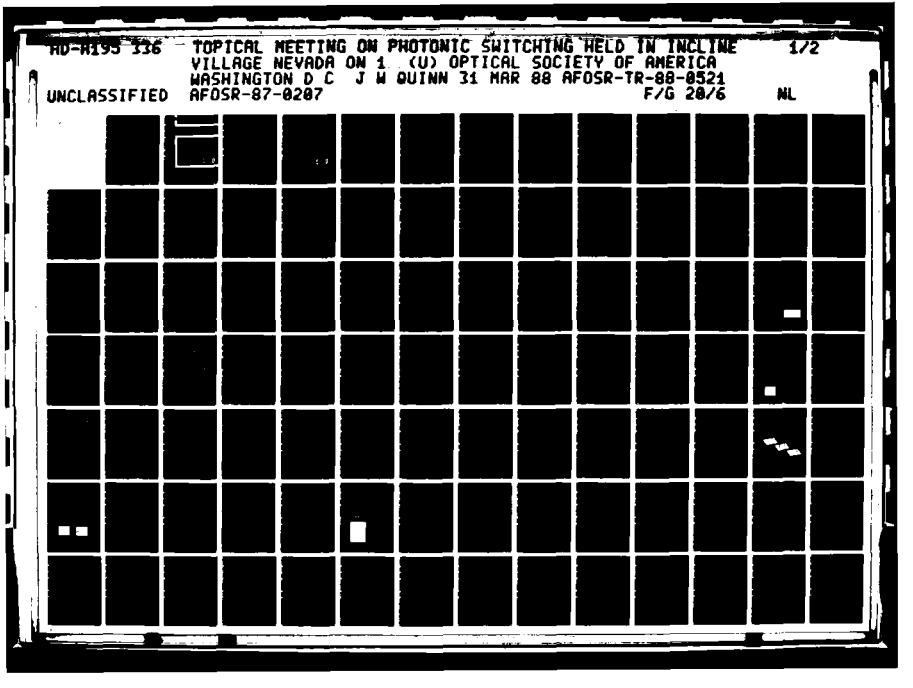
AD-A195 116 TOPICAL MEETING ON PHOTONIC SWITCHING HELD IN INCLINE 1/2
VILLAGE NEVADA ON 1 (U) OPTICAL SOCIETY OF AMERICA
WASHINGTON D C J W QUINN 31 MAR 88 AFOSR-TR-88-0521
UNCLASSIFIED AFOSR-87-0207 F/G 20/6 NL

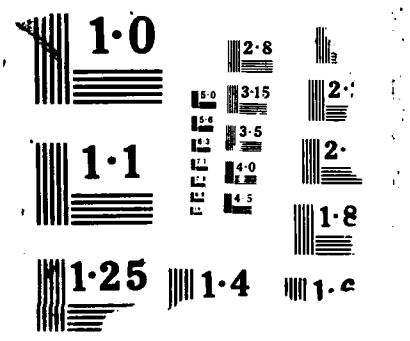
1·0
1·1
1·25
1·4
2·8
3·15
3·5
4·0
4·5
2·
1·8

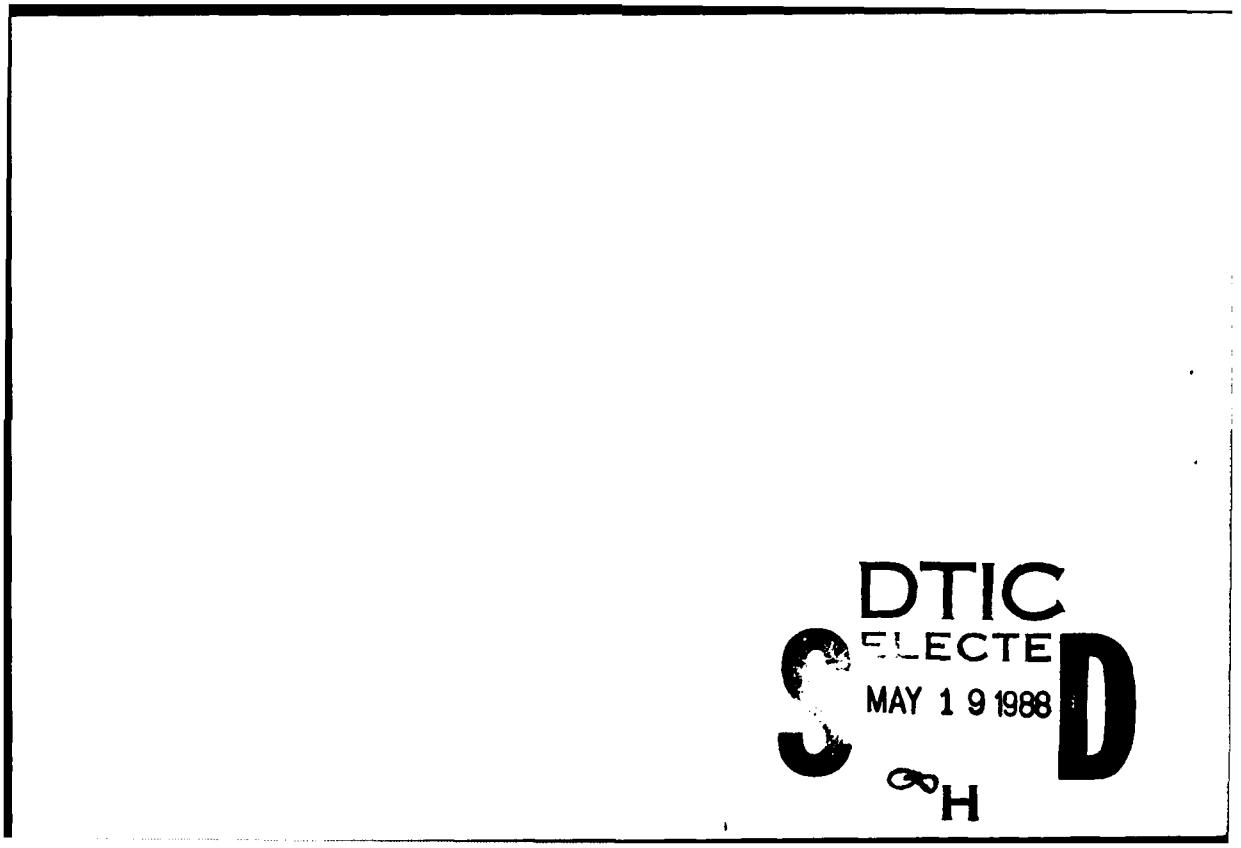
DTIC
ELECTE
MAY 1 9 1988
S
D
H

Unclassified

SECURITY CLASSIFICATION OF THIS PAGE

REPORT DOCUMENTATION PAGE

Form Approved OMB No. 0704-0188

1a. REPORT SECURITY CLASSIFICATION Unclassified	1b. RESTRICTIVE MARKINGS n/a
2a. SECURITY CLASSIFICATION AUTHORITY	3. DISTRIBUTION/AVAILABILITY OF REPORT Approved for public release-distribution unlimited
2b. DECLASSIFICATION/DOWNGRADING SCHEDULE	
4. PERFORMING ORGANIZATION REPORT NUMBER(S) AFOSR-87-0207	5. MONITORING ORGANIZATION REPORT NUMBER(S) AFOSR-TR- 88-0521
6a. NAME OF PERFORMING ORGANIZATION Optical Society of America 6b. OFFICE SYMBOL (If applicable)	7a. NAME OF MONITORING ORGANIZATION Department of the Air Force- Air Force Office of Scientific Research
6c. ADDRESS (City, State, and ZIP Code) 1816 Jefferson Place, N.W. Washington, D.C. 20036	7b. ADDRESS (City, State, and ZIP Code) AFOSR/NE Building 410 Bolling AFB, Washington, D.C. 20332-6448
8a. NAME OF FUNDING/SPONSORING ORGANIZATION 8b. OFFICE SYMBOL (If applicable) 8 AFOSR/NE BLDG 410 BOLLING AFB, DC 20332-6448	9. PROCUREMENT INSTRUMENT IDENTIFICATION NUMBER ~~F~~ AFOSR-87-0207
	10. SOURCE OF FUNDING NUMBERS PROGRAM ELEMENT NO. 61102F; PROJECT NO. 2305; TASK NO B2; WORK UNIT ACCESSION NO.
11. TITLE (Include Security Classification) Organization of a Topical Meeting on Photonic Switching	
12. PERSONAL AUTHOR(S) J. W. Quinn	
13a. TYPE OF REPORT Final	13b. TIME COVERED FROM 87/03/15 TO 88/03/31
14. DATE OF REPORT (Year, Month, Day) 88/03/31	15. PAGE COUNT
16. SUPPLEMENTARY NOTATION	

17. COSATI CODES		
FIELD	GROUP	SUB-GROUP

18. SUBJECT TERMS (Continue on reverse if necessary and identify by block number)

19. ABSTRACT (Continue on reverse if necessary and identify by block number)

This meeting provided a forum for the presentation of both invited and contributed original papers on the subjects of devices and architectures suitable for switching, multiplexing, or routing optical signals. This meeting fostered and enhanced interaction between two groups that share a common interest in exploring possible applications of photonics switching technology; people working on optical switching devices and components; and people working on future switching systems and networks. Papers covered the following areas: devices and phenomena for switching applications and switching systems and network architectures utilizing optical switching technologies.

20. DISTRIBUTION/AVAILABILITY OF ABSTRACT ☒ UNCLASSIFIED/UNLIMITED ☐ SAME AS RPT ☐ DTIC USERS	21. ABSTRACT SECURITY CLASSIFICATION Unclassified
22a. NAME OF RESPONSIBLE INDIVIDUAL ~~Jarus W. Quinn~~ Schlossberg	22b. TELEPHONE (Include Area Code) 202/~~223-8130~~ 767-4908 22c. OFFICE SYMBOL NE

DD Form 1473, JUN 86 Previous editions are obsolete.

SECURITY CLASSIFICATION OF THIS PAGE

Unclassified

(2)

TOPICAL MEETING ON

PHOTONIC SWITCHING

Summaries of papers presented at the Photonic Switching Topical Meeting

March 18–20, 1987

Incline Village, Nevada

Sponsored by the

Lasers and Electro-Optics Society of IEEE
Optical Society of America

In cooperation with

Communications Society of the
Institute of Electrical and Electronics Engineers

Optical Society of America
1816 Jefferson Place, N.W.
Washington, D.C. 20036
(202) 223-8130

Articles in this publication may be cited in other publications. In order to facilitate access to the original publication source, the following form for the citation is suggested:

Name of Author(s), Title of Paper, Topical Meeting on Photonic Switching, Technical Digest Series, 1987 Volume 13, (Optical Society of America, Washington, D.C. 1987) pp. xx-xx.

ISBN Number
Conference Edition 0-936659-50-5
Postconference Edition 0-936659-70-X

Library of Congress Catalog Card Number
Conference Edition 86-063951
Postconference Edition 86-063952

IEEE Catalog Number 87TH0173-5

TABLE OF CONTENTS

TUESDAY, MARCH 17, 1987

LOWER LOBBY

6:00 PM-9:00 PM REGISTRATION/REFRESHMENTS

WEDNESDAY, MARCH 18, 1987

LOWER LOBBY

7:30 AM-6:00 PM REGISTRATION/SPEAKER CHECKIN

LOBBY

7:30 AM-8:30 AM CONTINENTAL BREAKFAST

PROSPECTOR/RUBICON ROOM

8:30 AM-11:40 AM
WA PLENARY SESSION: 1

8:30 AM
OPENING REMARKS
Peter W. Smith, *Meeting General Cochair*

8:50 AM
Linking Technology and Applications, Stewart D. Personick, *Meeting Program Cochair*

9:30 AM (Plenary Paper)
WA1 Overview of Switching Needs for 1990-2000 Plus, Eric Nussbaum, *Bell Communications Research, Inc.* Fiber optics and information services needs will drive new switch requirements. Necessary functional capabilities will include variable bandwidth assignment, high speed reconfigurability, modularity, and distributed intelligence capability. (p. 2)

LOBBY

10:20 AM-10:50 AM COFFEE BREAK

WEDNESDAY, MARCH 18, 1987—*Continued*

PROSPECTOR/RUBICON ROOM

10:50 AM (Plenary Paper)
WA2 Electronic Switching Technologies for Digital Logic, Robert W. Keyes, *IBM T.J. Watson Research Center.* Modern computers represent information as binary digits, the positions of switches. The great success of the transistor in providing these switches is described and projected through the coming decades. (p. 4)

11:40 AM-1:30 PM LUNCH BREAK

PROSPECTOR/RUBICON ROOM

1:30 PM-5:20 PM
WB Joint Photonic Switching and Optical Computing Plenary Session, T. Kenneth Gustafson, *National Science Foundation, Presider*

1:30 PM (Plenary Paper)
WB1 Photonic Switching Components: Current Status and Future Possibilities, John E. Midwinter, *University College London, U.K.* The range of components becoming available for routing signals in optical networks is vast and varied. We review their character and typical performance and point to the network characteristics they support. (p. 8)

2:20 PM (Plenary Paper)
WB2 Optical Digital Computers, Alan Huang, *AT&T Bell Laboratories.* (p. 9)

LOBBY

3:10 PM-3:40 PM COFFEE BREAK

PROSPECTOR/RUBICON ROOM

3:40 PM (Plenary Paper)
WB3 Optical Neural-Net Computer, Demetri Psaltis, *California Institute of Technology.* (p. 9)

4:30 PM (Plenary Paper)
WB4 Switching System/Network Architectural Possibilities, Tadahiko Yasui, Katsuaki Kikuchi, *NTT Electrical Communications Laboratories, Japan.* We describe the present status of optical switching technology and endeavors to enhance the advantages of optical switching systems. (p. 11)

5:20 PM BREAK

LAKESIDE ROOM

6:00 PM-8:00 PM CONFERENCE RECEPTION

THURSDAY, MARCH 19, 1987

LOWER LOBBY

8:00 AM–5:00 PM REGISTRATION/SPEAKER CHECKIN

LOBBY

8:00 AM–8:30 AM CONTINENTAL BREAKFAST

PROSPECTOR/RUBICON ROOM

8:30 AM–10:00 AM
ThA PHOTONIC SWITCHING SYSTEMS
H. Scott Hinton, *AT&T Bell Laboratories, Presider*

8:30 AM (Invited Paper)
ThA1 Switching Requirements for Broadband Integrated Services Digital Networks, O. Fundneider, *Siemens AG, F. R. Germany.* Introducing broadband services in integrated services digital networks has important impacts on switching technology. The architectural and technological aspects for broadband ISDN are discussed with respect to possible uses of optical switching. (p. 18)

9:00 AM
ThA2 Optical Broadband Communications Network Architecture Utilizing Wavelength-Division Switching Technologies, Syuji Suzuki, Kunio Nagashima, *NEC Corporation, Japan.* Wavelength synchronization is introduced in wavelength-division communications networks. A synchronized wavelength-division switching system, based on semiconductor optical integrated circuits, is also proposed. (p. 21)

9:15 AM
ThA3 Photonic Switching and Digital Cross-Connect Systems, Jonathan A. Nagel, *AT&T Bell Laboratories.* Wideband switches are being introduced into the network. This paper discusses their functions, general features, and potential applications for photonic switching technology. (p. 24)

9:30 AM
ThA4 Optical Switching in Coherent Lightwave Systems, M. Fujiwara, S. Suzuki, K. Emura, M. Kondo, K. Manome, I. Mito, K. Kaede, M. Shikada, M. Sakaguchi, *NEC Corporation, Japan.* Integration of optical switching networks and coherent transmission systems was studied. Space-division switching experiments in a 100-Mb/s optical FSK transmission system using closely spaced (< 5 GHz) transmitter wavelengths were carried out with a $LiNbO_3$ optical switch. (p. 27)

THURSDAY, MARCH 19, 1987—*Continued*

9:45 AM
ThA5 Photonic Switching Demonstration Display, J. R. Erickson, C. G. Hseih, R. F. Huisman, M. L. Larson, J. V. Tokar, G. A. Bogert, E. J. Murphy, R. T. Ku, *AT&T Bell Laboratories.* A switching demonstration display has been built to show the feasibility of routing digital video through a guided-wave photonic switch. (p. 30)

LOBBY

10:00 AM–10:30 AM COFFEE BREAK

PROSPECTOR/RUBICON ROOM

10:30 AM–12:00 M
ThB SWITCHING ARCHITECTURES
Alan R. Tedesco, *Bell Communications Research, Inc., Presider*

10:30 AM (Plenary Paper)
ThB1 Introduction to Switching Networks, Vaclave E. Benes, *AT&T Bell Laboratories and Columbia U.* We present a broad tutorial description of connecting network concepts and structures, divided into three categories: combinational, probalistic, and operational, each with suitable examples. (p. 34)

11:15 AM
ThB2 Deterministic and Statistic Circuit Assignment Architectures for Optical Switching Systems, A. de Bosio, C. De Bernardi, F. Melindo, *Centro Studie Laboratori Telecomunicazioni, Italy.* Two architectures are proposed: the first utilizes nonblocking networks operated with label-address techniques; the second uses blocking networks exploiting the wide band of the optical elements. (p. 35)

11:30 AM
ThB3 Dilated Networks for Photonic Switching, Krishnan Padmanabhan, Arun Netravali, *AT&T Bell Laboratories.* We present novel switches optimized for low crosstalk using directional couplers in $LiNbO_3$ as switch elements. The switch has a simple routing algorithm and an optimum number of elements. (p. 38)

11:45 AM
ThB4 Self-Routing Optical Switch with Optical Processing, P. R. Prucnal, D. J. Blumenthal, P. A. Perrier, *Columbia U.* The experimental demonstration of a self-routing optical switch, in which routing information is processed optically on a bit-by-bit basis, is presented. (p. 42)

12:00 M–1:30 PM LUNCH BREAK

PROSPECTOR/RUBICON ROOM

1:30 PM-3:00 PM
ThC PHOTONIC SWITCHES: 1
Rod C. Alferness, *AT&T Bell Laboratories, Presider*

1:30 PM (Invited Paper)
ThC1 Optoelectronic Hybrid Switching, R. I. MacDonald, *U. Regina, Canada.* The principles, performance and some possible uses of optoelectronic switching matrices are reviewed, and their advantages and disadvantages compared with other techniques of wideband switching are considered. (p. 46)

2:00 PM
ThC2 Photonic Switching with Stripe Domains, E. J. Torok, J. A. Krawczak, G. L. Nelson, B. S. Fritz, W. A. Harvey, F. G. Hewitt, *Sperry Advanced Optics CTC.* This paper describes an all-optical crossbar switchboard for optical fibers. It is fast, solid state, nonblocking, latching, polarization insensitive, and can handle large numbers of fibers. (p. 49)

2:15 PM
ThC3 Single-Mode Fiber Switch with Simultaneous Loop-Back Feature, W. C. Young, L. Curtis, *Bell Communications Research, Inc.* A moving fiber-array switch providing a bypass function and a simultaneous loop-back circuit has been demonstrated. Fabricated with single-mode fibers the insertion losses for the bypass and on-line positions are 0.38 and 0.33 dB, respectively. (p. 52)

2:30 PM
ThC4 All-Fiber Routing Switch, S. R. Mallinson, J. V. Wright, C. A. Millar, *British Telecom Research Laboratories, U.K.* We report an optical crosspoint switch using a high-index waveguide sandwiched between two polished fiber coupler blocks. (p. 55)

2:45 PM
ThC5 All-Optical Switch for Signal Routing Between Fibers, C. R. Paton, S. D. Smith, A. C. Walker, *Heriot-Watt U., U.K.* An optically bistable nonlinear interference filter has been operated as a spatial switch to route an optical signal carrying video information between fibers. (p. 58)

LOBBY

3:00 PM-3:30 PM COFFEE BREAK

THURSDAY, MARCH 19, 1987—*Continued*

PROSPECTOR/RUBICON ROOM

3:30 PM-5:00 PM
ThD PHOTONIC SWITCHES: 2
Takakiyo Nakagami, *Fujitsu Laboratories, Ltd., Presider*

3:30 PM
ThD1 Monolithically Integrated Optical Gate 2 × 2 Matrix Switch using a GaAs/AlGaAs Multiple Quantum Well Structure, A. Ajisawa, M. Fujiwara, J. Shimizu, M. Sugimotc, M. Uchida, Y. Ohta, *NEC Corporation, Japan;* K. Asakawa, *Optoelectronics Joint Research Laboratories, Japan.* A 2 × 2 optical matrix switch, monolithically integrating multiple quantum well gate and optical circuits fabricated by a reactive ion beam etching method, is described. The switch size can be as small as 3 mm × 1.2 mm. Low crosstalk (20 dB at 9 V) is achieved. (p. 62)

3:45 PM
ThD2 Silicon Carrier-Enhanced Electrooptical Guided-Wave Switch, J. P. Lorenzo, R. A. Soref, *Rome Air Development Center.* An all-silicon 1.3-μm wavelength electrooptical switch is demonstrated for the first time. Partial 2 × 2 switching is observed during minority carrier interjection. (p. 65)

4:00 PM
ThD3 4 × 4 Ti:$LiNbO_3$ Switch Array with Full Broadcast Capability, G. A. Bogert, *AT&T Bell Laboratories.* We present a Ti:$LiNbO_3$ optical switch array which provides full broadcast capability. The architecture integrates directional couplers, *Y*-branches, and intersecting waveguides. The device operates at 13 V and exhibits measurement-limited crosstalk. (p. 68)

4:15 PM
ThD4 New Architecture for Large Integrated Optical Switch Arrays, P. J. Duthie, M. J. Wale, I. Bennion, *Plessey Research (Caswell), Ltd., U.K.* We propose a new reflective switch-array architecture and describe process-tolerant waveguide reflectors. Experimental results from a reduced 8 × 8 Ti:$LiNbO_3$ switch array are presented and used to derive practical maximum array sizes. (p. 71)

4:30 PM
ThD5 System Considerations for Lithium Niobate Photonic Switching Technology, W. A. Payne, H. Scott Hinton, *AT&T Bell Laboratories.* This paper discusses several components and system areas that require development prior to the successful implementation of lithium niobate technology for photonic switching. (p. 74)

4:45 PM
ThD6 High-Speed Δβ-Reversal Directional Coupler Switch, R. C. Alferness, L. L. Buhl, S. K. Korotky, R. S. Tucker, *AT&T Bell Laboratories.* An optical directional coupler switch designed for low crosstalk operation for both switch states with multigigahertz toggle rates is described. Experimental and theoretical results are presented. (p. 77)

5:00 PM BREAK

PROSPECTOR/RUBICON ROOM

8:00 PM
ThE POSTDEADLINE PAPERS
John E. Midwinter, *University College London, Presider*

LOWER LOBBY

8:00 AM-5:00 PM REGISTRATION/SPEAKER CHECKIN

LOBBY

8:00 AM-8:30 AM CONTINENTAL BREAKFAST

PROSPECTOR/RUBICON ROOM

8:30 AM-10:00 AM
FA PHOTONIC DEVICES: 1
William J. Stewart, *Plessey Research (Caswell), Ltd., Presider*

8:30 AM (Invited Paper)
FA1 Photonic Switching Devices Based on Multiple Quantum Well Structures, D. A. B. Miller, *AT&T Laboratories.* Quantum well semiconductor structures can be used to make several different electrically and/or optically controlled modulators and switches. Physics and uses are reviewed. (p. 82)

9:00 AM
FA2 Room Temperature Excitonic Nonlinear Absorption in GaAs/AlGaAs Multiple Quantum Well Structures Grown by Metalorganic Chemical Vapor Deposition, H. C. Lee, A. Hariz, P. D. Dapkus, A. Kost, M. Kawase, E. Garmire, *U. Southern California.* A strong saturation effect of the excitonic absorption in GaAs/AlGaAs MQW structures grown by MOCVD has been achieved at room temperature, with low saturation intensity (249 W/cm^2). (p. 85)

9:15 AM
FA3 Hard-Limiting Optoelectronic Logic Devices, P. Wheatley, M. Whitehead, P. J. Bradley, G. Parry, John E. Midwinter, *University College London, U.K.;* P. Mistry, M. A. Pate, J. S. Roberts, *U. Sheffield, U.K.* We report the first demonstration of a novel optoelectronic device for optical logic having an inverting characteristic that displays hard limiting and optical gain. (p. 88)

9:30 AM
FA4 Picosecond Optical Beam Coupling in Photorefractive GaAs, George C. Valley, Arthur L. Smirl, *Hughes Research Laboratories;* Klaus Bohnert, Thomas F. Boggess, *North Texas State U.* Picosecond optical beam coupling as a function of time delay is reported showing competition between photorefractive and free-carrier transient energy transfer and two-photon absorption. (p. 91)

9:45 AM
FA5 Nonlinear Optical Logic Etalon at Today's Fiber Communication Wavelengths, K. Tai, J. L. Jewell, W. T. Tsang, *AT&T Bell Laboratories.* We have constructed all-optical logic etalons operating in the 1.57-μm wavelength region using InGaAs/InP MQW structures. These etalons require several pJ switching energy, exhibit high on/off contrast with large on-state transmission and several ns recovery time, and have signal gain. (p. 94)

LOBBY

10:00 AM-10:30 AM COFFEE BREAK

PROSPECTOR/RUBICON ROOM

10:30 AM-12:00 M
FB HOLOGRAPHY AND BISTABILITY
Eric Spitz, *Thompson CSF, Presider*

10:30 AM (Invited Paper)
FB1 Wave Mixing in Nonlinear Photorefractive Materials; Applications to Dynamic Beam Switching and Deflection, Jean-Pierre Huignard, *Thomson-CSF, France.* Wave mixing in photorefractive crystals leads to new dynamic functions in optics. A review of the basic aspects of the beam interactions is presented as well as laboratory demonstrations of optically controlled beam deflection and switching devices. (p. 98)

11:00 AM
FB2 Design and Construction of Holographic Optical Elements for Photonic Switching Applications, M. R. Taghizadeh, I. R. Redmond, A. C. Walker, S. D. Smith, *Heriot-Watt U., U.K.* We report the simultaneous operation of a 2-D array of all-optically bistable switches in ZnSe nonlinear interference filter using a dichromated gelatin holographic array generator. (p. 104)

11:15 AM
FB3 Optical Threshold Mechanism using a Fiber Coupled Phase-Conjugate Mirror, Ram Yahalom, Aharon Agranat, Amnon Yariv, *California Institute of Technology.* We describe a new optical phenomenon in which the phase conjugate power of mutually incoherent light beams is determined by their relative input power. Its potential as a threshold mechanism is briefly discussed. (p. 107)

FRIDAY, MARCH 20, 1987—*Continued*

11:30 AM
FB4 Computational Properties of Nonlinear Optical Devices, Michael E. Prise, Norbert Streibl, Maralene M. Downs, *AT&T Bell Laboratories.* We derive the relationships between the optical properties of devices (transmission and contrast) and their potential computational properties (fan-in and fan-out), when used in an optical digital computer. The required accuracy of intensity levels in the system is discussed. (p. 110)

11:45 AM
FB5 Operating Curves for Optical Bistable Devices, P. Wheatley, John E. Midwinter, *University College London, U.K.* A method of presenting the steady state and dynamic responses of optical bistable devices is explained; it can be used to show the capabilities of such devices and their suitability for sequential logic. (p. 113)

12:00 M LUNCH BREAK

PROSPECTOR/RUBICON ROOM

1:30 PM-3:00 PM
FC PHOTONIC DEVICES: 2
W. Jack Tomlinson, *Bell Communications Research, Inc., Presider*

1:30 PM (Invited Paper)
FC1 Optical Amplifiers for Photonic Switches, R. M. Jopson, G. Eisenstein, *AT&T Bell Laboratories.* Optical amplifiers will play an important role in photonic switches. We describe the basic properties and limitations of practical optical amplifiers. (p. 116)

2:00 PM
FC2 170-ps Fast Switching Response in Bistable Laser Diodes with Electrically Controlled Saturable Absorber, Akihisa Tomita, Shunsuke Ohkouchi, Akira Suzuki, *NEC Corporation, Japan.* Fast switching in a bistable laser diode was achieved by controlling the carrier density electrically through the loss section electrode. The turn-off time was reduced to 170 ps. (p. 119)

2:15 PM
FC3 Organic Materials for Nonlinear Optics, R. D. Small, J. E. Sohn, K. D. Singer, M. G. Kuzyk, *AT&T Engineering Research Center.* Organic and polymeric materials are discussed in the context of nonlinear optics, including our development of doped poled polymer glasses for use in nonlinear optics. (p. 123)

2:30 PM
FC4 Physical and Optical Properties of Cd(Se,S) Microcrystaliites in Glass, D. W. Hall, N. F. Borrelli, *Corning Glass Works* Commercially available filters and experimental glasses containing Cd(Se,S) microcrystallites are studied using x-ray diffraction, TEM, wet-chemical analysis, photoluminescence, and linear and nonlinear absorption measurements. (p. 125)

2:45 PM
FC5 Dynamics of Photonic Switching in Indium Antimonide, H. A. MacKenzie, J. Young, H. A. Al-Attar, *Heriot-Watt U., U.K.* Results are presented which characterize both the dynamic switching and noise dependence of single bistable channels and the transfer of switching in adjacent channels. (p. 128)

LOBBY

3:00 PM–3:30 PM COFFEE BREAK

PROSPECTOR/RUBICON ROOM

3:30 PM–5:00 PM
FD TIME-DIVISION SWITCHING
Flavio Melindo, *CSELT, Presider*

3:30 PM (Invited Paper)
FD1 Photonic Time-Division Switching Technology, Hirokazu Goto, *NEC Corporation, Japan.* The principles and present state of optical time-division switching technology are described. Further studies aimed at the achievement of large-capacity switching systems are also discussed. (p. 132)

4:00 PM
FD2 A 1.5-Gb/s Time-Multiplexed Photonic Switching Experiment, J. R. Erickson, R. A. Nordin, W. A. Payne, M. T. Ratajack, *AT&T Bell Laboratories.* We describe a time-multiplexed photonic switch that routes 45-Mb/s channels which are block multiplexed to 1.5 Gb/s. The switch is nonblocking and capable of broadcasting. (p. 135)

4:15 PM
FD3 4-Gb/s Optical Time-Division Multiplexed System Experiments using Ti:$LiNbO_3$ Switch/Modulators, R. S. Tucker, S. K. Korotky, G. Eisenstein, U. Koren, G. Raybon, J. J. Veselka, L. L. Buhl, B. L. Kasper, R. C. Alferness, *AT&T Bell Laboratories.* We demonstrate the use of high-speed Ti:$LiNbO_3$ switch/modulators in a 4-Gb/s optical time-division multiplexed fiber transmission system based on mode-locked semiconductor lasers. (p. 138)

FRIDAY, MARCH 20, 1987—*Continued*

4:30 PM
FD4 Optimizing Photonic Variable-Integer-Delay Circuits, Richard A. Thompson, *AT&T Bell Laboratories.* For three different structures, we investigate the total number of photonic switches and the number of switches through which a photonic signal must pass. (p. 141)

4:45 PM
FD5 Photonic Switch Architecture utilizing Code Division Multiplexing, T. S. Rzeszewski, A. L. Lentine, *AT&T Bell Laboratories.* Code-division multiplexing is a means of making a multiplicity of input channels orthogonal, so that any input to a code division (CD) switch can be switched to any output. This type of switch is nonblocking and has inherent broadcast capability. A photonic implementation of a CD switch and combinations of CD with time, space and wavelength division switching are discussed. (p. 144)

5:00 PM CLOSING REMARKS

WEDNESDAY, MARCH 18, 1987

PROSPECTOR/RUBICON ROOM

8:30 AM–11:40 AM

WA1–2

PLENARY SESSION: 1

Overview of Switching Needs for 1990-2000+

E. Nussbaum
435 South Street, Room 2A-213
Bell Communications Research
Morristown, NJ 07960

Summary

Research and development underway 30 years ago brought about today's world of stored program controlled digital switching. The confluence of three key elements was the trigger for this new era in switching--the transistor, the basic concepts of stored program controlled computing, and the techniques of digital communication in the form of PCM. Today, roughly one quarter of the world's 400 million telephone lines are served by central offices deploying most of these technologies. Though stored program gave these switches considerable new flexibility for customer features and allowed great strides in automation and simplification of maintenance and operations, the new technology was primarily deployed as a one-for-one cost reduction element for its electromechanical predecessors in the existing network--effectively a replacement vehicle between existing mainframes.

Today the prime technological driving force in the network is, of course, fiber optics. Along with that has come an enormous increase in the speed capability of the driving electronics, allowing for high speed data interchange and digital encoding of all information up to and including full motion video. These elements, together with the associated progress in computing power and storage capabilities, are the foundation of the so-called information age in which all forms of information are transmitted, stored, and processed electronically, be they voice, data, image, or video. To meet these "information age" needs, the next generation of switch, unlike previous generations in electronic switches, will require major new functionality in the switching network and its control, and most probably a redefinition of the role of the switch in the conventional telephony hierarchy. Some specific characteristics required to meet the needs in this new era include:

A. Capability for switching high bandwidths measured into the hundreds of Mb/s as opposed to the 64 kb/s standard rate prevalent to date.

B. Dynamic bandwidth assignment capabilities to allow a user to "dial up" the amount of bandwidth needed for the occasion, be it a low bandwidth interactive data transfer, or speech, or a high speed burst of data for bulk loading, or "continuous high speed data" such as full motion video.

C. Non-symmetric bandwidth capabilities allowing a user to have differing upstream and downstream channel capabilities as required, since users will often be using communication nets to access remote data bases with a query that is very brief compared to the response data supplied.

D. A very fast switching reconfigurability, be it fast circuit or high speed packet switching, to allow multiple routing paths for the multimedia mix of traffic necessary to meet the information needs described above.

E. Broadcast or multipoint capability to more readily allow the use of telecommunications networks for conferencing, narrowcasting, and even full fledged broadcasting (as in cable TV).

F. New topological structures that distinguish the function of switching individual channels within a whole facility at some points in a hierarchy, while switching larger "hunks' elsewhere in the hierarchy, driven by the dramatic change in the cost ratio of switching and transmission with the advent of fiber optic transmission systems.

G. Increased reliance on distributed intelligence and control to separate physical control of switching configurations from the geographic constraint of the associated controller, and instead allow for a

network of "data bases" interconnected at high speeds (again using a fiber optic technology) to control an entire network in a far more efficient and flexible manner.

Put together these factors all indicate the next generation of switch is unlikely to be a one-for-one physical and functional replacement from today's switching technology. The combination of technological and service triggers will instead help redefine the structure of the entire network and the nature of the services it can provide.

For optical switching to play a major role in this next generation of communication networks it must fulfill the requirements of the vast majority of the aforementioned points. To do so, it must compete with steadily improving costs and performance of silicon and the coming GaAs alternatives. To meet the functionality requirement in large scale networks, optical switches will have to be able to individually and rapidly switch the multiple channels of information and signaling emanating from each fiber, provide the capability for individual buffering and reconfiguration of bits for digital network interfaces and synchronization, and perform optical regeneration if information is to be kept in an all optical domain over large geographic areas. The limitations of performing these functions at the electronic level are primarily the cost of the E/O interfaces required, and of the extensive multiplex and demultiplexing necessary to separate and isolate channels. At the performance level the limitations occur when speeds of more than several hundred Mb/s per second are to be switched. The future of optical switching as a ubiquitous technology to move us towards all optical domain networks depends on its ability to meet these functional needs and to compete economically with the electronic alternatives.

It seems likely that to achieve that will require a total rethinking of traditional network structures and elements into a form that bears little relationship to the current partition of transmission, switching and control elements. Probable earlier steps to introduce more optics into switching might include its use in such areas as: a) lower functionality (cross connect) switching at limited high level points in the network and b) hybrid optoelectronic structures performing relatively simple high speed functions (e.g. multiplexing) combined with more conventional electronic implementation of complex lower speed functions. Modular structures to allow such technology upgrades are an important overall consideration in new switch and network architectures.

Overview of Electronic Switching Technologies for Digital Logic

Robert W. Keyes

T. J. Watson Research Center
P. O. Box 218
Yorktown Heights, NY 10598

Modern computation depends on the representation of information in digital form. "Digital" means that there are a discrete set of signal values. All contemporary electronic logic uses just two digits, binary representation of information. There are two recognizable signal values. A binary unit of information is known as a bit. It can be represented by the position of a switch of the familiar ON-OFF type. The state of the switch or the signal is also conveniently represented by a 0 or a 1.

- Why Switches? -

One might wonder: why digital? The answer is well-known, although not always well-remembered. Although representation of information by a continuous signal that can have an infinite number of values can represent an infinite amount of information, the ability to use this capacity is limited by noise and the accuracy of measuring instruments. Digital representation means that only a discrete set of standard signal values must be distinguished. Arbitrary accuracy in the representation can be obtained by the use of enough digits.

One might further ask: why binary? The answer lies in the requirement that the signal values that represent the digits must be well-separated; the digits must be recognizable in spite of attenuation and distortion suffered in transmission from one place to another and in spite of the imperfections of sending and receiving devices. The clearest separation is afforded by using only two signal values. It is also easy to make physical devices with two clearly distinguishable physical states, e.g., there is or is not a magnetic bubble at a certain location, a ferromagnetic torus has two low energy states, a relay contact is either open or closed. Obviously other number systems could be used. Some have been investigated, but none has led to machines with the reliability, accuracy, and speed of binary digital computers. Thus the state of the art of computation is closely related to the state of development of electronic on-off switches.

- The Transistor -

Although many physical phenomena of a switching character are known, large digital systems have only been realized with three: relays, vacuum tubes, and transistors. These three types of devices depend on essentially the same mode of operation, which, though simple and familiar, also is sometimes forgotten. One of the two signal values applied to an input terminal establishes a connection between an output terminal and one of the power supply leads. The other input signal value opens this connection and permits the output to assume the value of the other power supply lead. Thus the values of the output are determined by power supply voltages distributed throughout the system.

Although relays and vacuum tubes have been used to construct large systems, they were rapidly displaced by transistors not long after the invention of the latter device. The transistor fitted the needs of systems containing thousands of logic gates for devices of low cost, high reliability and low power dissipation extremely well. Furthermore, the transistor turned out to have almost unlimited potential for miniaturization; the pace of improvements in all aspects of transistor performance stagger the imagination and defy all suggestions of problems that seem to limit the technology. The experience of the past two decades lends confidence to the extrapolation of current trends to a considerable distance into the future.

- The Future -

The themes that have characterized transistor development through the past two decades have been integration and miniaturization, the latter being an essential element of the former. These directions have been the key to low cost, low power, and high reliability, and, in addition, have led to high speed through reduction of capacitances and of the distances between elements. The history of miniaturization and integration can be projected to provide a basis for a picture of the chips of the future. Such projections will be presented. The picture obtained differs so dramatically from the chips of today that the forecast is hard to accept. Yet progress has continued in the face of similar doubts in the past.

Quite a few effects inhibit progress to smaller dimensions and higher levels of integration. New fabrication techniques offering finer resolution, more accurate alignment, and greater control must be developed. Electric fields increase, accelerating the deleterious effects of hot electrons. High-speed systems demand large currents; current densities increase with miniaturization. The high current densities cause electromigration, increase the losses at contacts, and affect the operation of devices.

Integration poses its own set of problems. Highly integrated chips in high-speed systems consume large amounts of power that must be supplied through miniaturized contacts to the chip and removed by elaborate cooling means. Increasing off-chip communication capacity is also needed by increasingly integrated chips that are part of a large system. Even chips that constitute a self-contained system use increasing word lengths that need more off-chip contacts. The amount of wire necessary to provide communication on a chip also increases rapidly with increasing levels of integration.

Digital switching is used in a variety of information-handling products, such as memories, microprocessors, and high-speed gate arrays, each filling some niche in a cost-functionality space. Attack on each usually proceeds simultaneously on several technical fronts, as the existence of several types of transistor and their flexibility in fitting into a wide variety of circuit configurations offers many options. Bipolar transistors and field-effect transistors, NMOS and CMOS, silicon and gallium arsenide constantly compete for a place in applications. Limitations of one technology may provide opportunities for another.

The speed of switching devices and comparisons of speed among devices attract large amounts of attention. Speed can be measured at various levels. A single device can be selected and tuned to demonstrate high speed switching. This is more difficult in an integrated ring oscillator, where ten or twenty devices must all operate simultaneously. Large load capacitances that must be charged and possible variability among devices must additionally be taken into account in functional units of useful size. Speed in a large mainframe computer is dependent not only on the properties of switching devices but on the ingenuity of engineers in

supplying power and removing heat at high densities and in providing a compact network of interconnections among chips. The large numbers of components demand attention to economic considerations. The significance of simple measures of speed to performance in complex applications is often obscure.

- Conclusion -

The difficulties that one sees in realizing the extrapolations of transistor switches into the future are the challenges that the scientists and engineers who will be responsible for implementing the technologies of the future will have to face. History provides reason to believe that the challenges will be successfully met.

WEDNESDAY, MARCH 18, 1987

PROSPECTOR/RUBICON ROOM

1:30 PM–5:20 PM

WB1–4

JOINT PHOTONIC SWITCHING AND OPTICAL COMPUTING PLENARY SESSION

T. Kenneth Gustafson, National Science Foundation,
Presider

PHOTONIC SWITCHING COMPONENTS: CURRENT STATUS AND FUTURE POSSIBILITIES

J E Midwinter
University College London
Torrington Place
London WC1E 7JE

I. INTRODUCTION

The interest in optical switching seems to stem from several factors. One might well be cost, avoiding the need for two opto-electronic interfaces at the switching node. Further to that, in a local or campus network, the low insertion loss and bandwidth of single mode fibre offers the possibility of truly "transparent" networks, in which the format and data rate are set by the communicating terminals and the routing is achieved independently in a way that does not require synchronous or rigidly formatted data streams. Such switches may also support bidirectional operation both within the fibre and the switch. Another attribute of such technology is likely to be the provision of very large communication bandwidths as well as the usual optical advantages of low cross talk and distortion.

These factors are applied most readily in networks in which an incoming fibre carries data from a single user to a single user so that wideband circuit switching without multiplexing is required. However, often some form of multiplexing will be needed, with the result that the incoming and outgoing fibres will be carrying multiple services simultaneously, travelling to or derived from diverse locations. In these circumstances, the switch must perform a more complex operation. At present, two approaches appear to be under study, based upon WDM and TDM. The former case reduces to the circuit switched situation having dispersed wavelengths while the latter requires a much more sophisticated accurately timed switch structure, placing a very high premium on the timing accuracy.

II. ELECTRICALLY CONTROLLED EXCHANGE-BYPASS UNITS.

The basic building block for most switches is some form of four port element having the characteristic that two input ports, A & B can be connected directly (bypass) or crossed (exchange) to the two output ports C & D. Key operating parameters are the insertion loss, the cross talk level, the wavelength response, the switching time and precision. In single mode switches, the polarisation properties can also be important. One family of devices is based upon optical fibres. The simplest involves optical fibres connected via micro-optic elements (lenses, beam splitters etc) that are moved electro-mechanically or fibres themselves that are physically moved. Such devices lend themselves more to multimode than single mode operation, will generally have low insertion loss (particularly for multimode) and good cross talk characteristics but are inevitably rather slow in operation (order milliseconds), imprecisely timed, relatively insensitive to wavelength or polarisation but are physically bulky. They lend themselves to use within simple wideband video security networks. They do not appear to be more generally applicable.

Another class of fibre based devices is based upon fibre interferometers or "waveguide directional couplers", almost certainly using single mode fibre. For example, one might form a Mach-Zehnder Interferometer with two parallel single mode fibres fused at two points to form two 3dB directional couplers.

This leads to a four port coupler whose transfer characteristics depend upon the relative phase length of the two fibre paths between the two couplers. Changing one path relative to the other by a half wavelength switches the device from exchange to bypass or vice-versa. Such a change is readily induced by electrical heating of one arm. By the same token, thermal drift is likely to be problem. As with all fibre based devices, elements of this type can exhibit extremely low insertion loss and are potentially broad band. However, if the arms are unbalanced (unequal length), then the transfer characteristic becomes wavelength sensitive. The device may also be polarisations sensitive. Response time is expected to be slow, typically milliseconds and with relatively large dimensions (mm. to cm.). Once again, the devices seem most suited to use in circuit switched video surveillance or studio networks where switch set-up time is unimportant.

A totally different class of electrically controlled exchange bypass units emerges from the use of the electro-optic effect in guided wave integrated-optic form and commonly made by Titanium diffusion into Lithium Niobate crystal substrates. The exchange bypass unit so formed has two diffused waveguides that for part of their length run parallel and sufficiently close for their evanescent fields to interact. Switching is achieved by means of suitably placed electrodes that change the relative refractive indices in the two guides. These devices can have relatively low insertion loss, perhaps 1dB or better, although low loss coupling to fibre is difficult. Cross talk can easily be a problem. Fabricating large arrays poses major technological problems, since the devices are long (typically mm.) and confined to a single wiring plane. It appears that up to 16x16 may be possible on a single chip. Most devices are polarisation sensitive but clever design can overcome this. They can switch very fast, well into the sub-nanosecond regime, but present substantial capacitance to the drive circuit. Given a matrix occupying a large area (sq.cms), exploiting this speed to synchronously reset/set is almost certainly more difficult to achieve than switching a monolithically integrated electronic cross point. However, once the optical path is established, it offers "infinite" and bi-directional data bandwidth. Such elements are capable of very fast multiplexing or demultiplexing given electrical synchronisation. Wavelength response is also limited, typically to a few percent of the centre wavelength.

III. WAVELENGTH ROUTING

The growing availability of tunable sources and receivers opens possibilities of using a passive guided-wave network in a communication mode equivalent to that of free space radio communications, with terminals indentified by means of optical frequency. Some semiconductor lasers can be made to tune by the use of an external cavity over a range of 50-100nm, corresponding to more than 10,000 GHz, and in the case of those developed for coherent communication systems, can exhibit stabilities of better than 1MHz. Assuming channel spacings of 2GHz, one might speculate that as many as 5000 parallel and simultaneous channels could become accessible. Using less sophisticated lasers of the monolithically integrated type, a few tens to a few hundreds of wavelengths are accessible by electrical control.

At the receiver end, the coherent receiver selects its wavelengths primarily by means of the tunability of its local oscillator, a similar laser to the remote transmitter, although it is likely in a network using very many

wavelengths that some previous band-filtering might be desirable. A wide variety of techniques exist ranging from tunable filters based upon electro-optic directional coupler designs to those fabricated in fibres by means of grating structures impressed on the waveguide to simpler bulk dispersive elements interposed in the light path. Non-linear interactions in the fibre may also seriously limit perfromance. In any case, the network is transparent and passive and could be bi-directional (single fibre per terminal) and probably of a star format with central power splitting node. Alternatively, a dispersive element could be included at the central node although how this would be done for more than a small numbers of outgoing fibres is unclear. In principle, such wavelength switched networks looks extremely powerful given good tunable sources and receivers at competitive prices.

IV. OPTICALLY ACTIVATED SWITCHES

Studies in non-linear optics have led to a variety of optically activated switches, mainly based on optical bistability, that have led to much speculation on optical computing but have generated little interest for switching. Optical activation opens up interesting new opportunities in control and interconnection, particularly when coupled with free space (2 dimensional) optical "wiring" and the possibility of normally addressed planar arrays of devices, since the wiring rapidly becomes a limiting factor in other optical matrix concepts. Optical logic gates span a huge range of switching speeds from ps to ms but tend to require similar switching energies, at present in the 1E-9 to 1E-6 Joule range (ie 1000 gates at 1Gbit/s = 1kW to 1MW power!). It is expected that pico-joule sensitivities will be possible in time with bistable laser and other hybrid devices reaching femto-joule levels. Bistable gates are operated as threshold logic elements and thus incur all its normally associated problems. Hence there is growing interest in alternative approaches involving hard limiting opto-electronic circuits, preferably with good I/O isolation. However, the bistable element does imply a memory capability and this has been demonstrated in simple time-slot interchange switches although the engineering problems involved in constructing a large switch look formidable.

An alternative approach is to explore hybrid opto-electronic matrices, combining optical wiring and control, electronic logic and photodetectors and electro-absorption modulators monolithically integrated as I and O elements. This approach promises to combine the interconnect strengths of optics with the high speed logic strength of small electronic logic circuits and hence to lead to large ultra-fast optically controlled arrays. In time, all optical logic solutions may emerge and some novel approaches to their logical design have already been postulated that draw heavily on ideas generated in studies of optical computing. The technology for optically activated switches is still at an early stage of development although a variety of very interesting ideas can be discerned already. The major gain arise from optical wiring which provides very accurate timing control at high data rates (in excess of 1Gbit/s per port), thus opening up the possibility of switching packet or TDM data from ultra wideband highways.

WB2

Optical Digital Computers

Alan Huang
AT&T Bell Laboratories
Holmdel, NJ 07733

OPTICAL NEURAL COMPUTERS

Demetri Psaltis

California Institute of Technology
Department of Electrical Engineering
Pasadena, California, 91125

The development of optical computers of any type is based on the notion that semiconductor technology imposes limitations in the performance of current computers which prevent them from being effectively used for the solution of a class of interesting computational problems. If optics is used instead, these limitations will be lifted and we will therefore be able to now solve these interesting problems. Global connectivity is perhaps the most distinctive feature of optics vis-a-vis semiconductor technology, and the development of optical neural computers can be viewed as an attempt to exploit this feature. In a neural network each elementary computational unit, the neuron, directly communicates to thousands of others, while in electronic computers each gate is typically connected to only two or three gates. With optics it is feasible to realize the dense connectivity that is evident in neural networks. This provides the impetus for examining neural network models of computation to get ideas about how to build optical computers whose performance is clearly better than their electronic counterparts.

A neural network consists of two basic components: a large collection of neurons and a dense network of connections. Neurons are typically modeled as thresholding elements and information is stored in the strength of the connections largely through error driven learning. If during a learning phase the response of the network is correct then the connections remain unaffected. Otherwise they are modified to eventually produce a desired response. Within this basic framework (large number of neurons, dense connections, and learning by modifying the connections) numerous models have been developed that attempt to explain different aspects of natural neural systems. These models have attracted the attention of computer scientists and engineers and have served as a source of ideas for building computers that are well suited for solving the types of problems that humans are good at. A prime example of such a problem is pattern recognition; we do it extremely well but current computers do it poorly. The hope is that even a partial understanding of how pattern recognition is done in a neural network, will prove helpful in designing computers that solve the problem. Neural computers derive their potential advantages largely from the fact that they are specialized. A particular neural computer will be a machine that is tuned to solve a specific set of problems. Experimental versions of such neural circuits have been built using either both optics and electronics. Optics is a technology that is particularly well suited for building neural computers because of the extensive connectivity it can provide. A neural optical computer can be built by arranging the neurons in a planar geometry and using the third dimension to globally interconnect the neural planes with light. It is the relative easy access to the third dimension that we have in an optical system that gives this technology an edge over electronic neural nets.

Overview of Switching System/Network Architectural Possibilities

Tadahiko Yasui and Katsuaki Kikuchi

NTT, Electrical Communications Laboratories,
3-9-11, Midori-cho, Musashino-shi, Tokyo, 180, Japan

1. Need for optical switching systems

To ensure the provision of high-speed, broadband services, new telecommunications networks should be constructed using both high-speed, broadband switching systems as well as high-speed transmission systems.

Optical technology has become a practical reality for high-speed transmission systems, and optical fiber transmission systems are rapidly replacing metallic-cable in long-haul transmission systems. As the bit-rate of optical fiber transmission systems increases beyond 1Gbps and the repeater-spacing continues to increase, it becomes more and more necessary to develop high-speed switching systems. It is difficult, however, to fabricate high-speed switching facilities using conventional electrical technologies, because the bandwidth and cross-talk problems inherent in electrical technologies do not allow high-speed operations. A very promising candidate for solving these problems is a high-speed optical time-division switching system in which it is not necessary to convert the high-speed optical signals to low-speed electrical signals.

It is also expected that optical fibers will penetrate into the present copper-wire subscriber loop networks. Therefore, optical fibers are essential for the provision of enhanced high-speed, broadband services of the future. In optical subscriber networks, two different switching functions must be performed; one is line concentration for broadband bidirectional services, and the other signal distribution for CATV services. Optical technologies have made space-division switching networks almost independent of transmission bit-rate. Such networks are suitable for realizing the two functions mentioned above. Optical line-concentration will contribute very much to the construction of cost-effective optical subscriber loop networks.

An optical communications network can be realized by combining an optical switching system with optical fiber transmission lines without the need for electonic-optical and optical-electronic converters. Such optical communications networks are expected to offer both enhanced functions and high performance in the provision of high-speed, broadband services of the future.

2. Switching Network Architectural Possibility

To fully realize high-speed time division switching networks, it is necessary to clarify the potential advantages of optical switching networks over electronic switching networks.

The relevant Optical and electrical technologies are shown together in relation to device fabrication and interconnection techniques in Fig. 1.

Optical signal transmission features low loss, wide bandwidth and non-inductiveness, while electrical signal transmission has a speed limit due to the product of the resistance and capacitance in the electrical line. Optical interconnection exhibits excellent broadband transmission characteristics, and is essential for a high-speed operation. Optically controlled optical devices (OCOD) are capable of attaining a very high switching speed on the order of picoseconds [1]. In contrast, electrically controlled optical devices (ECOD) cannot achieve such high-speed operation, because the switching speed in such devices is limited by electrical control signals. Therefore, an optical time division switching system with OCODs and optical interconnection will be able to realize a very high-speed operation.

In such synchronous systems as time division switching networks, one of the most difficult problems arising from high-speed operation is clock skew caused by differences in propagation delay time among optical signals through different optical paths. One solution to this problem is to use a two-dimensional beam steering technique [2] which exploits the a non-interaction feature of photons. Two-dimensional arrays of optical memories are incorporated in this novel switching networks.

Electronic devices can realize virtually the same speed of operation as ECODs. Therefore, for the time being, time division switching networks are likely to be constructed with opto-electronic integrated circuits (OEICs), which incorporated the best advantages of both optical and electrical technologies - electronic logic circuits and optical interconnections. Wavelenghth division technologies, however, make it possible to extend the throughput of a switching network without increasing the operating speed. Thus, optical switching systems with ECODs also have their own merits over conventional electronic switching systems with OEICs.

Optical technology has the great advantage of being able to transfer two-dimensional images using fiber bundles or graded index fibers without the need to convert into electrical signals. In this application, image switching networks are required to exchange images transmitted through such transmission media.

3. Optical Switching Technological Possibility

Eight-by-eight optical matrix switches, which are the basic components in the construction of an optical space division switching system, have already been demonstrated. These switches appear to have the capability required by small-size optical switching systems. Recently, some small-size system experiments using such optical matrix switches have been reported.[3],[4] To realize large-size optical switching systems, such as telecommunications switching networks, however, it is necessary to clarify that the problems of loss accumulation and cross talk

can be overcome.

The key devices supporting the development of optical time division switching networks are high-speed optical switches and memories. Many studies of optical bistable devices are currently being conducted in a number of countries. Recently, semiconductor optical bistable devices based on either laser diodes or multiple quantum well structures have been attracting special interest. Optical time switches using either fiber delay lines or bistable laser diodes as optical memories have been demonstrated. [5],[6],[7] Furthermore, optical retiming and regenerating techniques are essential to synchronizing high-speed optical signals.

References

[1] P.W.Smith, "On the Physical Limit of Digital Optical Switching and Logic Elements", Bell Syst. Tech. Jour., Vol.61, 1982

[2] P.Gravey, et al., "Optical Switching Techniques for High Capacity Exchanges", ISS'84, 1984

[3] S.Suzuki, et al., "An Experiment on 32-lines Optical Space-division Switching", Natl. Conv. IECE Japan, 156, 1986.

[4] T.Matsunaga, et al., "Optical Space-division Switching System", ISS'87, 1987. (To be published)

[5] T.Matsunaga, et al., "Experimental Application of LD Switch Modules to 256Mb/s Optical Time Switching", Electron. Lett., Vol.21, No.20, 1985.

[6] R.A.Thompson, et al., "Experimental Photonic Time-slot Interchanger Using Optical Fibers as Reentrant Delay-line Memories", OFC'86, 1986.

[7] S.Suzuki, et al., "An Experiment on High-speed Optical Time-division Switching", IEEE J.Lightwave Tech., Vol.LT-4, No.7, 1986.

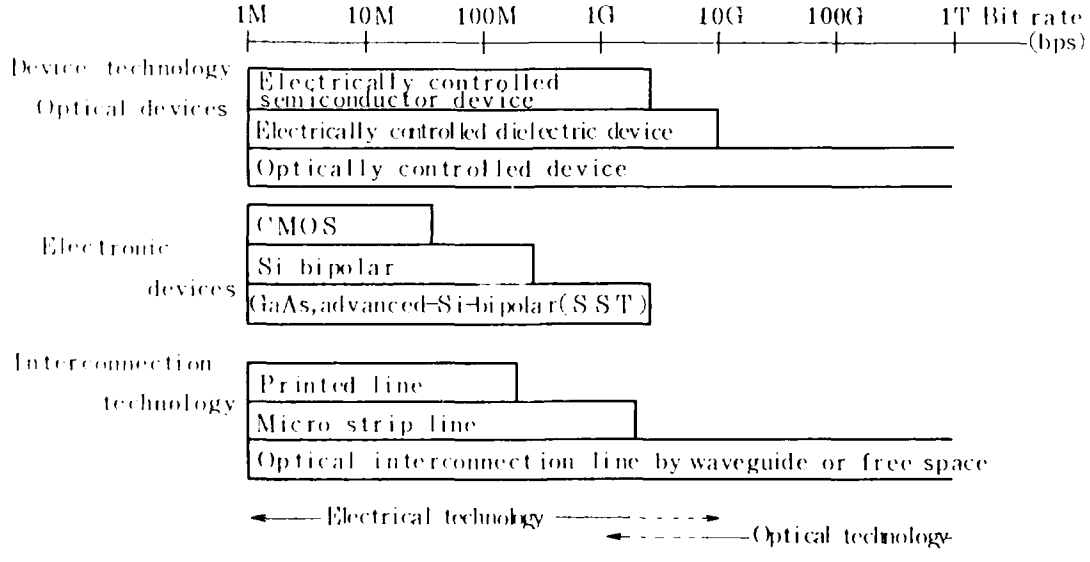

Fig. 1. Comparison of optical and electrical technologies

THURSDAY, MARCH 19, 1987

PROSPECTOR/RUBICON ROOM

8:30 AM–10:00 AM

ThA1–5

PHOTONIC SWITCHING SYSTEMS

H. Scott Hinton, AT&T Bell Laboratories, *Presider*

Switching Requirements for Broadband-ISDN

O. Fundneider, Siemens AG, N ZL SV,
P.O. Box 70 00 76, D-8000 Munich 70

1. Introduction

Telephone, telex and data networks today span the whole world and enable any parties to communicate with each other regardless of distance or time. In spite of their efficiency, these networks have one basic shortcoming: they are service-dedicated networks. A special terminal, a special network and a special service is required for each type of information. The users of the communication networks, however, would like to be able to use all types of information in one session.

As a result of technological advances, in particular those in the fields of microelectronics, optical technologies and software, it has now become possible to overcome the present situation with the aid of the ISDN concept. The fundamentals of ISDN have already been internationally standardized as have the essential points for narrowband services up to 64 kb/s. Work at the present time is concentrated on broadband services in the ISDN. Standards organizations, technologists and developers throughout the world are involved in this work.

2. Broadband ISDN Services

Most communications experts are of the opinion that, in the long term, all communications services can be integrated in one universal network: the ISDN. In the short term, the following brodband service categories result from the broadband introduction strategies of network operators; provision will be made for them within the BB-ISDN concept:

- Circuit-switched distribution services (e.g. for TV programs) together with the standard telephone service for private households: the picture quality must be at least as good as the conventional TV quality here; HDTV should not be impaired. These requirements necessitate bit rates of 30 to 140 Mb/s for conventional quality and at least 140 Mb/s for HDTV, the actual rate being dependent on the type of picture encoding used. It should be possible for households to receive 3 to 4 TV programs simultaneously.
- Circuit-switched interactive bearer services with bit rates of approx. 30, 45, 140 Mb/s for data applications and for moving-picture services with TV quality, e.g. for film retrieval, broadband videotex, video conference, videophone.
- Block-switched (high-speed packet switched) bearer services with carrier bit rates of up to 140 Mb/s: the carrier channel can accommodate numerous (e.g. 100) virtual circuits here

with an effective bit rate per virtual circuit of up to 10 Mb/s, increasing later to 100 Mb/s. Possible applications here are the flexible interconnection of LANs or PABXs or data applications e.g. communication from stations with a high-definition screen.

In addition to these broadband services, the BB-ISDN must of course also include ISDN narrowband services.

3. The User Access to the Broadband ISDN

A new broadband user interface is necessary for the broadband services. International standardization is tending towards a broadband universal interface S_B, offering approx. 150 Mb/s in each transmission direction.

This transmission capacity can, for example, be broken down into the following channels by using synchronous multiplexing: in addition to the channels which have already been standardized for the ISDN basic access (2 x B + D: with B = 64-kb/s channel and D = signaling channel), a 140-Mb/s channel will be offered, which can be subdivided into 4 channels of approx. 34 Mb/s each or 3 channels of approx. 45 Mb/s each. The channels with 140, 34 or 45 Mb/s can be circuit switched or block switched.

All signaling (information exchange between user and network when the network facilities are being requested) takes place over the D channel. In the case of TV-program distribution with 140 Mb/s per program, additional 140-Mb/s channels will be necessary from the network to the subscriber, made available to the subscriber in a suitable manner: if the TV programs are switched, 3 additional 140-Mb/s channels suffice; if all TV programs are transmitted en bloc to the user, considerably more additional 140-Mb/s channels will be required (e.g. 32).

The glass fibers providing the subscriber connection are fed to the first switching system in a star configuration.

4. Demands on the Switching System

The channels offered at the user/network interface are multiplexed with suitable equipment for transmission over the subscriber line and fed to the appropriate switching networks in the switching system. The signaling information is fed within the switching system to the connection control equipment.

In order to avoid cost-intensive conversions between optical and electrical signals, multiplexing should also be carried out optically when optical switching systems are used; wavelength multiplexing and, if necessary, synchronous time division multiplexing are possibilities here; in the case of TV channels distributed en bloc, multiplexing can be performed with the aid

of optical carriers very close together and reception with the aid of heterodyning.

In the care of public switching systems, the attenuation of the subscriber lines, the switching networks and the internal switching-system links, necessitates amplification and, when distortion, jitter and crosstalk are present, also often requires regeneration of the digital signals. Optical amplification and regeneration is therefore crucial for the widespread application of optical switching systems in public networks.

From a functional point of view the following types of switching networks can be distinguished: circuit-switching networks for B channels and for 34-, 45- and 140-Mb/s channels, and switching networks for block and packet switching. Some of these switching networks can, if necessary, be realized as one physical switching network, e.g. a synchronous broadband TDM switching network could circuit switch 34- and 140-Mb/s connections or 45- and 140-Mb/s connections; another example is the theoretically possible provision of circuit-switched connections for different bit rates via a block-switching network. The switching principles -circuit-, block- and packet switching -, in this order, represent an increase in the information-processing requirement for forwarding user information.

Optical switches will be of particular interest for high bit rates and, initially, for small circuit-switching networks; block- and packet-switched connections and circuit switched connections with lower bit rates can, at first, be offered via electronic facilities. Further development of optical signal processing could lead in the long term to block switching being realized also by optical means. Regarding public switching systems, special consideration must be given to stringent requirements concerning low volume, low power dissipation, lifetime and performance. In the case of performance, requirements must be met even when the behavior of some users is incorrect.

5. Summary

The great advances made in the field of optical transmission are the prerequisites for economic realization of a broadband ISDN even if, initially, the switches are operated electronically. Optical switching systems will at first be more suitable for small systems with lower requirements than those required for large public switching systems: examples are protection switching facilities in transmission systems, remote units, small PABX's. The promising beginnings discernable in the areas of optical amplification, coherent transmission, optical switching and optical computing can, if appropriate development continues, be expected to give further, effective impulse to innovation in communications engineering.

OPTICAL BROADBAND COMMUNICATIONS NETWORK ARCHITECTURE UTILIZING WAVELENGTH-DIVISION SWITCHING TECHNOLOGIES

Syuji SUZUKI and Kunio NAGASHIMA

C&C Systems Research Laboratories
NEC Corporation, 4-1-1 Miyazaki, Miyamae-ku, Kawasaki, 213, Japan

1. Introduction

Substantial needs for broadband communications networks have been increasing with the advent of new technology and growing interest in visual information services. Optical switching systems and optical-fiber transmission systems will be indispensable to realize future broadband communications networks. In particular, wavelength-division (WD) switching system and wavelength-division multiplexed (WDM) transmission systems, making full use of extremely high optical carrier frequencies and enjoying widely ranging bit-rate independency for individual channels, have potential capability for extension to wide-area broadband networks. This paper proposes optical broadband network architecture using WD switching systems and WDM transmission systems.

2. Design principle in WD channel arrangement

Large line-capacity optical switching system realization will be difficult without the introduction of optical itegrated circuits. InP semiconductor materials are expected to be most suitable for the optical integrated circuits, because they allow the integration of optical active elements and the emission spectra for InGaAsP/Inp active layers lie in a low-loss region of silica fibers. In InP variable wavelength filters, their wavelength tuning ranges are generally controlled by their refraction indexes. One-percent refraction index control possibility in InP materials has been reported using the free-carrier plasma effect[1] or the nonlinear optical properties in multiple quantum well (MQW) structures[2]. Hence, the 150Å tuning range, in case of the 1.5μm region, in the variable wavelength filter is expected to be realized. Recently, WD channel spacing narrower than 1Å has been estimated, using distributed feedback InP filters [3]. Therefore, optical switching systems, based on the InP optical integrated circuits, will be able to handle more than 100-WD channels with 150Å tuning range.

The most serious difficulty in realizing such narrow channel spacing is wavelength drift caused by temperature variation in light sources. The drift rate is as large as about 1Å/°C in InP matrials. The introduction of wavelength network synchronization is proposed to solve this problem. On the analogy of the clock synchronization in the conventional time-division digital networks, subject, mutual and independent synchronization can be utilized in the WD communications network. Figure 1 shows a basic model of a subject synchronized WD communications network as an example. A wavelength reference light source, whose output wavelengths are stabilized, is mounted in the network and internal channel wavelengths in all WD switching systems are

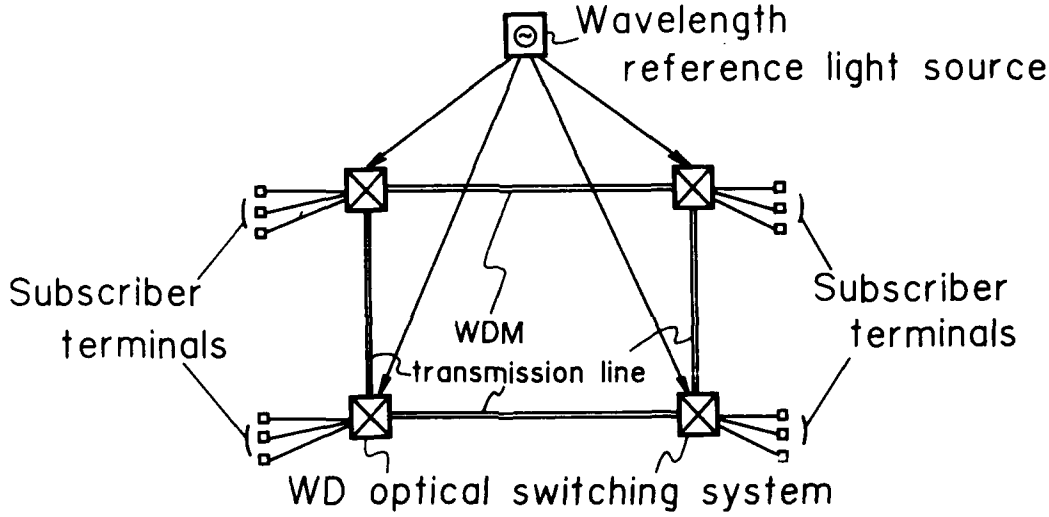

Fig. 1. Wavelength synchronized optical communications network

synchronized to the reference light supplied from the light source. As a result, individual channel wavelengths in all optical switching systems can be locked to the same value. Hence, an individual WD switching operation can be free from wavelength drift.

3. Wavelength synchronized WD switching system

In this section, a new wavelength switch (λ switch), based on a variable wavelength filter and an optically controlled madulator, is first proposed and then its expandability is discussed. Figure 2 shows the proposed λ switch, where an input WDM signal is split and parts are led to individual variable wavelength filters, each of which extracts a specific wavelength signal from the input signal. The output optical signal from the variable wavelength filter is then applied to an optically controlled modulator and is intensity-modulated onto a preassigned-wavelength light carrier, which is extracted from the wavelength reference light by a fixed wavelength filter. Through

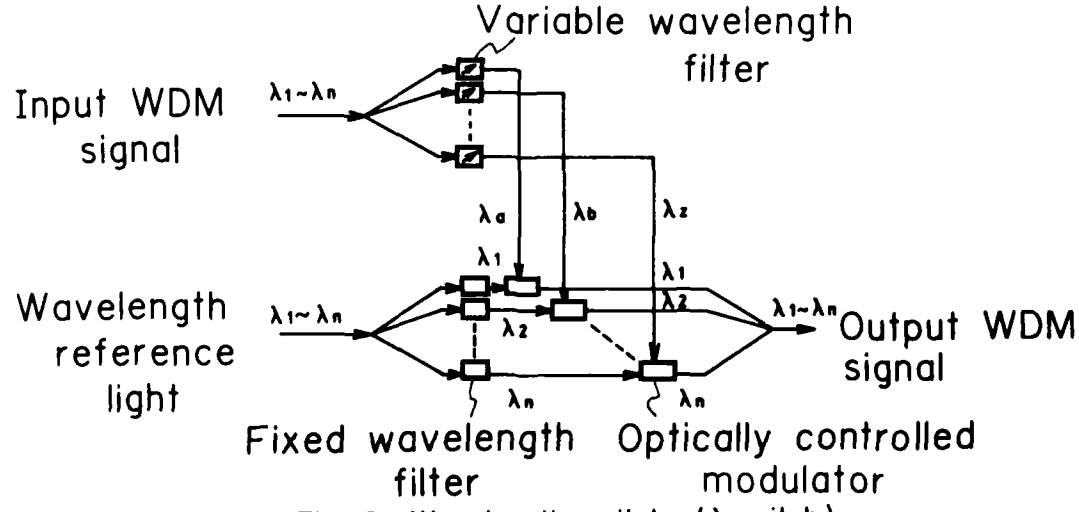

Fig. 2. Wavelength switch (λ switch)

this process, the input wavelengths λa, λb, ... , λz, in Fig. 2, are converted into wavelengths λ1, λ2, ... , λn, respectively, without loss of intensity modulated information, which results in wavelength interchanging. Moreover, wavelength synchronization has also been realized, because the λ switch output wavelengths are accurately the same as the reference light wavelengths. Optical amplifiers, such as laser diode amplifiers or optical fiber Raman amplifiers, will be used to compensate for WDM signal and reference light attenuations, both in the WD switching systems and in the WDM transmission lines. The optically controlled modulator will be realized using optical nonlinear devices such as an MQW etalon [4]. The realization of the monolithic integrated λ switch in a single InP chip is most desirable.

Multi-stage switching networks are necessary to construct large-capacity switching systems. A new λ^n switching network is proposed for this purpose. As shown in Fig. 3, wavelength multiplexers (WMUX) and demultiplexers (WDMUX) are mounted in inter-stage connections. Between individual WDMUX output ports and individual WMUX input ports, an optical path is provided, thereby giving each λ switch potential connectivity to every next-stage λ switch. The λ^n switching network can provide more than ten thousand line capacity, using λ switches having a few hundred WD channels.

4. Conclusion

Optical broadband network architecture, using WD switching systems based on InP optical integrated circuits, was proposed. The wavelength network synchronization introduction will enable the network to utilize a large number of WD channels without the wavelength drift. The new wavelength synchronized WD switching system, using the λ switch and the λ^n switching network, will provide large line capacity and play an important role in partnership with the WDM transmission systems in the future broadband wide-area networks.

References

(1) K.Kishino et al., IEEE J, QE-18, p343, 1982
(2) H.Yamamoto et al., Elec. Let., vol.21, No.13, p579, 1985
(3) R.C.Alferness et al., Appl. Phys. Let., 49(3),pl25, 1986
(4) J.L.Jewell et al., Appl. Phys. Let., 46(10), p918, 1985

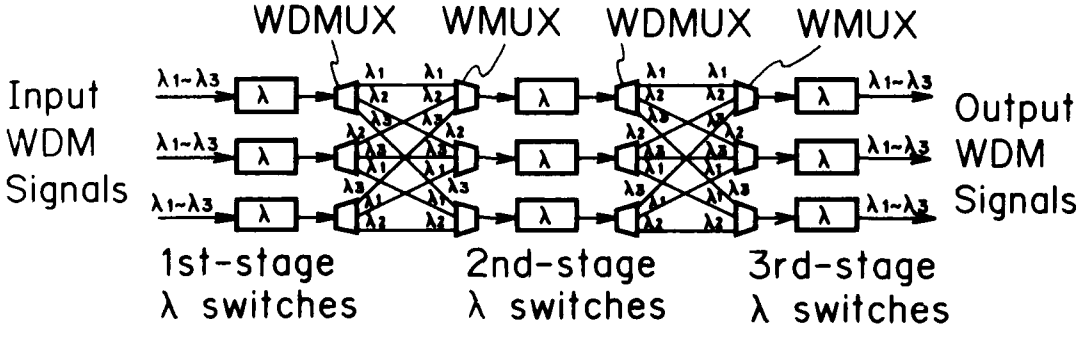

Fig. 3. λ^3 switching network

Photonic Switching and Automatic Cross-Connect Systems

Jonathan A. Nagel

AT&T Bell Laboratories
Crawford Hill Laboratory
Holmdel, New Jersey 07733

Introduction

There will be an explosion of digital facilities as more and more lightwave systems are installed in the next few years. The size and complexity of junction offices where transmission facilities are interconnected will increase, and rearrangements will be more frequent than in the past. Because of these factors, wideband digital switches will replace manual cross-connects at junctions.

In this paper, we will discuss the new generation of wideband switches. These switches may offer the best opportunity to use optical switching technology for commercial products. However, major breakthroughs will be needed before photonic switching can practically compete with electronics. Progress is being made in optical switching, but advances in VLSI technology seem to be keeping pace. There are existing or planned electronic digital cross-connect switches at bit rates up to 140 Mb/s.

Automatic Cross-Connect Systems

Digital facilities are interconnected at junctions through manual cross-connect frames. These consist of jack panels with built-in bridging so that traffic can be manually reconfigured, tested, or rolled with no loss of service. An Automatic Cross-Connect System (ACS) is a digital switch that will replace manual cross-connects, and will allow rearrangements, testing, and cross-connects to be done automatically under local or centralized remote control.

An ACS differs from a voice circuit switch in signal bandwidth, connection holding time, and deployment in the network. The ACS will cross-connect digital signals at rates ranging from 64 kb/s to wideband signals of 45 Mb/s and above. Voice circuit switches cross-connect 64 kb/s circuits for dialed telephone calls. An ACS connection may last from minutes to years, while a voice circuit connection is usually a few minutes long and seldom lasts for more than a few hours. Finally, voice circuit switches are physically located at terminal offices, and ACS switches will be at facility junctions.

There are existing products that cross-connect 64 kb/s (DS0) circuits, and there will be products that cross-connect at the 1.5 Mb/s (DS1), 45 Mb/s (DS3), and 140 Mb/s rates. A digital cross-connect system includes multiplexing if the external interface is at a faster bit rate than the switched signals. Examples are the DACS 1/0™ that interfaces at the DS1 level and switches DS0's, and planned products that interface at the standard DS3 level and switch DS1 signals. Requirements have also been written for a Digital Cross-Connect System (DCS 3/X) that interfaces at a synchronous DS3 rate and cross-connects DS1, DS0, and 384 kb/s signals.* Applications that include multiplexing are less likely to be near term candidates for photonic switching, because optical signal processing would be required.

---

* Synchronous DS3 Digital Cross-Connect System (DCS 3/X) Generic Requirements, Bellcore Technical Advisory TA-TSY-000233.

Cross-Connect Operations

A remotely controlled digital cross-connect switch with either electronic or photonic technology would have the same tasks that are now done by hand at jack panels. Examples of operations at a wideband digital cross-connect switch are:

- Facility Grooming - Transmission systems carry traffic in multiplexed bundles. When traffic is added or dropped at different points along the route, demultiplexing and multiplexing is necessary to keep line fill high. Grooming is probably the most important function of any level cross-connect.
- Restoration - Cable cuts or other failures of lightwave routes can result in massive service outages. A wideband switch could be used to quickly re-route priority traffic.
- Facility Protection - An equipment failure can lead to partial outage along a route. Many transmission systems have automatic protection switching for this eventuality, and a wideband switch could take over this function.
- Facility and Service Provisioning - Broadband connections are established through the network by cross-connecting different transmission systems. Wideband switches will be used to test and cross-connect links remotely.
- Testing and Performance Monitoring - Broadband circuits are monitored at cross-connect points, without interrupting service, by bridging signals into a common test set.
- Customer Control - For customers who lease private networks, automatic cross-connects represent an opportunity to do their own rearrangements. Security precautions would prevent customers from controlling the public network.

General ACS Requirements

Switching time requirements for automatic cross-connects are not well defined, because of the wide variation in possible applications. However the time between disconnect and connect should be less than 50 ms to avoid dropping voice circuit calls. Other considerations may call for faster switching times.

In the next 5 years, DS3 cross-connects will grow enormously, so that there will be many offices with 1000-2000 DS3 switch terminations. Even larger cross-connects will be needed if broadband digital services become popular. However, the required size of DS3 switches would be reduced if a higher cross-connect level were introduced.

It should be possible to bridge cross-connected signals to any other port, mostly for test access. This feature would also be used when rolling circuits, bridging onto the head end of a link and switching the tail end to minimize disconnect time.

Reliability is an important issue for automatic cross-connects, because the failure of a large wideband switch could knock out much of the traffic in a network with no chance for restoration. Equipment failures should be protected, and outage time minimized. Circuit performance objectives will determine how much noise and crosstalk in the switch can be tolerated.

The sum of equipment and operating costs of any ACS switch should be less than those for an equivalent manual cross-connect system. Operating cost savings are hard to estimate, but equipment costs of manual cross-connect systems can set a scale for wideband switch costs. For example, the installed equipment cost of a manual DS1 level cross-connect including multiplexing and demultiplexing from the DS3 level is $10-$20 per equivalent voice-circuit termination. Therefore an ACS that interfaces at DS3 and cross-connects DS1's should be priced in this range.

Multiplexing is a large part of the cost of a manual cross-connect system, so that the target cost of a non-multiplexing wideband switch is low. For example, the cost of a DS3 manual cross-

connect is only about $1 per equivalent voice-circuit termination, setting a scale for ACS systems that cross-connect and interface at the DS3 level.

Photonic Switching and the ACS

A variety of devices and architectures have been proposed for optical switches. For example, arrays of Lithium Niobate directional couplers have been built into NXN electronically controlled optical switches. There are many problems with this kind of switch. The polarization of all the optical signals must be well controlled, so that polarization maintaining fibers and connectors must be used, and regeneration may be necessary. When a coupler is left in one state for a time, as could be the case in an ACS switch, the optical power drifts from one port to another because of slow charge accumulation at the electrodes. To remedy this situation, the voltage across the electrodes must be continuously adjusted. In a large array the voltages on each individual device must be separately controlled. There are also difficulties with crosstalk and losses in large arrays due to polarization and photorefractive effects. Finally, the large scale integrability of these devices has not been demonstrated.

These problems can be solved, but in the meantime electronic switches are being designed for most levels of digital cross-connects. The increasing reliability and lower costs of VLSI technology will favor electronic switches, as will applications that include multiplexing. Optical switching will be practical when growth in broadband services leads to larger cross-connects with vastly increased traffic and faster switching speeds, stretching semiconductor technology to the limits. The establishment of standard cross-connect rates of over 400 Mb/s, or of optical interface standards such as SONET should give impetus to photonic switch development. A photonic switch will only be used in a particular application when it can compete on a cost basis with an electronic switch having the same features. Progress in photonics is being made, but major breakthroughs will be required.

There are ACS applications for optical switches at high bit rates that do not involve multiplexing. For example, an optical switch could be used for equipment protection switching, operating at the line rate of 1.7 Gb/s or higher. No multiplexing would be needed since the line interface and switch rate would be the same. The switch would not need to be large since there are usually less than 50 fiber pairs on a single route. A line rate optical switch could also be used for route restoration, although reroute traffic around the network in such large bundles would be awkward.

Conclusion

Optical switching and signal processing technology are still in the research stage, while electronic wideband switches are being planned for all levels of digital cross-connects in the network. Increasing traffic in the future may require cross-connects at speeds not easily attainable by electronics, and thus provide an opportunity for optical switches. Such a switch will have requirements and cost targets that are similar to currently planned wideband digital switches for cross-connect applications.

Optical Switching in Coherent Lightwave Systems

M.FUJIWARA, *S.SUZUKI, K.EMURA, M.KONDO, K.MANOME
I.MITO, K.KAEDE M.SHIKADA and M.SAKAGUCHI

Opto-Electronics Res.Labs. *C&C Systems Res. Labs.
NEC Corporation
4-1-1 Miyazaki, Miyamae-ku, Kawasaki 213, Japan

Introduction

Broad-band networks providing various kinds of services, such as video and high speed data communications, have received increasing attention in not only local-area networks(LANs) but also wide-area networks(WANs). Recent progress in optical fiber transmission has already made worldwide point-to-point transmission links possible. Coherent lightwave technology would further make evolution in transmission length and information capacity. Optical switch would be a key technology for achieving all optical broad-band WANs, where switching and routing functions will be accomplished in optical domain as well as transmission. A possible architecture of global WAN is illustrated in fig.1. Optical communication utilizing both inland and under-sea optical fiber transmissions, together with satellite communication, will play an important role in broad-band global WANs. With these networks, broad-band communication/ distribution services will be offered to all over the globe.

This paper presents a study on integration of optical switching and coherent lightwave technology, which would be important for achieving broad-band WANs. Some experimental results with a LiNbO3 optical switch and an optical FSK heterodyne transmission system are reported.

Optical switching in coherent lightwave systems

There are three possible types of optical switching: time-division(TD), space-division(SD) and wavelength-division(WD) switching.(1) Since various different demands are placed on the broad-band services, networks are desired to be transparent both in terms of band-width capability and modulation format. SD and WD switchings could easily construct transparent networks while TD would require rigid data formatting and syncronization. Furthermore, SD and WD switchings are fit to coherent lightwave systems, where information of wavelength is essential. Specifically, SD switching using optical switch matrices, such as a LiNbO3 guided-wave type(2), is suitable for coherent systems because it is able to preserve every information the input optical signals have.

Since SD switching seems to be practical from the today's technological stand point, SD optical switching networks would be put in practical use with direct detection system at first. Introduction of coherent detection technology to these SD optical switching networks will remove the constraints of number of subscriber lines and distance. The number of subscriber lines are restricted by both insertion loss and optical crosstalk value of optical switch matrices.(3) Increased span loss margin with coherent detection allows more cascaded connections in optical

switch matrices. In addition, optical crosstalk can be rejected at the receiver end by introducing distinct emitting wavelengthes to each subscriber. The increased span loss margin also can be allotted to transmission line loss. In that case, networks which are located at a long distance would be directly linked to each other. Moreover, the optical switching networks where each subscriber has its own emitting wavelength would easily be integrated in future WDM networks where both SD and WD optical switchings and dense coherent WDM transmission would be utilized.

Experiments

In order to demonstrate the advantages described above, SD optical switching experiments have been carried out using a LiNbO3 switch and an optical FSK heterodyne transmission system.(4) The experimental set-up is shown in fig.2. Two transmission terminals and one receiver terminal are connected via transmission fibers and a switch. Two 1.55 μm wavelength flat FM response phase tunable DFB-DC PBH LDs were used as FSK transmitter light sources (LD1,LD2;optical carrier frequency f1, f2). At the receiver terminal, a balanced receiver and a dual filter detection system were employed. Each transmitted signal was a 100Mb/s FSK signal with frequency deviation of 800 MHz.

Receiver sensitivity as high as -55dBm(BER=10^{-9}), which is 8.5 dB higher than direct detection, was obtained for each transmitter. The interchannel interference characteristics were measured with LD1 and LD2 being driven simultaneously. Figure 3(a) shows power penalty change with channel separation Δf(=f2-f1) which was monitored in IF signals (fig.3(b)). The parameter in fig.3(a) is optical crosstalk value(CT) at the entrance of the receiver. In the case of 0dB CT, two channel signals reached the reciever with equal optical power. In the case of Δf being above 2GHz, no interference effect was observed even if CT is 0dB. With 2GHz wavelength spacing, more than 10^4 emitting wavelengthes can be assigned to subscribers within the 1.3-1.55μm low loss window. This result clearly shows that constraint in number of subscriber lines caused by optical crosstalk can be neglected in a SD switching network with coherent detection. Span loss margin exceeded 60dB in this system. A SD optical switching network containing 500 subscribers can be constructed with 7 stage cascaded connection of 8x8 LiNbO3 switch matrices.(3) Therefore a 500-line SD optical switching network and 100km transmission would be possible in this system assuming 4dB switch insertion loss and 0.25dB/km fiber loss.

Conclusion

Integration of optical switching and coherent lightwave technology was considered. Switching experiments using a LiNbO3 optical switch and a FSK heterodyne transmission system was carried out. SD switching networks with coherent technology would be important sub-systems in future large scale WDM networks.

References

(1) M.Sakaguchi and H.Goto, First Optoelctronics Conference (OEC'86) technical digest,d9-3,pp.192(1986)
(2) M.Kondoet al., Technical digest of 5th IOOC and11th ECOC

vol.1, pp.361(1985)
(3) S.Suzuki et al., Natl. Conv. IECE Japan,pp.133(1986)
(4) K.Emura et al., to be published in Electron.Lett.

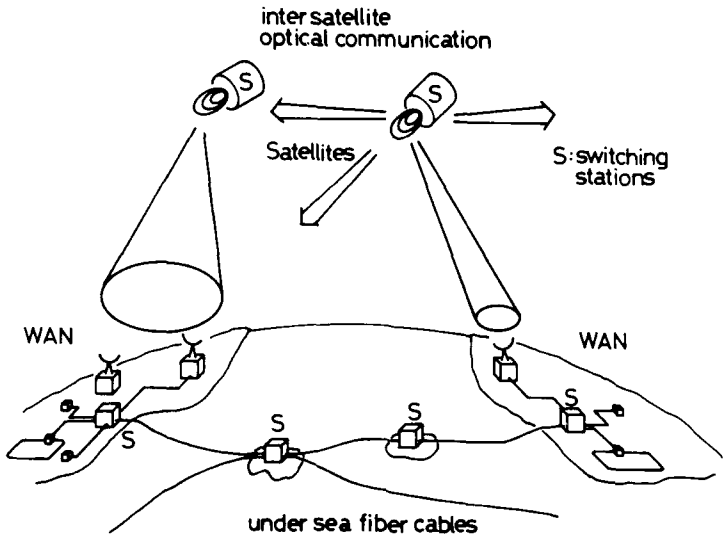

Fig.1 Architecture of global wide-area networks(WANs).

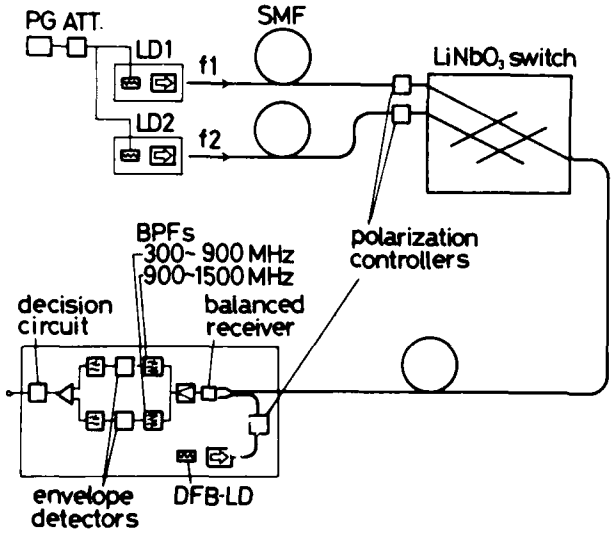

Fig.2 Set-up for SD switching experiments in FSK transmission system.

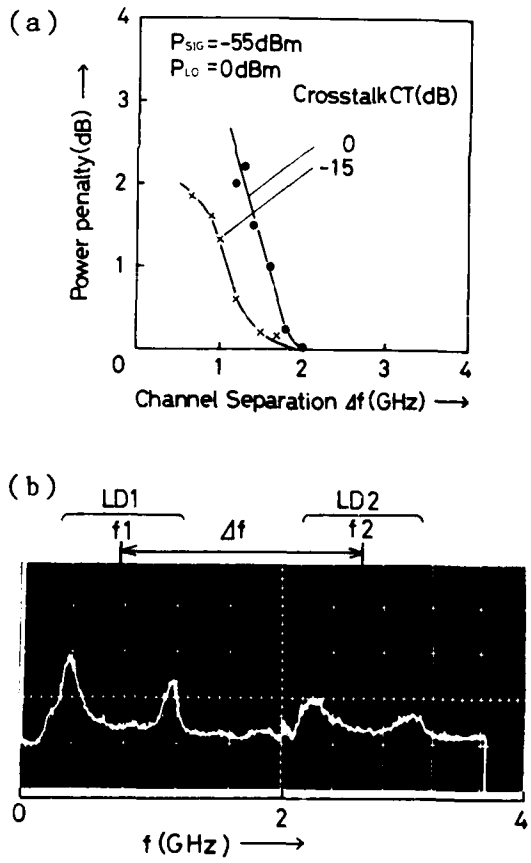

Fig.3 Interchannel interference characteristics(a) and IF spectrum(b).

A Photonic Switching Demonstration Display

J. R. Erickson
C.G. Hseih
R.F. Huisman
M.L. Larson
J.V. Tokar
AT&T Bell Laboratories
Naperville-Wheaton Rd.
Naperville, IL 60566

G.A. Bogert
E.J. Murphy
AT&T Bell Laboratories
555 Union Boulevard
Allentown, PA 18103

R.T. Ku
AT&T Bell Laboratories
2525 No. 12th Street
Reading, PA 19603

1. INTRODUCTION

As fiber optic communication proliferates, it becomes important to explore the possibilities of photonic switching. As a near-term photonic switching technology, titanium-diffused lithium niobate ($Ti:LiNbO_3$) needs to be evaluated by its use in experimental systems. In this display, a $Ti:LiNbO_3$ array switches video from cameras to monitors.

We will first give a system overview and trace a signal through the system. Next, the photonic switch will be explained, followed by a description of the electronics.

2. SYSTEM OVERVIEW

This experimental switch operates as a photonic cross connect: a reconfiguring space switch. Figure 1 shows the experimental system; the photonic switch is in the center, surrounded by electronics that control the photonic switch and by video equipment that generates and receives data. In Figure 1, each camera creates analog video which is digitized and fed to a laser transmitter. The transmitter launches the data into a fiber that connects to the photonic switch, where the optical bit stream is routed to any one of four outputs. After leaving the switch, the optical pulses are reconverted into analog video that enters the monitors.

3. PHOTONIC SWITCH

In building a photonic switching system, a host of tradeoffs confront the device and system designers. We mention some of the tradeoffs made in building this demonstration.

3.1 Architecture

The switch in our display uses 16 directional couplers to make a 4x4 crossbar architecture (see the center of Figure 1). The crossbar is non-blocking in the wide sense, any idle input will have a path to any idle output as long as a connections are set up according to a specific algorithm[1]. Although architectures exist that have better SNR than the crossbar[2] [3], the crossbar performs well for the number of couplers employed, and since the crossbar is a planar architecture, no noise is introduced by crossing waveguides[4].

3.2 Polarization

This demonstration uses single-polarization directional couplers and polarization-maintaining (PM) fiber from the lasers to the switch. The fiber end on the laser side is lensed to increase the power coupled into the PM fiber and the fiber is attached to the photonic switch using rectangular silicon grooves[5] [6].

3.3 Electrodes

To enable tuning both cross and bar states, the demonstration switch uses two-segment reverse $\Delta\beta$ electrodes and therefore requires 32 electronic drivers, two for each coupler[7].

3.4 Performance

This crossbar photonic switch has been refined several times, each showing an improvement over the previous generation [5]. Figures 2 and 3 summarize the improvements. Each box represents the set of 16 couplers for one switch. The box center line is the median with the upper and lower sections representing the upper and lower quartiles of the data. The box whiskers extend to the farthest data points. In Figure 2, for example, the median switching efficiency for the 16 couplers of switch 3 is ~27 dB; the upper quartile extends to ~31 dB and the lower quartile to ~22 dB, with all coupler switching efficiencies above 17 dB and less than 37 dB. All these data were taken with fiber attached to the switch, and are practical system measurements, not measurements taken under controlled laboratory conditions before fibers were attached[5]. Since the third and fourth switches have reverse $\Delta\beta$ electrodes, and therefore two voltages for each state of each coupler, we average the two electrode voltages before comparing them to previous switches. Switches 3 and 4 were made from the same mask and similar processing. Switch 3 is the switch used in the display and has run reliably for nine months. From these data we see that the best-case and worst-case switching efficiencies improved (from switch 1 to switch 3) and that the switching-efficiency medians are several dB better in the later switches (see Figure 2). The bar state voltages decrease in later iterations, easing the high-voltage requirement on the drive electronics and increasing the potential switching speed (see Figure 3). From Figure 3 we see that switches 2, 3 and 4 have much more tightly clustered voltages and approach the goal of uniformity across the array.

4. ELECTRONICS

A microcomputer controls the display; it accepts connection requests, decides which couplers must change state, and generates a bit pattern, two bits for every coupler. The observer sees the pattern of existing connections by a graphic representation on the microcomputer screen. Observers listen to instructions and touch-in connection requests at a remote telephone that connects to a voice synthesizer and tone decoder inside the microcomputer. Alternatively, the demonstration can cycle connections autonomously. Cameras and monitors used in the display are NTSC commercial units.

The lightwave transmitters and receivers are generally used back-to-back as lightwave repeaters, but in this application, the transmitters turn 90 Mb/s electronic data into light pulses that enter the photonic switch. On the output of the switch, the receivers sense the pulses, recover the clock, and reconstruct the electronic data stream. Serial-to-parallel and parallel-to-serial conversions are designed in ECL logic, and the photonic switch drivers are operational amplifiers.

5. ACKNOWLEDGEMENTS

We thank G.H. Zimmerman, H.S. Hinton, and F.T. Stone for their administrative support. We acknowledge the contributions of M. Dautartas, R.J. Holmes, and Y.S. Kim for *Ti:LiNbO*$_3$ process development. B.C. Roe and W.C. Bourland designed the drive electronics and ECL hardware. D.M. Armin helped assemble the electronics.

REFERENCES

1. V.E. Benes, *Mathematical Theory of Connecting Networks* and *Telephone Traffic*, New York, Academic Press, 1965, pp. 77-9.

2. R.A. Spanke, "Architectures for Large Nonblocking Optical Space Switches," *IEEE Journal of Quantum Electronics*, Vol. QE-22, No. 6, June 1986, p. 964.

3. M. Kondo et al., "32 Switch-Elements Integrated Low-Crosstalk *LiNbO*$_3$ 4x4 Optical Matrix Switch," IOOC-ECOC '85, Venice, Italy.

4. H.S. Hinton, "A Nonblocking Optical Interconnection Network Using Directional Couplers," *IEEE GLOBECOM*, Nov. 26-9, 1984, 26.6, pp. 885-90.

5. G.A. Bogert, E.J. Murphy, and R.T. Ku, "A Low Crosstalk 4x4 *Ti:LiNbO*$_3$ Optical Switch with Permanently Attached Polarization-Maintaining Fiber Arrays," *IGWO* '86, PDP3, Feb. 27, 1986, Atlanta, GA.

6. E.J. Murphy et al., "Self-Oriented Arrays of Polarization Maintaining Fiber," *OFC '86*, PDP2, Feb. 25, 1986, Atlanta, GA.

7. H. Kogelnik and R.V. Schmidt, "Switched Directional Couplers with Alternating $\Delta\beta$," *IEEE Journal of Quantum Electronics*, Vol. 18, pp. 4012-6, 1979

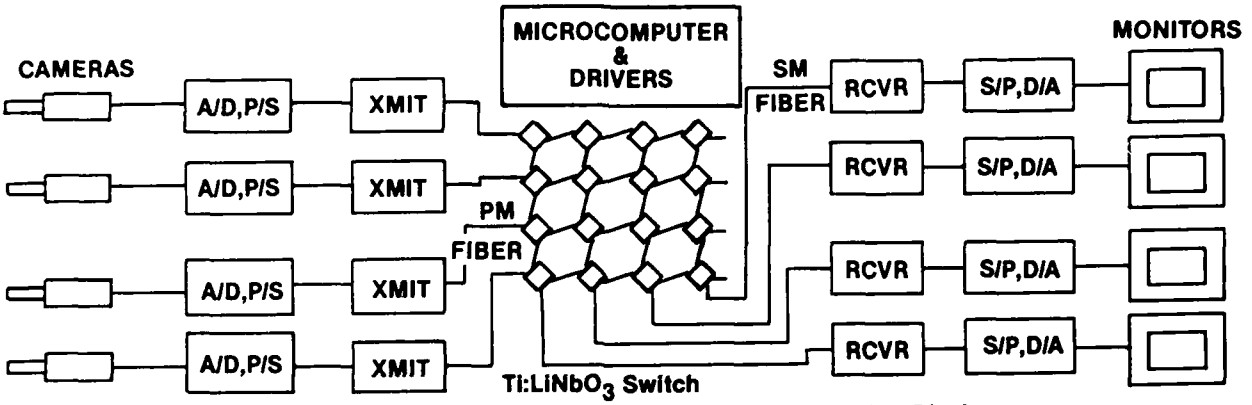

FIGURE 1 - A 4×4 Photonic Switching Demonstration Display

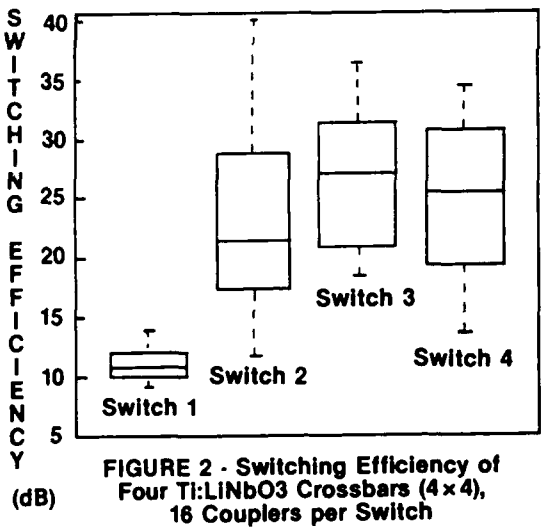

FIGURE 2 - Switching Efficiency of Four Ti:LiNbO3 Crossbars (4×4), 16 Couplers per Switch

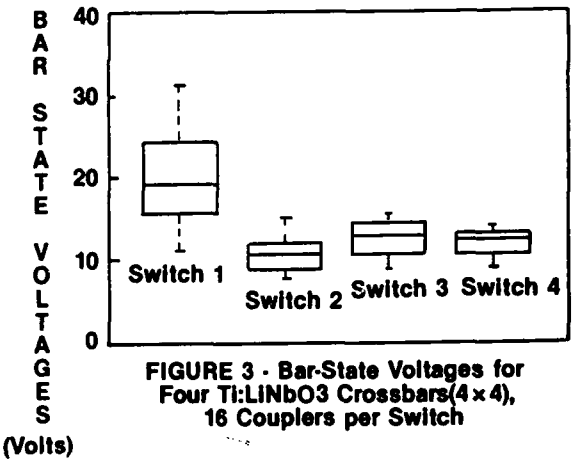

FIGURE 3 - Bar-State Voltages for Four Ti:LiNbO3 Crossbars(4×4), 16 Couplers per Switch

THURSDAY, MARCH 19, 1987

PROSPECTOR/RUBICON ROOM

10:30 AM–12:00 M

ThB1–4

SWITCHING ARCHITECTURES

Alan R. Tedesco, Bell Communications Research Inc., *Presider*

INTRODUCTION TO SWITCHING NETWORKS

Václav E. Beneš
AT&T Bell Laboratories
Murray Hill, NJ 07974

ABSTRACT

We present a broad tutorial description of connecting network concepts and structures, divided into three categories: combinatorial, probabilistic, and operational, each with suitable examples.

Among the combinatorial aspects we single out the semi-lattice of network states, notions of mismatch and overflow, group theory applications such as the reduction of states by symmetries, construction of nonblocking networks, and topological characterization of such network properties as rearrangeability and nonblocking.

The probabilistic ideas we cover are (i) modeling of network operation, (ii) definition of loss (probability of blocking), (iii) load-loss relationships. Finally, such operational issues as good routing choices and time-space swaps and shuffles (time-division and/or packet switching) are touched on.

DETERMINISTIC AND STATISTIC CIRCUIT ASSIGNEMENT ARCHITECTURES FOR OPTICAL SWITCHING SYSTEMS

A. de Bosio , C. De Bernardi, F. Melindo
CSELT - Centro Studi e Laboratori Telecomunicazioni, 10148 Turin Italy

The size of an optical switching network based on 2x2 optical switching elements, is limited by a series of factors: the relatively small phisical size of the substrate (no more than 100x75 mm for $LiNbO_3$), the phisical size, loss and crosstalk of the switching element, the loss introduced by the fiber-substrate coupling and the large radii (more than 1 cm) imposed to the waveguide to keep bend loss around few hundredths of dB/degree.

These limitations make it quite difficult to realize on a $LiNbO_3$ substrate a switching network, topologically organized as an N dimension array, with N greater than 10-16, if directional couplers are utilized as switching elements.

In the absence of efficient optical signal regenerators and optical memories, the improvement of an optical switching component can then be obtained, at least in a first step, by both improving the interconnections and switching element characteristics and minimizing the number of switching elements at a parity of the switching network dimension.

This approach seems particularly appropriated for those architectures, called Deterministic Circuit Assignement Architectures (DCAA), which rely on nonblocking networks operated according to synchronous fast packet switching strategies, for which the problem is to find a fast switch setting algorithm, yet keeping low the number of switching elements.

If on one side the "defects" of the optical switching elements lead to architectures based on non blocking multistage switching networks operated according to FPS schemes, on the other hand their "qualities", that is their wide bandwidth and small switch setting time (few psec), make them well suited for architectures, called Statistic Circuit Assignement Architectures (SCAA), which are based on asynchronous switching strategies and on few switching element networks whose blocking characteristics are compensated by the multiplexing capability of the optical system as a whole.

Table 1 shows some characteristics of four switching networks (numerical values are computed for N=8). The first three belong to the permutation network cathegory and are therefore utilizable for systems based on DCA architectures. The fourth belongs to the single path network cathegory, that is has exactly one pass between every arbitrary input/output pair and therefore is not able to connect its inputs to its outputs in any arbitrary way. This network and even simpler networks are well suited for systems based on SCA architectures.

Among the permutation networks, Benes network has the smallest number of stages, but the best algorithm for switch setting on a single process machine

NAME	E(n)	S(n)	CONTROL	BLOCK
BENES	$2^{n-1}(2n-1)$	2n-1	CONCEN-TRATED	NO (REARR.)
	20	5		
ODD-EVEN MERGE	$(n^2-n+4)2^{n-2}-1$	n(n+1)/2	DISTRIBUTED	NO
	19	6		
BITONIC SORTER	$(n^2+n)2^{n-2}$	n(n+1)/2	DISTRIBUTED	NO
	20	6		
OMEGA (DELTA)	$n\,2^{n-1}$	n	DISTRIBUTED	YES
	12	3		

$N=2^n$: network dimension

E(n) :number of elements

S(n) :number of stages

Numerical values computed with N=8

Tab. 1 - Networks' main features

runs in O(NlogN) time. Odd-even Merge network has a smaller number of elements than Bitonic Sorter (BS) network, but has paths with different lenghts and less regular structure. The BS network shows a good tradeoff between the number of elements and switch setting time because it works as a selfrouting network if any switching element is associated to a comparator for switch setting.

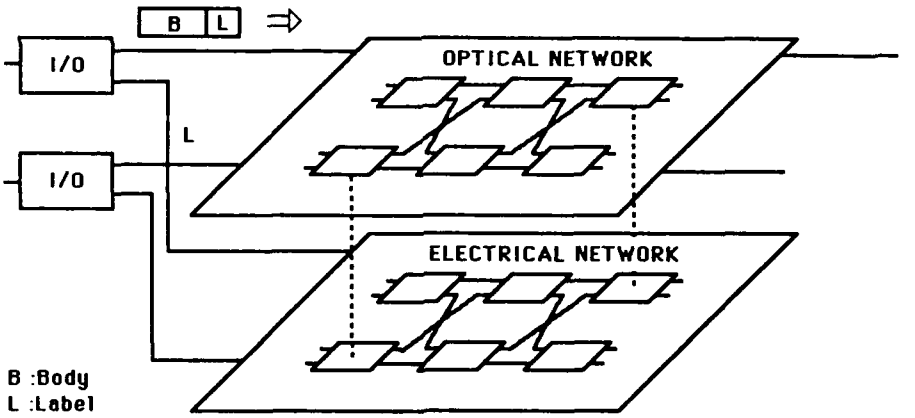

Fig. 1 - Optical switching with selfrouting electrical control

Fig. 1 shows the utilization of a BS network in an optical switching system of a DCA architecture. The input information is transformed in packets of identical size with a label and a body. The labels are sent, at the same time, to an electrical network which is topologically identical to the optical network. The autosetting of each electrical switching element causes the setting of an homologous optical switching element. When the electrical network is completely positioned, the bodies of the packetized information are sent through the optical network.

Fig. 2 shows a model based on a SCA architecture: I1,..,In and O1,..,On are respectively inputs and outputs of a switching network RC;

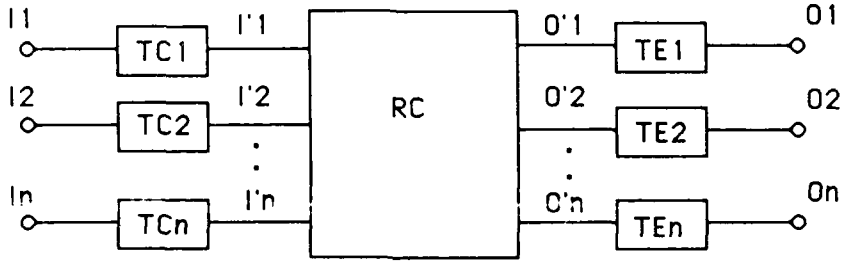

Fig. 2 - Model based on a SCA architecture

TC1,..,TCn are "time compressors" and TE1,..,TEn "time expanders". Each TC receives from an input line bursts of data of variable lenght and interarrival time; data are stored and then sent to RC at a higher bit rate , that is in a shorter time, exploiting the wide band of the optical switching elements; the inverse operation is made by each TE; the path assignement in RC is made when data are ready to be sent from any TC.

As the time compression reduce the data packets collision probability, also blocking networks, like OMEGA or DELTA, characterized by a small number of switching elements and low setting time, can be utilized for such scheme, yet providing end to end protocols for error recovery.

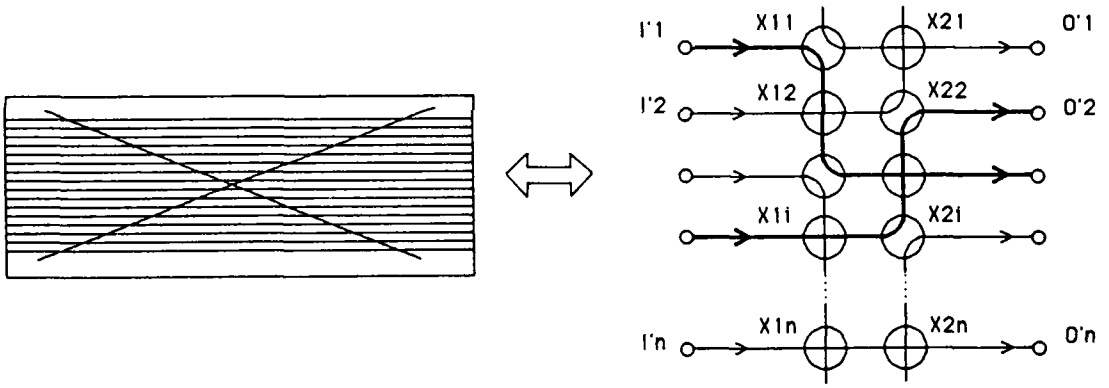

Fig. 3 - Near-neighbour mesh network

Also much simpler networks can be employed, like the ring, the bus, or the near-neighbour mesh (NNM) represented in fig. 3 which is equivalent to a linear array, but provides optical connections both from a high order input to a low order output and viceversa. Estimates made on this structure showed that on a 100x10 mm $LiNbO_3$, a 30 input/output NNM can be implemented using X junctions with a loss of 7.35 dB and a crosstalk of 25dB.

In conclusion, two switching systems based on two different switching architectures have been proposed: they both utilize electro-optical elements also suitable for semiconductor implementation. However, in order to implement electro-optical systems of large dimensions, many problems are still to be solved: among them, the interconnection problem becomes remarkable, especially when logarithmical-growth networks, like those discussed in this paper, are employed.

ThB3-1

Dilated Networks for Photonic Switching

by

Krishnan Padmanabhan
Arun Netravali

AT&T Bell Laboratories
600 Mountain Avenue
Murray Hill, NJ 07974

SUMMARY

Introduction

Wideband optical signals can be switched under electical control using directional couplers between Ti:$LiNbO_3$ waveguides on a planar $LiNbO_3$ crystal [1]. The basic switching element is a directional coupler with two active inputs and two active outputs. Depending on the control voltage at the junction of the two waveguides, either of the two inputs can be coupled to either of the two outputs. Several architectures have been proposed to construct an NxN (N > 2) switch with the 2 x 2 directional coupler as the basic element [2-4]. These architectures are analogs of similar architectures known in electronic switching [5]. However, due to the difference in characteristics of the electronic and optical switching elements, performance and optimization of the optical architectures is significantly different.

For the optical architectures, the performance may be characterized by the following parameters: (a) Optical path loss (worst case), (b) Crosstalk (worst case), and (c) the number of switching elements necessary to implement an NxN switch. Since regeneration is expensive in the optical domain, the largest switch that can be implemented using directional couplers is usually limited by either (a) or (b) above.

In the electronic domain, multistage, rearrangeably non-blocking Clos-Benes [5] networks decrease sharply the number of switch elements from N^2 required for a cross-bar to $\frac{N}{2}$ (2 log N-1). Such multistage networks have (2 log N-1) stages and the same optical path length. If the crosstalk* is assumed to be from the adjacent channel in each of the couplers, the number of directional couplers contributing to the crosstalk for any path is (2 log N-1). It turns out that based on a given budget for the crosstalk, crosstalk limits the size of the switch more than the optical path length [2,3,7]. An architecture called "Active Splitter-Combiner" [3] limits crosstalk substantially at the expense of switching elements which are increased to 2N(N-1).

Dilated Architectures

Our novel architectures, called dilated networks, allow us to reduce the number of switching elements for a given crosstalk budget without significantly changing the optical path length. These are based on the premise that a 1 x 2 splitter (or combiner) is currently implemented using the same device structure as a 2 x 2 directional coupler simply by deactivating one of the inputs. We create dilated networks in which a path connecting an input to an output passes through a controllable number (say K) of couplers which have two active inputs. All the rest of the couplers (2 log N-K) that this path passes through have only one active input and therefore contribute little to the crosstalk.

* Crosstalk due to intersecting waveguides on the substrate is not considered here due to space limitations. See [6].

Although such dilation can be performed on most rearrangeably non-blocking networks [6], we illustrate it on a Benes network shown in Figure 1. In this figure, the first stage of the Benes network is explicitly brought out. It contains N active splitters each with only one active input. This input can be directed to one of the two N x N Benes networks. Using the routing algorithm of the next section, any input can be connected to any output after rearrangement such that no path contains a coupler with two active inputs. However, now the size of the network has increased by almost a factor of two compared to Benes network. The dilated Benes network, has N x (2 log N) elements and an optical path of (2 log N).

The architecture can be improved by trading off the amount of crosstalk with the number of switching elements without changing the optical path length. To illustrate this, consider Fig. 2 in which the first stage now consists on N/2 switches each functioning as 2 x 2 couplers. Keeping the rest of the network the same, we see that any optical path contains only one directional coupler containing two active inputs. The number of devices is reduced by N/2. In general, if K (K < 2 log N) stages contain couplers with two active inputs, then we save KN/2 switches. These K-stages with 2-active couplers have to be placed in the outermost columns of the network.

Routing Algorithm

The routing algorithm is a modified looping algorithm [8]. We first apply looping procedure to the two outer columns (Fig. 1) to set the switches for the desired permutation and then show that the N active paths are directed to the two center subnetworks in such a way that the two outer columns of these two subnetworks have only one active input per switch. This process recurses until subnetworks become 2 x 2 switches. If inputs in Fig. 1 are numbered 1, ..., N then dual $\hat{i}$ of input i is defined as

$$\hat{i} = \begin{cases} i + 1, & \text{if } i \text{ is odd} \\ i - 1, & \text{if otherwise} \end{cases}$$

Let Π be the desired permutation, then follow:

(a) choose a new switch i which has not been connected to either center switch. If all switches are connected, then exit.

(b) $j = i$

(c) connect switch j to center switch 1

(d) connect switch $\hat{j}$ to center switch 2

(e) connect output switch $\Pi(\hat{j})$ to center switch 2

(f) connect output switch $\widehat{\Pi(\hat{j})}$ to center switch 1

(g) If $\Pi^{-1}(\widehat{\Pi(\hat{j})}) = i$, then go to (a), else choose $j = \Pi^{-1}(\widehat{\Pi(\hat{j})})$ and go to (c).

We now show that the two center subnetworks are dilated Benes networks of size N/2. N lines of either of these subnetworks go to (N/2) 2 x 2 switches inside the network. At any such switch, the two input lines come from two dual switches in the outer stages of Fig. 1. The above looping algorithm guarantees that only one of the latter switches sends its input to a subnetwork. Thus every 2 x 2 switch in the input stage of a subnetwork has only one active input. Since the subnetworks are recursively constructed, this condition ensures that they are dilated Benes networks of size N/2.

Conclusions

We have derived dilated architectures to reduce the crosstalk without significant increase in the number of switching elements or optical path lengths. Although not shown here due to space limitation, these architectures require the smallest number of elements for a given crosstalk from couplers [6].

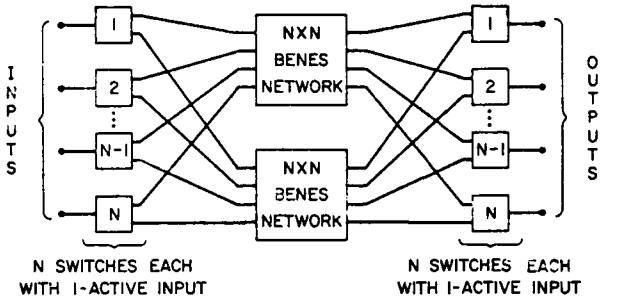

FIGURE 1. DILATED BENES NETWORK.

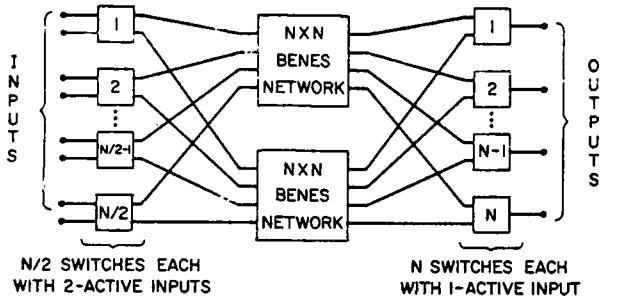

FIGURE 2. DILATED BENES NETWORK WITH FIRST STAGE CONTAINING 2X2 COUPLERS.

References

(1) R. C. Alferness, "Guided-wave devices for Optical Communication", IEEE Journal of Quantum Electronics, QE-17, pp. 946-957.

(2) H. S. Hinton, "A Non-blocking Optical Interconnection Network Using Directional Couplers", IEEE Global Telecommunications Conference, Nov. 1984.

(3) R. A. Spanke, "Architectures for Large Non-blocking Optical Space Switches", IEEE Journal of Quantum Electronics, vol. QE-22, 1986, pp. 964-977.

(4) P. Granestrad, et.al., "Strictly Non-blocking 8 x 8 Integrated-Optic Switch Matrix in Ti:$LiNbO_3$", IGWO'86, 1986 pp.26-28

(5) G. Broomell and J. R. Heath, "Classification Categories and Historical Development of Circuit Switching Technologies", Computing Surveys, vol. 15, 1983, pp. 95-133.

(6) K. Padmanabhan and A. N. Netravali, "Dilated Rearrangeable Networks for Photonic Switching" (to appear).

(7) G. A. Bogert, E. J. Murphy and R. T. Ku, "A Low Crosstalk 4 x 4 Ti:$LiNbO_3$ Optical Switch with Permanently Attached Polarization-Maintaining Fiber Arrays", IGWO'86, pp. 348-356.

(8) D. C. Opferman and N. T. Tsao-Wu, "On a Class of Rearrangeable Switching Networks", Part I: Control Algorithm", Bell Syst. Tech. J., vol. 50, 1971, pp. 1579-1600.

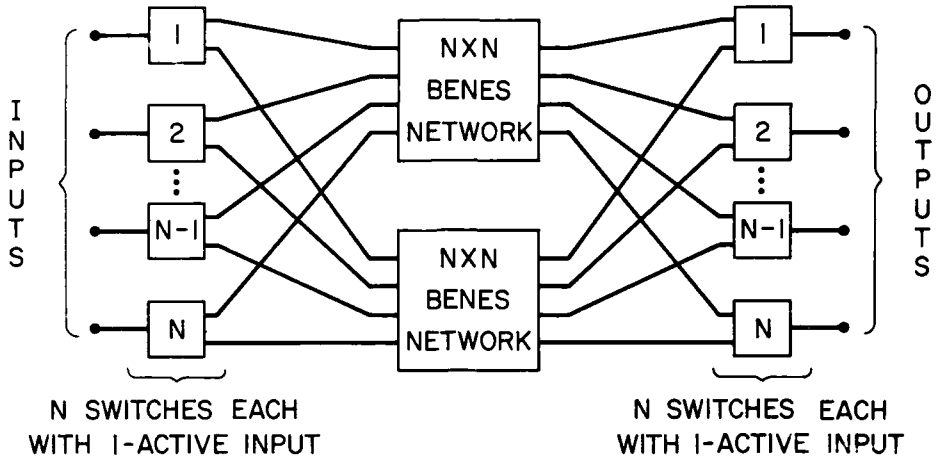

FIGURE 1. DILATED BENES NETWORK.

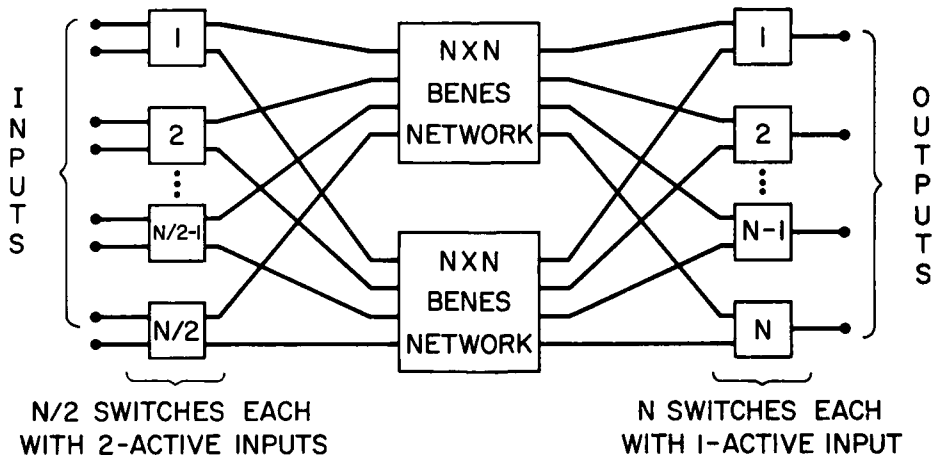

FIGURE 2. DILATED BENES NETWORK WITH FIRST STAGE CONTAINING 2x2 COUPLERS.

Self-Routing Optical Switch with Optical Processing

P. R. Prucnal, D. J. Blumenthal, P. A. Perrier

Lightwave Communications Research Laboratory
Center for Telecommunications Research
Columbia University
New York, N.Y. 10027

Self-routing switching architectures can reduce the propagation delay of data through a switching network. In the self-routing process, the data is encoded with a destination address which accompanies it through the switching network. This destination address may be contained in each bit, or in the packet header. Each switching node processes this destination information to route the data through the switch. Propagation delay is reduced by processing the destination address in real time, rather than prior to transmission.

Self-routing optical switching systems will experience a bottleneck if routing decisions are executed under electronic hardware control. This bottleneck can be relieved if optical processing techniques are used to perform routing decisions.

In this talk, a self-routing integrated optic switch with optical processing is presented and experimentally demonstrated. The self-routing technique is based on encoding each bit with its destination address, using code-division multiple access (CDMA) [1,2]. Each bit is replaced by a pseudo-orthogonal CDMA sequence corresponding to the destination address. At each switching node, the received CDMA sequence is optically correlated with a stored destination sequence, producing the appropriate switching decision for each bit.

The experimental layout is shown schematically in fig. 1. Encoded optical data entering the switch is distributed to both the switch and an optical routing controller. At the controller, individual data bits are correlated with a predetermined sequence using a fiber optic delay-line transversal filter. Correct correlation of data with the stored sequence

results in an autocorrelation peak which activates the switch (pass state). Incorrect correlation results in a cross-correlation function, leaving the switch closed (block state).

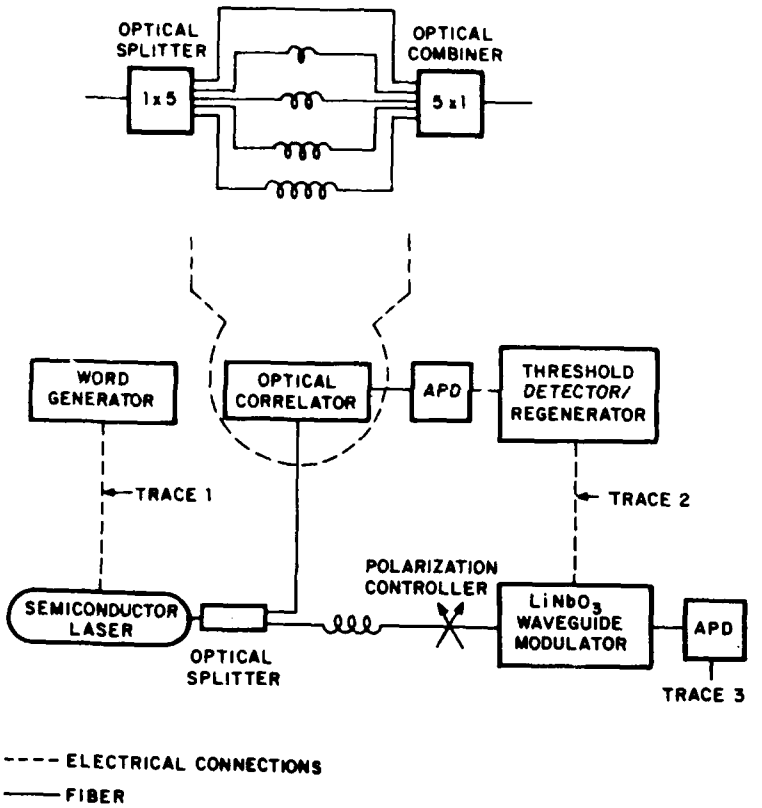

fig. 1: block diagram of the self-routing experiment.

Demonstration of self-routing optical data is seen in fig. 2. A series of binary ones is transmitted to alternating destinations 1 and 2. The alternating CDMA sequences 1 and 2 are shown in trace A. Sequence 1 generates an autocorrelation function at the output of the fiber optic correlator and triggers the generation of a switching pulse (trace B). Sequence 2 generates a cross-correlation function which does not generate a switching pulse (trace B). The switching pulses permit only chip sequence 1 to pass through the modulator (trace C).

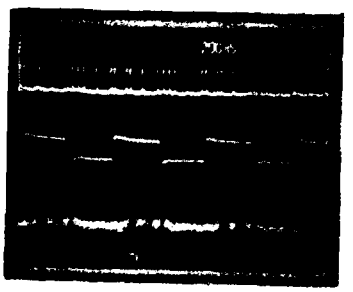

a: alternating 32-bit electronic CDMA chip sequences.

b: electronic switching pulses.

c: self-routed data.

fig. 2: self-routing optical data

Optical self-routing may also be performed using other schemes such as time-division multiple access (TDMA) [2,3]. TDMA provides more efficient bandwidth utilization than CDMA. It is anticipated that an experiment demonstrating optical TDMA self-routing will also be completed and discussed in this talk.

The implementation of optical self-routing is useful for networks in which the protocol is realized using optical processing [4]. It is also applicable to broad-band integrated services networks, where several varieties of wide-band information are supported [5].

REFERENCES

[1] P.R. Prucnal, M.A. Santoro, and T.R. Fan, "Spread Spectrum Fiber-Optic Local Area Network using Optical Processing," Journal of Lightwave Technology, LT-4 (5), 547-554 (1986).

[2] P.R. Prucnal, M.A. Santoro, and S.K. Sehgal, "Ultra-fast All-optical Synchronous Multiple Access Fiber Networks," Journal of Selected Areas in Communications, in press.

[3] P.R. Prucnal, M.A. Santoro, S.K. Sehgal, and I.P. Kaminow, "TDMA Fiber Optic Network with Optical Processing," Electronics Letters, submitted.

[4] A. Husain, J. Warrior, P.R. Haugen, N. Murray, M. Beatty, and L.D. Hutcheson, "Optical processing for future computer networks," Optical Engineering, 25 (1), 108-116 (1986).

[5] H. Suzuki, T. Takeuchi, and T. Yamaguchi, "Very High Speed and High Capacity Packet Switching for Broadband ISDN," IEEE ICC '86, Vol. 2, Paper 24.3, 749-754 (1986).

THURSDAY, MARCH 19, 1987

PROSPECTOR/RUBICON ROOM

1:30 PM–3:30 PM

ThC1–5

PHOTONIC SWITCHES: 1

Rod C. Alferness, AT&T Bell Laboratories, *Presider*

ThC1-1

Optoelectronic Hybrid Switching

by

R.I.MacDonald
Professor, NSERC-SaskTel Chair
University of Regina
Saskatchewan S4S 0A2
CANADA

1. Introduction

Optical methods have proved extremely successful for signal transmission and have very quickly formed the basis for a maturing industry. Other applications of optics to informatics are less natural. For example, it has been recognised that wideband transmission implies a future need for wideband switching, but the development of optical switches has proved difficult. Similarly the concept of optical computing may have great promise, but its present state is very primitive.

Electronic technology has also been remarkably successful in adapting to higher and higher speeds. In fact the generation of signals to be sent over wideband optical links and the subsequent use of these signals universally employs electronic circuits. It is safe to predict that for the foreseeable future much wideband equipment will be built with some mix of electronic and optical methods. There is already considerable interest in optical signal distribution within electronic equipment.

The presence of both optical and electronic signals in a single, hybrid system gives the opportunity to make use of the optoelectronic interface itself. Wideband switching is an application for which this approach seems very practical. Optoelectronic space- division matrices have already been shown promising for wideband switching applications. Optoelectronic frequency- division switches have also been demonstrated to have potential.

By definition an optoelectronic switch receives an optical signal but yields an electronic signal (or, rarely, the reverse.) Switching is due to some process that occurs in the conversion of the signal from one form to the other. The device thus inherently embodies a portion of an optical repeater stage and forces a double conversion of the signal between optical and electronic form. This feature is often seen as a disadvantage by comparison with optical switches through which an optical signal can pass unmolested in principle, if not in fact. Many practical situations, however, require optoelectronic conversion at a switching centre for purposes such as remultiplexing or even the collection of billing data. If the required wideband performance can be obtained by optoelectronic techniques, there may be no real reason not to use them.

2.Optoelectronic Switching Matrices:

(a)Space division

Space division optoelectronic switch matrices make use of optical transmission paths, with their excellent crosstalk immunity, to distribute incoming signals to crosspoint switches. These are switchable detectors that convert the optical signals to electrical ones only when in their sensitive state. By summing the detected electrical signals from a group of such detectors, each receiving a different optical signal, the basic N x 1 column unit of a space division switching matrix is formed. In a full matrix M such units are used, interconnected only by the optical signal distribution paths. The switching performance of such a matrix is determined by two characteristics of the basic unit: the effectiveness of sensitivity switching in the detectors and the electrical crosstalk of detected signals between units.

Sensitivity switching has been demonstrated in both photodiodes and photoconductors. With photodiodes an off-state reduction of up to 90 dB in the level of the detected signal is relatively easily obtained by applying a forward bias to raise the diode capacitance, and thus reduce photovoltaic response. Such switches exhibit isolation, defined as the ratio of on- state to off- state response, that increases with frequency over the detection bandwidth of the diode. Photoconductors can be turned off simply by applying no bias at all, so that the photogenerated charges do not drift. Frequency-independent isolation in excess of 70dB has been demonstrated over detection bandwidths up to 4 GHz in GaAs switchable photoconductors.

Work to develop photodiode- based optoelectronic switches has been carried out at several laboratories. In general the conclusion was reached that good performance could be obtained with discrete detectors, but integration was difficult because of the high conductivity of silicon substrates, the need for large aggregate forward bias current, and the complexity of the detectors and the circuitry for signal summation. Such problems can be largely eliminated by the use of photoconductors. When these devoce are made in III-V compounds they can be about as sensitive as a silicon pin diode because of the presence of photoconductive gain. They can have very high frequency response and their zero- bias off- state simplifies signal summation to a "wired- OR" connection. The availability of semi- insulating substrate material provides a barrier against charge leakage that facilitates monolithic integration of the detectors with high isolation. The main disadvantage is the noise associated with high dark current. There is evidence that low dark current, switchable GaAs photoconductors can be made, but the power budget of reasonably- sized optoelectronic switch matrices permits the use of relatively noisy detectors in any case. Photoconductors in materials such as InP and in silicon grown on insulating substrates have also been found interesting in this application.

It has been experimentally demonstrated that GaAs photoconductors can be integrated at 500 micrometer spacing into

switching arrays that maintain 50dB isolation over the frequency range from zero to at least 1.3GHz /1/. These results imply that for digital signals at the corresponding rate, switch matrices of up to several hundred inputs could be fabricated in physical sizes smaller than would be possible with optical waveguide switching technology. Higher frequencies can be obtained with redesign of the detectors and possibly greater detector spacing.

With the development of integrated methods of optical signal distribution, arrays of switching photoconductors may be relatively inexpensive to fabricate, since the device technology is very simple. As well as future applications in high rate communications switching, such matrices have unique properties of use in signal processing. Reconfigurable, broadband lattice filters of a very general type can be obtained by optoelectronically switching fibre delay lines. Among other advantages, the optoelectronic matrix can naturally provide the required loop gain without the need for optical amplification.

(b)Frequency division

There are several concepts of frequency division optoelectronic switching in early stages of study. In one form the signals to be switched are frequency- multiplexed before being imposed on an optical carrier. They can be selected during the process of detection by applying a local oscillator signal to the bias of a photodetector so that the detector output contains the required multiplexed channel, frequency- shifted to pass through an electronic filter.

3.Reference

/1./ R.I.MacDonald, D.K.W.Lam,"Optoelectronic Switch Matrices: Recent Developments", Opt. Eng. 24, pp220- 224, 1985

PHOTONIC SWITCHING WITH STRIPE DOMAINS

E.J.Torok, J.A.Krawczak, G.L.Nelson, B.S.Fritz, W.A.Harvey, and F.G.Hewitt,
Advanced Optics CTC, Sperry, Box 64525, St Paul MN 55164-0525

This paper describes a cross-bar switchboard for optical fibers. The switchboard is all optical, solid state (i.e. no moving parts), rugged, wide temperature, fast (2μsec), non-blocking, latching (i.e non-volatile), requires no initial polarization, is capable of switching both digital and analogue signals, and is theoretically capable of handling very large numbers of inputs and outputs in a single stage. The light is deflected from input fiber to any output fiber by a stripe domain deflection element, so there are no splitting losses; the efficiency does not decrease as more outputs fibers are added.

Stripe domain films[1,2] are made by liquid phase epitaxy. A 20 mil thick transparent non-magnetic single crystal garnet substrate such as gadolinium gallium garnet ($Gd_3Ga_5O_{12}$) is dipped into a melt and a 25 μm bismuth substituted rare earth iron garnet film (for example $Bi_{.7}Lu_{2.1}Fe_5O_{12}$) is grown. The film is magnetic with a $4\pi M$ of 1800 Oe and a uniaxial anisotropy field of approximately 150 Oe with easy axis normal to the film plane. Long straight regularly spaced magnetic domains form spontaneously in such films, as shown in figure 1. Both the orientation and spacing (grating constant) of these domains can be changed by application of an external magnetic field. The stripes align themselves parallel to the direction of the field, and the stripe spacing varies inversely as the strength of the applied field. A 25 μm film for example may have stripes whose grating constant can be varied from 7 μm to 2 μm. This corresponds to a change of deflection angle of 14° in the polar direction and 360° in the azimuthal direction.

The magnetization in the film is nearly normal to the film plane, and has only a small in-plane component. The normal component alternates from stripe to stripe in order to minimize the demagnetizing energy. When light is passed through the film, the part that passes through one stripe has its polarization rotated by an amount FD where F is the Faraday constant of the material and D is the film thickness. The light that passes through the adjacent stripe has its polarization rotated an angle -FD. The film acts as a phase diffraction grating whose diffraction efficiency depends on the film thickness. For example, when each stripe rotates the polarization 90 degrees, the zero order disappears entirely, and all light goes into the higher orders. When the film is thick enough, and the incident light enters at an angle to the normal, all orders become negligible except the one that exits at an angle nearly equal and opposite in sign to the entrance angle, i.e. the Bragg angle. The deflection efficiency in this case can be shown to be[2]

$$Eff = \exp(-\alpha D)\sin^2(2FD/\pi) \qquad (1$$

where α is the absorption in nepers/cm, and F is the Faraday coefficient of the film in radians/cm. For light of wavelength 0.8μm , a good film will have α = 86 nepers/cm and F = 104 rad/cm. Film compositions with much higher bismuth content have been made, but not perfected. They have F as high as 270 rad/cm.

When a mirror is placed behind a stripe domain deflector, the rotation of the polarization in each stripe is doubled, and the deflection efficiency is increased as if the film were twice as thick.

If a partially reflecting layer is put on the other surface, so that the film is enclosed in a resonsnt optical cavity, or etalon, the efficiency can be shown to be:

$$Eff = (4F/\pi)^2(\alpha+\{\alpha^2+(4F/\pi)^2\}^{1/2})^{-2} \qquad (2$$

This offers an advantage in higher efficiency as well as the convenience of using a thinner film. For example, a 25 μm thick film with F=104 rad/cm and α=86 nep/cm has an efficiency of only 2%. When a mirror is placed behind it, the efficiency rises to 7%. When an etalon is formed by placing a partially reflecting layer on the other side of the deflector, the efficiency rises to 30%. Without that partially reflecting layer, the maximum deflection efficiency is 20% and is obtained when the film thickness is 75μm. Future films with F=270 should yield Eff=61%.

Since the Faraday effect rotates the polarization angle of an incoming beam regardless of the initial polarization angle, the deflector works for any polarization at all or any superposition of polarization; thus a stripe domain light deflector works for unpolarized light.

A fiber-optic switchboard can be made using stripe domain light deflection elements. The principle is shown in figure 2: Light from a particular input fiber in a bundle is focused by an input lens onto its own facet of a multifaceted pryamidal reflector (which is really the pavillion of a gem). The light is reflected by the facet and focused by a relay lens onto a light deflecting element. There is a mirror behind each deflecting element. The deflector deflects that beam of light back through the relay lens which focuses the deflected light onto the original spot on the facet. The angle of incidence of the deflected light onto the facet determines which output fiber the light reaches. Each output fiber has an output lens to focus the light into the fiber. This is an imaging system, with images of the tip of an input fiber forming on the gem, on the deflector, again on the gem, and finally on the output fiber.

Note that for full efficiency, it is necessary to be able to image any input fiber onto the end of any output fiber, and, indeed, to be able to image all input fibers simultaneously onto the end of any output fiber. In order for the light to stay in the output fiber it is also necessary that the light enter within the numerical aperture of the output fiber. These two conditions put constraints on the design of the switchboard and are the reason for the multifaceted reflector.

Each output lens is focused on the gem, so the output lens focuses all of the light into the output fiber. This changes

what essentially is an analogue deflector system into a digital deflector system. Small changes in deflection angle don't cause the light to miss the output fiber; all the light has to do to enter the proper fiber is to hit the corresponding output lens.

Since light beams don't block each other when they cross, all inputs and outputs can be operating simultaneously, in a non-blocking fashon.

The current status of the project is that a 4x4 fiber-in photo-detector out switchboard for high resolution video signals has been demonstrated and a 2x2 fiber-in fiber-out switchboard has been demonstrated. An 8x8 fiber-in fiber-out design is currently being built, and will be discussed at the conference.

REFERENCES

1. T. R. Johanses, D. I. Norman and E. J. Torok, J. Appl.Phys. 42,1715 (1971)
2. G. L. Nelson and W. A. Harvey, J. Appl. Phys. 53 1687 (1982)
3. E. J. Torok and J. A. Krawczak, to be published

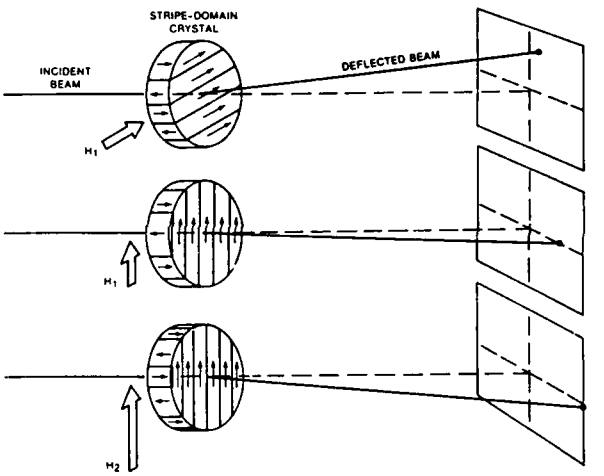

Figure 1: A stripe domain deflector acts as a two dimensional light deflector. The stripes align themselves with an applied magnetic field, and rotate when the field rotates. The stripe spacing becomes smaller when the field is increased.

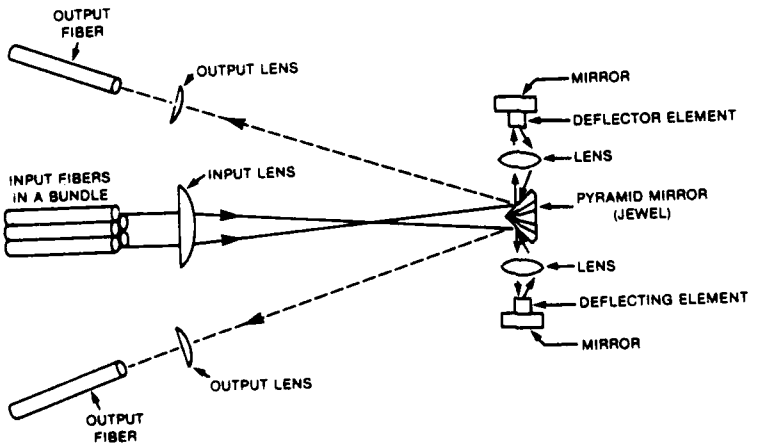

Figure 2: A fiber-optic switchboard.

SINGLE-MODE FIBER SWITCH WITH SIMULTANEOUS LOOP-BACK FEATURE

W. C. Young and L. Curtis

Bell Communications Research
331 Newman Springs Road
Red Bank, New Jersey 07701

INTRODUCTION

As applications for lightwave systems expand, new challenges for photonic switches are constantly evolving and some of these challenges can be satisfied by moving-fiber type switches. In the case of optical fiber networks having many regenerative nodes, it is necessary to bypass those nodes that are not in use and to ensure that in-operative nodes are not permitted to enter the network and cause a total network failure.[1] In this paper, we report on a moving-fiber-array switch that provides these important switching functions in evolving single-mode fiber (SMF) networks. In particular, the switch is designed to provide the bypass function through only one SMF butt-joint; therefore, it exhibits very low insertion loss and permits networks to be designed that have a large number of off-line nodes for a large percentage of the time. A second feature of this switch is that while in the bypass position the switch establishes an optical loop-back circuit, for the regenerative node (a receiver/transmitter combination), permitting self-testing of the node. If the self-test is negative, due to an in-operative node, then the switching function (switching to the on-line position) can be blocked thereby avoiding a total network failure. In the event a node failure occurs after switching, the actuator is de-energized and the switch returns to the normal position (bypass position). In the on-line position the optical path through the switch uses low loss single-mode fiber to multimode fiber (SMF/MMF) "photon-bucket" type joints between the line input and the node's receiver, and again only one SMF/SMF joint between the node's transmitting SMF and the network's SMF. Solenoid actuation is used for achieving the on-line position and a compression spring is used to return and hold the switch in the bypass position.

SWITCH DESIGN

The switch is configured with two linear arrays of fibers, a 4-fiber array (2 MMFs and 2 SMFs) on the line-in side of the switch and a 3-fiber array (2 MMFs and 1 SMF) on the line-out side of the switch, as shown in Figures 1 and 2. The on-line switch position is achieved and maintained by energizing a solenoid that moves the 3-fiber array into transverse alignment with the stationary 4-fiber array. The on-line position and the optical paths through the switch are shown in Figure 1. The bypass position and its optical paths are shown in Figure 2. In the latter position the arrays are held in transverse alignment by a compression spring; the solenoid is not energized. As shown in these figures, the critical switching functions are achieved through only one SMF/SMF joint.

Because of the small mode field diameter of single-mode fibers, about 10 microns, the fiber joints in moving SMF switches must achieve transverse alignment to within about 1.5 microns in order to achieve a joint loss of 0.5 dB.[2] The precision arrays in this switch were fabricated with preferentially-etched silicon v-grooved chips, and the precise transverse alignment between the arrays was achieved by the meshing of the positive and negative chips.[3/4] The fabrication of the arrays is done by interleaving the fibers and chips and epoxying them into a robust assembly. The next step is to polish the endface perpendicular to the v-groove structure using a procedure that results in a slight recessing of the fiber endfaces below the chip's end surface. This recessing protects the fiber endfaces from damage during the movement of the array. An index-matching fluid was also used in the final assembly to minimize reflections and to provide lubrication. Since precise transverse alignment in the fiber joints was achieved by the mating of the precision v-grooves in the positive and negative chips, the only accuracy necessary during the movement of the array is that required to ensure that the appropriate grooves are meshed. The precise sub-micron alignment is achieved by the mating of the precision groove structures.

RESULTS

A low loss moving-fiber-array switch that provides a bypass function while simultaneously providing a loop-back circuit has been demonstrated. The insertion losses, using 1300 nm optimized single-mode fiber, for the bypass and on-line positions were 0.38 dB and 0.33 dB, respectively. The other paths through the switch are "photon-bucket" type joints (SMF/MMF) and have losses less than 0.2 dB. The switching speed, which was not optimized in the design, is about 25 msec. for the solenoid actuated on-line position and about 15 msec. for the bypass position (compression spring actuated).

REFERENCES

1. K. W. Loh et al., "Fail-Safe Nodes for Fiber Networks," OFC 86, Atlanta, GA, MD3.

2. D. Marcuse, Bell Syst. Tech. Journal, 56, 703 (1977).

3. C. M. Miller, Bell Syst. Tech. Journal, 57, 91 (1978).

4. W. C. Young and L. Curtis, "Moving Fiber Array Switch for Multimode and Single-Mode Fibers," IOOC'81, San Francisco WKG.

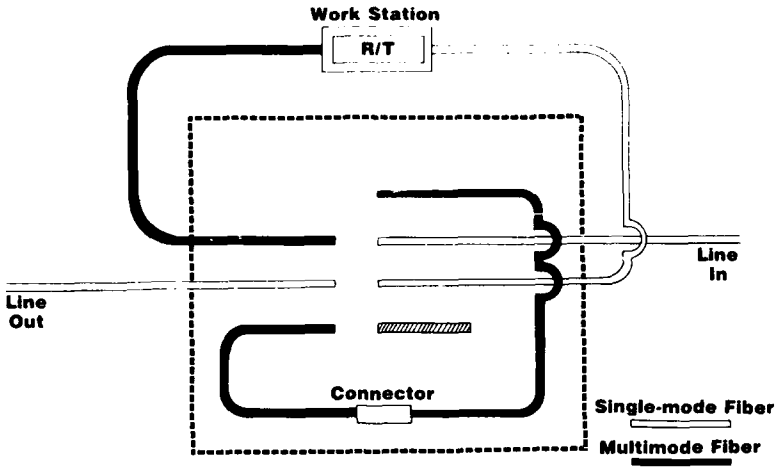

1. Schematic Of Switch In The On-Line, With Loop/Back Position

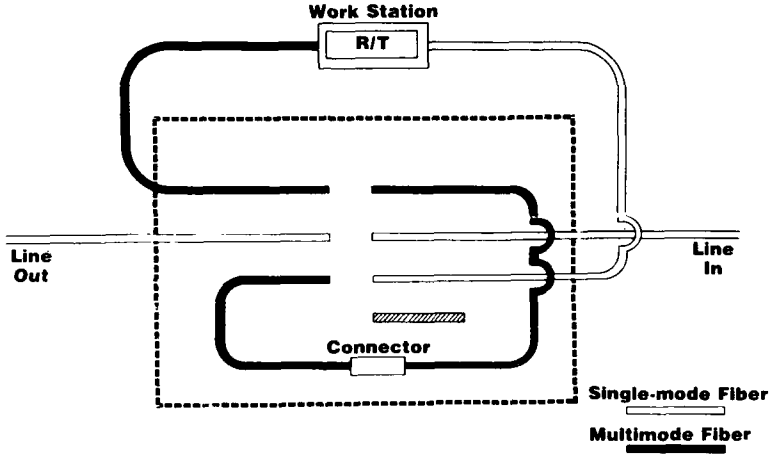

2. Schematic Of Switch In The Bypass Position

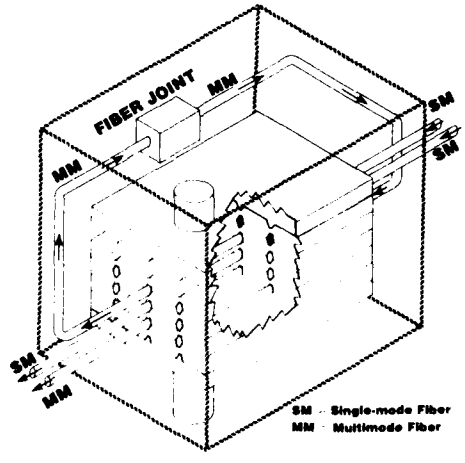

3. Moving Fiber Array Switch Details

An All-Fibre Routeing Switch

S R Mallinson, J V Wright, C A Millar
British Telecom Research Laboratories,
Martlesham Heath,
IPSWICH, UK.

A key functional element for advanced single-mode optical fibre networks is a 2x2 crosspoint switch for routeing optical signals (1). Such a switch would be used to configure an optical system and would not necessarily need to have a fast switching characteristic. An all-fibre device would be attractive because of the low transmission loss and ease of coupling to system fibre, and a basic building block for many fibre-based devices is the polished fibre coupler (2).

In this paper we describe a new switch principle which relies on the coupling between two polished fibre coupler blocks through a high index interlay waveguide whose refractive index is higher than the effective mode index of the fibres (Figure 1). Switching is effected by the input radiation coupling from the interlay waveguide into the second fibre (cross-coupled state) or recoupling into the first fibre (straight-through state). The half-coupler blocks were constructed with a 25 cm radius of curvature, and the top surfaces polished to within a micron of the edge of the fibre core (3). Accurate glass ribbon spacers were used to align the two blocks in parallelism and separated by typically 20 μm, and the interstice was filled with a transparent high index oil to form a slab waveguide. A two dimensional Beam Propagation Model (BPM) has been applied to investigate the behaviour of the optical power distribution in the two fibres and the interlay waveguide as a function of the waveguide and fibre propagation parameters. In the model, an optical field distribution, corresponding to the fundamental mode of the isolated fibre is established in one arm of the coupler and propagated through the device in small steps. Initially, the fibre is well isolated from the high index region and the field propagates without change. But within $\pm$ 1.5 mm of the device centre there is a strong interaction with high-order modes in the high index region and power couples to the opposite arm. The evolution of the power distribution at the beginning, in the middle and at the end of the interaction region for strong cross-coupling is shown in Figure 2. Generally, the nature of the interaction is such that either (a) power predominantly remains in the first fibre, or (b) is strongly coupled to the second fibre with low loss, or (c) is strongly coupled to the film with no subsequent recoupling, according to the film refractive index and thickness. These three regimes are observed in practical devices.

The outputs from both arms of the coupler when white light was launched into one input arm exhibited large extinctions at well-defined wavelengths, determined by the waveguide thickness and index (4). By varying either parameter, the outputs at a particular input wavelength were investigated, and observed to undergo periodic variations as predicted by the BPM model. Two methods of obtaining switching action were investigated: (i) by varying the waveguide thickness using a piezoelectric translator and (ii) by varying the waveguide index using a liquid crystal interlayer.

(i) The output from both arms as a function of the voltage applied to the translator (proportional to the waveguide thickness) is shown in Figure 3, for an input wavelength of 1.3 μm and oil index (n_D) of 1.49. The best crosstalk obtained was 10 dB, and switching speeds of around a few milliseconds are envisaged. Whilst acknowledging that the crosstalk associated with this particular device is unrealistic for a practical switch, it is a partial consequence of the non-optimised coupler design and is predicted by the BPM model. The device has the advantage of being constructed with system fibre, and has a very low excess loss.

(ii) A nematic liquid crystal interlay switch was constructed by depositing a polymer alignment layer on both coupler blocks. This induced homogeneous alignment of the liquid crystal, parallel to the fibre axis. An ac voltage was applied to electrodes embedded in the blocks in order to rotate the liquid crystal director in the plane of the film perpendicular to the fibre axis, thus effecting a large index change for the horizontal polarisation of the input optical field. The best crosstalk achieved was 8 dB at a drive voltage of 100V p-p, the further degradation in performance from (i) being attributed to waveguide losses and imperfections. Switch-on speeds were several milliseconds but the switch-off was slow (seconds) due to orientational relaxation of the liquid crystal molecules.

Although the performance of these switches is at present modest, an important principle has been established: that efficient cross-coupling is possible using high index materials. Until now, it has generally been perceived that interlay materials should have a refractive index equal to or less than the effective mode index. However, an interlay waveguide structure permits the use of much higher index materials; a relaxation which introduces the possibility of using a wide range of commercially-available liquid crystal compounds and many other optically-interesting materials. It is anticipated that computer modelling of the generalised structure will yield device geometries with much-improved crosstalk and insertion loss performances.

The Director of Research at BTRL is acknowledged for permission to publish this paper.

References:

(1) A M Hill; Journal of Lightwave Technology LT-4, 7, p785, 1986.
(2) R Bergh, G Kotler, H Shaw; Electronics Letters 16, p929, 1980.
(3) B K Nayar, D R Smith; Optics Letters 8, p543, 1983.
(4) C A Millar, S R Mallinson, M C Brierley; submitted to Optics Letters.

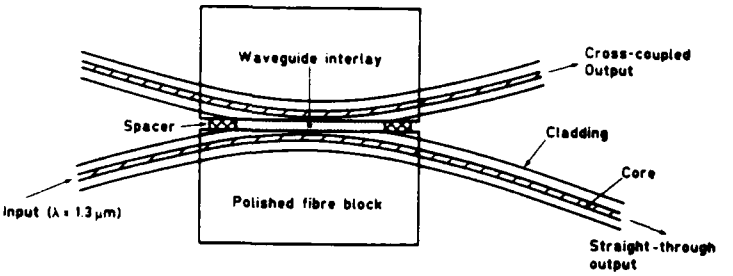

FIGURE 1 INTERLAY COUPLER.

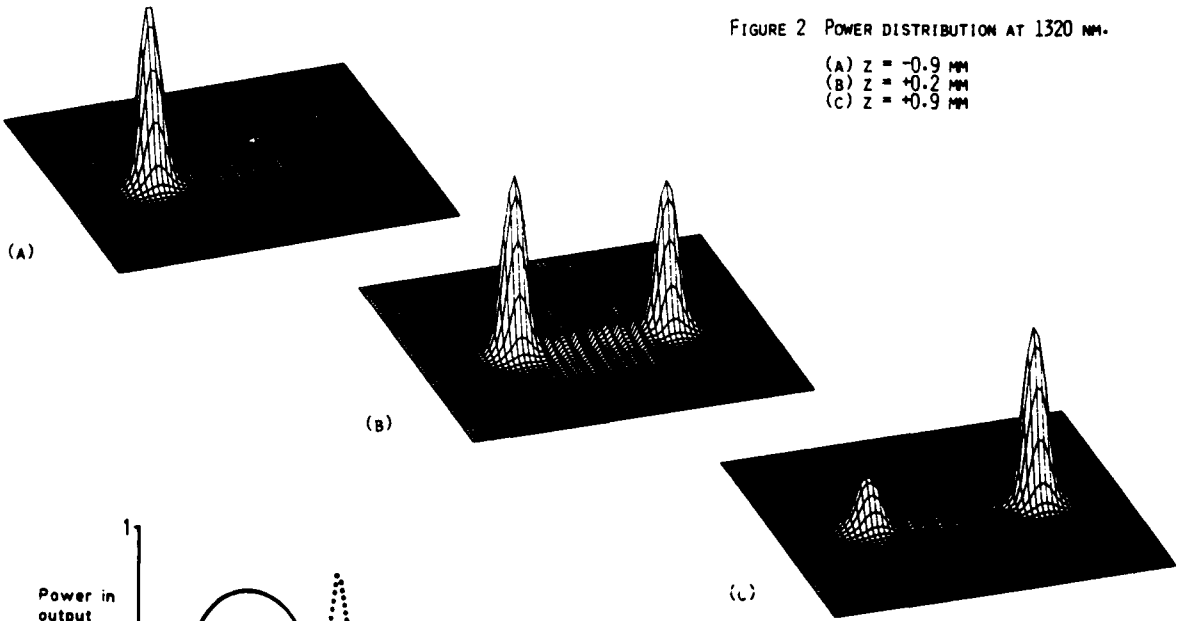

FIGURE 2 POWER DISTRIBUTION AT 1320 NM.
(A) Z = -0.9 MM
(B) Z = +0.2 MM
(C) Z = +0.9 MM

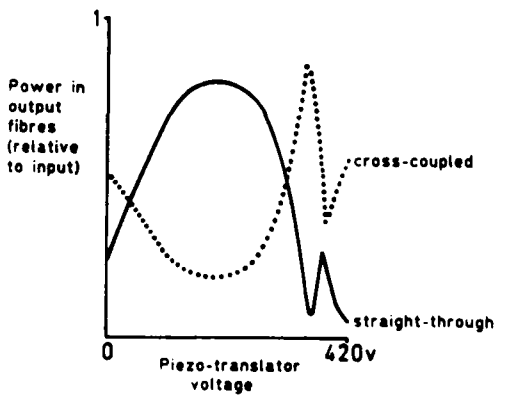

FIGURE 3 COUPLER OUTPUT AS A FUNCTION OF PIEZO-TRANSLATOR VOLTAGE.

ThC5-1

An All-Optical Switch for Signal Routing Between Fibres

C.R. Paton, S.D. Smith and A.C. Walker

Dept. of Physics, Heriot-Watt University, Edinburgh EH14 4AS, U.K.

Non-linear interference filters (NLIF) incorporating ZnSe spacers were first shown to exhibit optical bistability in 1984 [1,2]. Since then they have been successfully used in a number of digital optical circuit demonstrations [3]. Although these devices, which rely on a thermally induced nonlinearity, have limited low-power switch speeds (0.1 μs-100 μs) they have a very high transmission bandwidth, up to several THz, and can therefore act as an all-optical relay. They are therefore excellent candidates for spatial switching, or signal routing applications. A single NLIF may be configured as a 2 x 2 spatial switch by using both reflection and transmission outputs, as shown in fig. 1. An array of such devices may be used to form a non-blocking switch network or crossbar switch [4].

We have recently demonstrated such an all-optical spatial switch by using a single ZnSe NLIF to redirect a broad-band signal between a pair of optical fibres. The beam from an argon laser was intensity modulated with a video signal (from a TV camera) using an acoustic-optic modulator. This modulated beam was then injected into a length of multimode fibre (core diameter 50 μm) using a microscope objective. A graded-index (GRIN) rod lens was used at the other end of the fibre to focus the light onto the NLIF, and two more GRIN lenses were positioned to collect the reflected and transmitted beams and inject them into a pair of similar fibres. The light from the remote ends of these fibres was detected, and the amplified signals fed to a pair of TV monitors. With the power injected into the input fibre held below the critical switch level a picture was seen on the monitor fed from the reflected output. In this low-transmission region of the NLIF characteristic, the transmitted power was not sufficient to give a

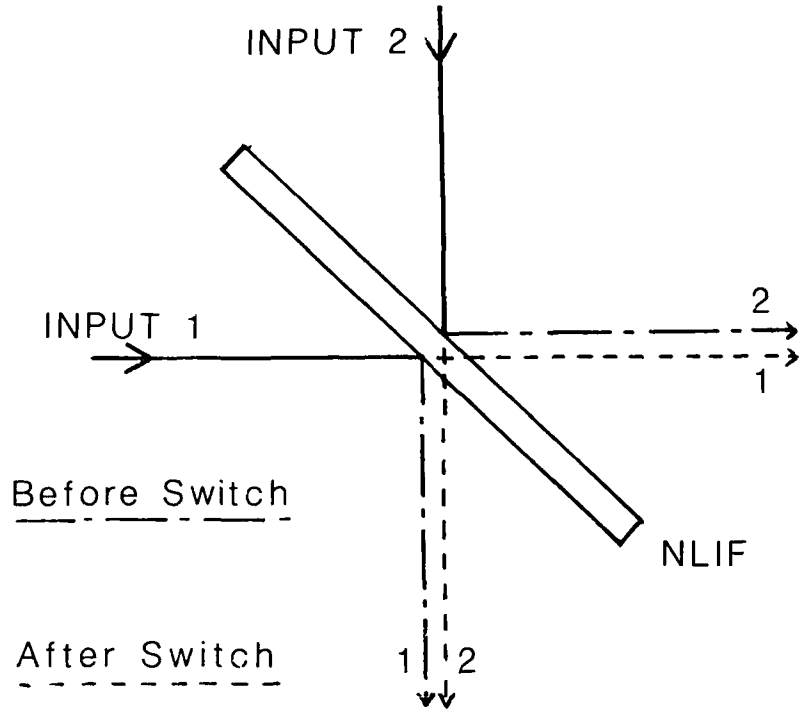

Fig. 1 - Optical 2x2 Spatial Switch

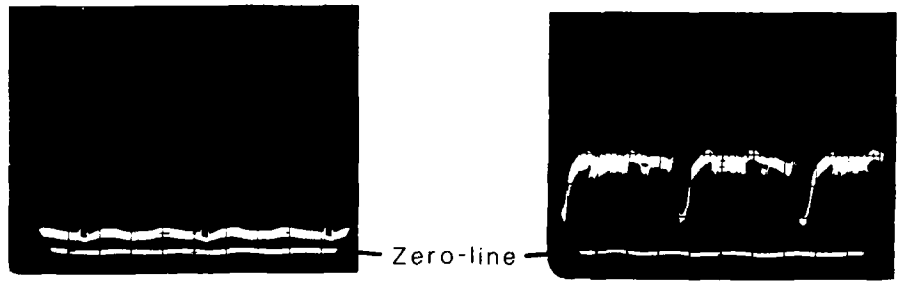

a) Before Switch

b) After Switch

Fig. 2 - Transmitted Video Signals

picture on the other monitor. When the power was increased slightly to switch the NLIF into its high-transmission region, this situation was reversed, and the picture was transferred onto the other monitor. The relative amplitudes of the transmitted video signals are shown in fig. 2, both below and above the switching point. The switch between high reflection and high transmission states can be achieved by transmitting a positive or negative pulse (relative to the average power level) along the input fibre from the modulator.

The input GRIN lens was imaging the fibre core onto the NLIF device with an approximately 2:1 magnification giving an estimated spot-size of $\sim$ 100 μm. The power required to switch to the high transmission state was $\sim$ 100 mW. Much lower operating powers (milliwatts) can be achieved with such devices using smaller spot-sizes, i.e. in conjunction with single-mode fibres. For example, an all-optical switch of this type has been operated with $\leq$ 4 mW of 830 nm radiation in a $\sim$ 10 μm spot and a bistable response demonstrated using a cw GaAlAs laser diode. Operating powers below a milliwatt are expected for structured devices with dimensions of a few μm.

Factors determining insertion loss and switch contrast will be reviewed and the optimisation of such parameters discussed.

References

[1] S.D. Smith, J.G.H. Mathew, M.R. Taghizadeh, A.C. Walker, B.S. Wherrett, and A. Hendry, Opt. Commun. 51, 357 (1984).

[2] G.R. Olbright, N. Peyghambarian, H.M. Gibbs, H.A. Macleod and F. van Milligen, Appl. Phys. Lett. 45, 1031 (1984).

[3] S.D. Smith, A.C. Walker, F.A.P. Tooley, J.G.H. Mathew and M.R. Taghizadeh, Optical Bistability III (Springer Verlag, Proc. in Phys. 8) p. 8 (1986).

[4] A.A. Sawchuk and T.C. Strand, Proc. IEEE 72, 758 (1982).

THURSDAY, MARCH 19, 1987

PROSPECTOR/RUBICON ROOM

3:30 PM–5:00 PM

ThD1–6

PHOTONIC SWITCHES: 2

Takakiyo Nakagami, Fujitsu Laboratories, Ltd.,
Presider

A Monolithically Integrated Optical Gate 2x2 Matrix Switch Using GaAs/AlGaAs Multiple Quantum Well Structure

A.AJISAWA, M.FUJIWARA, J.SHIMIZU, M.SUGIMOTO
M.UCHIDA, Y.OHTA

Opto-Electronics Res. Labs. NEC Corporation
4-1-1 Miyazaki, Miyamae-ku, Kawasaki 213, Japan

K.ASAKAWA

Optoelectronics Joint Res. Labs.
1333 Kamiodanaka, Nakahara-ku, Kawasaki 211, Japan

1. Introduction

A small size matrix switch is desired for constructing large scale optical switching systems. An optical gate matrix switch which consists of optical splitters, combiners and gates has advantages of its simple construction and ability of non-blocking and point-to-multipoint connections. So far this kind of switch (1) was hybrid and it seemed difficult to interconnect optical gates with optical circuits.

This paper reports a 2x2 small size optical gate matrix switch which integrates monolithically electro-absorption type multiple quantum well (MQW) optical gates (2,3) with optical circuits including optical splitters and combiners which are constructed with corner mirrors (4) fabricated by reactive ion beam etching (RIBE) method.

2. Design and Fabrication

A 2x2 optical gate matrix switch structure is shown in Fig. 1. The switch consists of four optical gates, two 1x2 optical splitters and two 2x1 optical combiners. These components are monolithically integrated on a GaAs/AlGaAs MQW wafer grown by MBE method. To obtain a small size matrix switch, corner mirrors are arranged in the optical splitter and combiner circuits. Optical switcing between input and output ports can be made by selecting the on-off state in four optical gates.

An MQW gate has higher extinction ratio at low bias voltage than a double hetero (DH) structure gate (5). Since at the longer wavelength than the exciton absorption peak the MQW has low absorption loss, it is suitable for optical circuits. A diagram of the MQW optical gate with p-i-n structure is shown in Fig. 2. The MQW consists of 28 GaAs quantum well layers, each 80Å thick, separated by 80 Å AlGaAs barrier layers and has absorption edge at about 835nm wavelength.

Corner mirrors used for constructing the optical splitters and combiners are fabricated by RIBE method. An SEM photograph for a corner mirror is shown in Fig. 3. The etched facet has excellent perpendicularity and smoothness. The switch dimensions are 3mm length and 1.2 mm width.

3. Experimental Results

Measurements of extinction characteristics of the MQW gates and optical loss of the matrix switch were made using an 860nm wavelength laser diode, because at this wavelength the MQW had large electro-absorption changes and low intrinsic absorption loss.

Figure 4 shows the extinction ratio for the MQW gate, 1mm in length, as a function of applied voltage. High extinction ratio of 20dB at 9V reverse bias voltage was achieved. A low crosstalk (20dB) 2x2 switching operation was obtained.

Total optical loss was 24dB, excluding input/output to waveguide coupling loss, divided as follows : 3dB splitting loss, 9dB propagation loss (3dB per mm), 8dB mirror loss (2dB per mirror) and 4dB scattering loss in splitter and combiner circuits. The mirror loss and the scattering loss will be decreased by optimizing the process in fabricating optical circuits.

4. Conclusion

2x2 monolithically integrated optical gate matrix switch using a GaAs/AlGaAs MQW structure was demonstrated. Large scale optical switching systems can be realized by designing low loss optical circuits and integrating this kind of switch and optical amplifiers.

5. Acknowlegements

The authors are grateful to M.Sakaguchi and N.Nishida for suggesting and guiding for this work.

Reference

(1) M.Kobayashi et.al.,IOOC-ECOC'85 Technical Digest Vol.III,73
(2) T.H.Wood et.al.,Elect. Lett.,21, 693, (1985)
(3) K.Wakita et.al.,Elect. Lett.,22, 907, (1986)
(4) P.Buchmann et.al.,J.Lightwave Tecnology,LT-3,785,(1985)
(5) H.Iwamura et.al.,Jpn.J.Appl.Phys.,22,L751,(1983)

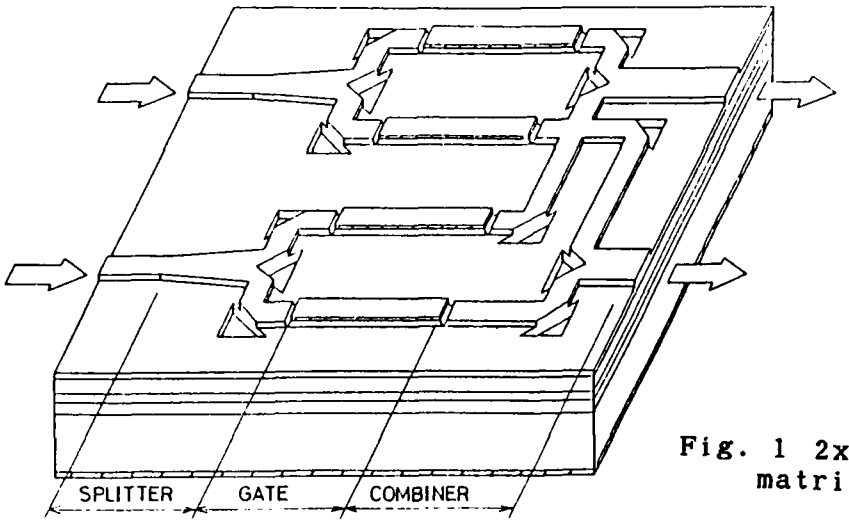

Fig. 1 2x2 optical gate matrix switch structure

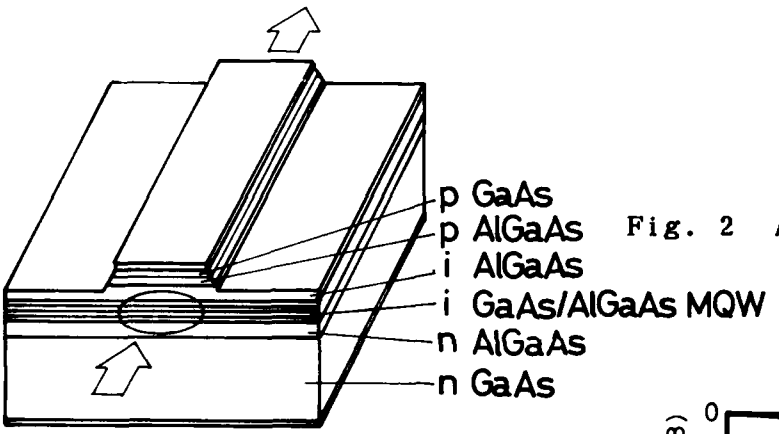

Fig. 2 An MQW optical gate

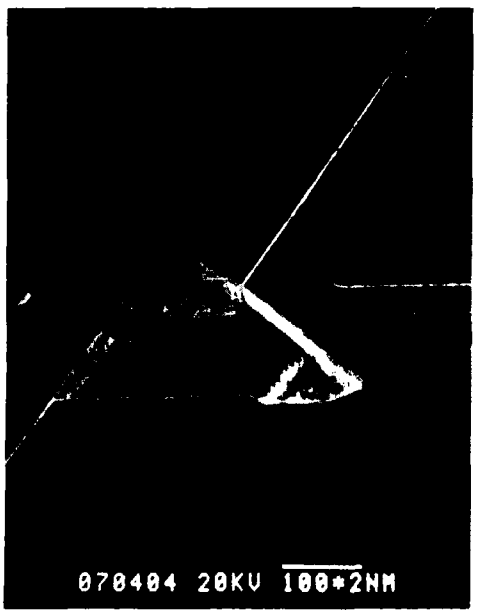

Fig. 3 Corner mirror SEM photograph

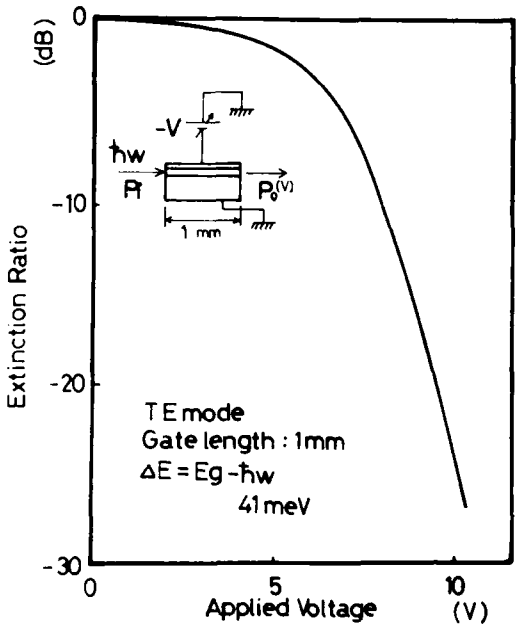

Fig. 4 Gate extinction ratio as a function of applied voltage

SILICON CARRIER-ENHANCED ELECTROOPTICAL GUIDED-WAVE SWITCH

J.P. Lorenzo and R.A. Soref
Rome Air Development Center
Solid State Sciences Directorate
Hanscom AFB, MA 01731-5000

Experimental results on an all-silicon 1.3 μm 2 x 2 optical switch are presented in this paper. Waveguiding of 1.3 μm light has been shown to be feasible in silicon with little attenuation expected for doping concentrations below $10^{17}cm^{-3}$.(1) This and other state-of-the-art developments(2) has led to the monolithic opto-electronic device under study in this work. A schematic view of the integrated device structure is shown in figure 1. The active region is integrated at the crossing intersection of two raised rib channel waveguides. Each device chip consists of three individual bi directional 2 x 2 devices with different crossing angles and rib widths. The chip is polished in a special mounting jig to delineate the ridge waveguide ends. Electrooptical interactions are induced by actively altering the refractive index profile under a metallurgical p+/n junction at the waveguide intersection region shown in figure 2. An index decrease in this region is created with injected carriers.(1) Refractive index change near the junction is estimated to be 1.5×10^{-3} for $10^{18}cm^{-3}$ free holes.(3)

Geometries similar to figure 1 are fabricated in 6.5 μm thick ($N_d = 5 \times 10^{15}cm^{-3}$) crystalline silicon epitaxial layers grown on degenerate n-type ($N_d = 2 \times 10^{19}cm^{-3}$) Si substrates. These raised rib structures are delineated using standard photolithographic techniques and dry plasma etching.

A typical cross-sectional geometry is shown in figure 2. Vertical optical confinement is achieved at the n/n^+ interface with an impurity induced index step of 1.8×10^{-2} and lateral confinement provided by the

silicon/SiO_2 rib walls. Prior to dry etching a p^+ region is formed along the intersection using a boron diffusion. Hole injection from this forward biased p^+/n junction supplies excess carriers for active switching.

Initial tests were made with a highly multimode device with a 20 μm rib width and 40 μm intersection width. The active region was 2000 μm long. InGaAsP DHB laser diodes were used for end fire coupling into one channel waveguide at either 1.3 μm or 1.55 μm. The near-field radiation pattern of both channel outputs was imaged on an infrared vidicon and displayed on a video monitor. Resolution of spatial variations of the optical output pattern was calibrated by correlation with actual device dimensions. With a video line scanner, horizontal variation and relative switching intensity between output intensity peaks was measured. Forward bias junction currents as low as 600 A/cm^2 resulted in partial 2 x 2 switching wherein a few percent of the optical energy was transfered to the cross channel. The device appear to be bi-directional in nature i.e. signals can be launched or received at any of the four ports.

We also observed mode modulation phenomena. At low forward bias current densities (600 A/cm^2) some 1.3 μm excited modes can be extinguished while others are enhanced. Individual modes are observed to move laterally within the multimode channel. A more pronounced increase in the cross channel (e.g. port 4) mode structure and output intensity occurs at current densities near 1000 A/cm^2 while the signal in output port 3 decreases. The induced lateral shift of mode groups across an output waveguide is measured to be 5.7 microns at 1000 A/cm^2.

We observe electroluminescence phenomena during forward biasing of the p^+/n junction. The junction luminescence is optically guided and emitted

at all four ports. At room temperature and 600 A/cm^2, ~ 0.2 μW of emitted optical power is measured. Since shorter wavelength light is self absorbed, we believe a spectral analysis will show this emission is longer than 1.05 μm, consistent with radiative recombination due to isoelectronic centers (phosphorous/boron) in the junction region. This device could be used as a modulated optical source in a monolithically integrated silicon optical-interconnect system.

References:

1. R.A. Soref and J.P. Lorenzo, IEEE J. of Quant. Elec., June '86.

2. O. Mikami and H. Nakagome, Electr. Lett. 20, 299, Mar. '84.

3. R.A. Soref and B.R. Bennett, IEEE J. of Quant. Elec., Jan. '87.

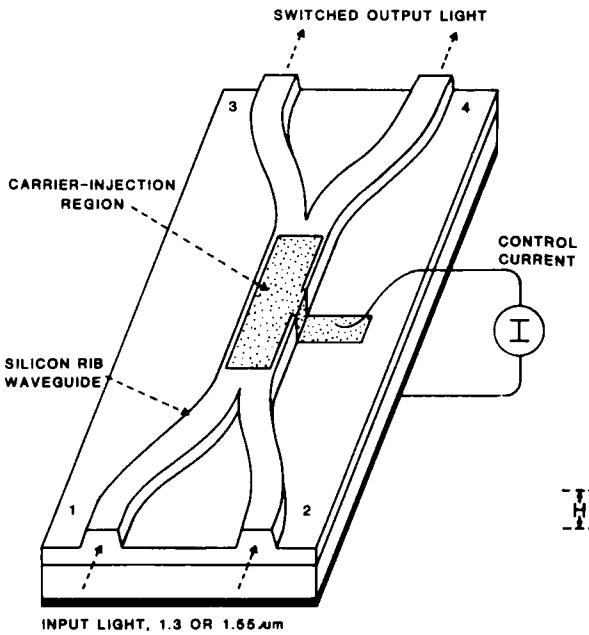

Fig. 1

Schematic of 2 x 2 (4 port) Si integrated optical switch.

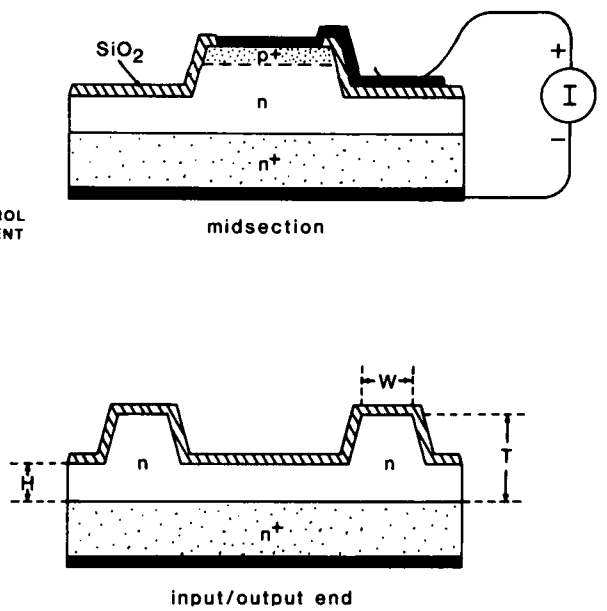

Fig. 2

Cross section of rib guides and p^+/n Si junction region.

4x4 $Ti:LiNbO_3$ Switch Array with Full Broadcast Capability

G. A. Bogert
AT&T Bell Laboratories
Union Boulevard
Allentown, PA 18103-1285
(215) 439-5295

Recently, $Ti:LiNbO_3$ optical switch arrays have received significant attention with several NxN arrays reported in the past year [1,2,3]. While there has been considerable improvement in the performance and complexity of the arrays, all have been of the crossbar architecture. The crossbar architecture, while providing nonblocking point-to-point operation, does not allow for the broadcast function, a highly desirable characteristic for an array.

The device presented here is a nonrearrangeable and nonblocking 4x4 switch array with a passive splitter and active selector architecture [4,5] permitting both broadcast and point-to-point operation. The passive splitter and active selector concept is shown schematically in Figure 1.

The device was fabricated using Ti diffused waveguides in Z-cut, y-propagating $LiNbO_3$. After the indiffusion at 1050 C for 6 hours, a CVD SiO_2 buffer layer was deposited and Al electrodes deposited and photolithographically defined. The device was designed to operate with the TM polarization at λ =1.3μm.

Several different components were required to realize this architecture: directional couplers, 50/50 splitters, and waveguide crossovers. While significant work on directional couplers had already been performed, further development of low-loss Y branches using s-bends and intersecting waveguides was performed and will be presented.

Insertion losses for the 16 paths of the array ranged from 11.6dB to 13.9dB with an average of 12.8dB. 6 dB of this is due to the broadcast nature of the device; each path includes two 3dB splitters. A 4 dB improvement in the loss of this array is expected with a redesign of the individual features.

The average operating voltages for the twelve directional coupler switches were ≈ 13 volts for the bar state and ± 9 volts for the cross state. Uniform $\Delta\beta$ electrodes and reverse $\Delta\beta$ electrodes were utilized for the bar and cross state, respectively. Switching efficiencies were measurement limited (<-

35dB).

The device was mounted and wirebonded onto a printed circuit board compatible with standard edge connectors. The single-mode fiber arrays were attached using silicon V-groove technology.

In summary, we have demonstrated the first nonblocking switch array which provides both full broadcast capability and point-to-point operation. It operates with reasonable voltages and provides exceptional switching efficiency.

I would like to acknowledge the contributions of F. Sandy for fabrication of the device; M. Dautartas, R. J. Holmes, and Y. S. Kim for process development; Y. Chen for fiber array attachment; J. R. Erickson, R. A. Nordin and M. T. Ratajack for project motivation and system expertise; R. Spanke for design of the architecture, and F. T. Stone and W. A. Payne for project support.

REFERENCES

[1] A. Neyer, W. Mevenkamp, and B. Kretzschmann, Integrated and Guided-Wave Optics '86, Atlanta, GA, WAA2, Feb. 86.

[2] P. Granestrand, L. Thylen, B. Stoltz, et. al., Integrated and Guided-Wave Optics '86, Atlanta, GA, WAA3, Feb. 86.

[3] G. A. Bogert, E. J. Murphy, and R. T. Ku, Integrated and Guided-Wave Optics '86, Atlanta, GA, PDP 3-1, Feb. 86.

[4] R. A. Spanke, IEEE Journal of Quantum Electronics, Vol. QE-22, No. 6, June 1986, p.964.

[5] K. Habara and K. Kikuchi, Electronics Letters, Vol. 21, No. 14, July 1985, p. 631.

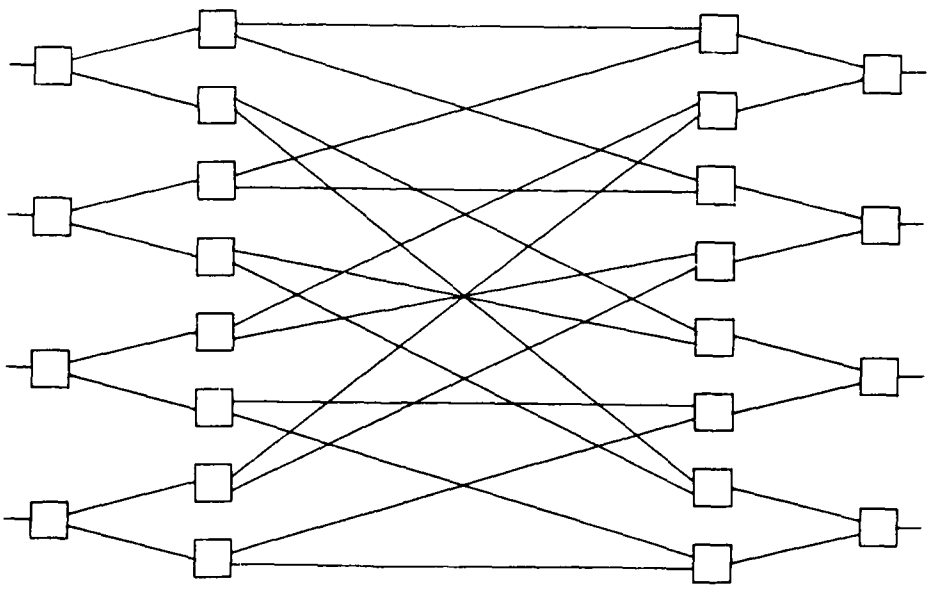

FIGURE 1

A New Architecture for Large Integrated Optical Switch-arrays

P J Duthie, M. J. Wale, I Bennion
Plessey Research Caswell Limited, Allen Clark Research Centre
Caswell, Towcester, Northants. UK

We propose a new reflective switch-array architecture, and describe process-tolerant waveguide-reflectors. Experimental results from a reduced 8 x 8 Ti:$LiNbO_3$ switch-array are presented and used to derive practical maximum array sizes.

Introduction

Optical switching will be required in future broad-band optical telecommunication systems where electrical components will not be able to switch the multi-GHz bandwidths envisaged. Optical switches have been described by several authors, e.g. [1] Arrays of optical switches integrated onto a single substrate have also been reported, [2], [3], [4]. These switches are essentially transparent to data rate and protocol. The largest array reported to date is an 8 x 8 crossbar switch [4], whereas many applications require very much larger switches. A major cost in an optical switching system will be the attaching of fibres to the chips. It is therefore desirable to maximise the number of switches on a single substrate, and to minimise the number of fibre connections.

Array Architectures

The first report of an integrated optical switch array was of a blocking five-switch 4 x 4 array [2]. Sixteen switches were required for a strictly non-blocking 4 x 4 switch [3] and 64 for a similar 8 x 8 switch [4]. A reduced switch design has been proposed by Marom [5]. This architecture allows non-blocking switches to be fabricated on smaller substrates than the equivalent strictly non-blocking switches. We now propose a reflective switch architecture which reduces the size of both non-blocking and strictly non-blocking switches and simplifies the problem of fibre alignment.

Integrated optical devices have a large aspect ratio determined by the interaction lengths of the device elements, together with the high loss of small radii curved waveguides. Present day device integration is restricted by the available 3" substrates. If the optical path can be folded, then a greater degree of device integration is possible. Tietgen [6] has described a 180^0 reflector based on a directional coupler. This device required electro-optic tuning to compensate for the imprecision in polishing the coupler to the required length. We have investigated a new design of reflector, whereby the waveguides are separated before reaching the reflection-coated polished edge of the substrate. A detailed account of the properties of these Ti: $LiNbO_3$ devices will be presented at the meeting. If the waveguides in a switch array are reflected in the manner described above, then a further set of switches can be interleaved with those before the reflectors. Figure 1 shows an 8 x 8 crossbar switch following this principle. As the inputs and outputs appear on the same edge of the substrate, only a single fibre-array need be aligned to the waveguides. Optimisation of alignment will be simpler than when two arrays are simultaneously aligned. The single reflection of figure 1 can be extended to multiple reflections, opening up a variety of possible architectures.

Reduced 8 x 8 Ti:$LiNbO_3$ Switch Array

In order to predict the properties of large switch-arrays, we have fabricated a number of small Ti:$LiNbO_3$ switch arrays based on the reduced 8 x 8 design reported by Marom [5]. Twenty-eight reverse $\Delta\beta$ directional coupler switches are defined in Z-cut $LiNbO_3$. To assess the effect of coupler properties varying across the substrate, we made devices with a variety of coupler inter-waveguide gaps. The switches are 4mm long, with Al electrodes over a SiO_2 buffer layer. The total length of the array is 68mm. One array is shown in Fig. 2. The devices were measured with TM polarised light of wavelength 1.3μm. For devices with the gap varying between 3μm and 5μm, the switching voltages varied between 27 and 35V, and the bias voltages varied between 5V and 21V. Differences between nominally identical test switches on either side of the arrays were of similar magnitude, but because the metallisation uniformity was optimised along the length of the array, rather smaller variations were observed on the array chips. A more detailed report of switch properties will be presented at the meeting.

Maximum Array Sizes

To calculate the maximum array size which can be made on a given substrate, we must know the switch-cell size, the switch crosstalk, the maximum permissable total crosstalk and the switch architecture. In the switch described above, the cell-length is 5.6mm. If a 2mm switch-length is used, as in reference 4, then the cell-length will be 3.6mm. If 3mm, then the cell-length will be 4.6mm. As the loss in an optical switch array can be arranged to be path-independent, the crosstalk is calculated by adding the crosstalk ofthe switches traversed by the signal. Thus for an n x n crossbar switch, the total crosstalk may be found by adding the crosstalk of 2n-2 bar states and one cross-state. For a permissable optical SNR of 11dB, corresponding to a BER of 10^{-7}, sufficient for video services, with crosstalks of -26dB (bar) and -26dB (cross) [1]; this corresponds to 31 switches - or a 16 x 16 array. To build such an array on a 70mm substrate would require a cell-length of 2.3mm. If however a reflective design was adopted, then the cell-length would be ~4.6mm.

Conclusion

We have described a new process-tolerant waveguide reflector, and an demonstrated an 8 x 8 reduced Ti:$LiNbO_3$ switch array. We have proposed a new reflective switch architecture and shown that a 16 x 16 switch array can be fabricated on a 3" wafer.

Acknowledgements

We thank R. Gibbs, E. Hindson and J. Hendy for assistance in device fabrication.

References

1 'Optical Switching and Modulation in Parallel Dielectric Waveguides', H. F. Taylor, J. Appl. Phys. Vol. 44 No 7 pp3257-3262

2 'Experimental 4 x 4 Optical Switching Network' R. Schmidt and L. Buhl, Electronics Letters Vol. 12 No 22 pp575-577

3 '4 x 4 Ti:$LiNbO_3$ Integrated-optical Crossbar Switch Array' L. McCaughan and G. Bogert, Appl. Phys. Letts., Vol 47 No 4 pp348-350

4 'Strictly Non-blocking 8 x 8 Integrated Optic Switch Matrix in Ti:$LiNbO_3$' P. Granestrand et al OFC/IGWO '86, Atlanta, WAA3

5 'Integrated Optics Switch Array Network Decomposition'
E. Marom, Optics Communications, Vol. 58, No2, pp92-94
6 '180^0-Turns in Integrated Optics'
K. Tietgen and R. Kersten, Optics Communications Vol. 36 No 4 pp281-284

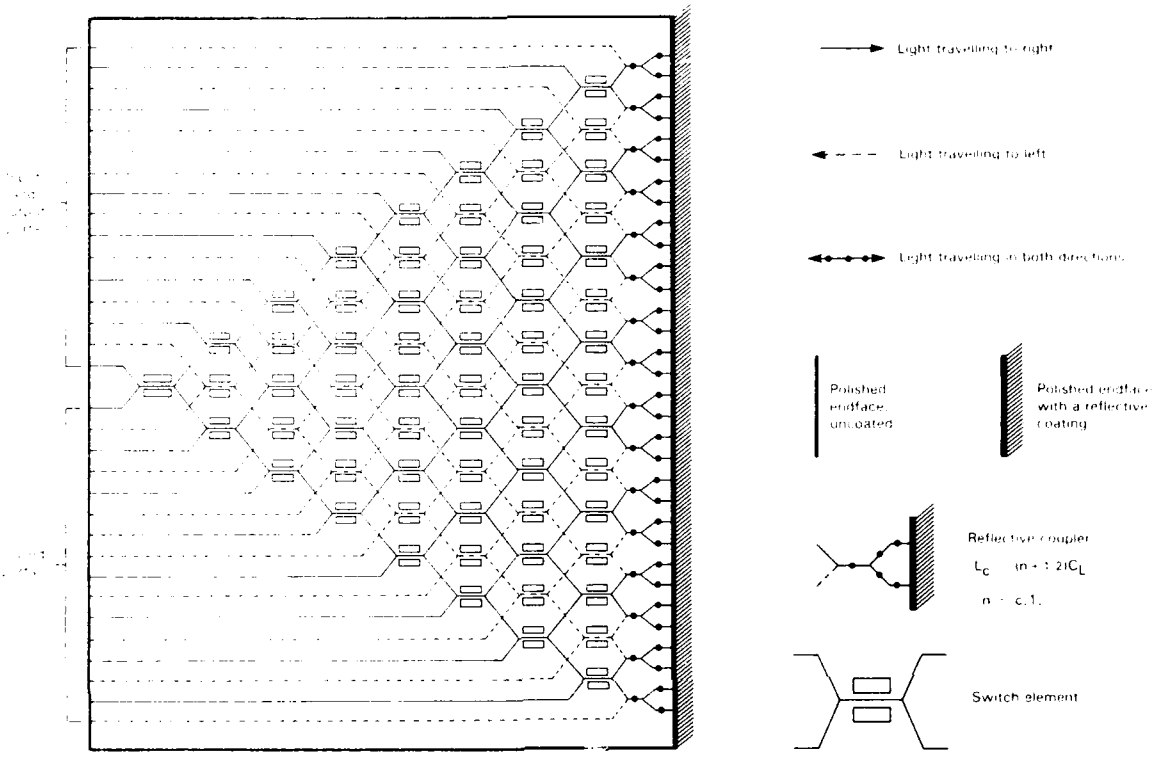

Fig 1 Strictly nonblocking reflecting 5 x 8 switch array

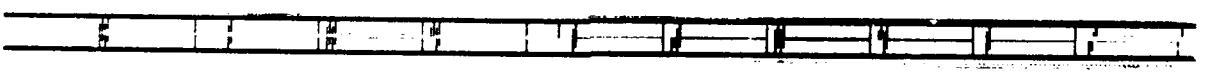

Fig 2 An 8 x 8 reflecting switch array in Ti:LiNbO

SYSTEM CONSIDERATIONS FOR THE LITHIUM NIOBATE PHOTONIC SWITCHING TECHNOLOGY

W. A. Payne
H. S. Hinton

AT&T Bell Laboratories
Naperville, Illinois 60566

1. INTRODUCTION

This paper discusses several system areas that require development prior to the successful implementation of the lithium niobate technology for photonic switching. The paper first describes several components required in a photonic switching system as well as the status of their development. It then discusses the system architectural areas that either require development or resolution. The final area discussed is the need for viable applications for photonic switching.

2. PHOTONIC COMPONENTS REQUIRING DEVELOPMENT

There are three major technical areas essential to eventual development of a $Ti{:}LiNbO_3$ photonic digital switching system. The first of these components is the directional coupler itself. The second factor is the further development of polarization maintaining fiber (PM fiber) which is used to interconnect different $LiNbO_3$ substrates as well as the driving lasers to the substrates. The third component is a thresholding optical amplifier. This amplifier cannot be a standard linear amplifier but one that has a threshold capability which allows it to improve the signal-to-noise ratio (SNR) of the photonic signal passing between the $LiNbO_3$ substrates.

2.1 Directional Couplers Device Design And Fabrication The center piece of the $Ti{:}LiNbO_3$ technology is the directional coupler [1]. These couplers can be interconnected to create larger photonic switching systems. The main limitation in interconnecting a large group of directional couplers to form a large switching network is the individual coupler crosstalk [2] [3]. At the current time switching matrices have been fabricated with 16 directional couplers all having crosstalk less than -30 dB [4].

2.2 Polarization Maintaining Fiber To minimize the required drive voltages, directional couplers have been optimized to operate on a single linear polarization. In most cases this is the TM polarization. This requirement reduces the required voltage from approximately 50 volts to the 10 to 15 volt range. These lower voltages are desired to allow high speed switching of the directional couplers. As light propagates through standard single-mode fiber its state of polarization can be changed. Thus, linearly polarized light injected into a single-mode fiber can have an elliptical polarization when it reaches a $LiNbO_3$ switching device. Another complicating factor is that the polarization effect of the fiber does not remain constant over time. To solve this problem PM fiber is required from the laser source to the $LiNbO_3$ substrates and between substrates.

2.3 Optical Amplifiers Most of the optical amplifiers under investigation are linear amplifiers [5]. These amplifiers have the disadvantage of amplifying the low level noise signals as well as the desired signals. Thus, the noise in the system is amplified along with the signal. With these type of optical amplifiers the SNR of a system limits its eventual size. In the ideal case there would be no amplification for signals below a given intensity level. Once an intensity threshold has been surpassed a large gain is desired [6]. A saturated or maximum value of output intensity is also desired. This type of thresholding amplifier is required to both amplify and improve the SNR of the signals passing between substrates of a dimensionally large photonic switching system.

3. SYSTEM ARCHITECTURAL CONSIDERATIONS

There are three main system level areas that need further study for the development of the lithium niobate technology. First we must find adequate switching techniques and architectures that provide good optical performance as well as a rich set of interconnection permutations. The maintenance of synchronization in a photonic network will be a very difficult task and is the second area of

importance. The third area would be concerned with the incorporation of transmission formats that allow easy integration of photonic switches.

3.1 Switch Architectures And Techniques There is a need to explore the implementation of larger switching matrices using the directional coupler arrays currently available. Most of the work has been on 4x4 arrays [4], but there has been an 8x8 array recently reported [7]. All of these have been crossbar configurations, and any larger matrices will be limited in size by the amount of crosstalk introduced to the signal. Recently there has been a report on other switch topologies [3] which reduce the crosstalk introduced to the signal.

There is also the need to enhance the interconnection richness through the introduction of time division switching. To date there have been only a couple of approaches reported [8][9]. These and/or other techniques need to be further refined to insure the use of photonic switching technology for a large set of applications.

3.2 Synchronization Some degree of synchronization must be maintained in the lithium niobate photonic switches. In order to maintain synchronization framing will likely need to be placed over the data stream [10]. Variation in the signal phase relationship at the switch occurs due to wander and jitter on the optical fiber (temperature variations, etc.). The framing bits must be processed (electronically) and then the optical data stream could be delayed appropriately by some type of elastic store. The electronic processing is performed on the order of the network frame time (currently $\approx 125\ \mu s$). The storage mechanism could be implemented using similar signal delay techniques to those described in [8][9]. Another alternative might be to use some sort of feedback mechanism to the optical sources of the network to insert/remove signal delay. The point is that there will need to be relatively complex synchronization electronics as well as possibly elastic storage capability at the photonic switch. The need for synchronization is not one unique to the photonic switch; the method of providing it in the photonic domain however needs more attention and study [10].

3.3 Transmission Formats As the transmission bit rates increase it becomes very difficult to reconfigure the lithium niobate array such that there is no loss of information. Thus gaps will probably need to be placed between information bursts or time slots. These gaps are considered reconfiguration overhead and should be minimized in order to get the highest transmission throughput. This fact promotes the use of a block multiplexing scheme where for example an entire DS3 frame becomes the basic switching quanta.

The recommended format (SYNTRAN [11]) for multiplexing DS0 and DS1 signals to the DS3 rate provides for byte interleaving thus allowing the DS0s and DS1s to be easily identifiable. Transmission formats for signals above the DS3 rate however, are currently viewed to involve bit multiplexing (ex. SONET [12]). Although this relieves the need for large amounts of high speed memory in the transmission equipment, it places a heavy burden on the rate of reconfiguration of the switching system. If gaps need to be placed in the information stream then transmission formats should be reevaluated to reduce the necessary overhead.

As an example, in the FT series G transmission systems a 1.7 Gb/s data stream contains 36 frames of DS3 information. The bits of these frames, plus overhead bits, are interleaved and mixed to the point that individual DS3 frames can not be extracted from the stream unless that stream is at least partially demultiplexed down to DS3 channels. By requiring that the DS3 frames be block multiplexed onto the high speed channel with a small gap between them, individual extraction and insertion of DS3 frames should be possible. This also reduces the rate of reconfiguration of the switch array.

4. APPLICATIONS/CONCLUSIONS

Perhaps the key component required to drive the $Ti{:}LiNbO_3$ technology into the marketplace within the next three to five years is a *good* application. A *good* application requires that the strengths of this new technology be used. The strength of directional couplers is their ability to control extremely

high bit-rate information. The high data rates allowed by this technology eliminate the needs for highly parallel electronic switching architectures and all of the problems associated with them (demultiplexing/multiplexing, wide high speed data busses, electrical crosstalk, large amounts of circuitry, etc.). The technology currently is however limited by several factors: 1) the electronics required to control them limits their switching speed, 2) the long length of each directional coupler prevents large scale integration, 3) for large switching systems thresholding optical amplifiers will be required to clean-up and amplify the signals as they pass from substrate to substrate, and 4) some sophisticated high speed electronic processing is still required for synchronization between the transmission and switching equipment.

REFERENCES

[1] R. C. Alferness and R. V. Schmidt, "Directional Coupler Switches, Modulators, and Filters Using Alternating Delta-Beta Techniques," IEEE Trans. Circ. and Sys., Vol. CAS-26, No. 12, Dec. 1979, pp. 1099-1108.

[2] H. S. Hinton, "A Non-Blocking Optical Interconnection Network Using Directional Couplers," Proceedings of the IEEE Global Telecommunications Conference, Vol. 2, pp. 885-889, November 1984.

[3] R. A. Spanke, "Architectures for Large Nonblocking Optical Space Switches," IEEE Journal of Quantum Electronics, Vol. QE-22, No. 6, June 1986, pp. 964-967.

[4] G. A. Bogert, "A Low Crosstalk 4x4 $Ti{:}LiNbO_3$ Optical Switch with Permanently Attached Polarization-Maintaining Fiber Arrays," Topical Meeting on Integrated and Guided-Wave Optics, Atlanta, Georgia, pp. PDP 3.1-3, February 1986.

[5] S. Kobayashi and T. Kimura, "Semiconductor Optical Amplifiers," IEEE Spectrum, May 1984, pp.26-33.

[6] Y. Silberberg, "All-Optical Repeater," Optics Letters, Vol. 11, No. 6, June 1986.

[7] P. Granestrand et al, "Strictly Nonblocking 8x8 Integrated-Optic Switch Matrix in $Ti{:}LiNbO_3$," Topical Meeting on Integrated and Guided-Wave Optics, Atlanta, Georgia, paper WAA3, p. 4, February 1986.

[8] R. A. Thompson and P. P. Giordano, "Experimental Photonic Time-Slot Interchanger Using Optical Fibers as Reentrant Delay-Line Memories," Topical Meeting on Integrated and Guided-Wave Optics, Atlanta, Georgia, paper TUB4, p.26, February 1986.

[9] H. Goto et al, "An Experiment On Optical Time-Division Digital Switching Using Bistable Laser Diodes and Optical Switches," Proceedings of the IEEE Global Telecommunications Conference, Vol. 2, November 1984, pp. 880-884.

[10] J. R. Erickson et al, "A 1.5 Gb/s Time-Multiplexed Photonic Switching Experiment," Submitted to this Conference.

[11] G. R. Ritchie,"SYNTRAN- A New Direction for Digital Transmission Terminals," IEEE Communications Magazine, Vol. 23, No. 11, November 1985, pp 20-25.

[12] R. Boehm, "Synchronous Optical Networks Concept," Technical Requirements Industry Forum (TRIF), St. Louis, MO, April 1985.

High-Speed $\Delta\beta$-Reversal Directional Coupler Switch

R.C. Alferness, L.L. Buhl, S.K. Korotky,
and R.S. Tucker

AT&T Bell Laboratories
Crawfords Corner Road
Holmdel, NJ 07733
(201) 949-2062

Waveguide electro-optic directional coupler crosspoints find use in many applications including modulators and switches for optical fiber communication.[1] Recently there has been significant progress in titanium-diffused lithium niobate ($Ti{:}LiNbO_3$) devices in both of these areas.[2],[3] To date, however, the emphasis of the device performance for modulation has been speed, drive voltage, and insertion loss; whereas, for switching it has been level of integration crosstalk, and insertion loss. Presently, for example, the switch arrays can be reconfigured only relatively slowly (0.1-1 GHz) and are appropriate for space division switching applications. However, optical switches capable of low crosstalk at reconfiguration rates above 1 GHz are important for time-division switching applications such as optical time-division multiplexing (OTDM).[4] The requirements for use in modulation and switching are, in fact, not necessarily conflicting. In this paper we describe a directional coupler crosspoint structure designed specifically for switching at multi-gigahertz reconfiguration rates with low (< -20 dB) crosstalk in both switch states.

Important to fast reconfiguration times and device integration is that the two switch states are achieved with a single-pole-throw, that is it is necessary to change the voltage on only one terminal to switch between states. Our design for achieving this form of operation is shown schematically in Fig. 1. It consists of a waveguide directional coupler and a coplanar waveguide electrode. The structure is configured as a $\Delta\beta$-reversal switch [5] so that both states may be attained with low crosstalk without strict fabrication tolerances. The reversal of the applied phase mismatch required to achieve a low crosstalk cross state is built into the electrode by shifting the position of the electrode at the midpoint of the directional coupler interaction length. As shown, a three-electrode structure (i.e. coplanar waveguide) is required to achieve a push-pull index change on z-cut lithium niobate. The electrode may be driven as a lumped element, or, for very high-speed operation, as a traveling-wave line as illustrated. A resonant design is also possible. To minimize the voltage swing required to switch between crossover (cross) and straight-through (bar) states for a strict $\Delta\beta$-reversal switch, the directional coupler length and interwaveguide gap are chosen so that the coupler is approximately 2 coupling lengths long.[5]

For the present device the coupler length is $\sim$1 cm and the gap is 5.5 μm. The waveguides were fabricated using 1000 Å thick, 6 μm wide titanium strips that were diffused at 980 °C for 4 hours. The electrode transmission line has a gap/width ratio of 0.75, yielding a characteristic impedance of 32 Ω. It consists of 3 μm thick electroplated gold. The center line has an end-to-end dc resistance of 5 Ω.

The dc operation of this switch, the crossover efficiency versus drive voltage, is shown in Fig. 2. Both the cross and bar states can be achieved with low crosstalk (better than -25 dB) by changing a single control voltage. The switch voltage is 9 volts. To our knowledge this is the first demonstration that crosstalk levels for both switch states suitable for switching applications can be achieved with a single drive voltage. We have measured the switch

crosstalk at a reconfiguration rate of 1 MHz and found the crosstalk to be better than -20 dB.

We expect the high frequency operation to be limited by optical/electrical velocity mismatch and electrical losses that destroy the balanced (equal but opposite) index change over the first and second halves of the coupler, which is required to achieve a low crosstalk cross and bar state. These effects were examined by calculating the response of a traveling-wave $\Delta\beta$-reversal switch to a sinusoidal electrical drive. Both walkoff and rf losses are taken into consideration. We have assumed that the 1 cm active length corresponds to 2.3 coupling lengths. The peak-to-peak drive voltage for the calculation was chosen to minimize the crosstalk and is approximately 1.4 times the voltage necessary for switching at dc. The calculations summarized in Fig. 3 indicate that crosstalk levels lower than -20 dB should be possible for toggle-rates as high as 4 GHz with a device having 1 cm active length. Measuring low crosstalk at high repetition rates can present a problem. To improve the sensitivity of the measurement we employ a optical sampling arrangement similar to that reported previously.[6] Results for high-speed operation will be reported at the conference.

In summary we describe a traveling-wave $\Delta\beta$-reversal directional coupler optical switch capable of very low crosstalk operation in both switch states at gigahertz rates. Such high-speed crosspoints will be important for tree-configured OTDM switch architectures.

REFERENCES

[1] R.C. Alferness, IEEE J. Quantum Electron. **QE-17**, 946 (1981).

[2] S.K. Korotky, G. Eisenstein, A.H. Gnauck, B.L. Kasper, J.J. Veselka, R.C. Alferness, L.L. Buhl, C.A. Burrus, T.C.D. Huo, L.W. Stulz, K. Ciemiecki Nelson, L.G. Cohen, R.W. Dawson, and J.C. Campbell, J. Lightwave Technol. **LT-3**, 1027 (1985).

[3] P. Granestrand, B. Stolz, L. Thylen, K. Bergvall, W. Doldissen, H. Heinrich, and D. Hoffmann, Elec. Lett. **22**, 816 (1986).

[4] R.S. Tucker, G. Eisenstein, U. Koren, S.K. Korotky, G. Raybon, J.J. Veselka, L.L. Buhl, and R.C. Alferness, in proceedings of Conf. on Optical Fiber Comm., Reno, Nevada, 1987, paper WO2.

[5] H. Kogelnik and R.V. Schmidt, IEEE J. Quantum Electron. **QE-12**, 396 (1976).

[6] R.C. Alferness, N Economou, and L.L. Buhl, Appl. Phys. Lett. **37**, 597 (1980).

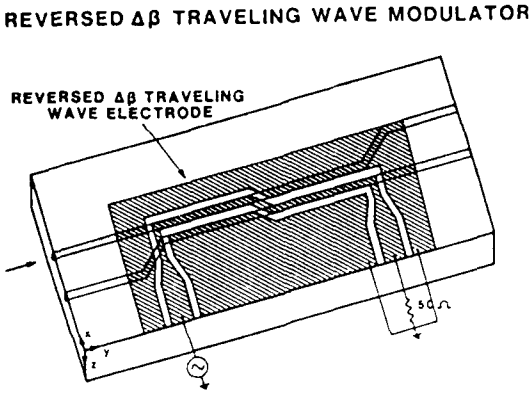

Fig. 1: Schematic of the single-pole traveling-wave $\Delta\beta$-reversal directional coupler switch

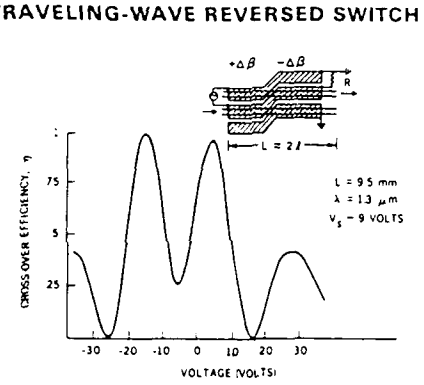

Fig. 2: Experimental switching curve (dc) for coupler configured with a geometry-induced $\Delta\beta$-reversal

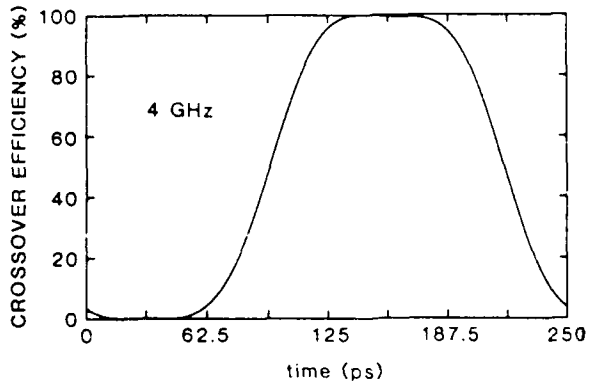

Fig. 3: Calculated response of 1 cm switch at 4 GHz. Optical/Electrical velocity mismatch and rf propagation loss are taken into account.

FRIDAY, MARCH 20, 1987

PROSPECTOR/RUBICON ROOM

8:30 AM–10:00 AM

FA1–5

PHOTONIC DEVICES: 1

William J. Stewart, Plessey Research (Caswell) Ltd.,
Presider

PHOTONIC SWITCHING DEVICES BASED ON MULTIPLE QUANTUM WELL STRUCTURES

D. A. B. Miller,

AT&T Bell Laboratories,

Holmdel, New Jersey 07733

Quantum well (QW) structures consist of alternate thin (e.g. 100 Å) layers of two different semiconductors such as GaAs and AlGaAs. Electrons and holes tend to be confined in the semiconductor with the narrower band gap (e.g. GaAs). New physical properties result from this confinement, and these properties can be engineered through choice of layer thicknesses and compositions. One specific consequence of confinement is that the optical absorption spectrum is changed significantly compared to conventional semiconductors, acquiring a step-like structure and also relatively sharp and strong absorption peaks at the edges of the steps even at room temperature. These peaks are called exciton absorption resonances, and they are normally only seen at low temperatures in conventional semiconductors.[1]

One mechanism associated with these resonances, the quantum-confined Stark effect (QCSE),[2,3] is unique to QW's at any temperature. In the QCSE, electric fields applied perpendicular to the QW layers cause the exciton peaks to move in energy. The most obvious application of this is to optical modulators.[3] The changes of absorption coefficient are large, and devices can be made that are only microns thick but that show substantial modulation (e.g. 3 dB) for applied voltages of 5-10 V; such devices can operate with the light propagating perpendicular to the layers. It is also possible to make waveguide devices where the light propagates along the layers. These can show much greater modulation depth (e.g. 10 dB) and can have lower drive voltages (e.g. < 1V) [4] These devices all operate by absorption, and hence do not reroute the information in the way that a directional coupler does. Their insertion loss

need not be very high, and they have been demonstrated to operate at high speeds (e.g. 100 ps). Recent calculations suggest that it may be possible to make refractive devices such as directional couplers based on the changes in refractive index associated with the QCSE.[5] These calculations also predict that the chirp in absorption modulators will be small. Although most of the work has been on GaAs/AlGaAs material operating at $\sim$ 850 nm, other materials have been investigated for longer wavelength applications. Recently, very clear QCSE has been observed in InGaAs/InP QW's at $\sim$ 1.6 μm.[6]

The QCSE can also be applied to make devices that are controlled by light by making structures that incorporate both a photodetector and a QCSE modulator. Several such "self electro-optic effect devices" (SEED's) have been demonstrated, including optically-bistable switches and optical level shifters.[7,8] The bistable devices are capable in principle of performing logic operations. 2×2 arrays of integrated devices have been reported with good uniformity,[8] and recently fully-functional 6×6 arrays have been demonstrated. Such devices are promising for possible parallel optical architectures for photonic switching.

Much work remains to be done to apply QW devices to practical photonic switching systems. The devices do however have several attractions: they operate at room temperature; they have relatively low operating energy densities; and they are compatible with semiconductor laser diodes, detectors and electronics in wavelengths, powers, voltages, and materials systems.

References

[1] See D. S. Chemla and D. A. B. Miller, J. Opt. Soc. Am. **B2**, 1155 (1985) for a discussion of quantum well optical properties.

[2] D. A. B. Miller, D. S. Chemla, T. C. Damen, A. C. Gossard, W. Wiegmann, T. H. Wood, and C. A. Burrus, Phys. Rev. **B32**, 1043 (1985)

[3] For a recent summary of work on modulators and the QCSE, see D. A. B. Miller, J. S.

Weiner, and D. S. Chemla, IEEE J. Quantum Electron. **QE-22**, 1816 (1986)

[4] J. S. Weiner, A. C. Gossard, J. H. English, D. A. B. Miller, D. S. Chemla, and C. A. Burrus, (to be published)

[5] J. S. Weiner, D. A. B. Miller, and D. S. Chemla, (to be published)

[6] I. Bar-Joseph, C. Klingshirn, D. A. B. Miller, D. S. Chemla, U. Koren, and B. I. Miller, (to be published)

[7] D. A. B. Miller, D. S. Chemla, T. C. Damen, T. H. Wood, C. A. Burrus, A. C. Gossard, and W. Wiegmann, IEEE J. Quantum Electron. **QE-21**, 1462 (1985)

[8] D. A. B. Miller, J. E. Henry, A. C. Gossard, and J. H. English, Appl. Phys. Lett. **49**, 821 (1986)

Room Temperature Excitonic Nonlinear Absorption in GaAs/AlGaAs Multiple Quantum Well Structures Grown By Metalorganic Chemical Vapor Deposition (MOCVD)*

H. C. Lee, A. Hariz, and P. D. Dapkus
Department of Electrical Engineering and
Center for Photonic Technology
University of Southern California, Los Angeles, CA 90089-0483

and

A. Kost, M. Kawase, and E. Garmire
Department of Electrical Engineering and
Center for Laser Studies
University of Southern California, Los Angeles, CA 90089-1112

Room temperature excitonic nonlinear absorption in multiple quantum wells (MQW) has great potential for making low-power high-speed optical switching devices. The required ultrathin multilayers have been grown by both molecular beam epitaxy (MBE) and metalorganic chemical vapor deposition (MOCVD). Efficient, narrow-linewidth luminescence and low-threshold laser operation have been achieved in MQW's with both techniques. However, virtually all of the reported work to date dealing with nonlinear optical properties has employed MBE-grown materials [1], [2], [3]. The implementation of arrays of photonic switches in optical computing and processing systems will require large area devices with uniformity that exceeds the capability of current technology. The potential advantages of MOCVD for large area, multiple wafer growth of these complex structures provides motivation to explore this technique for their fabrication. In this paper, the growth by MOCVD of GaAs/AlGaAs MQW structures that exhibit narrow-line, room temperature excitonic absorption are reported. We further describe the linear and nonlinear optical properties of these structures and discuss the implications of this work for the construction of large area arrays of switches.

Narrow linewidth excitonic absorption in MQW structures requires a low concentration of free carriers and ionized impurities to avoid screening and Stark broadening of the exciton. Additionally, low threshold nonlinear effects require relatively long minority carrier lifetimes in the quantum wells. These conditions present a set of conflicting requirements upon the MOCVD growth conditions. The purity of GaAs grown by MOCVD increases rapidly with decreasing growth temperature. The highest purity materials are grown in the range 600-650C [4]. On the other hand, the highest luminescence efficiency and longest minority carrier lifetimes in MQW structures and in AlGaAs bulk materials are observed in structures grown at relatively high temperatures (~750C) [5]. The tradeoffs required to achieve excitonic absorption at room temperature in these structures have been investigated. The photoluminescence, excitation spectra, and absorption properties of single quantum well (SQW) and MQW structures grown under a variety of growth conditions have been used to determine the optimal growth conditions for the fabrication of these devices. These characteristics will be discussed and an optimization methodology that does not require the growth of thick multilayers will be described.

Fig. 1 shows the PL spectra of three representative MQW structures grown at various temperatures and the dependence of the relative PL intensity upon excitation intensity of each. The structural properties of these samples are annotated in Table I. The samples grown at lower temperature have narrower PL linewidth and lower PL efficiency than those grown at higher temperatures. These effects are the result of lower free carrier concentration in the GaAs wells and higher trap density in the AlGaAs barriers, respectively, in the samples grown at lower temperatures. Note that the traps in the low temperature sample saturate at moderate excitation intensities.

Sample #	TMG Source	Growth Temp	Background Concentration	Periods	Tw well Thickness	Tb barier Thickness	Al Comp.	Ehh (eV)	Elh (eV)	FWHM (meV)
v158	TA5	650 C	6 E 14	61	100 A	100 A	0.32	1.4571	1.4659	15.4
v159	TA5	700 C		61	100 A	100 A	0.32	1.4553	1.4663	18.8
v160	TA5	750 C		61	100 A	100 A	0.32	1.4588		20.8
v136	AV4	730 C	4 E 16	51	100 A	100 A	0.32	1.4588		>20

Table 1

The substrates of MQW samples have been removed by selective etching and PL measurements performed on the first grown layers to confirm that the linewidths observed were uniform throughout the structures. In addition, linear absorption measurements have been performed after the substrates were removed. Results from samples V136, V158, and V159 are shown in Fig. 2. Enhanced absorption near the band edge, ascribed to the exciton resonance, is observed in samples with lower carrier concentration. The sample with the high carrier concentration shows no exciton absorption feature. Higher resolution evidence for the presence of excitonic absorption is observed in room temperature excitation spectra of sample V158 shown in Fig. 3. The heavy and light hole exciton transitions are well resolved in this case. The excellent correspondence observed between the PL and the absorption measurements in MQW samples and the previous correspondence in the PL of SQW and MQW materials has allowed us to further optimize the materials by growing SQW structures and monitoring the PL of these structures.

Absorption saturation has been observed in these materials both on and off the exciton resonance. The cw excitations were provided by a dye laser/mode-locked argon ion laser system. Styryl-9M dye was used to provide wavelengths in the range 780nm-900nm. The bleaching of excitonic absorption is clearly seen in the absorption spectra at various excitations shown in Fig. 4. Low saturation intensity (249 W/cm2) is obtained. The extrapolation method of saturation intensity will be further explained in detail.

In conclusion, excitonic nonlinear absorption in GaAs/ AlGaAs MQW structures has been observed in samples whose growth conditions were optimized for this purpose. The conditions required for the observation of these effects in MOCVD grown materials will be described and the most recent results in this ongoing program to develop low threshold switches in MQW structures will be reported.

* This work has been partially supported by AFOSR grants 84-0305,85-0297, by NASA Grant No. NAG 3-529, and by USC' s Joint Services Electronics Program F49620-85-C-0071.

References

[1] D. S. Chemla, D.A.B. Miller, P. W. Smith. Optical Engineering, vol. 24, no. 4, pp. 556-564, 1985.

[2] D. S. Chemla, J. Lumin. 30, pp. 502-519, 1985.

[3] D. A. B. Miller, D. S. Chemla, D. J. Eilenberger, P. W. Smith, A. C. Gossard, W. T. Tsang, Appl. Phys. Lett., 41 (8), pp. 679-681, 1982.

[4] P. D. Dapkus, H. M. Manasevit, K. L. Hess, T. S. Low, G. E. Stillman, J. Crystal Growth, 55, pp. 10-13, 1981.

[5] R. C. Miller, R. D. Dupuis, P.M. Petroff, Appl. Phys. Lett., 44 (5), pp. 508-510, 1984.

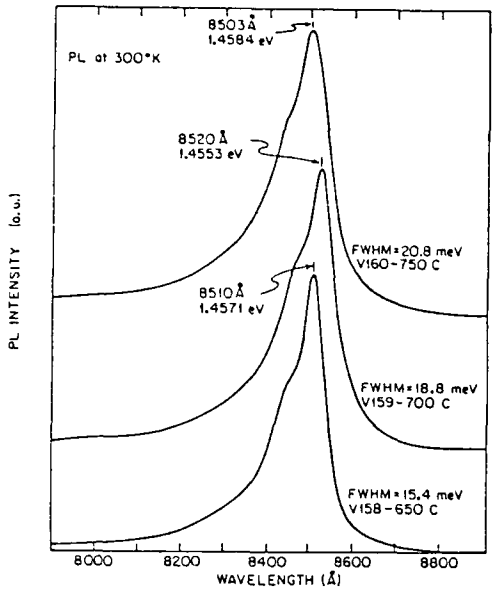

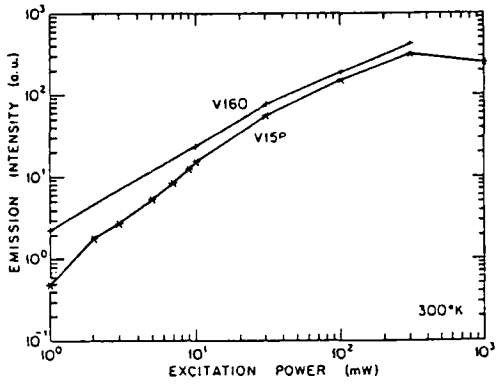

Fig. 1(a) Photoluminescence spectra of MQW structures grown at 650 C, 700 C and 750 C.
Fig. 1(b) Photoluminescence intensity versus excitation power of two MQW structures grown at 650 C and 750 C.

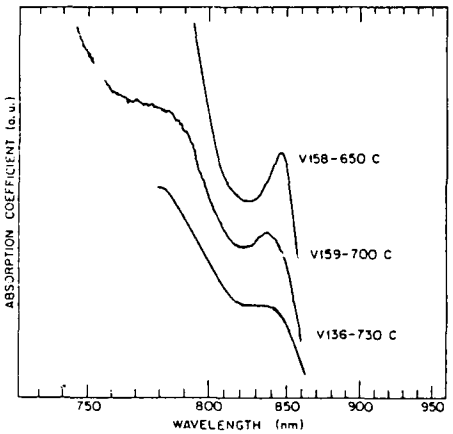

Fig. 2 Absorption spectra of MQW structures grown at 650 C, 700 C, and 730 C.

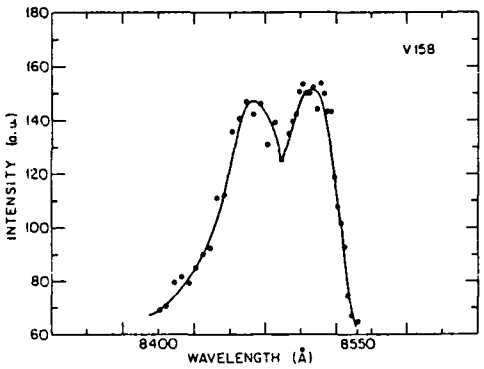

Fig. 3 Excitation spectrum of sample v158 (grown at 650 C). Detection wavelength was fixed at 856nm.

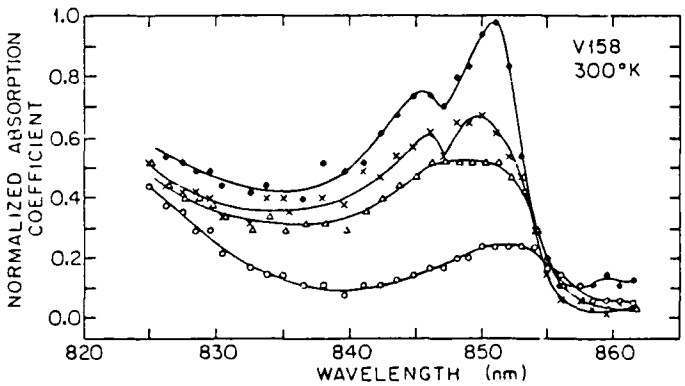

Fig. 4 Aborption saturation versus wavelength at different excitation intensities. (♦): 25W/cm2; (x): 251W/cm2; (Δ): 752W/cm2; (o): 7520W/cm2.

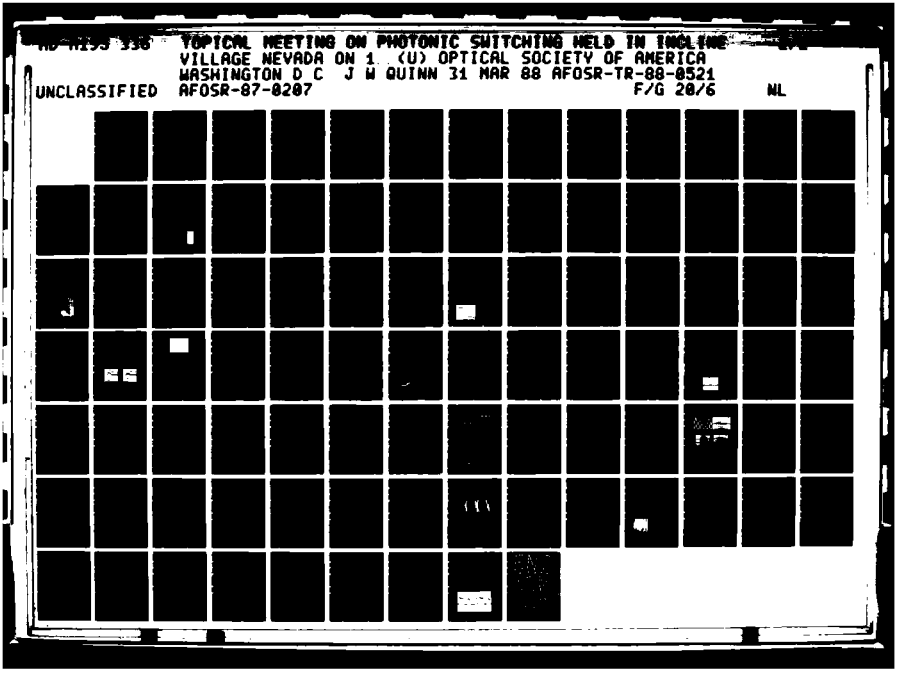
TOPICAL MEETING ON PHOTONIC SWITCHING HELD IN INCLINE
VILLAGE NEVADA ON 1 (U) OPTICAL SOCIETY OF AMERICA
WASHINGTON D C J W QUINN 31 MAR 88 AFOSR-TR-88-0521
UNCLASSIFIED AFOSR-87-0207 F/G 20/6 NL

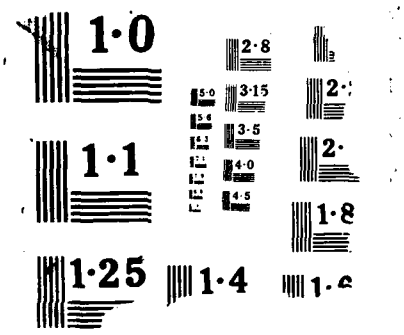
1·0
1·1
1·25
1·4
2·8
3·15
3·5
4·0
4·5
5·0
2·
1·8

A Hard-Limiting Opto-Electronic Logic Device

P.Wheatley,M.Whitehead,P.J.Bradley,G.Parry,J.E.Midwinter

Dept of Electronic and Electrical Engineering
University College London,
Torrington Place, London, WC1E 7JE

P.Mistry,M.A.Pate,J.S.Roberts

Dept of Electronic Engineering,
University of Sheffield,
Mappin Street, Sheffield, U.K.

We report the first demonstration of a novel non-resonant opto-electronic device suitable for optical logic, but which is not bistable. The operation of the device is based on the principle of a current driven multiple quantum well electro-absorption modulator which was first established in the 'self-linearized modulator' (1). By including electronic gain in the device and exploiting the limiting response of the device outside the self-linearising region, the device can be used as a logic gate with high optical gain and outputs which are 'hard limited'. The device, although it is not all-optical, does overcome many of the serious shortcomings of optical bistables device which have been outlined in ref.2.

The device consists of a photo-transistor in series with a photo-conductive electro-absorption modulator between a constant voltage supply and ground. The photo-absorption of the modulator should increase with applied voltage at least up to the supply voltage. A constant optical power, referred to as the pump beam, is applied to the modulator and a second, variable, optical power, referred to as the signal, is applied to the base of the photo-transistor.

The operation of the device is as follows. The signal beam causes the photo-transistor to pass a photo-current roughly proportional to the signal power. Because of the transistor gain the effective quantum efficiency is much greater than unity. The pump beam gives rise to photo-current through the modulator which is proportional to the power absorbed, but since there is no gain here, the quantum efficiency is less than one. To obey Kirchhoff's current law, these two currents must be equal. If they are not, then charge builds up on the modulator affecting its absorption in such a way as to equalise the two currents (1). The absorption of the modulator has a

maximum and mimimum value and if the transistor current requires the absorption to be above or below this range, charge builds up in such a way as to reduce quantum efficiency thereby equalising the currents. Absorption in these cases is constant. Thus as the signal is increased from zero, the transmitted power is firstly high and constant, then falls off rapidly and for large signals is low and constant.

The device was realised using a commercially available discrete silicon photo-transistor and a GaAs/AlGaAs multi-quantum-well electro-absorption modulator, grown by the SERC Central Facility at the University of Sheffield using MOVPE. The device is shown schematically in fig.1. The pump beam had a wavelength of 865nm and the signal beam was given by an LED. The experimental response curve, fig.2, shows an almost ideal hard limiting response with large flat noise thresholds on either side. The region in between exhibits a smooth slope with an optical gain of about ten. Although the constrast is poor, the full change in transmission of the modulator was used.

Several other features of this device configuration are worthy of note. Placing two photo-transistors in parallel forms a dual input OR gate, two in series a dual input AND gate. In case, truly independent input ports and good I/O isolation are achieved. We also note that the absence of positive feedback, as in bistable devices, means none is affected by the critical slowing down phenomenon. The discrete components are fundamentally fast, substantially sub-nanosecond, and in monolithic form the device is expected to exhibit very fast logic with a power-speed in the sub pico-joule range.

In conclusion, we have demonstrated what we believe to be the first potentially cascadable three-terminal optical logic device, overcoming the major problems of optical bistable devices. Although the device is not all-optical, it uses optical input and output and only requires a d.c. voltage supply. It is not critically dependent on any parameter and its present weaknesses are largely technological and are not fundamental physical limitations.

References

1. MILLER, D.A.B., CHEMLA, D.S., DAMEN, T.C., WOOD, T.H., BARRUS, C.A., GOSSARD, A.C. and WIEGMANN, W., "Novel optical level shifter and self-linearized optical modulator using a quantum well Self-Electro-optic Effect Device", Optics Letters 9 (1984), p.567.

2. KEYES, R.W., "Optical logic-in the light of computer technology", Optica Acta 32 (1985), p.525.

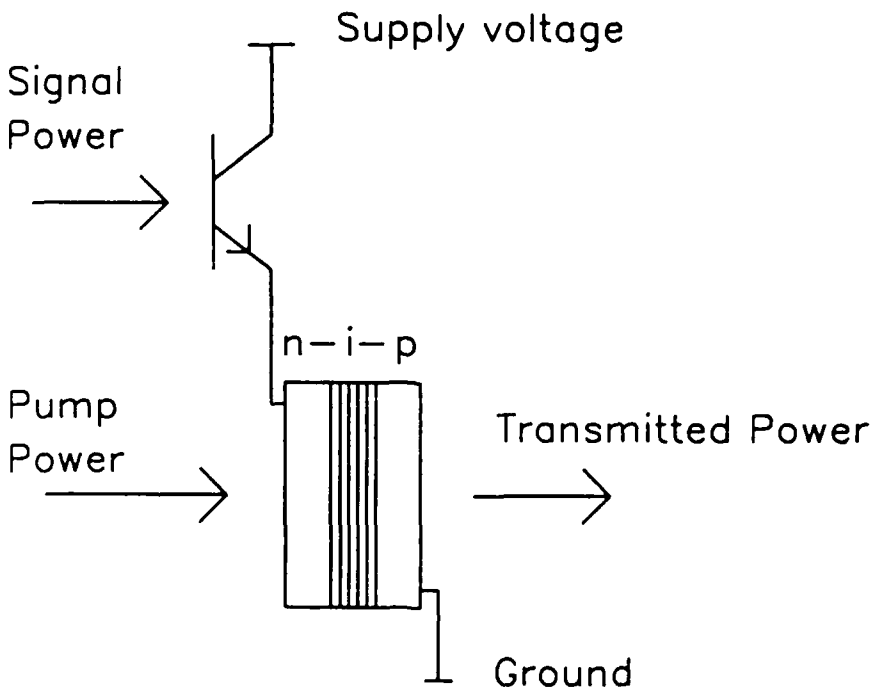

Fig 1. Schematic Diagram of Device

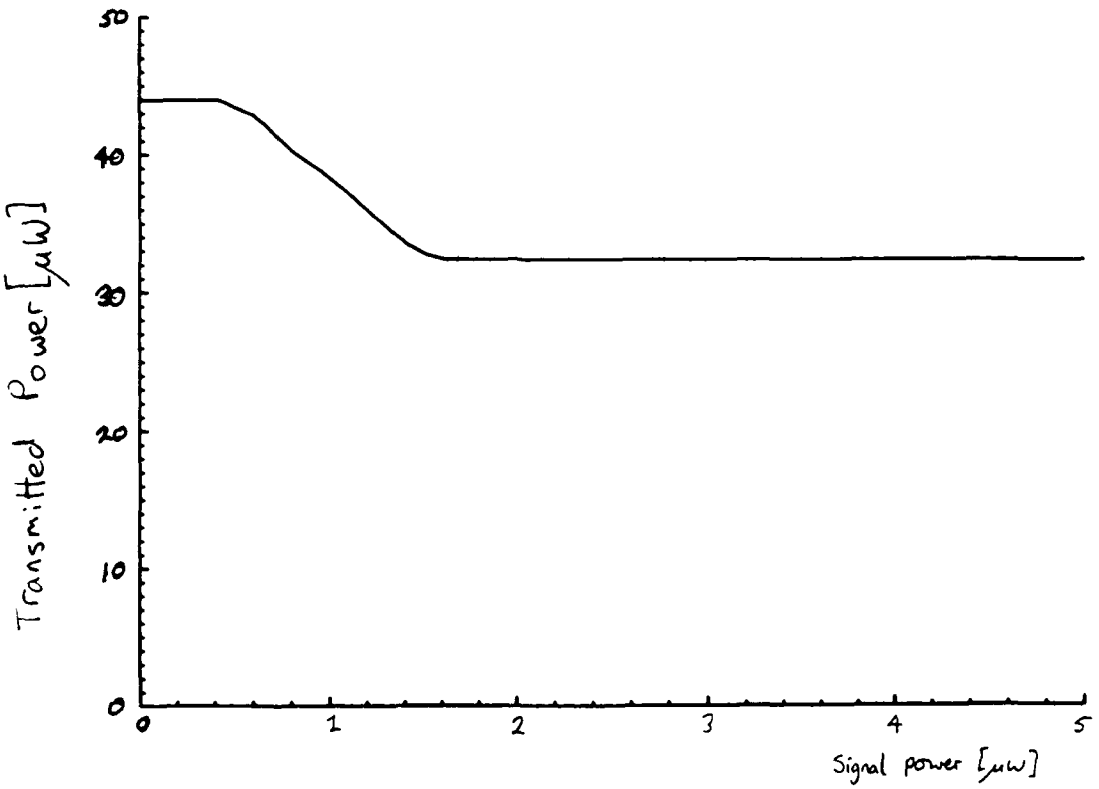

Fig 2. Input-Output Characteristic

Picosecond optical beam coupling in photorefractive GaAs

George C. Valley, Arthur L. Smirl,
Hughes Research Laboratories
3011 Malibu Canyon Road
Malibu, CA 90265
(213) 317-5435

Klaus Bohnert, Thomas F. Boggess
Center for Applied Quantum Electronics
Department of Physics
North Texas State University
Denton, TX 76203

We recently reported observations of the photorefractive effect in GaAs using beam coupling with 40-picosecond pulses.[1] In these observations, several effects interact to modify the transmission of a weak probe pulse in the presence of a strong pump pulse from that experienced by the weak probe pulse alone. The photorefractive effect transfers energy from one beam to the other in a direction controlled by the crystallographic axes.[2] Transient energy transfer due to the free-carrier grating transfers energy from the strong pump to the weak probe.[3] Two-photon absorption due to the presence of the strong pump causes enhanced probe loss. In addition, effects of lesser importance such as saturation of the donor and acceptor absorption at the EL2 and EL2+ levels, absorption gratings, and free-carrier absorption modify the probe transmission in the presence of the pump.

We have previously presented results for spatially and temporally overlapping beams that show a net photorefractive energy transfer from 1 to 10% for fluences of 0.1 to 10 mJ/cm^2.[1] A fluence of 0.1 mJ/cm^2 corresponds to 1 $pJ/\mu m^2$ or assuming a 1 μm by 1 μm pixel, a picojoule per pixel. Here we present beam coupling results at a fluence of 2.3 mJ/cm^2 for probe delays of -40 to +60 ps. Fig. 1 shows experimental results for the normalized change in probe transmission, $\Delta T/T$, as a function of delay; the ratio of probe to pump energy incident on the crystal is 1:23 while the period of the pump-probe interference pattern is 1.7 μm. The two sets of data correspond to two orientations of the GaAs crystal, one in which the photorefractive effect transfers energy from the pump to probe (upper curve) and vice versa (lower curve). Note that the maximum transfer of about +2% is obtained for probe delay of -10 ps. This compares to about -4% for zero delay.

The results shown in Fig. 1 can be understood qualitatively in terms of the time dependence of the three major effects. There are three properties of each effect

that are known qualitatively: sign of the normalized probe transmission, delay of the probe relative to the pump, and the temporal width. Two-photon absorption is always negative, its delay dependence is symmetric about zero, and it follows the pump intensity profile (a Gaussian with a 43-ps full width at 1/e of intensity) as shown by the dot-dash curve in Fig. 2. The photorefractive component, which can be unambiguously separated from the experimental results by differencing the two sets of data in Fig. 1, is either positive or negative depending on crystal orientation, shows a maximum for a probe that leads (negative delay) the pump beam, and has a temporal width that is roughly that of the pump. The maximum lags zero delay because the build-up time for the photorefractive grating is substantially greater than the pulse length, so that a trailing pump sees a larger grating than a leading pump. Transient energy transfer is always positive for a weak probe beam, is larger for a trailing pump pulse, and has a temporal width roughly that of the pump squared because this process is proportional to intensity cubed while the photorefractive and two-photon absorption are proportional to intensity squared. Summing the dashed curve, the dot-dash curve, and the positive and negative solid curves (corresponding to the photorefractive effect for the two crystal orientations) yields the small dashed curves shown on Fig. 2. These curves are in good qualitative agreement with the results in Fig. 1.

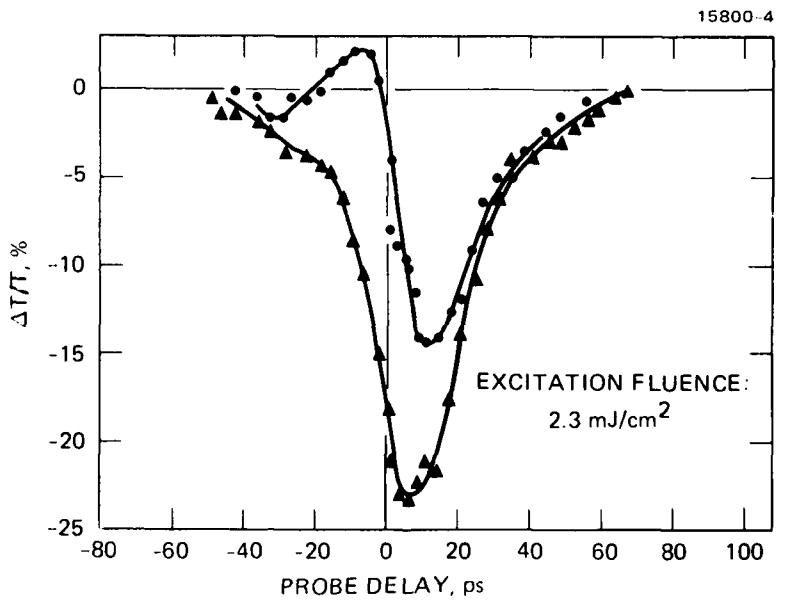

Fig. 1. The normalized change in probe transmission as a function of time delay between the two pulses for an excitation fluence of 2.3 mJ/cm^2, a grating spacing of 1.7 μm and a pump-to-probe ratio of 23:1. The sample was rotated by 180° about the surface normal between measurements represented by the triangles and the dots.

A detailed computational model of transient energy transfer in GaAs has been used to interpret the zero-delay data,[1] and results from this code for non zero pump probe delay will be compared to the data in Fig. 2 and used to determine optimum parameters for optical switching.

References

1. G.C. Valley, A.L. Smirl, M.B. Klein, K. Bohnert, and T.F. Boggess, Opt. Lett. **11**, 647 (1986).
2. M.B. Klein, Opt. Lett. **9**, 220 (1985).
3. V.L. Vinetskii, N.V. Kukhtarev, and M.S. Soskin, Sov. J. Quantum Electron. **7**, 230 (1977).

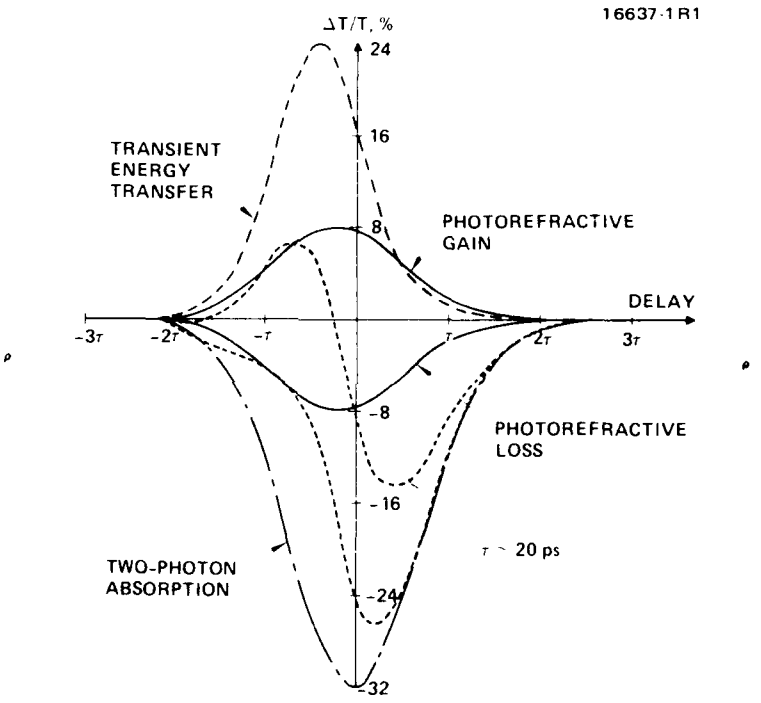

Fig. 2. Model of the probe delay dependence of the normalized probe transmission including transient energy transfer, two-photon absorption, and photorefractive energy transfer. The dashed curve represents transient energy transfer. The two solid curves represent the photorefractive energy gain or loss for the two crystal orientations, and the dot-dash curve represents the two-photon absorption. The small dashed curves are the sum of the three effects for the two crystal orientations.

Nonlinear Optical Logic Etalon at Todays Fiber Communication Wavelengths

K. Tai
AT&T Bell Laboratories, Murray Hill, New Jersey 07974

J. L. Jewell and W. T. Tsang
AT&T Bell Laboratories, Holmdel, New Jersey 07733

$In_{0.53}Ga_{0.47}As$ lattice matched to InP has been used extensively as the material for lightwave sources and detectors for optical communication. Here, we report the first use of InGaAs/InP multiple quantum wells (MQW) in the form of a nonlinear optical Fabry-Perot etalon for all-optical logic operations [1]. The MQW sample consists of 100 periods of alternating undoped thin layers of InGaAs (100 Å) and InP (150 Å) grown by chemical beam epitaxy [2] on InP substrate. Fig. 1 shows its room-temperature absorption spectrum. The characteristic step-like absorption is clearly shown and the n=1 heavy- and light-hole excitons are resolved. The substrate is removed by polishing and etching. The bare MQW structure is then sandwiched and epoxied between two 92.5%-reflectivity (at 1.57 μm) cover slips to form an optical logic etalon (OLE). Experiments employed a pump-and-probe configuration using a 1.57 μm synchronously-pumped color center laser (15-psec) as the probe and a 1.06 μm mode-locked Nd:YAG laser (100-psec) as the pump. Fig. 2 shows room-temperature positive gatings based on saturation of absorption. It requires 24 pJ of the pump pulse to get 30% of transmission (Fig. 2(a)). Larger transmission can be obtained by increasing the switching energy. This shows the absorption can be saturated almost completely and the material is indeed of superior optical quality with very little nonsaturable background absorption. Fig. 3 shows negative gating based on refractive index effect. The on-state transmission is about 40%. The switching energy for a 5:1 contrast is 6 pJ. The input probe energy is 32 pJ. Thus, the signal gain for a 5:1 contrast, defined as the pulse energy ratio between the output (the transmitted probe) and the input (the pump), is about 2. Larger gains are possible, since we saw no noticeable change in the probe transmission from several up to 32 pJ. Refractive positive gating showed similar results. These results were obtained at 77 K because the probe wavelength could not be tuned below the absorption edge

at room temperature. Thus, we blue-shift the bandgap by operating at low temperature. The performance of OLE was found not differ much from about -50°C to liquid nitrogen temperature. We would expect similar results for room temperature operation if the laser wavelength could be tuned far enough. Presumably, one can also reduce the well thickness to blue-shift the bandgap. We have seen room-temperature positive and negative gatings for the 70-Å (64 wells) MQW sample. OLE should readily perform other logic operations such as AND, OR, and NOR, if more than one pump (or input) is used. Actually, the negative gating here can be readily interpreted as a NOR gate since additional input energy serves only to lower its already low output. The time response of OLE was determined by scanning the probe arrival time. We found the rise of switching follows the pump pulse. The recovery time (e^{-1}) is about 1.2 ns. We made crude estimate about the nonlinear absorption coefficient and refractive index by fitting data in Figs. 2 and 3. The values are on the same order of magnitude as those of GaAs MQW [3]. In conclusion, we have constructed the first *all-optical logic device operated* at todays communication wavelengths. This device exhibits several very attractive features, i.e., several-pJ switching energy, large contrast ratio (20:1, if desired), > 40% total transmission (or < 4dB insertion loss), several-ns recovery, and ≈2 signal gain. The other unique feature is its compatibility with optical communication technology in terms of materials, sources, and detectors. This fact may lead to some useful applications in optical communication and optical switching.

REFERENCE

1. J. L. Jewell, Y. H. Lee, M. Warren, H. M. Gibbs, N Peyghambarian, A. C. Gossard, and W. Wiegmann, Appl. Phys. Lett. *46*, 918 (1985).

2. W. T. Tsang, Appl. Phys. Lett. *45*, 1234 (1984).

3. D. S. Chemla, D. A. B. Miller, P. W. Smith, A. C. Gossard, and W. Wiegmann, IEEE Quantum Electron. QE-20, 265 (1984).

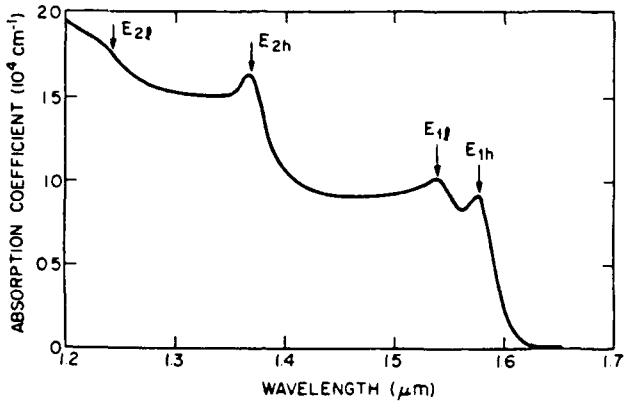

Fig. 1 A typical room-temperature absorption spectrum of CBE-grown InGaAs/InP MQW.

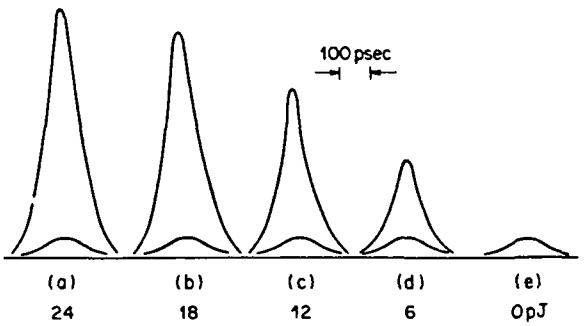

Fig. 2 Positive gating: A series of traces showing the transmitted probe for both on (with pump) and off (pump-blocked) states as a function of the pump pulse energy. Note detection is limited by the bandwidth of detector and oscilloscope.

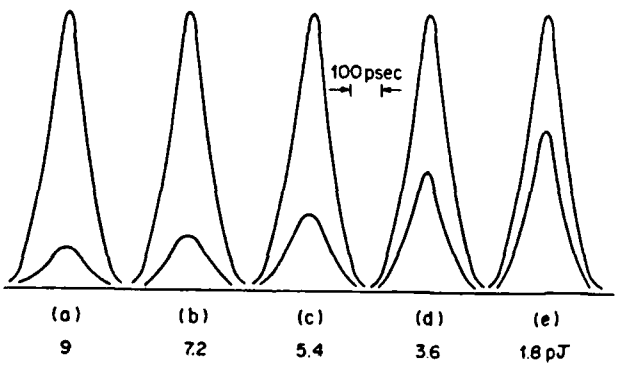

Fig. 3 Negative gating: A series of traces showing the transmitted probe for both on (pump-blocked) and off (with pump) states as a function of the pump pulse energy.

FRIDAY, MARCH 20, 1987

PROSPECTOR/RUBICON ROOM

10:30 AM–12:00 M

FB1–5

Eric Spitz, Thompson CSF, *Presider*

WAVE-MIXING IN NON LINEAR PHOTOREFRACTIVE MATERIALS APPLICATIONS TO DYNAMIC BEAM SWITCHING AND DEFLECTION

Jean-Pierre HUIGNARD

THOMSON-CSF, Laboratoire Central de Recherches

Domaine de corbeville, B.P. N° 10

91401 ORSAY Cedex (France)

The exchange of informations at high data rates between optoelectronic transducers is an important task encountered in all advanced architectures of high capacity parallel optical processors and optical transmission links. For these purposes, the use of all-optical techniques for large scale and very broad-band switching is currently the object of active researchs. For a limited number of input-ouput signals, integrated optical technologies using ligth propagation in electro-optic waveguides offer attractive performances. However, for the much larger switching capacities which will be required in the future, for example 1024 x 1024, the most attractive switch architecture should exploit the 2-D parallel space transmission of the optical beams (1-3). Because of the high degree of parallelism of this approach a switching time constant of few milliseconds would be convenient. The potentiel capabilities of such a switching technique are therefore very large, in particular if the connection between any light emitter and receiver can be reconfigured in real-time. The aim of the lecture is to show that the principle of reconfigurable interconnections can be demonstrated on the basis of wave mixing experiments with photorefractive crystals. The operating mode, of a 2-D optical switch is schematically shown in Figure 1. The point to point connection is established through the angular deflection of the beams emerging from the 2-D input light emitter array (semiconductor lasers, single mode fibers...). The reconfigurable interconnection plane which is the key element of this device consists

of an array of photorefractive crystals. By changing the spatial period of the dynamic photorefractive grating, the beam emitted by each pixel of the input array can be randomly switched in different spatial directions. For such purposes, photorefractive Bi_{12} SiO_{20} crystal (BSO) is a promising candidate on account of its high sensitivity for elementary grating recording and erasure [$S^{-1} \simeq 100\text{-}500$ μJcm^{-2} at $\lambda = 514$ nm - grating period $\Lambda = 6\,\mu m$ - Applied field $E_o = 6$ kV.cm^{-1}]. The attractive features of the BSO for the involved application are the following :

- The photoinduced index modulation persists in the dark for about 30 hours but may be erased through space charge relaxation under uniform illumination by one of the recording beam.
- The deflection of a beam in the near IR - typically at semiconductor laser wavelengths - persists for several hours after the writing beams are turned off because of the low crystal sensitivity at those wavelengths .

Since there is a wavelength change between the grating recording and readout steps (respectively $\lambda = 514$ nm and $\lambda = 850$ nm) we will review several original techniques allowing to maintain optimum Bragg diffraction of the near IR beam over a large scan angle. In the variable wavelength recording method (4-5) (IBM, Institut d'Optique, TH-CSF) the grating is produced by the interference of two beams emitted by a dye laser (Figure 2). Changing the recording wavelength produces both a modification of the grating period and of the slant angle of the fringes in the photorefractive BSO crystal. With this method, a scan angle of 12° of the beam at $\lambda = 850$ nm is achieved by varying the recording wavelength from $\lambda = 535$ nm to $\lambda = 575$ nm (Figure 3.a). The diffraction efficiency related to these experimental conditions is typically $\eta = 1$ % and a photograph of a part of the deflected spots is shown in Figure 3.b. In another technique (6) (E.T.H.) a non critical configuration for anisotropic Bragg diffraction can be found in biaxial photorefractive $KNbO_3$ crystals, thus allowing to obtain a signal beam deflection of 5.7° for a wavelength change of the control beams of $\Delta\lambda = 58$ nm.

The collinear Bragg diffraction method allows to achieve exact collinearity between the incident recording beams in the visible and the near IR readout beam (7) (figure 4.a). This technique exploits the spatial non linearities of the photoinduced space charge field in the photorefractive crystal. Exposing the crystal with two collinear grating vectors K_1 and K_2 generates through non linear mixing the new wave vectors $K_{NL} = mK_1 \pm nK_2$ which satisfy the Bragg condition for a readout wavelength λ_R such as $1/\lambda_R = m/\lambda_1 \pm n/\lambda_2$. The experimental demonstration of the method will be shown with the two recording wavelengths $\lambda_1 = 633$ nm ; $\lambda_2 = 514$ nm. Choosing $m = 2$, $n = 1$ ensures a collinear Bragg diffraction at the semiconductor laser wavelength $\lambda_R = 822$ nm (Figure 4.b). Since the method is based on the higher order non linearities in BSO it consequently results in low values of the diffraction efficiency (typically $\eta = 0.1$ %) - grating period $\Lambda = 3$ µm). The respective advantages of these beam deflection techniques which use optically induced variable gratings in photorefractive crystals will be discussed. In particular, emphasis will be placed on the crystal parameters allowing to attain much higher diffraction efficiencies and this mainly includes the crystal photoconductivity, the trapping center density and the impurity doping concentration. It thus follows that crystal of different origins may have significant differences in their photorefractive properties. We will show in particular that under optimized recording conditions, grating period $\Lambda = 20$ µm - applied field $E_o = 10$ kV.cm^{-1}, some BSO-BGO crystals exibit for the first time a steady state diffraction efficiency reaching $\eta \simeq 80$ % (8). Such high value of η constitutes a significant improvement allowing to envision their application to reconfigurable interconnection devices.

In conclusion, the dynamic holographic techniques in photorefractives crystals show attractive features since large deflection angles at millisecond speed are already achieved, in particular with BSO-BGO crystals. The extension of these principles to a full 2-D array of switching cells as well as further proposals for crystal optimization will be also presented.

References :

(1) J.W. GOODMAN, F.J. LEONBERGER, S.Y. KUNG - IEEE - 27 - 850 1984.

(2) R.I. MAC DONALD, D.K.W. LAM - Opt. Engi. 24 - 220 - 1985.

(3) P. GRAVEY - In Proceedings of the 7th ECOC 81 - Copenhagen 1981.

(4) G. SINCERBOX, G. ROOSEN - Appl. Opt. 22 - 690 - 1983.

(5) G. PAULIAT, J.P. HERRIAU, A. DELBOULBÉ, G. ROOSEN, J.P. HUIGNARD -JOSA -B - 3 - 306 - 1986.

(6) E. VOIT, C. ZALDO - P. GÜNTER - Opt. Lett. - 11 - 309 - 1986.

(7) J.P. HUIGNARD, B. LEDU - Opt. Lett - 7 - 310 - 1982.

(8) J.P. HERRIAU, D. ROJAS, J.P. HUIGNARD, J.M. BASSAT, J.C. LAUNAY - Ferroelectrics : To be published.

Figure captions

Figure 1 : Principle of a 2-D parallel switching device for reconfigurable interconnections.

Figure 2 : Elementary switching cell based on the dynamic grating recording with a variable wavelength laser source (dye laser).

Figure 3.a : Deflection angle of the IR beam - λ_R = 850 nm - versus the recording wavelength of the dye laser.

Figure 3.b : Photograph of a part of the deflected spots.

Figure 4.a : Wave-vector diagram illustrating the collinear Bragg diffraction based on spatial non linearities.

Figure 4.b : Application of the collinear Bragg diffraction in BSO to the steering of a light beam in a single mode fiber λ_1 = 633 nm, λ_2 = 514 nm.

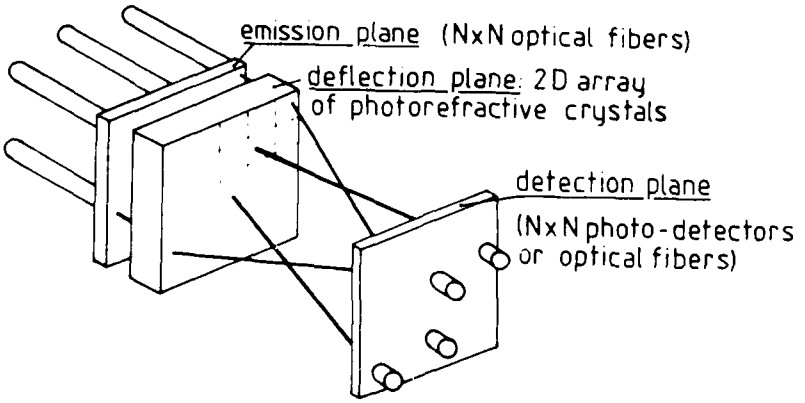

Fig : 1

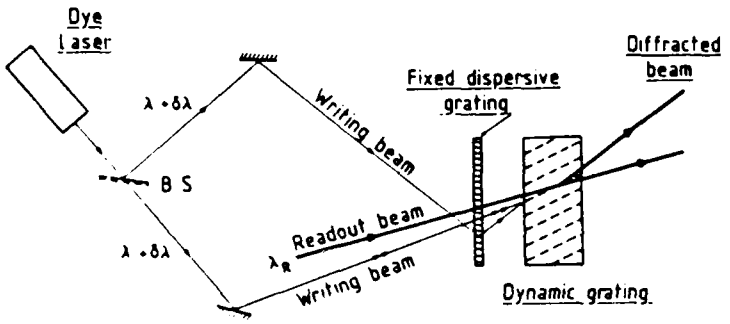

Fig : 2

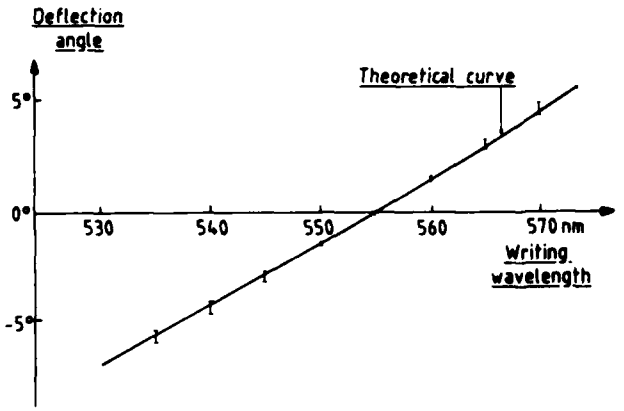

Fig : 3-a

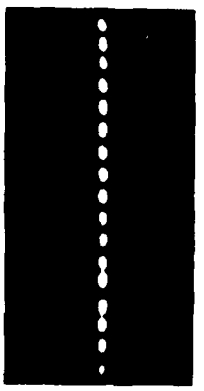

Fig : 3-b

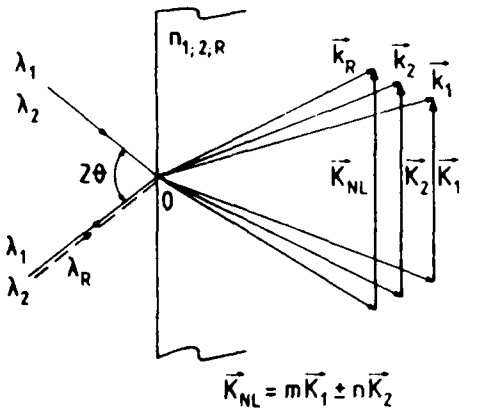
$n_{1;2;R}$
λ_1
λ_2
2θ
λ_1
λ_2
λ_R
0
$\vec{k}_R$
$\vec{k}_2$
$\vec{k}_1$
$\vec{K}_{NL}$
$\vec{K}_2$
$\vec{K}_1$
$\vec{K}_{NL} = m\vec{K}_1 \pm n\vec{K}_2$

Fig: 4-a

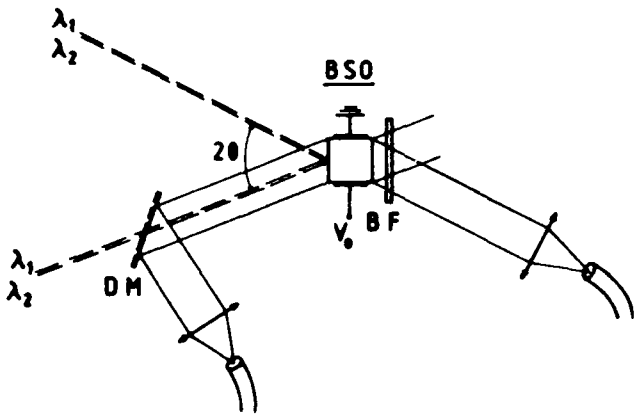
λ_1
λ_2
BSO
2θ
V_o
BF
λ_1
λ_2
DM

Fig: 4-b

FB2-1

Design and Construction of Holographic Optical Elements for Optical Photonic Switching Applications

M.R. Taghizadeh, I.R. Redmond, A.C. Walker and S.D. Smith

Department of Physics, Heriot-Watt University, Edinburgh EH14 4AS, U.K.

There has been a lot of interest in the possibility of the application of two-dimensional arrays of intrinsic optical bistable elements for cross-point switching in telecommunication systems and optical signal processing.

We have been successful in achieving low power (milliwatts) visible wavelength and room temperature operation of optical bistability in interference filters containing ZnSe material as their active element [1]. This, together with the high degree of uniformity achieved in the fabrication of these nonlinear interference filters (NLIF) led us to believe that simultaneous operation of two-dimensional arrays of bistable switches is possible provided we use two-dimensional arrays of laser beams to power individual elements. In the absence of laser diode arrays of sufficient power in the visible region, various methods of dividing one laser beam into a 2-D array of beamlets have been pursued by us. The most efficient of these techniques, by far, has been the use of holographic optical elements (HOE's).

Design and construction of dichromated gelatin (DCG) HOE's has been the subject of a great deal of attention in our laboratories both for generation 2-D arrays of laser beams and also as means of static interconnects for switching networks and optical computing applications.

High refractive index modulation capability together with high resolution and low absorption and scattering make dichromated gelatin almost

an ideal medium for recording holographic optical elements. However, DCG suffers from certain disadvantages compared with other holographic media (e.g. silver halides) such as short shelf life and low sensitivity which make it difficult to achieve consistent results. By adopting various pre- and post-processing techniques, we have been successful not only in achieving good consistency in DCG but also in predicting various parameters of individual HOE's such as diffraction efficiency, uniformity and bandwidth. All these parameters are of great importance in fabrication and application of these elements.

Fig. 1 shows the experimental set-up for construction and reconstruction of such holographic optical elements. The experiments have shown that 2-D arrays of holographic lenses with diffraction efficiencies approaching the theoretical limit (97 ± 2%) can be fabricated. These lenses are capable of generating diffraction limit spot sizes with uniformity of better than 2% between individual elements.

Using one of these HOE's together with high degree of uniformity (less than 3% variation in width and centre wavelength over an area of 5 mm^2) in fabrication of ZnSe NLIF's has allowed us to demonstrate simultaneous operation of an array of 5 x 5 intrinsic optically bistable switches on an 0.7 cm^2 of NLIF, which to our knowledge is the largest 2-D array of switches to date. The switching power of individual elements for spot diameter of 70 microns is ≈ 25 mW with a switch-on time of ≈ 100 μsec. This device has the basic characteristics of a novel optically addressable solid-state spatial light modulator. Various external sources including incoherent white light, infrared and a range of visible lasers have been used to address this device.

Currently under investigation is the possibility of constructing much larger arrays (> 100 x 100) using an automated exposure system.

In conclusion we have shown that dichromated gelatin HOE's are capable of efficiently generating uniform two-dimensional arrays of laser beams for optical signal processing and digital optical computing applications.

Acknowledgement

This work was supported by the EEC as part of a scientific cooperation with the Stimulation Action programme.

References

1. S.D. Smith, J.G.H. Mathew, M.R. Taghizadeh, A.C. Walker, B.S. Wherrett and A. Hendry

Opt. Commun., 51, 5 (1984).

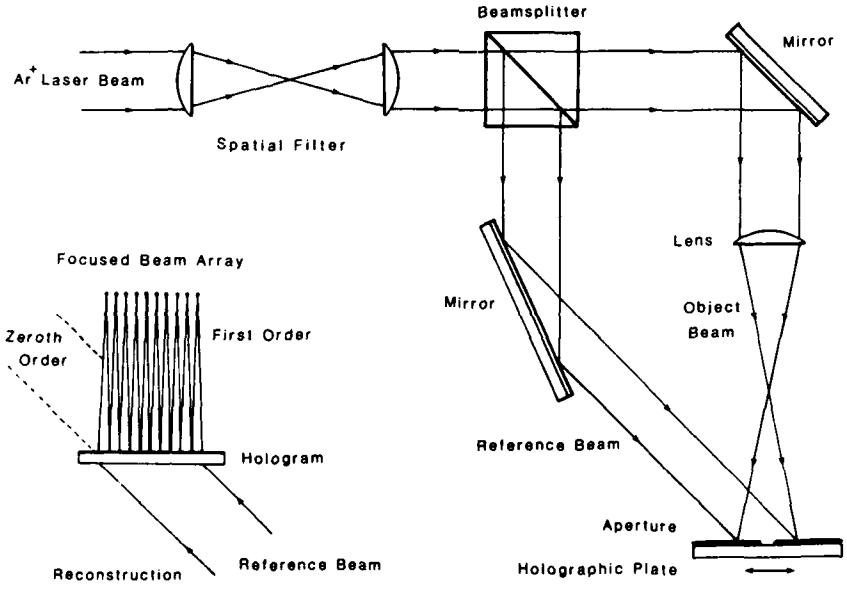

Fig. 1. Experimental arrangement for construction of holographic 2-D array generator.

Optical Threshold Mechanism Using Fiber Coupled Phase Conjugate Mirror

Ram Yahalom, Aharon Agranat and Amnon Yariv
California Institute of Technology
Pasadena, California 91125

The recent development of optical implementations of various data processing procedures created a demand for a sensitive all optical threshold device.[1] We henceforth present a possible mechanism for such a device, based on the coupling of mutually incoherent light beams by means of the fiber coupled phase conjugate mirror (FCPCM).[2,3]

Consider the experimental set-up described in Figure 1. Three mutually incoherent parallel beams are converged into a 40 cm long multimode fiber (with an incidence angle in the range of 0^0-10^0). The randomly polarized light diverging from the fiber is focussed onto the polarizer P, which is set in the horizontal direction. It is then focussed onto a $BaTiO_3$ crystal which serves as a self pumped phase conjugate mirror (PCM), aligned to reflect horizontally polarized light. The phase conjugated light of beams 1, 2 and 3 was measured by the detectors D1, D2 and D3 respectively. A fourth detector, D4, monitored the power incident on the PCM.

In the first set of experiments the interdependence of the phase conjugated light of two mutually incoherent beams (beams 1 and 2 in Fig. 1) coupled by the FCPCM was investigated. The sequence of the experiment was as follows: First the relative power of the input beams, (I_1 and I_2 respectively measured by D4), was set by governing the reflectivity of the beamsplitter BS1. The steady state phase conjugated light of each of the two beams (hereafter: $PC_1^{(0)}$ and $PC_2^{(0)}$) was then measured separately. And finally, the power of the steady state phase conjugated light of each of the two beams (hereafter: PC_1 and PC_2) was measured, while the two beams were coupled simultaneously to the fiber. It was found that only the stronger beam was phase conjugated, whereas the phase conjugated light of the weaker beam was suppressed to zero.

The qualitative results are summarized in Figs. 2 and 3. In Fig. 2(a) we present the results of a measurement of PC_1 as a function of I_2, while I_1 was held fixed. The same results as a function of the input power difference $\Delta I = I_1 - I_2$ are given in Fig. (2b). We see that PC_1 indeed depends on the input power difference ΔI, and not on I_1 alone. In Figure 3 we present the measurement of PC_1 as a function of ΔI along side the measurement of $PC_1^{(0)}$ as a function of I_1. We see here that the functional behavior of the two curves is very similar.

In the second set of experiments three mutually incoherent beams were coupled to the FCPCM. Here the inputs of beams 2 and 3 were held fixed (with $I_2 > I_3$) and I_1 was varied using the attenuator (ATN in Figure 1). In addition the phase conjugated light emerging from the PCM was temporally modulated by the chopper (CH in Fig. 1), enabling the use of the lock-in technique to improve the output SNR. It was found here that as long as $I_1 > I_2 + I_3$, only beam 1 was phase conjugated. Moreover, in the intermediate range where none of the input beams were stronger than the sum of the two others, no phase conjugated light was emitted.

A full theoretical explanation of these results is not yet completed. It is, however, obvious that the construction of a simple optical threshold device can be based on these phenomena. It is not yet clear if these results can be extended to the coupling of mutually incoherent spatially modulated light beams (images). Experiments to resolve this question are now under-way.

References:

1. "Demonstration of an All-Optical Associative Holographic Memory," A. Yariv, S. K. Kwong and K. Kyuma, Appl. Phys. Lett. 48, 1114 (1986).
2. "A Theoretical Model for Modal Dispersal of Polarization Information and Its Recovery by Phase Conjugation," A. Yariv, Y. Tomita and K. Kyuma, submitted to Optics Lett.
3. "Phase Conjugation of Mode Scrambled Optical Beams: Application to Spatial Recovery and Interbeam Temporal Information Exchange," R. Yahalom, K. Kyuma and A. Yariv, submitted to Appl. Phys. Lett.

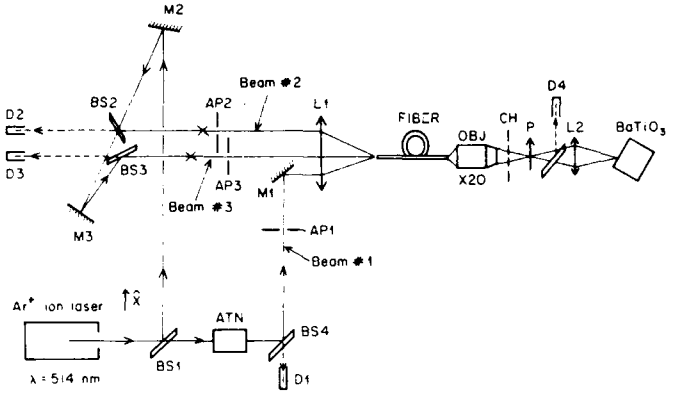

Fig 1

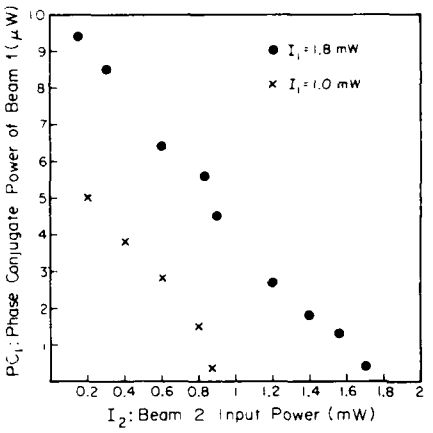

Fig 2(a)

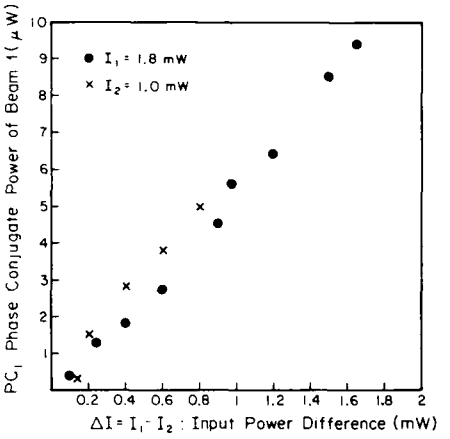

Fig. 2(b)

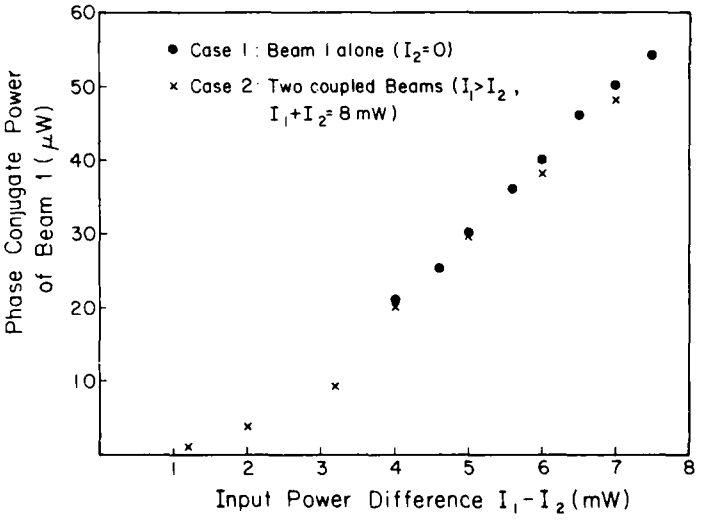

Fig 3

Computational Properties of Nonlinear Optical Devices

Michael E. Prise
Norbert Streibl
Maralene M. Downs

AT&T Bell Laboratories
Holmdel, New Jersey 07733

To design an optical digital computer it is essential to have a cascadable logic gate with a fanin and fanout of at least two. For a complete logical coverage it is necessary to have either a NAND or a NOR gate or have an AND and an OR gate and use dual rail logic to perform a spatial inversion. To built a general purpose computer without a ridiculous number of gates we must have loops in the system. That is the data must flow through the same gates more than once. This means one gate must be able to drive any other identical ones.

This analysis holds for a processor consisting off large arrays of identical nonlinear optical devices connected by imaging systems. Perhaps the interconnection will be a perfect shuffle or a symbolic substitution.

Here we analyze only devices which can be described in terms of input versus output power. In this case either reflected or transmitted power is the output power depending on whether we operate the device in reflection or transmission. Our treatment can be extended to devices which can not be charactarised so simply but more parameters are involved.

To use these devices as optical gates the inputs from previous devices are fed to the devices by our optical interconnection scheme. The transmission of the system is given by T_{sys}. We also introduce a bias beam P_{BIAS} which is incident on the device and can be adjusted. We have assumed that the bias beam cannot be adjusted independently for different elements on one array. The computational properties of a gate are:

- *fanin* which is the number of inputs
- *fanout* which is the number of outputs
- *threshold* which is the number of HI inputs required to switch the device

The *threshold* describes the logic function of the gate: for example, a NOR-gate has *threshold* = 1, whereas a four input AND-gate has *threshold* = 4. Obviously, *threshold* has to be bigger than 0 and less than or equal to *fanin*.

Figure 1 shows all the device parameters we consider for a noninverting device.

For inverting device the nomanclature is the same. In the case of bistable devices $\Delta P_{SW} = 0$

From this we can define a few figures of merit characterising the device: The *switching contrast* is given by

$$C_{SW} = \frac{P_{ON} - P_{OFF}}{P_{ON}} \tag{1}$$

The *switching transmission* is

$$T_{SW} = \frac{P_{ON}}{P_{OFF}} \tag{2}$$

The *relative switching window* is

$$\sigma_{SW} = \frac{\Delta P_{SW}}{P_{SW}} \tag{3}$$

We also include the differential transmission in the HI and LO states. For the device to perform the required logic functions
P_{BIAS} has to be chosen such that

- if there are *threshold* − 1 or less HI inputs, then the device does not switch,

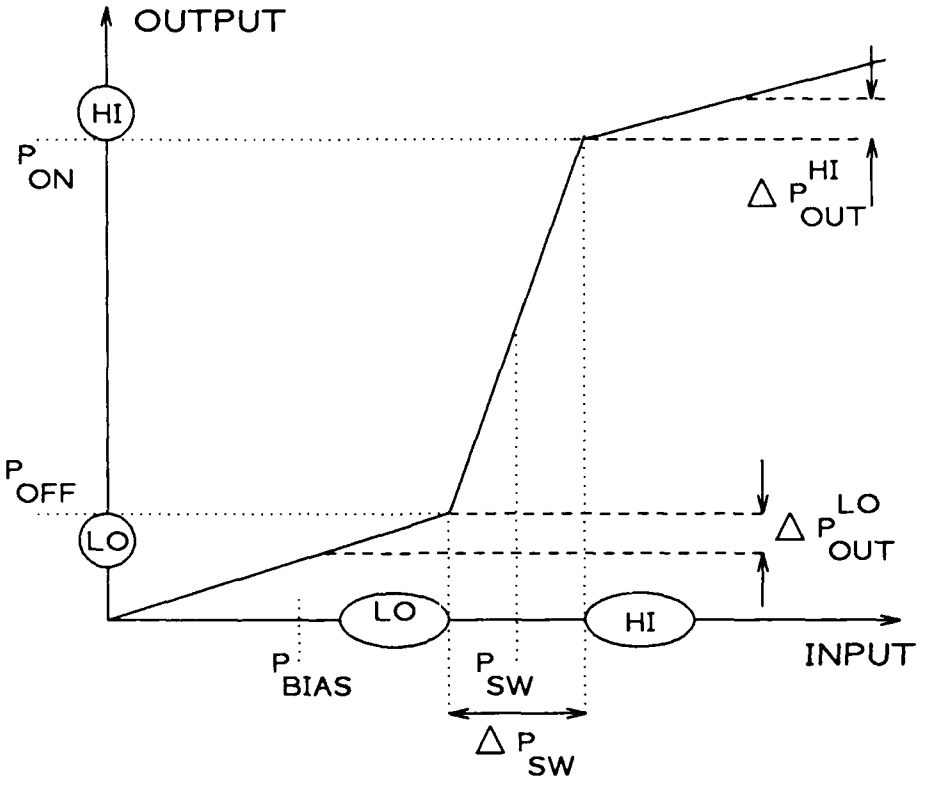

Figure 1. Characteristic of a thresholding devices

- if there are *threshold* or more HI inputs, then the device switches.

We can use this to derive the basic relationships between the optical and computational properties of device and the system. The effect of system error such as a variation in transmission for different parts of the system or a variation in the bias beam is simply to proportionally broaden the switching window. For instance in a system based on bistable devices an error in the bias beams accross the arrays of 10% would correspond to an effective switching window of 0.1. We can use the above to come up with inequalities relating the optical properties of the devices and interconnection systems with the computational properties which can be attained within given tolerances. We have then interpreted these inequalities graphically. We found it useful to define another parameter which we call the *gainparameter*. $T_{SW} * T_{eye/fanout}$. The physical meaning of this parameter is obvious, In figure 2 we plot the effective switching window (relative error in everything for a bistable device) versus the possible fanin for different *gainparameters*. We see a relatively small system gain dramatically alleviates the requirements on accuracy for this system.

From this and other plots we came to the following conclusions. which should serve to judge the computational merits of a proposed device or computer architecture:

- The devices must be infinitely cascadable and they must provide a fanin and fanout of at least two (including system losses). Further, they must allow the construction of any Boolean function (complete logical cover). Any device which does not fulfill *all* these conditions is useless for digital computing.
- Devices without internal feedback (transmission independent from transmitted power supply beam) do not rely on critical biasing, nor do they exhibit critical slowing down. They are highly desireable, since they reduce the required systems accuracy.

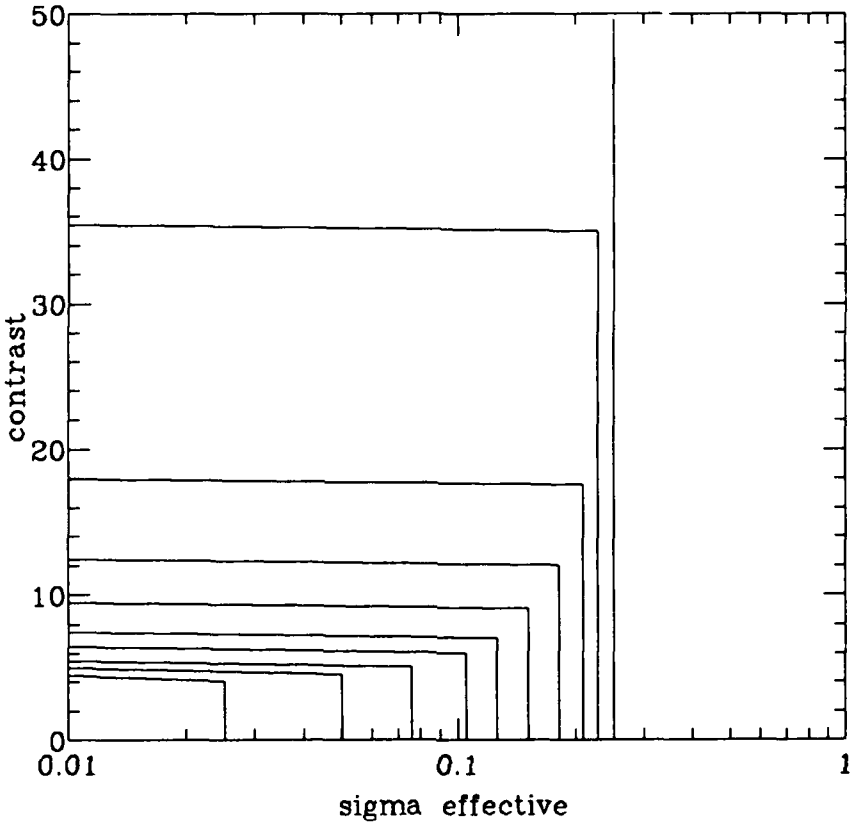

Figure 2. For an ideal binary device ($T_{HI} = T_{LO} = 0$) the *fanin* is plotted against the effective switching window σ_{eff} for switching contrasts C_{SW} of 0.1 to 1.0. We have set $T_{SYS} = 0.5$. The rightmost curve correspond to the largest C_{SW}. The area to the left of a curve is allowed.

- If *gainparameter* of the total system (devices + interconnects) is greater than 1 ("real gain") then the accuracy requirements on the system accuracy are much less severe. High absolute gain is in many cases not an advantage.
- The differential transmission of the devices in the upper and lower states is not very critical if the device does not have a high contrast and the fanin is small.
- As high a contrast as possible is desirable, but not at the expense of transmission. The key point to consider is again system accuracy. It will be very difficult to guarantee accuracies of 10% or better in a complex system.
- The development of devices which threshold with respect to a local reference would aleviate the requirements on systems accuracy. Similarly, local input renormalisation before each threshold operation is desireable.
- Generally, NOR-gates look better than for example AND-gates, since they have minimum threshold. Furthermore, a computer built out of NOR-gates need not use dual rail logic.
- Computer architectures requiring large fanins are unrealistic because of system accuracy problems

OPERATING CURVES FOR OPTICAL BISTABLE DEVICES

P. Wheatley & J.E. Midwinter

There is much interest in the use of optical bistable devices as logic gates for optical processors. Although desirable properties have been reported, it is difficult to see how these are offset by less desirable ones. All properties of the device can be controlled to a certain extent, principally by the bias conditions. Here we show how steady state and dynamic responses vary simultaneously with these parameters. These operating curves can be used to see the capabilities of a device or to choose the optimum bias conditions.

We use a simple model of a device whose steady state input-output is shown in Fig.1. The basic shape of this can be changed by varying the initial bias voltage in the case of a hybrid device or the initial detuning in a Fabry-Perot device. For an optical bistable device to be able to fan-out, an optical bias power is required. This is an optical beam whose power is less than the power required to switch the device on. When a further optical signal is applied, the device will switch on. Then fan-out is defined as the number of identical devices which can be driven by the output of this device. Fan-out is plotted as an operating curve. We draw a graph whose axes are the optical bias power and the optical signal power. Then contours of constant fan-out are drawn as broken lines.

If contrast is poor, then the output of one device may prevent the subsequent device from switching on. The shaded area on the graph, Fig. 2, shows where devices do not operate correctly due either to this or to other faults in bias conditions. The third response to be shown is the sum of the switch-on and switch-off times, plotted as solid lines.

The resulting graph gives an indication of how steady state properties vary with dynamic properties and thus indicates how device biassing can be optimised. It also highlights the difficult trade-offs inherent in operating such devices in sequential logic.

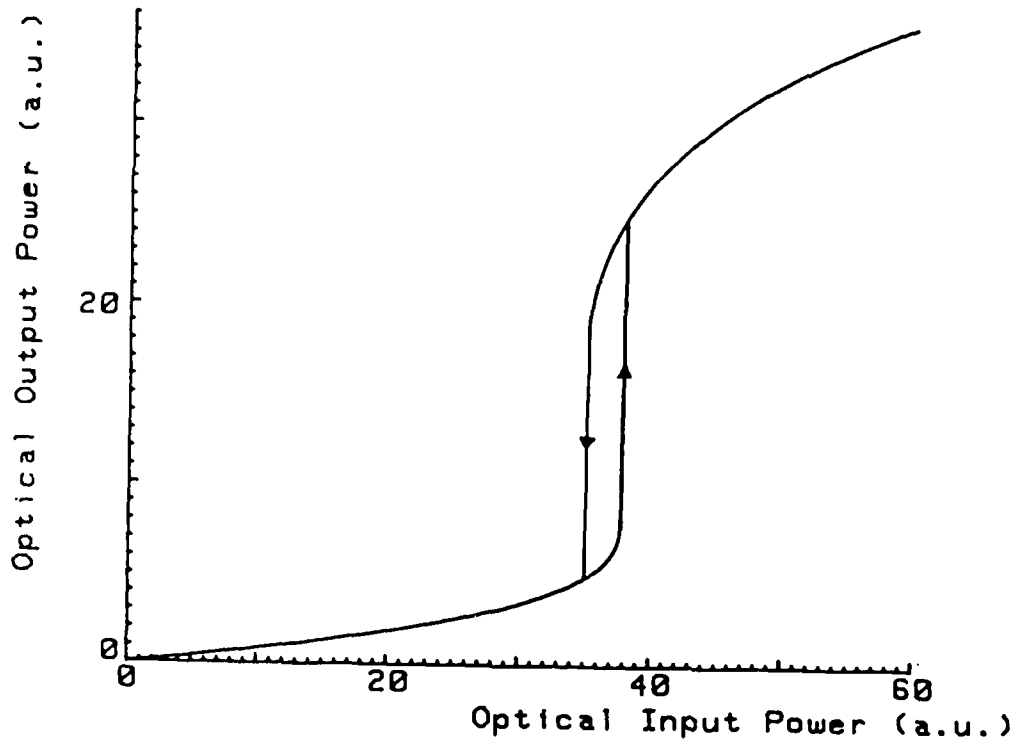

Fig 1. Typical Input-Output Characteristic

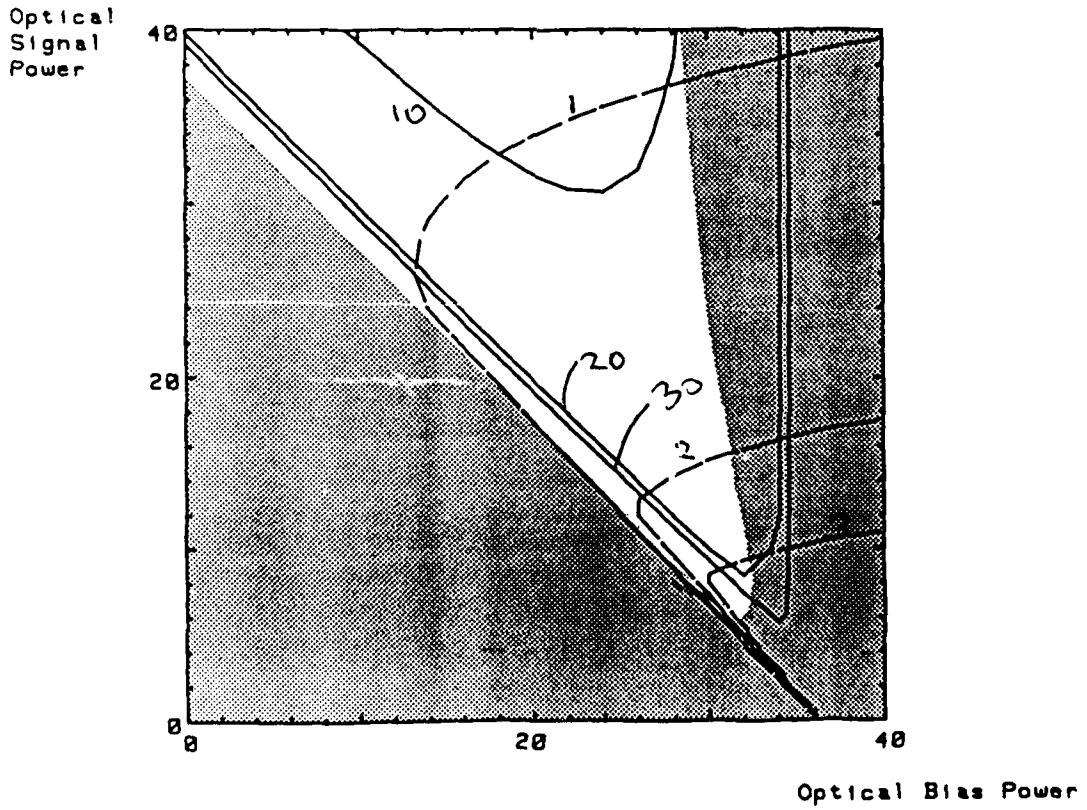

Fig. 2. Operating curves for 2 input OR gate

FRIDAY, MARCH 20, 1987

PROSPECTOR/RUBICON ROOM

1:30 PM–3:00 PM

FC1–5

PHOTONIC DEVICES: 2

W. Jack Tomlinson, Bell Communication Research, Inc., *Presider*

Optical Amplifiers for Photonic Switches

R. M. Jopson
G. Eisenstein

Bell Laboratories
Crawford Hill Laboratory
Holmdel, New Jersey 07733

Although semiconductor optical amplifiers[1,2,3,4] hold the promise of allowing lossless switch design, current optical amplifiers have properties that render them unusable in many applications. Two problems currently limiting their use are rapid Fabry-Perot variations in the gain spectra and bidirectionality of the gain. The figure below schematically illustrates the gain spectrum of a semiconductor optical amplifier. It can be seen that the broad (≈70-*nm*) semiconductor gain

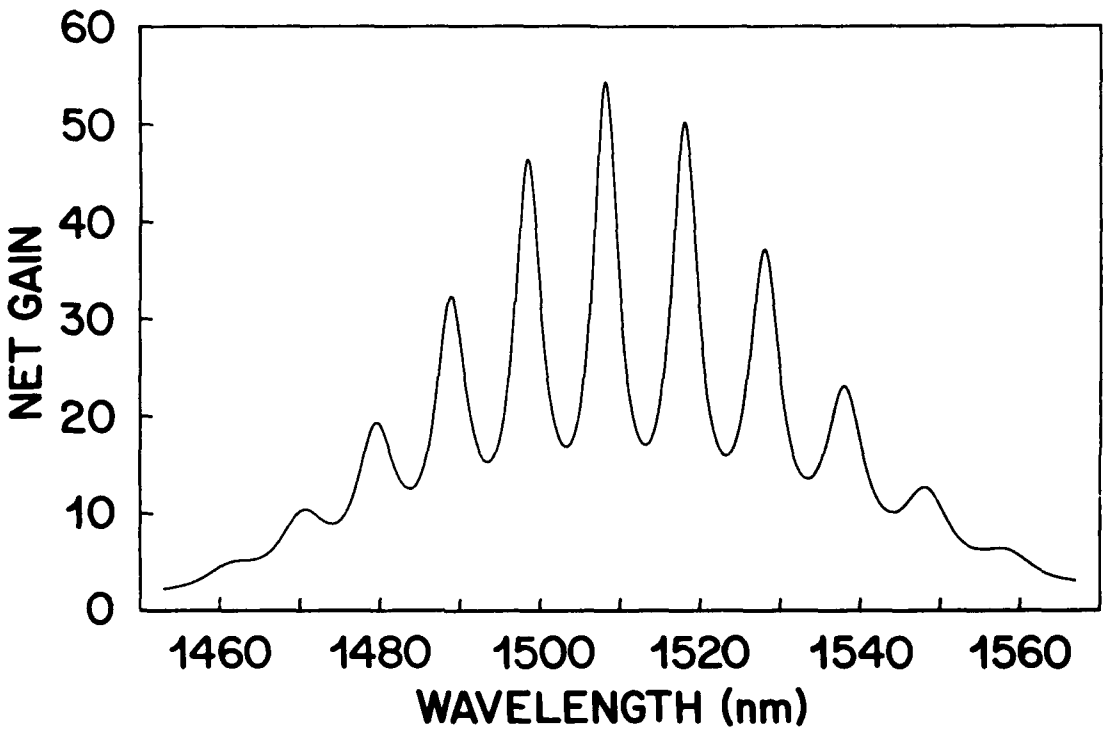

spectrum is multiplied by a rapidly varying Fabry-Perot spectrum. (The spacing between the Fabry-Perot peaks in the figure has been increased for illustrative purposes). Semiconductor optical amplifiers are usually made by putting an anti-reflective coating on the facets of a laser diode. It is the residual refectivity of the amplifier facets that causes Fabry-Perot resonances in the gain spectrum. The amplitude of this variation is determined by the product of the amplifier chip gain and facet reflectivity while the optical length of the amplifier waveguide determines the separation

between the peaks. Since optical amplifiers typically have Fabry-Perot periods of 1.3 *nm*, it can be seen that there are actually around 50 Fabry-Perot periods within the material gain bandwidth rather than the 7 illustrated in the figure. While is possible to obtain high gain from an amplifier with strong Fabry-Perot resonances, the use of such an amplifier obviously presents wavelength control problems to the switch designer. Other less obvious problems in amplifiers with strong Fabry-Perot structure are: 1) the locations of the Fabry-Perot peaks are strongly temperature dependent, 2) the location and gain of the peaks are sensitive functions of the bias current of the amplifier, 3) they have more cross-talk and lower saturated output power than amplifiers with a smooth gain spectrum, and 4) the backward reflected gain is comparable to the forward gain. Given these problems, it is unlikely that amplifiers with large Fabry-Perot resonances will be of much use in photonic switching systems.

Fortunately, coating technology is advancing rapidly and it is likely that amplifiers with a smooth gain spectrum will soon be available with net gains near 20 dB. However, the problem of bidirectionality in the amplifier gain will remain. Bidirectional gain becomes a problem when an amplifier is inserted into a system. All systems contain reflections arising from imperfectly matched transitions between different waveguides, changes in the waveguide or scattering within the waveguide. These reflections, when combined with the gain of the amplifier, lead once again to Fabry-Perot resonances in the system transmission spectrum. Again, the peak spacing of each set of resonances is determined by the optical path length between the reflections and the amplitude of the gain variation depends on the product of the net amplifier gain and the geometric mean of the system reflectivities. These resonances in system transmission will cause problems similar to those caused by resonances in amplifier gain; however, for systems, the spacing of the resonances is generally smaller than the signal bandwidth. Therefore, the problem of matching a signal wavelength to a peak in the amplifier gain spectrum is replaced by the problem of echoing in the signal channel.

As an example, consider the case of a perfect optical amplifier placed in a $LiNbO_3$ system that has a -30-dB reflection on each side the amplifier at a distance of 5 *cm* from the amplifier. The

period of the Fabry-Perot resonances in the system transmission will be 700 *MHz* resulting in an echo delay time of 1.5 *ns*. If we require that the Fabry-Perot variation in the system transmission be less than 3 dB, then from a generalized Fabry-Perot equation, we find that the amplifier gain can not be greater than 22 dB. Using an amplifier gain of 22 dB, the gain in the forward direction will then be 22 dB with a 3% echo train at 1.5 *ns* intervals while the gain in the backward reflected signal will be 12 dB, also with a 3% echo train. While it is possible that a system designer can accept performance degradation at this level, and it is likely that amplifiers with a net gain of 20 dB will be available soon, it is clear that the use of amplifiers with a net gain much greater than 20 dB requires major advances. First, amplifier facet reflectivities must be reduced by one or two orders of magnitude below those currently achieved and secondly, the problem of amplifier gain bidirectionality must be solved. One approach to this would be to reduce system reflectivities to -40 dB or lower. Another approach would be to either make the optical amplifier fundamentally unidirectional or to package it with an optical isolator. The latter method would require only minor changes to known techniques.

In this talk, we will discuss the facet reflectivity, chip gain, and coupling in current optical amplifiers and the effects of these parameters on amplifier performance. The interaction between the system and the amplifier will be discussed as well as some of the basic features of polarization effects, saturation, cross-talk and noise in optical amplifiers. Finally, we will predict near-term improvements expected for optical amplifiers and the implications of these improvements toward the use of optical amplifiers in systems.

1. J. C. Simon, J. Opt. Comm. **4**, 51, (1983).
2. M. J. O'Mohony, H. J. Westlake and I. W. Marshall, Br. Telcom. J. **3**, 25, (1985).
3. T. Mukai, Y. Yamamoto, and T. Kimura, Semiconductors and Semimetals, Volume 22: Lightwave Communications Technology, ed. W. T. Tsang (1985).
4. G. Eisenstein and R. M. Jopson, Int. J. Electronics **60**, 113 (1986).

170ps Fast Switching Response in Bistable Laser Diodes with Electrically Controlled Saturable Absorber

Akihisa Tomita, Shunsuke Ohkouchi, and Akira Suzuki
Opto-Electronics Research Laboratories, NEC Corporation,
1-1, Miyazaki 4-chome,Miyamae-ku,Kawasaki,Kanagawa 213, Japan

1.Introduction There has been great interest in optical data switching technology to meet increasing demand for massive data processing. Optical bistable devices have been considered as key elements for the optical data switching. Among the optical bistable devices, is a tandem electrode bistable laser diode (we will abbreviate this to BS-LD here). The BS-LD has various advantages over other optical bistable devices, such as large optical gain, high ON/OFF contrast, large optical output, and wide wavelength range for trigger light. The feasibility of BS-LDs as optical switching elements has been shown in 256Mb/s optical time division switching experiment[1]. The main factor limiting the BS-LD switching speed was the turn-off time rather than the turn-on time, as seen in most semiconductor optical bistable devices[2]. In order to achieve much faster switching operation in BS-LDs, it is necessary to reduce the turn-off time.

In this paper we have successfully demonstrated, for the first time, very fast switching operation in the BS-LD by controlling the carrier density and the carrier life time in the saturable absorber electrically. The turn-off time was reduced to less than 170ps. This improvement will enable to operate the BS-LD memory at more than 2Gb/s, about ten times faster than previously reported[1].

2.Experiment Figure 1 shows the structure of the BS-LD. The p-contact electrode of the 1.3μm InP/InGaAsP double channel-planer buried heterostructure laser diode[3] was divided into three sections 1,2, and 3. The p-contact layer was etched off between the each section for electrical isolation. In this experiment, sections 1 and 3 were connected in parallel and current I_1 was injected. These sections acted as gain sections. Small current (I_2) was injected into section 2, which acted as a loss section (satarable absorber). The BS-LD had a 35μm-width mesa structure to reduce parasitic capacitance.

Current-light output chracteristics are shown in Fig.2 as a function of current I_1, with constant current I_2. Hysteresis characteristics were controllable with I_2.

As shown in Fig.3, resonant-like frequency became higher when I_2 was larger, because absorption dumping and carrier life time decrease in the loss section. Since the light output responds to the carrier density change at the speed of resonant-like frequency, the higher resonant-like frequency gives the faster turn-off response. We chose bias current $I_1=I_{b1}$ and $I_2=I_{b2}$ so as to get the highest resonant-like frequency.

The experimental set up for the pulse response of the BS-LD is shown in Fig.4. Constant bias currents I_{b1}=53.5mA and I_{b2}=1.2mA were injected into the gain and loss sections, respectively. The peak amplitude for the turn-on current pulse and the reset current pulse was 26mA and -25mA, respectively. The rise time of both current pulse was 80ps. Total time resolution of the system was about 100ps. Figure 5 shows 170ps turn-off response for the BS-LD. The turn-off switching energy was estimated to be 10pJ. In the present experiment, no pattern effect was observed, because the excess carriers in the saturable absorber are pulled out electrically through the loss section electrode.

3.Discussion In the BS-LD with the loss section electrode, one can control hysteresis chacteristics and pulse response by changing the injection current I_2. The parameters which govern these device characteristics, such as absortion loss β, ratio of saturation parameter γ, etc., are closely related to carrier life time and carrier density in the saturable absorber[4]. For high speed switching, fast saturation(turn-on) and recovery(turn-off) of the absorption are needed. Fast saturation is achieved when β and γ are small. Though recovery time is affected by the RC time constant, high resonant-like frequency, i.e.small absorption and short carrier life time are preferable. Thus, it needs relatively high carrier density in the saturable absorber. However, the width of the hysteresis become narrow for high injection into the loss section. Optimization for the BS-LD sturucture and parameters will bring less than 100ps switching time.

4.Conclusion The BS-LD was shown to turn off at less than 170ps of switching speed and with 10pJ of switching energy by controlling parameters electrically through the loss section electrode. This is the highest speed bistable laser diode operation ever reported. The BS-LD seems to provide an attractive mean for high speed optical data switching.

References

[1]S.Suzuki et al.,IEEE J.Lightwave Tech.**LT-4**,894(1986)
[2]A.Migus et al.,Appl.Phys.Lett.,**46**,70(1985)
[3]I.Mito et al.,IEEE J.Lightwave Tech.**LT-1**,195,(1983)
[4]A.Tomita et al.,J.Appl.Phys.,**59**,1839(1986)

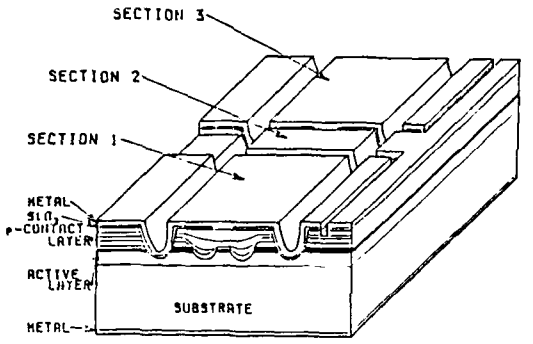

Fig. 1. Structure of a tandem electrode bistable laser diode.

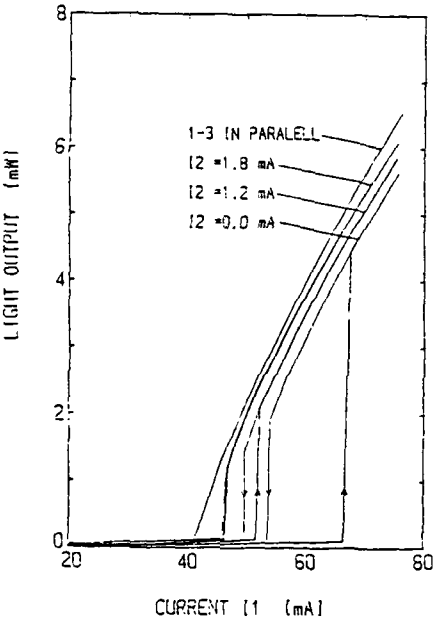

Fig. 2. Light-current characteristics for different bias current(I_2) into the loss section.

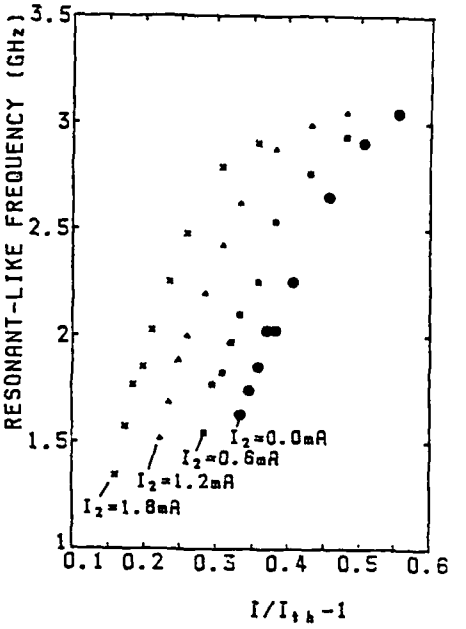

Fig. 3. Dependence of resonant-like frequency on the normalized excitation($I/I_{th}-1$) for different bias current(I_2), where I_{th} is defined as the threshold current when all the section are connected in parallel.

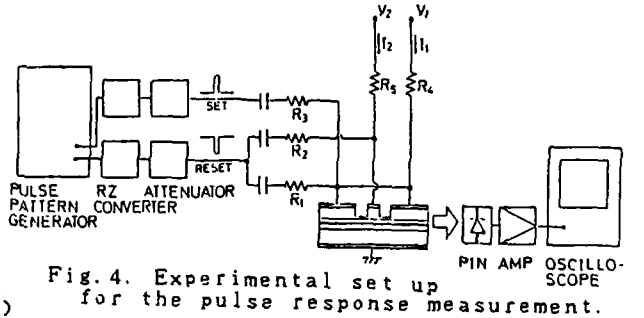

Fig. 4. Experimental set up for the pulse response measurement.

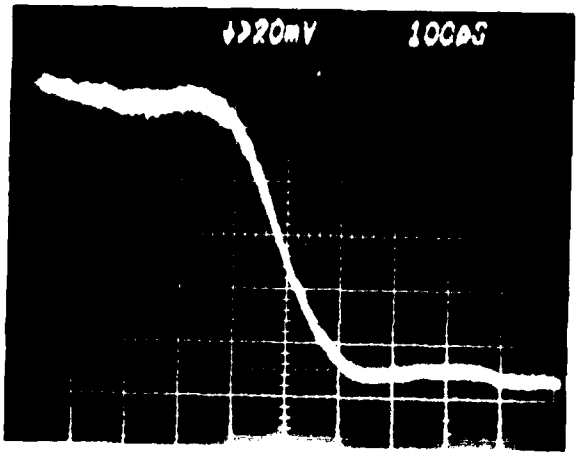

Fig. 5. Turn-off switching of the tandem electrode bistable laser diode. Horizontal: 100ps/div

ORGANIC MATERIALS FOR NONLINEAR OPTICS

R. D. Small, J. E. Sohn, K. D. Singer, and M. G. Kuzyk
AT&T, Engineering Research Center
P.O. Box 900, Princeton, NJ 08540

INTRODUCTION

Numerous investigations into the nonlinear optical properties of certain organic and polymeric materials have shown that these materials possess the largest observed optical nonlinearities.[1] [2] [3] [4] For implementation of all-optical and electro-optical communications and data processing systems, materials possessing large optical nonlinearities are required. Applications employing guided wave structures require materials that also are suitable for waveguiding and integration.

A variety of approaches to the fabrication of bulk organic nonlinear optical materials have been pursued including molecular crystals, crystalline polymers, Langmuir-Blodgett films, liquid crystals and liquid crystal polymers.[1] [3] Significant efforts in crystal growth [3] and single crystal thin film fabrication[5] [6] show promise for using organic and polymeric materials in applications using both second and third order optical nonlinearities.

We have recently demonstrated that molecularly-doped poled polymer glasses possessing reasonably large second-order nonlinear optical susceptibilities can be produced.[7] This new material class possesses several desirable properties for application to integrated optics, namely high optical quality, low dielectric constant and dielectric loss, the potential ability to be integrated with optical sources, detectors, and drive electronics, and the processability inherent to glassy polymers.

We will assess the potential applicability of organic and polymeric materials to integrated optics, discussing specific material properties important in these applications and progress in fabrication of optical structures from organic and polymeric materials.

NONLINEAR OPTICS

A brief description of nonlinear optical processes is necessary to understand the potential applications of organic and polymer materials in integrated optics. The macroscopic polarization P_i induced in a medium by an applied electric field is given by

$$P_i(t) = P_i^0 + \chi_{ij}^{(1)}(t)E_j(t) + \chi_{ijk}^{(2)}(t)E_j(t)E_k(t) + \chi_{ijkl}^{(3)}(t)E_j(t)E_k(t)E_l(t) + \cdots \quad (1)$$

where P_i^0 is the permanent polarization present in the material, $\chi_{ij}^{(1)}(t)$ the linear susceptibility, responsible for linear optics such as refraction and absorption, $\chi_{ijk}^{(2)}(t)$ the second order susceptibility which leads to effects such as second harmonic generation, the linear electro-optic (Pockels) effect, frequency mixing, and parametric amplification, and $\chi_{ijkl}^{(3)}(t)$ the third order susceptibility which leads to effects such as an intensity dependent index of refraction, optical bistability and optical phase conjugation. The odd order susceptibilities are nonzero in all materials, however, owing to the fact that $\chi_{ijk}^{(2)}(t)$ is a third rank tensor, the second order susceptibility is nonzero only if the material is noncentrosymmetric.

MATERIAL PROPERTIES

Glassy polymers possess several advantageous properties that are important for integrated optics. These properties include high optical quality, low dielectric constant and dielectric loss, and due to the processability inherent to glassy polymers, the potential ability to be integrated with optical sources, detectors, and drive electronics. Each of these properties will now be discussed in detail.

Optical Quality

Polymer glasses are widely used in the optics industry as bulk and micro optical components.[8] The most commonly used materials are polyacrylates, polycarbonates, and polystyrenes. Low optical losses are found with these materials due to their amorphous nature. Crystalline regions in a material cause scattering, thus reducing the optical quality.

Kaino has discussed the processes, both intrinsic and extrinsic, contributing to optical loss in polymer optical fibers.[9] Using the polymer glasses poly(methyl methacrylate), PMMA, perdeuterated PMMA, and polystyrene, it was found

that absorptive losses are very low (<0.1 dB/cm) at wavelengths between 0.5 and 1.0 μm, and that losses due to carbon-hydrogen overtones can be made lower than 0.1 dB/cm between 1 and 2 μm by deuteration.[10] [11]

High optical quality polymer waveguide structures were first reported in 1972 by scientists at Bell Laboratories.[12] Subsequently, several other methods were employed to produce low loss waveguides. The results have been reviewed elsewhere,[13] [14] and range from 0.5 dB/cm to less than 0.1 Db/cm. The high optical quality of these glassy polymer structures compares favorably with the propagation loss for devices fabricated in $Ti{:}LiNbO_3$ ($\sim$ 0.1 dB/cm).

Loss measurements for organic crystals have also been reported. Tomaru *et al* have produced optical channel waveguides of single crystal m-nitroaniline. [15] Scattering losses for a 5 mm long waveguide were reduced to 5 dB/cm with a laser zone-melting technique. Nayar has prepared single-crystalline, void-free benzil fibers (diameter 2-10μm) with a propagation loss estimated to be 2 dB/cm at 633 nm.[16] The quoted value was about 1 dB/cm greater than the attenuation in the bulk crystal. These values for crystalline materials are considerably higher than those measured in amorphous polymer glasses and in $Ti{:}LiNbO_3$; if crystals are to see application to guided-wave devices, these losses must be reduced substantially.

Dielectric Quality

The speed of lumped-element electro-optic devices is greatly determined by the dielectric properties of the electro-optic material. For instance, the bandwidth per modulating power ($\Delta f/P$) of a guided-wave modulator is given by[17]

$$\frac{\Delta f}{P} \propto \frac{1}{1 + \epsilon/\epsilon_0}, \tag{2}$$

where ϵ is the static dielectric constant. The rise time of a traveling wave modulator is given by $t_r \propto \sqrt{\epsilon/\epsilon_0} - n$,[18] thus a lower dielectric constant results in a faster device.

The dielectric properties of organic and polymeric materials are one of their more attractive properties. The dielectric constants of PMMA and polystyrene, which are typical polymer glasses, range from 2.5 - 3.5 depending on frequency. Also, the dielectric constant does not exhibit substantial dispersion in the modulating frequency ranges of interest. Dielectric loss will also degrade device performance and affect the switching power through its dissipative effects. Dielectric losses in polymer glasses are also low and nondispersive.

ELECTRO-OPTIC POLYMER GLASSES

We have prepared orientationally ordered electro-optic glassy polymer thin films.[7] [19] This is accomplished by dissolving an optically-nonlinear molecule, the azo dye disperse red 1, in PMMA. Thin films of the azo dye in PMMA are prepared by coating onto indium tin oxide coated glass; then a semi-transparent layer of gold is deposited on the film. The inversion center present in the amorphous solid solution of the dye in PMMA is removed using the technique of electric-field poling.

The poling process consists of first heating the film above its glass-rubber transition temperature, where, in the rubbery state of the polymer, molecular motion is enhanced. Next, a strong electric field is applied to the sample which tends to align the molecules. The sample is cooled and the electric field removed. The induced polarization is then locked in, resulting in a non-centrosymmetric material.

The nonlinear optical susceptibility can be calculated by assuming a non-interacting molecular ensemble at the poling conditions, and is given by, [7] [4]

$$\chi_{zzz}(-\omega_3;\omega_1,\omega_2) = N\beta_{333}(-\omega_3;\omega_1,\omega_2)\, f^{\omega_3} f^{\omega_1} f^{\omega_2} \left\{ \frac{p}{5} - \frac{p^3}{105} + \cdots \right\}, \tag{3}$$

where

$$p = \left\{ \frac{\epsilon(n^2+2)}{n^2+2\epsilon} \right\} \frac{\mu E_p}{kT}, \tag{4}$$

N is the number density, β_{333} is a component of the molecular nonlinear optical susceptibility, μ is the static dipole moment, E_p is the poling field, and where the f's are local field factors at the appropriate frequencies.

Second harmonic generation was measured in the films at a fundamental wavelength of λ=1.58μm. The d_{33} second harmonic coefficient, determined by measuring the second harmonic intensity as a function of angle, is: $d_{33} = 6.0 \pm 1.3 \times 10^{-9} esu$, which compares favorably with that of KDP ($d_{36} = 1.1 \times 10^{-9} esu$). Using the thermodynamic model and the properties of the measured film, namely that N=2.74×10^{20}, E_p=0.62MV/cm,

$\beta\mu = 525 \pm 100 \times 10^{-30} cm^5/esu$[7], $n = 1.52$, and $\epsilon = 3.6$; d_{33} is calculated to be $d_{33} = 7.5 \pm 1.5 \times 10^{-9}$ *esu*. The agreement between the experimentally determined value of d_{33} and the calculated value indicate that Equation (3) adequately describes the poled polymer solution.

It has been established experimentally that the origin of the electro-optic effect in organic materials is largely electronic.[4] This implies that the linear electro-optic coefficient can be estimated from the second harmonic coefficient.[4] By properly accounting for the dispersion (using a two level model), the electronic contribution to the electro-optic coefficient is calculated to be $r_{33}^{el} = 2.4 \pm 0.6 \times 10^{-12}\ m/V$ at $\lambda = 0.8 \mu m$, which compares favorably with that of GaAs ($r_{41} = 1.2 \times 10^{-12}\ m/V$).

Summary

The potential application of polymers, especially glassy polymers, to integrated optics is promising as evidenced by the pertinent material properties. A model nonlinear optical glassy polymer system was fabricated and evaluated. Its nonlinear optical properties compare favorably with those of other materials. Future optimization of nonlinear optical properties, along with the integrability, and high optical and dielectric quality of glassy polymers make this material class a promising one for use in integrated optics.

References

1. D. J. Williams, *Angew. Chem. Int. Ed. Engl.*, **23**, 690 (1984).

2. D. J. Williams, ed., *Nonlinear Optical Properties of Organic and Polymeric Materials*, ACS Symp. Ser. No. 233 (Washington D. C., 1983).

3. J. Zyss, *J. Molec. Electron.*, **1**, 25 (1985).

4. K. D. Singer, S. J. Lalama, J. E. Sohn, and R. D. Small, *Electro-optic Organic Materials*, in "Nonlinear Optical Properties of Organic Molecules and Crystals" edited by D. S. Chemla and J. Zyss, Academic Press, New York, 1986, in press.

5. See *inter alia* I. Ledoux, D. Josse, P. Vidakovic, and J. Zyss, *Opt. Eng.*, **25**, 202 (1986).

6. See *inter alia* G. M. Carter, Y. J. Chen, and S. K. Tripathy, *Opt. Eng.*, **24**, 609 (1985).

7. K. D. Singer, J. E. Sohn, and S. J. Lalama, *Appl. Phys. Lett.*, (1986), submitted for publication.

8. S. Musikant, "Optical Materials: An Introduction to Selection and Application", Marcel Dekker, Inc., New York, 1985.

9. T. Kaino, *Jpn. J. Appl. Phys.*, **24**, 1661 (1985).

10. T. Kaino, M. Fujiki, and K. Jinguji, *Rev. Elect. Commun. Lab.*, **32**, 478 (1984), and references cited therein.

11. P. Avakian, W. Y. Hsu, P. Meakin, and H. L. Snyder, *J. Polym. Sci. Polym. Phys. Ed.*, **22**, 1607 (1984), and references cited therein.

12. H. P. Weber, R. Ulrich, E. A. Chandross, and W. J. Tomlinson, *Appl. Phys. Lett.*, **20**, 143 (1972).

13. S. J. Lalama, J. E. Sohn, and K. D. Singer, *SPIE Proc.*, **578**, 168 (1985), and references cited therein.

14. W. J. Tomlinson and E. A. Chandross, "Organic Photochemical Refractive-Index Imaging Recording Systems," in *Advances in Photochemistry*, John Wiley & Sons, 1980, and references cited therein.

15. S. Tomaru, M. Kawachi, and M. Kobayashi, *Opt. Commun.*, **50**, 154 (1984).

16. B. K. Nayar, *Nonlinear Optical Interactions in Organic Crystal Cored Fibers*, p 153 in Reference 2.

17. I. P. Kaminow, J. R. Carruthers, E. H. Turner, and L. W. Stulz, *Appl. Phys. Lett.*, **22**, 540 (1973).

18. G. White and G. M. Chin, *Opt. Commun.*, **5**, 374 (1972).

19. K. D. Singer, S. J. Lalama, and J. E. Sohn, *SPIE Proc.*, **578**, 130 (1985).

PHYSICAL AND OPTICAL PROPERTIES OF Cd(Se,S) MICROCRYSTALLITES IN GLASS

D.W. Hall and N.F. Borrelli
Research and Development Division
Corning Glass Works
Corning, NY 14831

Since the demonstration of degenerate four-wave mixing in 'sharp-cut' filter glasses by Jain and Lind [1], considerable effort has been expended to understand the linear and nonlinear optical properties of glasses containing small amounts of Cd(Se,S) microcrystallites. This class of materials is promising for all-optical photonic switching devices: good optical quality samples are available, waveguide structures can be made using conventional ion-exchange techniques, the location of the absorption edge can be varied by composition changes across a wide range of wavelengths, and photo-recovery times on the order of ~ 10 ps have been reported [2,3]. Additional scientific interest in these materials comes from the observation of optical effects due to three-dimensional quantum confinement of photo-generated carriers [4] in specially treated samples.

We report on an extensive material and optical characterization of five commercially available Corning filter glasses containing thermally developed $CdSe_xS_{1-x}$ microcrystallites with selenium mole fraction in the range $0.28 \leq x \leq 0.74$, as well as several experimental glasses doped so as to contain crystallites of CdSe. Experimental techniques include wet-chemical analysis and X-ray diffraction for determination of crystallite structure and stoichiometry, transmission electron microscopy (TEM) for determination of crystallite size and distribution, and absorption and photoluminescence spectroscopy.

Absorption spectra obtained from thin-sections of the filter glasses are shown in Fig. 1. These data demonstrate that the steep absorption edge of 'sharp-cut' filters is due to the use of relatively thick (~ 2 mm) pieces of glass and not to the presence of a resonance that is fundamentally sharper than that

of bulk-crystal semiconductors. The location of the absorption edge of each of these filters is the same as that observed in bulk-crystal $CdSe_xS_{1-x}$ samples of the same selenium fraction [5]. We conclude on the basis of absorption, luminescence, and TEM data that quantum confinement effects have <u>not</u> been observed in these filter glasses, contrary to the analysis of others [6]. The distribution of crystallite diameters in one of the filters, CS 2-61, is shown in Fig. 2. Three-dimensional quantum confinement effects are anticipated when the crystallite diameter, d, satisfies the condition $d < d_{ex} \sim 80$ A [7], where d_{ex} is the bulk-crystal exciton diameter. Although some of the crystallites in the distribution satisfy this condition, an individual crystallite's contribution to the material's absorption coefficient or luminescence spectrum scales as the particle's volume so that optical properties are dominated by the larger, non-quantum confined particles.

Figure 3 shows absorption spectra of samples of an experimental CdSe-containing glass that have been given heat-treatments at various temperatures for 30 minutes. TEM confirms that higher treatment temperature produces crystallites with larger average particle diameter. An absorption band due to quantum confined transitions (e.g. peaked at 500 nm in the 595 C sample) appears and shifts towards lower-energy with increasing crystallite size until the band disappears (700 C sample) and the spectrum approaches that characteristic of the bulk crystal.

Experiments to measure the nonlinear coefficients of the filter glasses and quantum confined CdSe samples are under way. Pulses from 2 to 5 ps duration from a sync-pumped mode-locked dye laser are used to measure transmission as function of fluence. An example of data obtained for CS 2-61 at $\lambda = 600$ nm is shown in Fig. 4. Within our present pulse length range, no dependence on duration is observed; this is consistent with observations of other workers [2,3] that indicate hot-electron thermalization times on the order of 400 fs and electron-hole recombination times of $\geq$ 10 ps.

References

1. R.K. Jain and R.C. Lind, JOSA 73, 647 (1983).
2. M.Z. Nuss, W. Zinth, W. Kaiser, Tech. Dig. XIV Int. Quantum Elect. Conf. (IQEC), MBB2, San Francisco (1986).
3. G.R. Olbright, N. Peyghambarian, S.W. Kock, and B.D. Fluegel, submitted to Phys. Rev. Lett.
4. Al.L. Efros and A.L. Efros, Sov. Phys. Semicond. 16, 772 (1985).
5. D.W. Langer, Y.S. Park, R.M. Euwema, Phys. Rev. 152, 788 (1966).
6. J. Warnock and D.D. Awschalom, Phys. Rev. B 32, 5529 (1985).
7. L.E. Brus, J. Quantum Elec., QE-22, 1909 (1986).

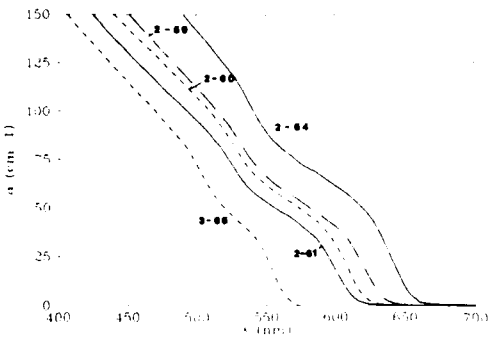

Fig. 1 Absorption spectra of Corning filter glasses containing Cd(Se,S) microcrystallites.

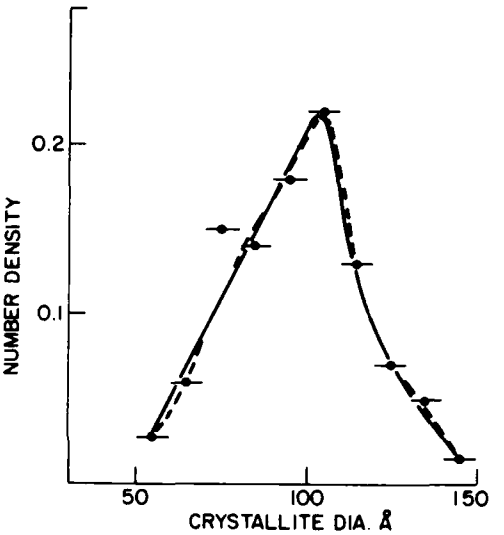

Fig. 2 Particle diameter distribution of CS 2-61 filter glass obtained by TEM.

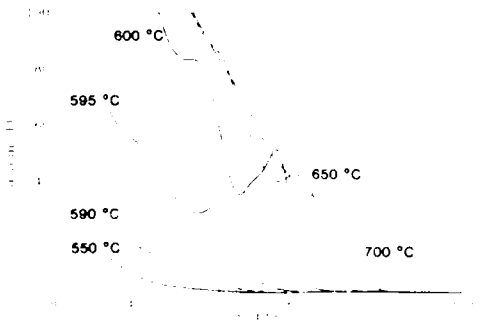

Fig. 3 Spectra of samples of a CdSe-containing glass receiving heat-treatment for 30 min.

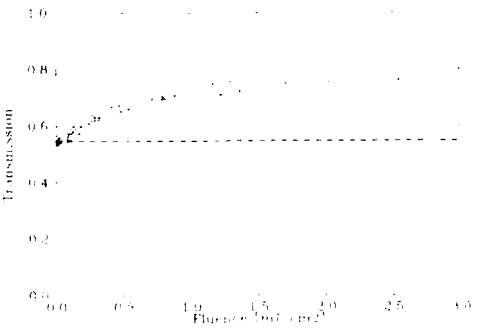

Fig. 4 Saturated absorption observed in CS 2-61 filter glass using 2 ps, 600 nm pulses.

The Dynamics of Photonic Switching in Indium Antimonide

H.A. MacKenzie, J. Young and H.A. Al-Attar

Physics Dept. Heriot-Watt University, Edinburgh EH14 4AS, U.K.

To obtain the full data processing potential of optical computing, the practical system may well evolve in the form of fast switching arrays of bistable elements which exploit the innate parallelism of optics. Such arrays will be required to operate efficiently with low incident powers, high switching speed, gain, good tolerance to noise and minimal cross talk between channels. An investigation of these competing criteria has been undertaken with an Indium Antimonide etalon using low power c.w. CO lasers, lead-salt diode lasers and other sources of switching signal.

The dynamic switching characteristics of the Indium Antimonide system have been studied to establish the optimal conditions for rapid switching and to assess the practical limits of the low power switching regime. In this mode of operation large differential optical gain may be achieved but as the operating point is very close to the switch point, the switching dynamics are subject to critical slowing down effects [1] and transient bimodality, both of which have been observed in our experiments. The role of noise in the system is crucial and we report a new study of noise dependent delay to switching [2,3] where noise assisted switching may be observed after a delay of μS (or in some cases mS) after the initiation of a weak control beam. The results of these experiments allow us to project stability criteria and the appropriate operating conditions for different noise levels in the system.

The assessment of the array potential of the InSb system has been investigated by measuring the crosstalk between adjacent optical channels under various operating conditions. In our system, the interchannel coupling

is diffusive and the diffusion length of photo-excited carriers in the InSb is typically 60 μm [4] at 80K. If one channel is allowed to switch, a switching wave then propagates to the other channel. If the photogenerated carrier density then exceeds the threshold for switching, the second channel will then switch and propagate the process through the array. The transfer of switching between adjacent channels spaced at up to 300 μm apart has been measured and transferred switch delays of up to 5 μS have been observed.

From these studies we make an assessment of the data rates, noise limitations, switching dynamics, and pixel densities which may be obtainable with the InSb system and which could be appropriately scaled to other semiconductor etalons.

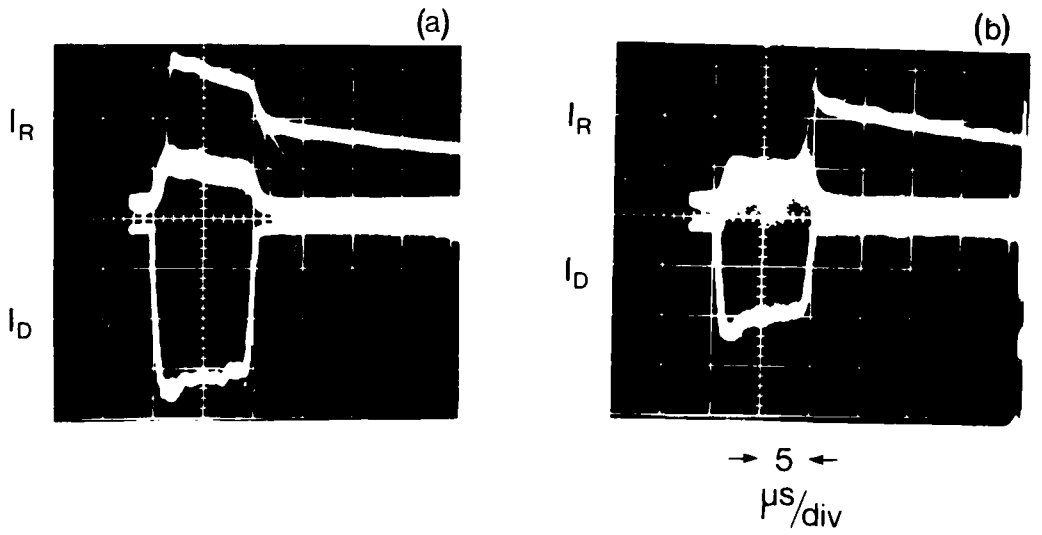

Oscilloscope traces (a,b) are each the superposition of 400 pulses showing critical slowing down effect and double peaked distribution which characterises transient bimodality. I_D is the input diode laser irradiance, I_R is the reflected CO laser beam.

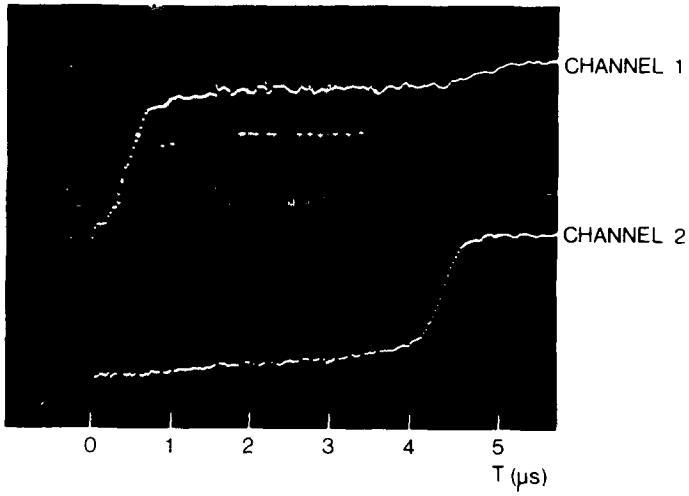

Figure showing outputs from both channels; channel 1 is switched on and ~ 4 μs later channel 2 is induced to switch. ΔP = 5.4% and x = 165 μm in this case.

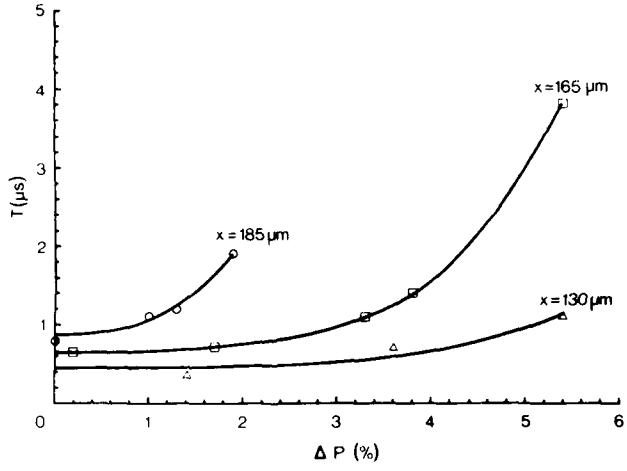

Graph showing time delay to switching for various hold-off powers ΔP and channel separations of 185, 165 and 130 μm. Where $\Delta P = (P_u - P_D)/P_u$, P_u = switch up power, P_D = switch down power.

References

[1] R. Bonifacio and L.A. Lugiato, Opt. Comm. 19, 172 (1976).

[2] F.A. Hopf and P. Meystre, Opt. Comm. 29, 239 (1979).

[3] D. Farina, M. Narducci, M. Yuen and L.A. Lugato, Opt. Eng. 19, 469 (1980).

[4] D.J. Hagan, H.A. MacKenzie, H.A. Al-Attar and W.J. Firth, Opt. Lett. 10, 187 (1985).

FRIDAY, MARCH 20, 1987

PROSPECTOR/RUBICON ROOM

3:30 PM–5:00 PM

FD1–5

TIME DIVISION SWITCHING

Flavio Melindo, CSELT, *Presider*

PHOTONIC TIME-DIVISION SWITCHING TECHNOLOGY

Hirokazu GOTO
C&C Information Technology Research Labs.
NEC Corporation, 4-1-1 Miyazaki, Miyamae-ku, Kawasaki, 213,Japan

1. Introduction

With growing interest in visual information services, substantial needs for broadband communications networks are increasing. Optical switching systems are expected to have advantages over conventional electronic switching systems for use in switching broadband optical signals. Space-division, wavelength-division and time-division switching networks will be used in optical switching systems. Compared with the two other switching networks, the time-division switching network has an inherent advantage in providing a good match with existing time-division optical fiber transmission systems. This paper describes the principles and the present state of optical time-division switching technology. Further studies are also discussed.

2. Principles of time-division switching

Figure 1 shows a basic time-division switching network. Input signals are time-multiplexed by a multiplexer onto an input highway which is connected to a time switch. The time switch performs the functions of interchanging every time-slot on the input highway and sending it to an output highway. Time-multiplexed signals on the output highway are separated into individual output lines by a demultiplexer. As a result, the exchange of information between incoming and outgoing channels has been accomplished.

Multi-stage switching networks, such as a Space-Time-Space network shown in Fig. 2, are necessary for achieving a large line-capacity network. The space switch consists of a crosspoint matrix, and its connections between inputs and outputs change every time-slot. Switching both in time switches and in space switches allows the exchange of information between different time slots on different highways.

3. Present state of optical time-division switching technology

Some studies of optical time switches, such as the one shown in Fig. 3, have been reported. An optical write gate leads the input optical highway to individual optical memories in turn. An optical read gate leads optical signals, memorized in optical memories, to the output optical highway in response to the controller's directions. High-speed optical memories and write/read gates are necessary for the construction of the optical time switch. An optical fiber delay line can be used as the optical memory[1]. Furthermore, several kinds of optical bistable devices have been developed. They fall into two categories, intrinsic and hybrid. A bistable laser diode[2] and a non-linear Fabry-Perot etalon[3] are intrinsic. A self-electro-optic effect device (SEED)[4] and monolithically integrated bistable device consisting of opto-electronic feedback circuits[5] are hybrid. An electro-optic switch and laser diode switch can be used as high-speed optical write/read gates.

The world's first experiment in optical time-division switching using fiber delay lines and directional coupler switch matrices was reported in 1983[1]. The current highest switching speed, 256 Mbps, has been achieved using bistable laser diodes and directional coupler switch matrices[6]. The bistable laser diode is a InP laser diode with a tandem electrode and has hysteresis characteristics in the relationships among an optical input power, output power and injection current, as shown in Fig. 4. It can be set and reset by applying optical pulse and current pulse, respectively.

4. Further studies

The following problems have to be solved before large-capacity optical time-division switching systems can be achieved.
(1) Realization of much higher optical highway speed:
Optical memories, which can memorize high-speed optical signals in order of giga-bits per second, will be required.
(2) Introduction of optical control circuits to prevent electronic control circuits from limiting highway speed:
Optically controlled logics and memories will be necessary.
(3) Realization of various timing circuits, such as a bit/frame synchronizer and a frame aligner:
These circuits are required to receive optical signals and to generate optical timing signals.
(4) Multiplexing and demultiplexing of signaling information in the interface between switching and transmission systems:
These operations will also be required to be performed by all-optical devices. The realization of optical multiplexer/demultiplexer interfacing with various hierarchy optical time-division trunk lines will be necessary.
To sum up the above discussion, the crucial points in developing large-capacity switching systems are the realization of high-speed, all-optical functional devices. They are now under extensive study worldwide in research concerned with optical signal processing and optical computing.

5. Conclusion

The present state of and further study objectives for optical time-division switching systems are described in this paper. The all-optical time-division switching system, including optical control circuits, will be required for the achievement of future optical time-division broadband telecommunications networks. The technology will be common to that of the optical computer. Therefore, the development of the optical time-division switching system will enhance the capability of achieving future optical computer and communications systems.

References

(1) H.Goto et al., OFC'83, MJ6 (1983)
(2) Y.Odagiri et al., CLEO'84, THJ3 (1984)
(3) D.S.Chemla et al., 14th International Conference on Quantum Electronics, MGG4 (1986)
(4) D.A.B.Miller et al., Appl. Phys. Lett., vol.45, p13 (1984)
(5) K.Okumura et al., IEEE J-QE, QE-21, p377 (1985)
(6) S.Suzuki et al., IEEE J-LT, LT-4, p894 (1986)

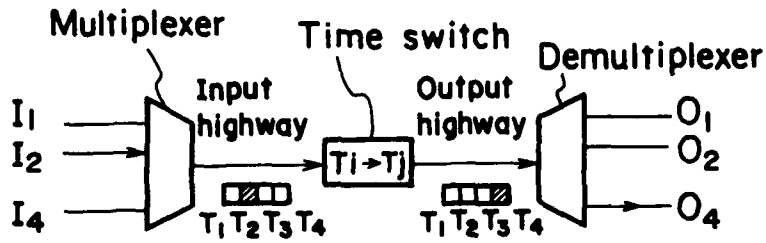

Fig.1. Basic time-division switching network

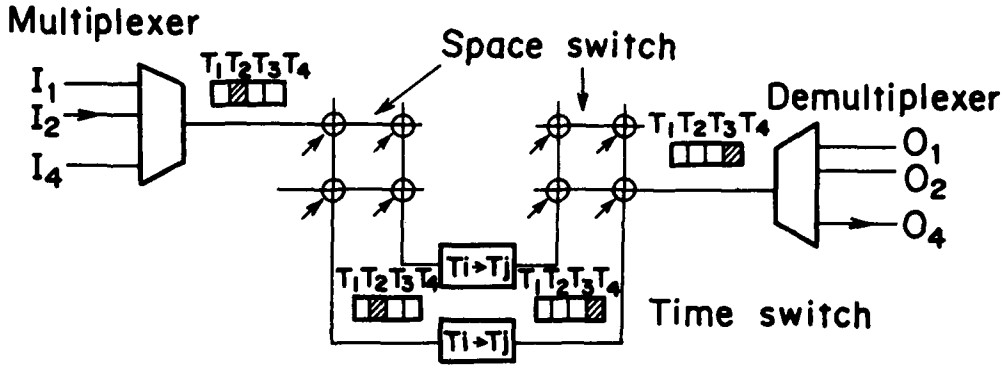

Fig.2. Three-stage time-division switching network

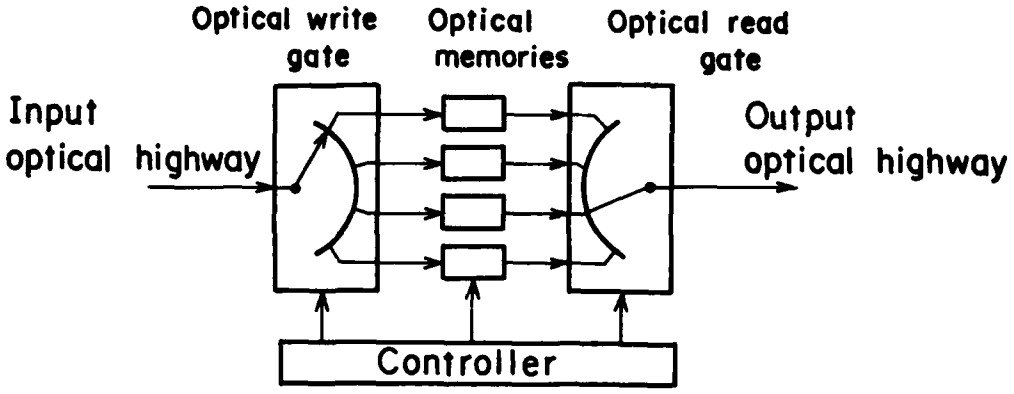

Fig.3. Optical time switch configuration

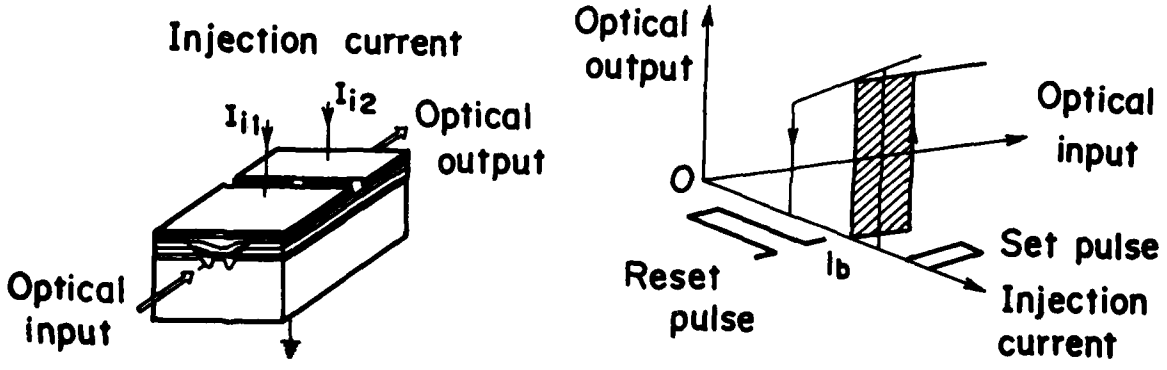

Fig.4. Bisable laser diode

A 1.5 Gigabit-per-Second, Time-Multiplexed Photonic Switching Experiment

J. R. Erickson
R. A. Nordin
W. A. Payne
M. T. Ratajack

AT&T Bell Laboratories
Naperville, Illinois 60566

1. INTRODUCTION and SYSTEM OVERVIEW

Current experimental $Ti:LiNbO_3$ switching systems need electronics for control, regeneration, and compensation for the imperfections of the photonic switching fabric. These early photonic switches do, however, have advantages over their electronic counterparts: 1) Their switching fabric can carry 100 Mb/s or 10 Gb/s with little modification, 2) Their switching fabric is synergistic with fiber transmission, especially when optical amplifiers can be used, 3) They provide valuable experience in optics and photonic switching, 4) They give insight into the future of optical switching and how the signaling and protocols of the network need to evolve to accommodate this emerging technology[1].

In this paper, we describe a time-multiplexed photonic switch which routes 45 Mb/s channels that are time-multiplexed to a data rate of 1.5 Gb/s (see Figure 1). The system will innovate on several frontiers: 1) The switch fabric will incorporate crossing waveguides, Y-branches, proton-exchange polarizers, and polarization-maintaining fiber, 2) It will demonstrate optical switching of time-multiplexed blocks of data, 3) It will switch gigabit data streams, and 4) It will have broadcast capability.

First, we describe the photonic switch features and fabrication, and follow with a description of the controlling electronics. We then describe the system and the data formats.

2. PHOTONIC SWITCH

We here explain the photonic switch architecture, and consider some fabrication issues.

2.1 Progress

In a few years $Ti:LiNbO_3$ technology has progressed from 2x2 photonic switch/modulators to 4x4 non-blocking switch arrays that switch video with no noticeable picture degradation [2]. Although VLSI in $Ti:LiNbO_3$ seems unlikely, 8x8 photonic switches on a single substrate have been reported and larger switches will follow, either on a single substrate or by interconnecting several substrates[3].

2.2 A Tree-Structured Architecture

To provide a strictly non-blocking switch fabric with broadcast capability, we chose a tree-structured architecture that uses passive splitters and active selectors[4] [5]. The left half of the fabric has passive Y-branches in a tree structure with the roots at the input. Power from each input is divided until it provides four equal-powered replicas to the center of the network. The selector side selects which of the four inputs will reach the outputs and voltage is applied to the appropriate couplers to direct the light to the desired output. The switch fabric has full broadcasting capability, i.e. any collection of subsets of the idle outputs can be connected to any of the inputs at any time.

2.3 Design and Fabrication of the Photonic Switch

In designing the photonic switch, several tradeoffs were made.

To keep the drive voltages low and to simplify the coupler design, we use single-polarization directional couplers. To preserve the polarization isolation of the laser, polarization-

maintaining fiber connects the laser transmitters to the $Ti{:}LiNbO_3$ switch. Further polarization filtering is done by proton-exchange polarizers that are fabricated at the switch inputs. Using this approach, polarization isolation better than -35 dB is expected[6].

This switch uses reverse $\Delta\beta$ electrodes which requires two electronic drivers for every directional coupler[7].

High-speed individual couplers have been fabricated, as have arrays of couplers operating at slow speed[8] [9]. This experiment proposes an array of couplers that can reconfigure in a few nanoseconds, thus requiring careful electrode design and high-speed electronic drivers.

G.A. Bogert et al. at the AT&T Bell Labs Allentown facility design and fabricate the lithium niobate devices; first versions of the switch are under test at AT&T Bell Labs near Chicago.

3. *SWITCH CONTROL*

A microcomputer reprograms connections using a memory and sequencer to control the switch drivers. The sequencer steps through the memory, extracting a bit pattern for the driver array once every timeslot. Reconfiguration takes place in a guard band that is between data blocks.

4. *SEMI-SYNCHRONOUS MULTIPLEXING*

Although bistable optical devices have been demonstrated, the integration necessary for a high-speed, photonic elastic store cannot be expected in the near term[10]. Photonic switching systems cannot easily bit-synchronize input data[11]. Using variable lengths of fiber on the switch inputs or switch-to-source feedback schemes, however, we can hope to align the incoming channels to within a reasonable number of bits. In this experiment we adopt a semi-synchronous format that uses block multiplexing and guard bands to broaden the allowed switching time.

Because multiplexing is done by blocks rather than bit by bit, a timeslot will have many bits all coming from the same input channel. Between the data blocks are three fields: guard bands, which allow the switch to reconfigure; clock recovery bits, which the receiver uses to extract clock; and flag bits, which alert the demultiplexer to the start of valid data. Each frame will contain several timeslots. Each timeslot will have a guard band, clock-recovery bits, flag bits, and data bits.

Using this format, the data need not be bit synchronized; we must only guarantee that during reconfiguration each channel is somewhere in its guard band. Once switched, the data enters the receiver, where the clock is extracted and the data demultiplexed. After demultiplexing, hardware at the receiving side finds the flag and marks the beginning of valid data. These data are then channeled to the desired 45 Mb/s sink.

Clock recovery is a critical issue. If the receiver takes half a timeslot to recover the clock, the system is impractical. If the frequency can be tightly controlled and the phase adjusted in a small number of bits relative to a total timeslot, the overhead will be a small fraction of the block size.

5. *CONCLUSIONS*

This experiment confronts several issues that are fundamental to guided-wave optical switching. 1) It illustrates several guided-wave optics functions in a single system. 2) It allows time-multiplexed switching of a number of interconnected and integrated directional couplers. 3) It demonstrates optical broadcasting. 4) It proposes a block-multiplexed data format.

REFERENCES

1. J.R. Erickson and H.S. Hinton, "Implementing a $Ti:LiNbO_3$ 4x4 Non-Blocking Interconnection Network," 578-38, SPIE 2nd Int'l Conf. Int. Optic Ct. Eng., Sept. 17-19, 1985, Cambridge, Mass.
2. J.R. Erickson et al. "A Photonic Switching Demonstration Display," submitted to this meeting.
3. P. Granestrad et al., "Strictly nonblocking 8 x 8 integrated-optic switch matrix in $Ti:LiNbO_3$," IGWO '86, WAA3, 26-28 Feb. 1986, Atlanta, GA.
4. R.A. Spanke "Architectures for Large Nonblocking Optical Space Switches," *IEEE Journal of Quantum Electronics*. Vol. QE-22, No. 6, June 1986, p. 964.
5. K. Habara and K. Kikuchi "Optical Time-Division Space Switches Using Tree-Structured Directional Couplers," *Electronics Letters* Vol. 21, No. 14, July 4, 1985, pp. 631-2
6. J.J. Veselka and G.A. Bogert, "Low Loss Proton Exchange Channel Waveguides and TM-Pass Polarizers in Z-cut $LiNbO_3$," submitted to IOOC/OFC '87.
7. R. V. Schmidt and R. C. Alferness "Directional Coupler Switches, Modulators, and Filters Using Alternating $\Delta\beta$ Techniques". *IEEE Trans. on Circuits and Systems* vol. CAS-26, no. 12, Dec. 1979
8. S. K. Korotky et al. "Fully Connectorized High-Speed $Ti:LiNbO_3$ Switch/Modulator for Time-Division Multiplexing and Data Encoding," IEEE Journal of Lightwave Tech., LT-3, No. 1, Feb. 1985, pp. 1-6.
9. G.A. Bogert, E.J. Murphy, and R.T. Ku, "A Low Crosstalk 4x4 $Ti:LiNbO_3$ Optical Switch with Permanently Attached Polarization-Maintaining Fiber Arrays," PDP3, IGWO '86, Atlanta, GA, Feb. 27, 1986.
10. H. Goto et al, "An Experiment On Optical Time-Division Digital Switching Using Bistable Laser Diodes and Optical Switches," Proceedings of the IEEE GLOBECOM, Vol. 2, November 1984, pp. 880-884.
11. W.A. Payne and H.S. Hinton, "System Considerations for the Lithium Niobate Photonic Switching Technology," submitted to this meeting.

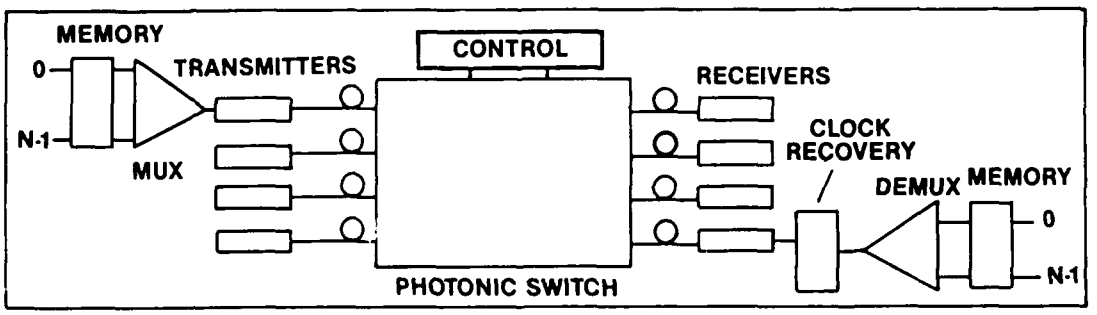

FIGURE 1 - A Time-Multiplexed, Photonic Switching System

4 Gb/s Optical Time-Division Multiplexed System Experiments using Ti:$LiNbO_3$ Switch/Modulators

R. S. Tucker, S. K. Korotky, G. Eisenstein, U. Koren, G. Raybon,
J. J. Veselka, L. L. Buhl, B. L. Kasper, and R. C. Alferness

AT&T Bell Laboratories
Crawford Hill Laboratory
Holmdel, N.J. 07733

Optical time-division multiplexing (OTDM) is potentially a useful technique for increasing the bit rate of lightwave systems beyond the bandwidth capabilities of drive electronics. We report here a novel optical multiplexing and demultiplexing scheme using mode-locked extended cavity injection lasers and Ti:$LiNbO_3$ waveguide switch/modulators. An OTDM experiment is described in which two separate lasers are mode-locked and externally modulated at 2 GHz, and then optically multiplexed to a bit rate of 4 Gb/s. The 4-Gb/s multiplexed signal is transmitted over 8 km of fiber, demultiplexed with a Ti:$LiNbO_3$ optical directional coupler switch, and received at low error rate. The experiments reported here extend our previous work on external modulation [1], OTDM using gain-switched lasers [2], and our work on mode-locking of extended-cavity injection lasers [3]. The mode-locked lasers provide an excellent means of generating short pulses at high repetition rates, using only narrow-band electronics. In addition, they offer the potential of good spectral purity - a key requirement for low distortion, high bit-rate transmission over long fiber lengths.

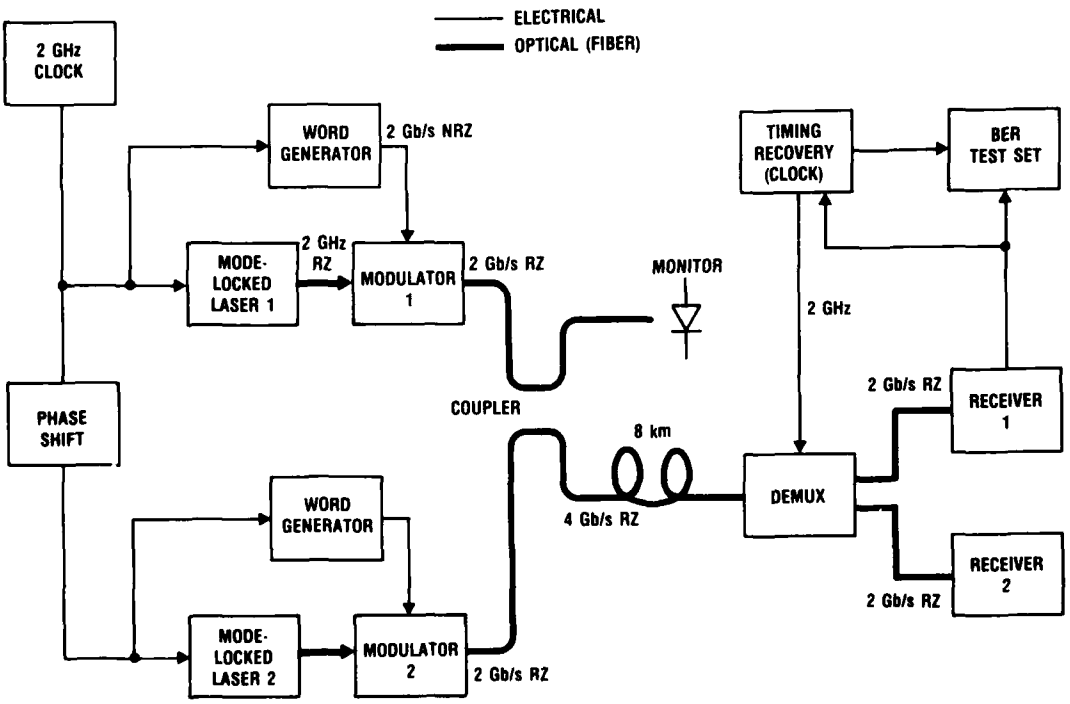

Fig. 1: Schematic of experimental setup.

The optical time-division multiplexed system is illustrated in Fig. 1. Two mode-locked lasers operate near 1.3 μm and generate pulse trains at a repetition rate of 2 GHz, and with durations of 20 ps FWHM. The gain media of the lasers are grown and selected so that their emission wavelengths are within 100 Å of one another and of the fiber zero dispersion wavelength. Data encoding of the laser pulses is carried out using Ti:$LiNbO_3$ waveguide modulators which are driven by non-return-to-zero (NRZ) pseudorandom word generators. The two lasers are driven by the same 2-GHz signal, which is also used to clock the word generators. Electrical phase shifters are used to provide an appropriate time delay of one-half of a bit period between the mode-locked pulses from the two laser transmitters. Additional phase-shifters (not shown) provide synchronization of the modulators with the mode-locked pulses. In the preliminary experiment described here, only one channel was modulated with pseudorandom data: the second channel was operated with a continuous string of "ones". Outputs from the two laser transmitters are combined in a 3-dB fiber directional coupler to give a multiplexed return-to-zero (RZ) signal at 4 Gb/s. This signal is monitored by a high-speed detector and is injected into an 8 km length of fiber.

At the receiver end of the system, the 4-Gb/s signal is demultiplexed using a Ti:$LiNbO_3$ directional coupler switch. Each demultiplexed signal is detected using a separate 2-Gb/s avalanche photodiode receiver, and errors are detected using a conventional error test set. A 2-GHz phase-locked loop at the output of receiver 1 provides timing recovery both for demultiplexing and error detection. Total losses of the switch/modulators in the transmitters and demultiplexer are in the range 4-5 dB.

One of the chief advantages of optical multiplexing is that the bandwidth requirements of the electronics are less than for a system with electronic multiplexing. In the present 4-Gb/s system the widest electronic bandwidth required is approximately 1.5 GHz (for the modulators and receivers). The clock and demultiplexer drive signals are narrowband 2-GHz sinusoids.

Fig. 2 shows the received 2-Gb/s eye pattern at the output of receiver 1 at an error rate of 10^{-10}. The bit error rate is plotted in Fig. 3 as a function of received power level. The curve on the the right characterizes the overall system performance, and indicates a sensitivity of -34 dBm for 10^{-9} error rate. For the 8 km fiber used in the present experiments, the received power was 10 dB above this level. The curve in the center of Fig. 3 is for only one channel operating (laser 2 switched off), and the left curve is for the 8 km length of fiber removed. The sensitivity of the system with no fiber was independent of whether laser 2 was on or off. We deduce from these results that there is negligible system penalty due to crosstalk in multiplexing and demultiplexing, and that other penalties (principally due to fiber dispersion) are small.

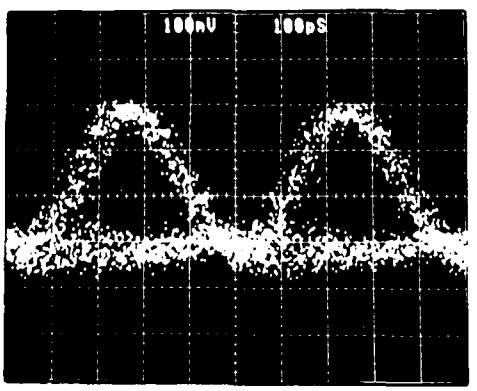

Fig. 2: 2-Gb/s eye pattern at output of receiver 1

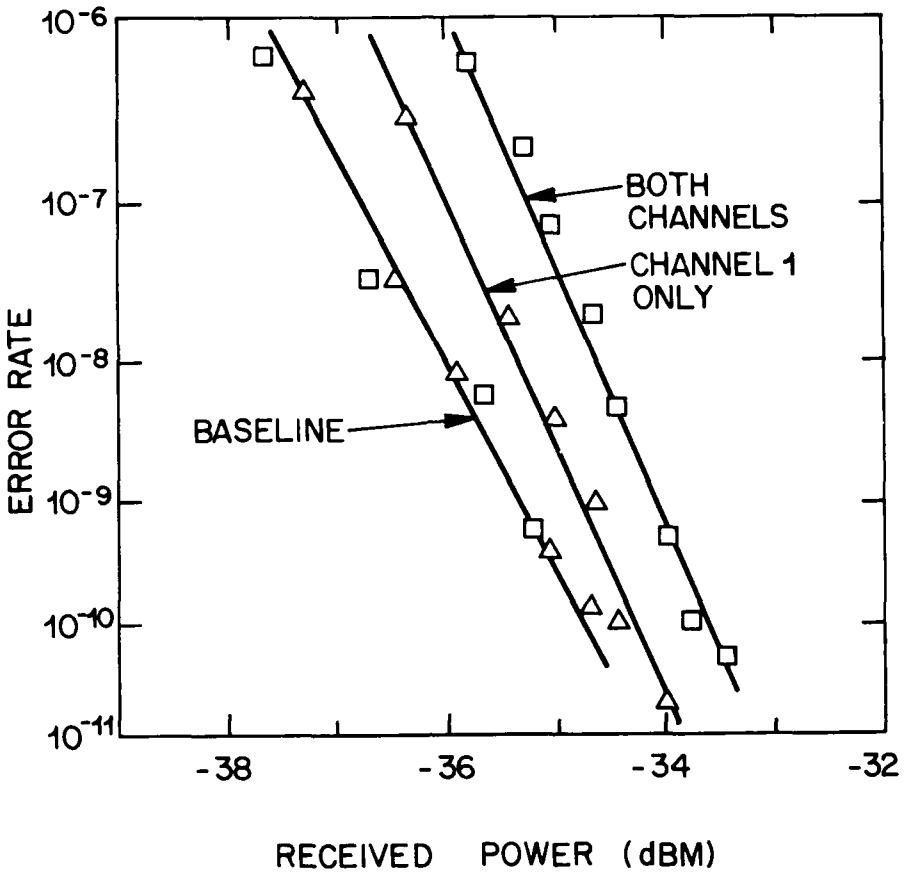

Fig. 3: Error rate versus received power

In summary, we have demonstrated that high-speed $LiNbO_3$ switches can be used in practical optical time-division multiplexed systems. The present experiments carried out at 4 Gb/s, but higher bit-rates should be readily achievable.

REFERENCES

[1] S. K. Korotky, G. Eisenstein, A. H. Gnauck, B. L. Kasper, J. J. Veselka, R. C. Alferness, L. L. Buhl, C. A. Burrus, T. C. D. Huo, L. W. Stulz, K. C. Nelson L. G. Kohen, R. W. Dawson, and J. C. Campbell, J. Lightwave Technol., LT-3, 1027 (1985)

[2] S. K. Korotky, L. L. Buhl, R. C. Alferness, G. Eisenstein, and J. J. Veselka, Technical Digest, Topical Meeting on Guided-Wave and Integrated Optics, Kissimmee, Florida, 1984, Paper TuA3.

[3] G. Eisenstein, R. S. Tucker, U. Koren, and S. K. Korotky, IEEE J. Quantum Electron., QE-22, 142 (1986)

Optimizing Photonic Variable-Integer-Delay Circuits

Richard A. Thompson

AT&T Bell Laboratories
Murray Hill, New Jersey 07974

1. Introduction. We present photonic circuits for temporal processing of photonic signals by a controlled variation in the delay of a photonic signal path. Since they provide variable delay in increments of some fixed elementary value, we call them *variable integer delays*. We present three structures, called *parallel*, *series re-entrant*, and *series feed-forward*. One application is in a photonic time-slot interchanger[1], [2] in which all the data from an input time-slot experience the appropriate delay to emerge in the assigned time-slot in the output. We optimize two parameters: the total number of switches in the structure (roughly proportional to cost) and the number of switches through which any photonic signal must pass (roughly proportional to insertion loss).

A parallel variable-integer-delay circuit with n integer-delay values requires n different fixed delay lines and two commutators. An input pulse is steered to the delay line that provides the desired delay and steered from that line to the output. Each commutator is a binary tree of 1-by-2 photonic switches; one implementation is to use 2-by-2 Lithium Niobate directional couplers with an unused input.[3] Such a binary tree with n outputs requires n−1 total switches and a pulse traverses $\log_2(n)$ switches from input to output. For parallel structures, the total switch count is 2(n−1) and the number of switches that a signal traverses is $2\log_2(n)$. Since we will show alternate structures for which both measures are about $\log_2(n)$, one might conclude that the parallel structures are poorer. However, if the variable-integer-delay circuits are part of larger systems that have commutators anyway, then the parallel structures may be superior.

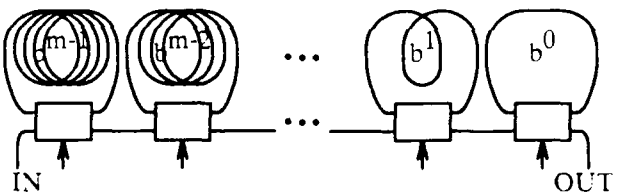

2. Series Re-Entrant Structure. The rightmost loop has delay equal to the fundamental unit of delay and each loop has a delay equal to b times the length of its right neighbor; b is called the *base*. A photonic pulse experiences a total delay

$$d = a_{m-1} b^{m-1} + \cdots + a_0 b^0$$

where b^i is the delay of loop i and a_i is the number of times the pulse enters loop i; $0 \le i < m$. Usually $a_i < b$ because, if not, the same total delay could be implemented with a higher-order loop and fewer switch traversals. In its extremes, $d_{min} = 0$ (nominally) if all $a_i = 0$ and $d_{max} = b^m - 1$ if all $a_i = b - 1$. Typically the designer knows the maximum delay and selects the number of switches m and the *base* b. For a given base, m is determined by solving the d_{max} equation for m,

$$m = \frac{\ln\left(d_{max}+1\right)}{\ln\left(b\right)},$$

and rounding up to the next integer. Selecting the *base* is more difficult.

If the photonic switches are expensive and if cost is the principal design issue, then an implementation with m = 1 is interesting to consider. However, a total delay of d times the delay of the only loop requires that a photonic signal traverse the switch x(d) = d + 1 times, resulting in considerable loss for a typical photonic switch in Lithium Niobate. Since the loss

can be reduced significantly by introducing one more switch, for m = 2 and a delay of d times the unit delay,

$$b = \sqrt{d_{max}+1} \text{ and } x(d) \le 2\sqrt{d_{max}+1}.$$

This expression above generalizes in m, but the number of switch traversals, x(d), is not monotonically decreasing as m increases.

The photonic switches, from which the structures are built, are characterized by poor crosstalk and high insertion loss. This motivates optimizing the architectures to reduce the number of switches through which a pulse traverses, over all values of delay. A pulse traverses the i-th switch once even if the i-th loop is not entered and traverses the i-th switch one additional time for each time the i-th loop is entered. Thus, the total number of switch traversals for a delay of d is

$$x(d) = \sum(1 + a_i) = m + \sum a_i.$$

In its extremes, $x_{min} = m$ when $d = d_{min} = 0$ and $x_{max} = mb$ when $d = d_{max} = b^m - 1$. We provide analyses for minimizing two variants of x(d), its *worst case* and its *average*.

The worst case number of switch traversals is

$$x_{max} = mb = \ln(d_{max}+1)\frac{b}{\ln(b)}.$$

Differentiating with respect to b and setting to zero has solution when $\ln(b) = 1$. The solution and the minimized worst case number of switch traversals are

$$b_{opt}^{wc} = e = 2.71828 \text{ and } x_{opt}^{wc} = 2.7 \ln(d_{max}+1) = 2.7\, m.$$

This *worst-case* analysis suggests that the optimal integer-valued *base* is 3.

Assuming the values for each a_i are uniformly distributed between 0 and b−1 inclusively, the average value for any a_i and the average number of switch traversals are:

$$\bar{a} = \frac{b-1}{2} \text{ and } \bar{x} = m + m\bar{a} = m\left(\frac{b+1}{2}\right) = \frac{\ln(d_{max}+1)}{\ln(b)}\frac{b+1}{2}.$$

Differentiating with respect to b and setting to zero has solution when $\ln(b) = \frac{b+1}{b}$.

This transcendental equation was solved by a short Newton-Raphson program. The solution and the minimized average number of switch traversals are

$$b_{opt}^{av} = 3.59112 \text{ and } \bar{x}_{opt} = 1.8 \ln(d_{max}+1) = 2.3\, m.$$

This analysis suggests that the optimal integer-valued *base* is 4, and not 3 as suggested above. The inaccuracy of this analysis is worsened if the a_i are not uniformly distributed between 0 and b−1.

3. Series Feed-Forward Structure. We identify three differences between the Feed-Forward structure and its equivalent Feed-Back (re-entrant) structure. Unlike the re-entrant case, where a pulse may traverse the same loop many times, here a loop may only be traversed once or by-passed by a pulse, and the *base* b is always 2. A Feed-Back structure with m loops has m switches while a Feed-Forward structure requires m+1 switches. The number of switch traversals is constant in the Feed-Forward structure, so there is no analysis of worst-case or average values. We compare the number of switch traversals in comparable Feed-Forward and Feed-Back structures.

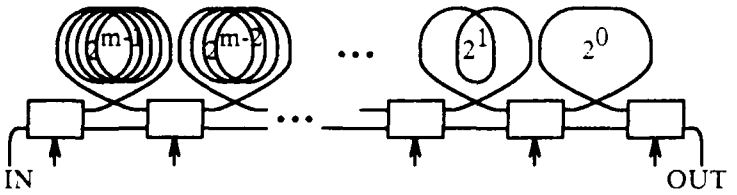

Consider a series structure with *base* b = 2 and m = M loops. In a Feed-Forward structure, the number of switch traversals is a constant

$$x^{ff} = \bar{x}^{ff} = M + 1.$$

In the equivalent Feed-Back structure, the worst case x(d) and average $\bar{x}$ number of switch crossings are:

$$x^{fb}_{b=2} \le 2M \quad \text{and} \quad \bar{x}^{fb}_{b=2} = 1.5\,M \quad \textit{implies} \quad \bar{x}^{ff} \le \bar{x}^{fb} \quad \textit{whenever} \quad M+1 \le 1.5\,M.$$

The right inequality is satisfied for any M ≥ 2; that is, any multi-stage structure. If the *base* in the re-entrant structure is squared to 4, past the worst-case minimum of 3 but close to the average-value optimum, then only half as many switches, M/2, are required to provide the same maximum total delay, d_{max}. Here,

$$x^{fb}_{b=4} \le 2M \ \textit{again} \ \text{and} \ \bar{x}^{fb}_{b=4} = 1.25\,M \quad \textit{implies} \quad \bar{x}^{ff} \le \bar{x}^{fb} \quad \textit{whenever} \quad M+1 \le 1.25\,M.$$

The right inequality is satisfied for any M ≥ 4. But, recalling that M is the number of loops in a Feed-Back structure with b = 2 and that the equivalent Feed-Back structure with b = 4 has half as many loops, the inequality is satisfied if the Feed-Back structure with b = 4 has 2 or more loops. To illustrate the optimality (for the average value) of b=4 in the re-entrant structure, if the original base had been cubed to a value of 8, then only one-third as many switches, M/3, are required to provide the same d_{max}. Here,

$$x^{fb}_{b=8} \le \frac{8}{3}M \quad \text{and} \quad \bar{x}^{fb}_{b=8} = 1.5\,M \quad \textit{again}.$$

Thus, for any Feed-Back structure with more than one loop in any *base*, the equivalent Feed-Forward structure (always base-2) has fewer (or, at most, the same) average number of switch traversals. If the average number of switch traversals is the critical characteristic, and we think it is, then the Feed-Forward structure is preferred for all but trivial cases.

REFERENCES

1. M. Kondo, et al., *High-Speed Opt. Time Switch with Int. Opt 1×4 switches and Single-Pol. Fiber Delay Lines*, Int'l Conf. on Int. Opt. and Opt. Fiber Comm., June 1983.

2. R. A. Thompson and P. P. Giordano, *Exp. Photonic Time-Slot Interchanger Using Opt. Fibers as Re-Entrant Delay Line Memories*, Opt. Fiber Comm. Conf., Feb. 1986.

3. J. E. Watson, M. A. Milbrodt, and T. C. Rice, *A Pol.-Independent 1×16 Guided-Wave Opt. Switch Integrated on Lithium Niobate*, J. of Lightwave Tech., Vol LT-4, November 1986.

A Photonic Switch Architecture Utilizing Code Division Multiplexing

T. S. Rzeszewski
AT&T Bell Laboratories
Naperville IL. 60566

and

A. L. Lentine
AT&T Bell Laboratories
Naperville IL. 60566

Code-Division Multiplexing (CDM) is a technique that can be used in photonic switching architectures. CDM can be used to make each optical input channel orthogonal to every other input channel so that the sum of all the orthogonalized input channels can be presented to a decoder at each output port of the switch. The actual output signal on each port can be selected to be anyone of the input signals by using the appropriate code for selection. This is possible because of the correlation property of an orthogonal code family.

$$\int_0^T \phi_i(t)\phi_j(t)dt = 1 \text{ for } i = j \qquad (1)$$
$$= 0 \text{ for } i \neq j$$

ϕ_i and ϕ_j are members of the code family that are used to orthogonalize the input bits, and T is the duration of any code sequence and the duration of any input bit. This is the means by which any input signal can be switched to any or all outputs (customers). Therefore, the resultant switch is non-blocking with broadcast capability. The basic structure of a switch that uses an orthogonal code family is shown in Figure 1.

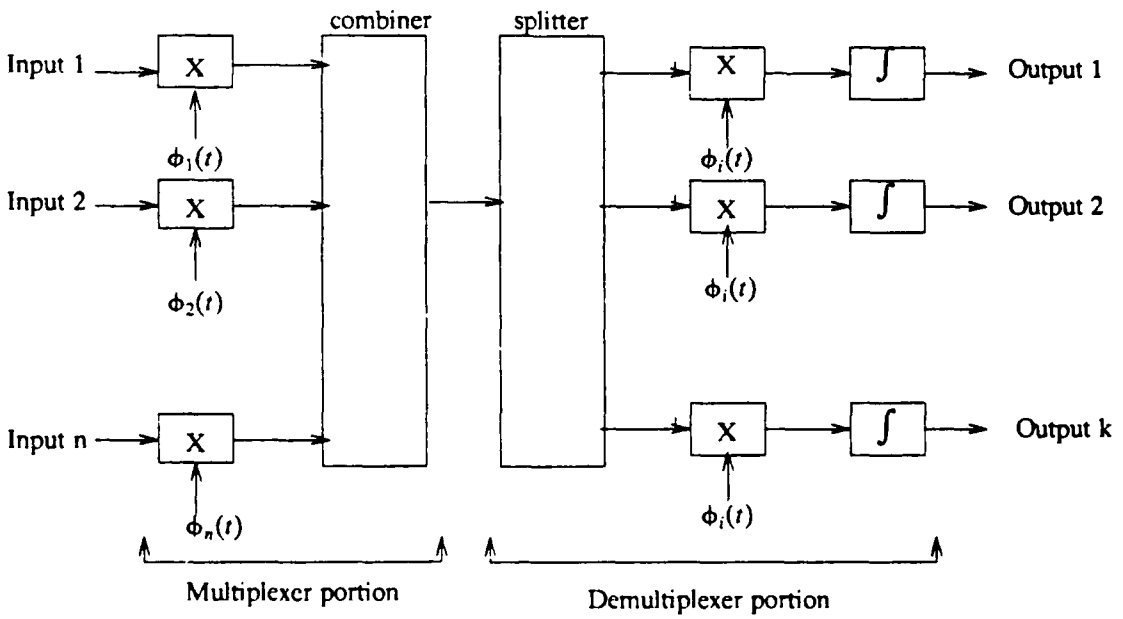

Figure 1. Basic code division switch

The input signals are each multiplied by the different members of the orthogonal code family. Therefore, the orthogonalized inputs can be represented as $\phi_i(t)$ times the input bits, where the input bits are a 1 or -1 for a duration of T, and $\phi_i(t)$ equals 1 or -1 for a duration T/n. If the input is a baseband signal, the output is a baseband signal of n times the input bandwidth. Therefore, an input to the summing circuit can be expressed as,

$$m_i(t)\phi_i(t), \tag{2}$$

where $m_i(t)$ is the information (+1 or -1) and $\phi_i(t)$ is the orthogonal code for the input channel.

The desired output from a multiplier on the right of Figure 1 after integration is:

$$m_i(t)\phi_i^2(t) \tag{3}$$

The undesired signals integrate to zero across the information bit interval. If $\phi_i(t)$ is a polar orthogonal code sequence, $\phi_i^2(t)$ is unity. Therefore, the output becomes m(t).

The code-division multiplexer portion of the switch can be implemented by using the orthogonal codes to modulate each information bit by shifting the phase of the optical carrier. This phase shift is controlled by one unique sequence from an orthogonal code family for each input channel. The resultant signal will be inphase during the time when the code has logical zeros and out of phase when the code is producing logical ones; this is phase shift key (PSK) modulation. Next, all the optical input signals that have been PSK modulated are added together in a passive combiner as shown in Fig. 1. The phase shifter can be realized by utilizing titanium diffused waveguides in lithium niobate with metal electrodes on the surface near a portion of the titanium channel. There is a change in the index of refraction of the material when an electrical signal is applied to the electrode, this produces the desired phase shift in the optical signal that is propagating in the waveguide [1]

The output of the phase shifter is the desired phase shift keyed (PSK) optical signal. Each orthogonal code word that controls the phase of the incoming signal lasts for exactly the duration of an information bit, and then repeats for the next and all subsequent information bit time intervals. The bandwidth of each coded input channel is increased by a factor that equals the number of bits in the length of the orthogonal code family. However, all the coded input channels occupy the same spectral density (frequency range). Further, all the coded channels may be added together and later be separated by correlating each coded channel with the appropriate member of the code family that was used for encoding. This will be performed on the output of the switch to select any input that is desired.

The demultiplexer portion of the switch uses a passive splitter to route the multiplexed signal to each output. Each output has a $Ti{:}LiNbO_3$ phase shifter to select or decode the desired input signal. The electrical input to this phase shifter is the member of the orthogonal code family which had been used to code the desired input signal. The output of the phase shifter consists of the analog sum of all of the coded input signals after they have passed through the decoder. The undesired signals have an equal number of zero and 180 degree phase shifts over the bit interval and the desired signal always has zero phase shift. When this analog signal is passed through an integrator, the undesired signals integrate to zero and only the desired signal remains. The integrator can be an optical bandpass filter, if a continuous optical path between the input and output is desired, or an electronic low pass filter, if coherent detection is utilized with subsequent electronic to photonic conversion.

If it is required to add more inputs to this type of a code switch, it is necessary to increase the bandwidth requirements of the switch proportionally. Therefore, the switch size on the input becomes limited by the bandwidth of the individual components that are available to implement the switch. The output size of the switch is limited by the losses associated with the summing circuit and the passive splitter.

Code division switching can be combined with time, space, or wavelength division switching to give more flexibility in switch design. For example several time multiplexed optical channels can be switched using a code division switch instead of a space switch. By adding time slot interchangers for each input and output the equivalent of a non-blocking time-space-time switch can be built. The

code division portion of the switch consists of two nx1 passive splitters instead of an nxn space switch. This is a large reduction in complexity and size for switches using $Ti{:}LiNbO_3$ directional couplers. However, if the switch is very large, the bandwidth requirements of the components which make up this switch may become too great. In this case, space or wavelength division can be used in conjunction with code division switching to reduce these bandwidth requirements.

One strategy for a switch design that must accommodate a large number of input channels is to group the input channels into m groups of n channels. The total number of input channels that this switch could handle is equal to n x m. A CD multiplexer is utilized for each group of n channels, and n is chosen to produce a high frequency operation consistent with the bandwidth of the technology that is used for implementation. This approach makes the speed requirement, and therefore the bandwidth, of the circuitry needed to implement a switch with n x m inputs equal to the requirement for an n input CD multiplexer; a speed reduction by a factor of m compared to that of a CD multiplexer that must handle n x m inputs. These individual CD multiplexers each fed one input port of a space switch or wavelength division switch as illustrated in Figure 2. The number of output ports is limited by the maximum size of the space switch or the number of lasers in the wavelength division switch.

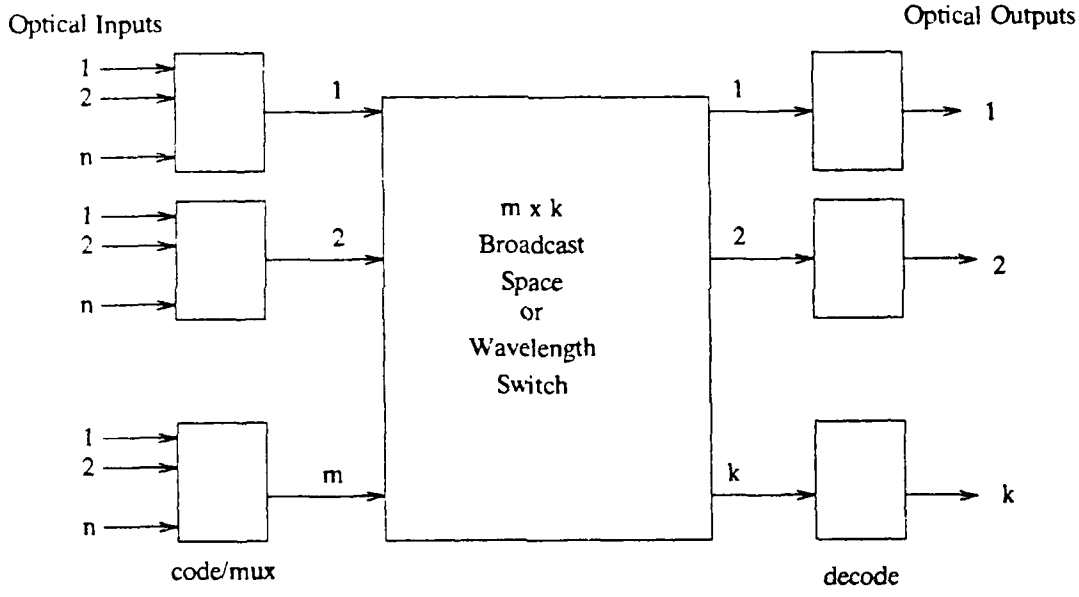

Figure 2. Code division combined with space or wavelength division switching

We have presented photonic switching using code division multiplex as an alternative or supplement to time, space or wavelength division switching. Code division switching uses orthogonal codes to select any of a multiplicity of inputs at each output. This type of switch is non-blocking and has inherent broadcast capability. CDM switches offer significant hardware savings compared to space switches of the same size and can be used in conjunction with space, time, or wavelength switching to provide greater flexibility in switch design.

REFERENCES

1. R. V. Schmidt and R. C. Alferness, *Directional Coupler switches, Modulators, and Filters Using Alternating* $\Delta\beta$ *Techniques*, IEEE trans. on Circuits and Systems, Dec. 1979, pp 1099 - 1108.

KEY TO AUTHORS AND PAPERS

KEY TO AUTHORS AND PAPERS—*Continued*

TOPICAL MEETING ON

PHOTONIC SWITCHING

POSTDEADLINE PAPERS

MARCH 18–20, 1987
INCLINE VILLAGE, NEVADA

TOPICAL MEETING ON
PHOTONIC SWITCHING

POSTDEADLINE PAPERS

Key to Authors of Postdeadline Papers

TOPICAL MEETING ON

PHOTONIC SWITCHING

POSTDEADLINE PAPERS

Thursday, March 19, 1987
8:00 P.M.

PDP1 "GaAs-AlAs Monolithic Microresonator Arrays", J. L. Jewell, A. L. McCall, A. C. Gossard, J. H. English, AT&T Bell Laboratories, A. Scherer, Bell Communications Research.

PDP2 "Ultrafast All-Optical Switch", S. R. Friberg, Y. Silverberg, M. K. Oliver, M. J. Andrejco, M. A. Saifa, P. W. Smith, Bell Communications Research.

PDP3 "Optical Logic And Switching Using Solitons", M. J. Doran, David Wood, British Telecom Research Laboratories.

PDP4 "A Digital Electrooptic Switch", Y. Silberberg, P. Perlmutter, Bell Communications Research.

PDP5 "Fast All Optical Switching In A Silicon On Sapphire Waveguide", H. Chelli, A. Nieceron, N. Paraire, A. Koster, H. Sauer, M. Carton, S. Laval, Institut d'Electronique Fondamentale, Universite-Paris Sud.

PDP6 "Low Drive Voltage 4x4 Ti:Linb03 Switch", I. Sawaki, T. Yamane, H. Nakajuma, Fujitsu Laboratories Ltd.

PDP7 "A Rigorous Analysis Of Intersecting Waveguides", L. McCaughan, Niraj Agarwal, University of Wisconsin.

PDP8 "Optical Amplification in Switching Networks", L. Thylen, P. Granestrand, A. Djupsjobacka, Ericsson Telecom.

GaAs-AlAs Monolithic Microresonator Arrays

J. L. Jewell
AT&T Bell Laboratories, Holmdel, NJ 07733

A. Scherer
Bell Communications Research, Red Bank, NJ 07701

S. L. McCall, A. C. Gossard, and J. H. English
AT&T Bell Laboratories, Murray Hill, NJ 07974

Miniaturization of optical logic devices has long been considered to be a key to minimizing their energy requirements but difficult to achieve[1-4]. We demonstrate a straightforward technique for fabricating arrays of GaAs/AlAs Fabry-Perot etalon devices (microresonators) as small as 1.5 μm in diameter. The growth of integrated GaAs-AlAs nonlinear etalons by molecular beam epitaxy[5] (MBE) represents a tremendous advance over previous fabrication techniques[6]. From the sample of reference 5 we have formed close-packed arrays of monolithic "posts" or microresonators 1.5-5 μm across by ion-beam assisted etching[7] and have performed optical NOR/OR gating experiments on them using picosecond pump and probe pulses. These microresonators represent a qualitative advance over the GaAs devices reported by Lee et al[8]. In that work pixels 9×9 μm square were formed in the active material only, and then sandwiched between dielectric mirrors in the usual way[6]. Growth of integrated devices by epitaxial techniques such as MBE allows us to etch right through both mirrors and the active material. This is critical since in an optimized nonlinear etalon the dielectric mirrors comprise most of the total thickness. The lateral optical confinement in these waveguiding structures allows efficient operation with diameters as small as one can focus the light. Elimination of carrier diffusion[9,10] out of the devices permits very close spacings. Reduction of energy requirements is expected due to the decreased volume of interaction. Finally, surface recombination[8,11] on the *sidewalls* of the microresonators should produce fast relaxation times. Our experiments show reduced energy requirements (factor of >8), essentially uniform response over small arrays, practically no crosstalk with *3-μm center-center spacing*, ~200 ps full recovery time, and thermal stability at 82 MHz operating frequency.

The MBE growth upon a GaAs substrate comprised 9½ pairs of AlAs/GaAs layers 813Å/594Å thick (quarter-wave-stack mirror) followed by a 1.6 μm GaAs spacer and 7 more AlAs/GaAs pairs (total thickness 4 μm). This design gives both mirrors ~90% reflectivities when the structure is intact on the substrate. Since the GaAs substrate has significant absorption at the wavelengths used, transmission was not monitored and the reflection was taken as the output. Thicknesses varied over the sample area. The etching was accomplished in a 5:2 Ar:Cl_2 gas mixture at 8×10^{-4} torr with an etch rate of ~1 μm/min. As seen in Fig. 1 the devices have vertical walls despite the deep etch and extreme variation (0-100%) in Al concentration.

For the optical measurements we used two 82-MHz mode-locked LDS 821 dye lasers tunable from ~780-950 nm. A Burleigh piezoelectric "inchworm" XYZ translator positioned the array of microresonators with high precision. The pump beam could be temporally varied over 330 ps to measure relaxation phenomena with ~15 ps resolution determined by the pulse durations. Our f/1.1 lens has a theoretical full width from zero to zero (FWZZ, i.e. the *entire* central lobe of the Airy disk) of 2.64 μm for the focused beam at 890 nm wavelength.

The MBE-grown etalon was not designed for high performance or even for this kind of gating. Prior to etching the lowest pump energy required for 5:1 contrast was ~20 pJ[5]. So far we have achieved similar or better response with 2.3 pJ pump (factor of >8 lower). The probe energy was 15 pJ. Fig. 2 shows a NOR gate response to 2.3 pJ input in a ~2.5 μm diameter pixel. In this and the following traces the left side of the pulse train shows the gate output with no input while the right side has the input present. Wavelengths are typically 850 nm for the input (pump) beam and 890 nm for the probe due to this etalon design. Results indicate that a ~2.5

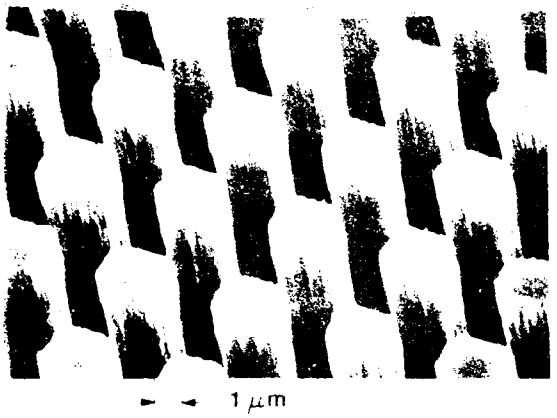

Figure 1

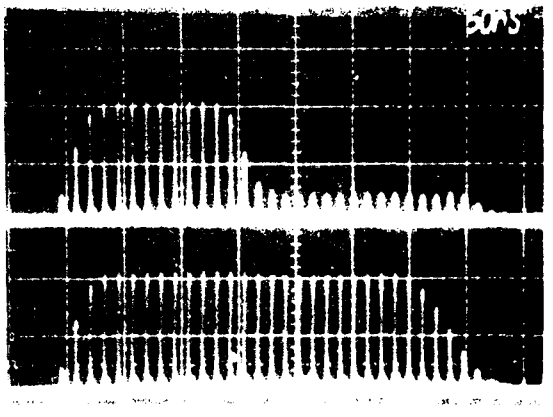

Figure 2

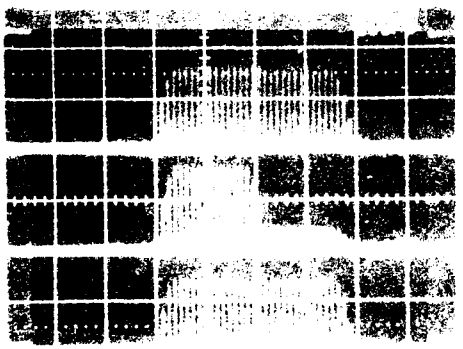

Figure 3

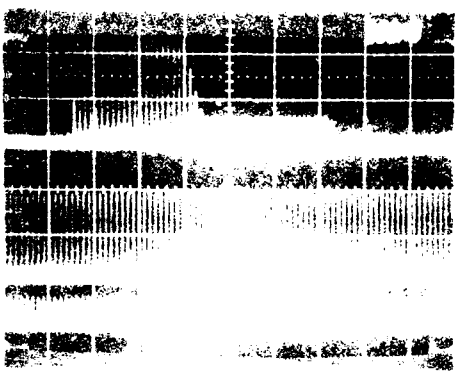

Figure 4

quantum well semiconductors, not just in bulk material.

Most data was taken with modulated pulse trains ~300 ns long and widely spaced to avoid thermal effects. However heating effects appear to be minimal since the response of a 5:1 contrast NOR gate was very similar with the pulses on *continually* at the 82 MHz mode-locked repetition rate as it was in the "thermal free" (~300 ns pulse train envelope) case. In Fig. 4 the upper trace shows the usual response, the middle trace is the "high" output (input beam blocked), and the lower trace has inut pulses present. In the latter two traces the lasers were on continually. The device still functions as a NOR gate, however the detector output shows a noticeable drop for the "high" signal. Saturation of the avalanche photodiode is believed to account for at least most of the difference since a similar drop was seen when the device was replaced by a highly reflecting mirror.

In conclusion we have demonstrated a qualitative advance in etalon optical logic device technology which improves most of the key device characteristics such as energy, speed, uniformity and crosstalk. In no way does the performance appear to be degraded; only good focusing is required. These first experiments with microresonators have confirmed our expectations of reductions in energy requirements, crosstalk, and recovery times. The thermal stability at 82 MHz offers additional encouragement to their eventual practicality. Exactly what percentage of the light actually coupled into the devices is not known. Microresonators designed for transmitted outputs should allow much more accurate quantitative measurements. High performance etalon designs, good fabrication of still smaller devices and possibly some reduction of operating temperature should allow us to push these devices close to the fundamental and statistical limits of performance[1,3].

References

[1] S.L. McCall and H.M. Gibbs, *Optical Bistability*, C.M. Bowden, M. Ciftan, and H.R. Robl, eds. (Plenum, New York, 1981), p. 1.

[2] R.L. Fork, Phys. Rev. A **26**, 2019 (1982).

[3] P.W. Smith, Bell System Tech. J., **61**, 1975 (1982).

[4] Robert W. Keyes, Optica Acta **32**, 525 (1985).

[5] S.L. McCall, A.C. Gossard, J.H. English, J.L. Jewell, and J.F. Duffy, Technical Digest, CLEO '86, (Optical Society of America, San Francisco, CA) paper FK3.

[6] J.L. Jewell, H.M. Gibbs, A.C. Gossard, A. Passner, and W. Wiegmann, Matl. Lett. **1**, 148 (1983).

[7] M.W. Geis, G.A. Lincoln, N.N. Alfremow, and W.J. Piazentini, J. Vac. Sci. Technol. **90**, 1390 (1981).

[8] Y.H. Lee, M. Warren, G.R. Olbright, H.M. Gibbs, N. Peyghambarian, T. Venkatesan, J.S. Smith, and A. Yariv, Appl. Phys. Lett. **48**, 751 (1986).

[9] J.L. Jewell, Y.H. Lee, J.F. Duffy, A.C. Gossard, and W. Wiegmann, Appl. Phys. Lett. **48**, 1342 (1986).

[10] D.J. Hagan, I. Galbraith, H.A. MacKenzie, W.J. Firth, A.C. Walker, J. Young, and S.D. Smith, in *Optical Bistability III*, H.M. Gibbs, P. Mandel, N. Peyghambarian, and S.D. Smith, eds. (Springer-Verlag, Berlin, 1986), p. 189. W.J. Firth, I. Galbraith, and E.M. Wright, *ibid.*, p. 193.

[11] Y.H. Lee, H.M. Gibbs, J.L. Jewell, J.F. Duffy, T. Venkatesan, A.C. Gossard W. Wiegmann, and J.H. English, Appl. Phys. Lett. **49**, 486 (1986).

Ultrafast All-Optical Switch

S. R. Friberg, Y. Silberberg, M. K. Oliver,
M. J. Andrejco, M. A. Saifi, and P. W. Smith

Bell Communications Research, Red Bank, NJ 07701

The importance of ultrafast all-optical switching devices stems both from their sub-picosecond switching time, which is faster than that feasible with electronic devices, and their compatibility with all-optical fiber data-transmission systems. Much of the work on such devices has been concentrated on optical bistable switches, which require optical materials with large nonlinearities if devices are to be small enough to respond at sub-picosecond speeds. However, waveguide devices such as the nonlinear optical coupler[1] or the birefringent fiber polarization switch[2] can operate at ultrafast switching rates even when fabricated from glass, a material with a small, fast electronic nonlinearity and a very low absorption.[3,4]

We present the first demonstration of substantially complete switching in a nonlinear coupler. For such a device, shown in Fig 1, low intensity light focused into waveguide (1) couples across to waveguide (2) in a coupling length L_C, and then couples back to waveguide (1), with this process continuing the length of the device. When this coupler is an integer number of coupling lengths long, low intensity input light emerges from one or the other of the waveguides. Otherwise, it emerges from a combination of both. When the intensity is increased, the coupling length is increased because of the waveguide nonlinearity. As a result, the light can be made to switch outputs by increasing its intensity. For a critical input power defined as P_C the coupling length becomes infinite. At powers greater than P_C, the input light essentially remains in the input waveguide. A nonlinear coupler of length L_C exhibits particularly useful switching characteristics as shown in Fig 2. At low intensities, light P_{in} focused into waveguide (1) emerges from waveguide (2). At intensities above P_C, the light emerges from waveguide (1), so that the coupler can serve as an optical AND gate logic device: two or more input intensities adding to less than P_C are channeled out through waveguide (2), whereas sums greater than P_C exit through waveguide (1).

Our nonlinear coupler is a weakly birefringent dual-core fiber with two 5 micron diameter cores that are 8 microns apart. The index difference between core and cladding is .0054 and the fiber is 2 m long. The measurement of the intensity-dependent response of the coupler was made with 80 psec pulses from a Q-switched, mode-locked 1.06 micron Nd:YAG laser. A pulse train of about 30 pulses was passed through a linear polarizer and half-wave plate so that an arbitrary linear polarization could be focused by a 5X objective into one of the fiber's cores. Light emerging from each core at the end of the fiber is imaged onto a FND-100 photodiode with a one nsec response time. To obtain data, the input polarization was rotated so that the output polarization

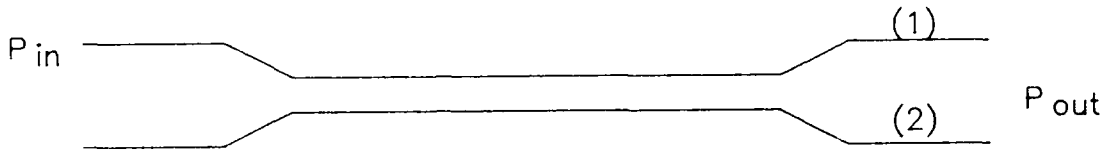

Fig 1. A nonlinear coupler. Light coupled into waveguide (1) emerges from waveguide (1) or (2).

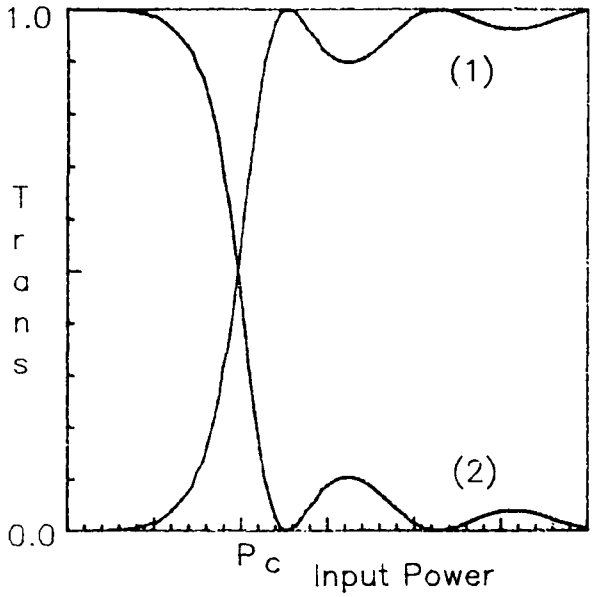

Fig 2. The response of a nonlinear coupler of length L_c

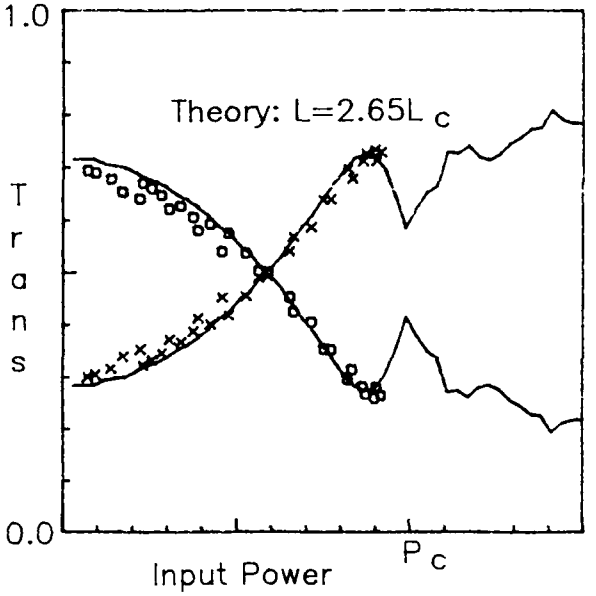

Fig 3. Data and fitted theoretical curve (solid lines) for a nonlinear coupler of length L_c

was linear at all power levels (the contrast ratio was 100/1). Two fast oscilloscopes were triggered to obtain simultaneous traces of the output of the two photodiodes. This gave 30 pairs of data points that included both rising- and falling-edge pulses from the pulse train. Because our experiments were performed with light pulses that had a continuously-changing instantaneous power, the fiber transmission measured with a slow detector is an average of the coupler transmission over the pulse duration.

The data points from one of our measurements is shown in Fig 3, where the horizontal axis is the sum of the peak powers of the two cores, and the vertical axis is the transmission (the peak power from one core divided by the sum of both cores). Light emerges primarily from one core at low intensity, and mainly from the other core at higher intensities, demonstrating substantially complete switching. The theoretical fit to the data is also shown, which assumes that the coupler is 2.65 L_C long, that the pulses have a sinc^2 intensity profile, and that the detectors have response times much slower than the pulses. This fitted

curve implies a critical power P_C for the coupler of 880 Watts, in very good agreement with 940 Watts estimated by assuming the nonlinear coefficient to be that of silica (3×10^{-20} m^2/W), by assuming a coupling length L_C of .75 m (= 2m/2.65), and by using the measured value of 20 microns^2 for the core cross-section. There is no evidence of any thermally induced refractive index changes. These changes would result from heating if the Q-switched, mode-locked pulse train were absorbed in the cores, and would produce differences in the coupling characteristics for rising- and falling-edge pulses of the train. They are not expected because of the low absorption of glass.

In conclusion, we have demonstrated the operation of an all-optical nonlinear coupler. Because it is fabricated from glass, it is capable of ultrafast switching: glass has an electronic nonlinearity that has been measured to respond at faster than 100 fsecs.[4] The critical power P_C required to completely switch the device is 880 Watts. It follows that a device one coupling length long would also switch at this power, and exhibit the nearly ideal response of Fig 2. The critical power for switching can be reduced by either reducing the core size, increasing the coupler length, or increasing the nonlinearity of the material, or by any combination thereof. For example, a one meter coupler with a 4 micron^2 core fabricated from SF-59 high nonlinearity glass would switch with 7 Watts, a power that might be obtained from a mode-locked semiconductor diode laser.[5] These results give convincing evidence that nonlinear glass couplers may become the first practical picosecond all-optical switching elements.

References

1. S. M. Jensen, IEEE J. Quantum Electron. QE-18, 1580 (1982).

2. S. Trillo, S. Wabnitz, R. H. Stolen, G. Assanto, C. T. Seaton, and G. I. Stegeman, Appl. Phys. Lett. 49, 1224 (1986).

3. S. R. Friberg and P. W. Smith, submitted to IEEE J. Quantum Electron., (1987).

4. I. Thomazeau, J. Etchepare, G. Grillon, and A. Migus, Opt. Lett. 10, 223 (1985).

5. Y. Silberberg and P. W. Smith, IEEE J. Quantum Electron. QE-22, 759 (1986).

OPTICAL LOGIC AND SWITCHING USING SOLITONS

N J DORAN and David WOOD

BTRL, Martlesham , IPSWICH, ENGLAND IP5 7RE

1. INTRODUCTION

Solitons occur in optical fibres with the propagation of short pulses in the negative group velocity dispersion regime. Solitons have the important property of dispersionless propagation and also behave in many respects as single entities. Nonlinear devices designed for optical switching respond to local intensities and thus do not function efficiently for typical ultrashort pulse envelopes. The device described here exploits the 'particle' nature of solitons to produce excellent switching characteristics for entire pulses and also serves to illustrate the necessity for using solitons as the essential 'bits' in ultrafast optical devices.

2. THE SOLITON SWITCH

The device consists of two fibre arms with approximately the same optical path length but which are otherwise dissimilar (either designed to have different group velocity dispersions or made from different dopants to give different nonlinear coefficients). These two fibres are joined at the input and output ends with couplers. Figure 1 shows the arrangement of the device.

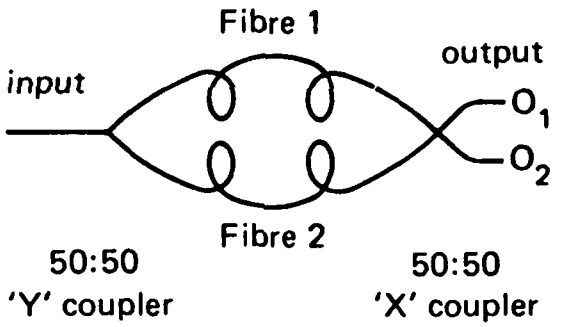

Figure 1

At the input a Y-coupler splits the pulse energy equally into the two fibre arms. The two pulses are then recombined at the output with an X-coupler. The final pulse from each arm of the output coupler is then a combination of the complex wave envelopes of the two pulses. The lengths of the two arms must be chosen so that the optical path lengths are the same. However, even two pulses arriving in coincidence would still have an arbitrary phase difference, due to sub wavelength differences in path length. The recombined pulses out of the output coupler are determined by this phase difference.

The nonlinearity in the fibre is a third order effect where the refractive index depends on the light intensity through the formula

$$n = n_0 + n_2 \times |E|^2 \tag{1}$$

where n_0 is the linear refractive index and n_2 is the nonlinear index of refraction. The propagation of pulse envelopes in a fibre with such a nonlinearity and negative group velocity dispersion is described by the Nonlinear Schrodinger equation (NLS) [1], [2].

$$i\frac{\partial u}{\partial z} + \tfrac{1}{2}\frac{\partial^2 u}{\partial t^2} + u|u|^2 = 0 \tag{2}$$

This is a normalised equation and there are transformations to take the variables back to real units. The normalised amplitude generated by a real pulse is proportional to $\sqrt{n_2/D_2}$ and the normalised distance, z, is proportional to $D_2 l/\tau^2$, where D_2 is the dispersion coefficient, τ the pulse duration and l the real distance. Hence equal real pulses in each fibre arm would have different normalised amplitudes and lengths, according to the differences in dispersion and nonlinear coefficients.

The NLS has bound state multisoliton solutions of the initial form [3],

$$u(z=0,\ t) = \frac{N}{\tau} \times sech(t/\tau) \tag{3}$$

when N is an integer. All such multisolitons have the property that $|u(z,t)|$ returns to its original form every $\pi\tau^2/2$ propagated. For $N=1$ the full solution is

$$u(z,\ t) = exp(-iz/2\tau^2) \times sech(t/\tau) \tag{4}$$

Note the phase factor $exp(-iz/2\tau^2)$ in the above formula. More generally, for all multisoliton bound states of the form $(N/\tau) \times sech(t/\tau)$, the solution can be written as

$$u(z,t) = exp(-iz/2\tau^2) \times f(z,t) \tag{4}$$

where $f(z,t)$ is periodic in z with period $\pi\tau^2/2$.

The overall phase is unimportant for the propagation in a single fibre. However, the outputs from the two arms of the X-coupler in figure 1 are determined by the relative phase of the pulses emerging from the two fibre arms. Our device is based on these two properties: that multisoliton bound states return to their original shape periodically, and that the output is sensitive to the relative phase acquired in the two arms.

The normalised NLS, equation (2), is taken to apply to both fibre arms. If the ratio of dispersion in *fibre* 1 to that in *fibre* 2 is α and the ratio of the nonlinear coefficients is β, then if the pulse in *fibre* 1 is $A \times sech(t)$ the normalised pulse in *fibre* 2 is $(\alpha/\beta)^{1/2} A \times sech(t)$. In real units the pulses entering each arm are the same. Thus if the normalised length in *fibre* 1 is L_1 then the normalised length in *fibre* 2, $L_2 = L_1/\alpha$. Again the real lengths are the same for both arms. The pulses entering the X-coupler have a *sech* form, if both the normalised amplitudes in each case are integers and the normalised lengths of each arm are equal to an integer number of soliton periods.

The device operates as follows. The arm length is chosen to fulfill the above condition for there to be an integer number of soliton periods in each arms. As the launched power is increased the threshold for generating solitons is reached, but the two emerging *sech* pulses will have different phase factors (for $\alpha \neq 1$). This means that, at the particular power levels when pure solitons are launched, we can switch all the energy into one or other of the two arms by an appropriate choice of the angle ϕ. At other power levels this will not be the case but as the power is increased the exact soliton launch power will be reached periodically to give total switching.

It only remains to determine the switching characteristics at intermediate power levels. This we do numerically; for a range of input powers we integrate directly the NLS (2) in each fibre arm, and then evaluate the overlap integrals to obtain the power in each of the two output ports O_1, O_2.

As an example we take $\alpha=4$, $\beta=1$ and a fibre length in each arm such the normalised length of *fibre* 1, $L_1=2\pi$ and hence the normalised length of *fibre* 2, $L_2=\pi/2$. Here the two arms have different dispersions but the same nonlinear coefficients. This could be realised practically since it is comparatively straightforward to fabricate fibres with different dispersions at the same wavelength. When $A \times sech(t)$ is launched in *fibre* 1, then the normalised pulse in *fibre* 2 is $2A \times sech(t)$. Hence pure soliton bound states are launched in each fibre when A is an integer. For this choice of length of arm the normalised lengths are exact soliton periods for

both arms. Thus at the end of the two fibre arms the pulse in *fibre* 1 has acquired a phase $-\pi$ (four soliton periods at $L_1=2\pi$) and the pulse in *fibre* 2 a phase $-\pi/4$ (one period at $L_2=\pi/2$). If the phase angle, ϕ in the output coupler is equal to $-3\pi/4$ and A is an integer, then the outputs from the two fibres into the coupler have the same *sech* shape and are in-phase. Hence all the power is transmitted out of port O_1 when A is an integer.

Below the characteristics of the device is shown in Figs 2a and b. Fig 2a shows the device is totally transparent for total input powers of 2 and 8 (to port O_1) and that there is a strong dip at around an input power of 4. Both the depth and width of this dip could not have been predicted but its existance is the feature of the device which is most remarkable.

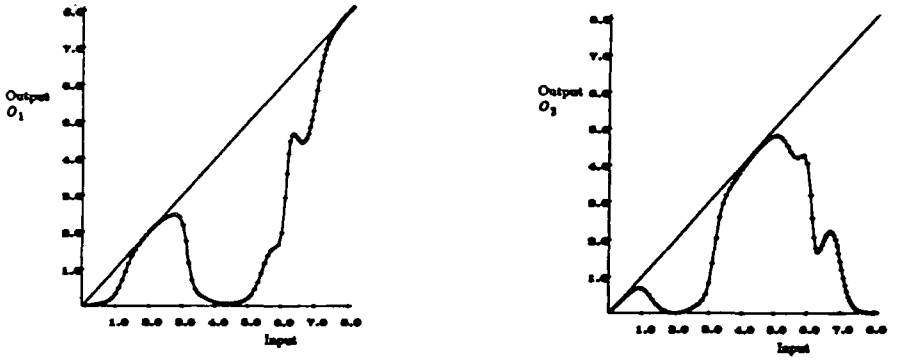

Figures 2a,b Output energy v input energy from ports O_1 and O_2 respectively.

Figure 2 shows that the device can work either as a nonlinear switch, or (if we neglect the output from one or other of the ports) it can perform the basic logic functions "Exclusive OR" and "AND". The calculated crosstalk is zero for output to O_1 and $\approx 16dB$ for switching to O_2.

Calculations have also been performed for non-integer values of $(\alpha/\beta)^{1/2}$. Good resonances can be obtained, although 100% switching is no longer possible.

3. CONCLUSION

A passive device has been presented which can perform both ultrafast optical logic and ultrafast spatial switching. The length of the device does not impose any restriction on the speed of operation since it can be operated either in a pipeline mode or can be made to perform many operations in parallel. The device requires careful interferometric alignment but it is capable in principle of providing passive switching of whole pulses at ultrafast speeds.

ACKNOWLEDGEMENT

We acknowledge the Director of Research, British Telecom for permission to publish.

REFERENCES

1. A Hasegawa and F Tappert Appl. Phys. Lett. 23, 142 (1973)

2. N J Doran and K J Blow IEEE JQE 19, 1883 (1983)

3. J Satsuma and N Yajima Prog. Theor. Phys. Suppl. 55, 284 (1974)

A Digital Electrooptic Switch

Y. Silberberg and P. Perlmutter

Bell Communications Research
331 Newman Springs Rd., Red Bank, NJ 07701

We propose and analyze a new 2X2 electrooptic switch structure that exhibits a step-like response to the switching voltage. This response eliminates the need for precise voltage control for switching, and it therefore enables the operation of many such elements by a single voltage source, as required for switching arrays. Moreover, because this characteristic applies to both polarizations in a lithium niobate device, it can be made polarization independent, and it should be insensitive to the wavelength of light.

Most electrooptic switches are interferometric in nature, i.e. they require a precise phase shift to achieve a switched state with low crosstalk. The directional coupler switch, for example, requires a phase shift of $\sqrt{3}\pi$ between its two waveguides to switch [1]. Because of small fabrication errors, this phase shift requires slightly different voltages for each switching element in a switching array. It is also very difficult to obtain switching in the two orthogonal polarizations simultaneously. Another class of 2X2 switches is based on modal interference. This class includes the Bifurcation Optic Active (BOA) switch [2], the TIR or X-switch [3] and the symmetric directional coupler switch [4], all exhibit a sinusoidal response to the applied voltage and therefore require precise voltage control as well.

The proposed device is shown in Figure 1. It is based on an asymmetric waveguide junction structure, composed from two unequal input guides, a double-moded central region and a symmetric output branching. The symmetry of the output branching can be broken by applying an external electric field. An asymmetric waveguide branching is known to perform mode sorting [5]. The fundamental or first order mode of the central region can be excited by launching light through the wider or the narrower input guides, respectively. The salient feature of the asymmetric Y-junction is the fact that mode sorting is obtained not at a particular point of operation, but for a range of parameters. By making the angle small enough one can assure mode sorting. The two normal modes in the junction area can now be routed to the required output guide by properly biasing the output branching. The fundamental mode will be directed to the arm with higher index of refraction if the bias is high enough. Due to the symmetry breaking operation, switching is not periodic or quasiperiodic, but depends only on the direction of the bias.

Figure 2 shows a simulation of light propagation in such a switch. The simulation assume a step index slab waveguide configuration, and it uses the local normal mode approach for the propagation analysis [6]. The input guides are 2.75 and 3.25 μm wide, the output guides are 3 μm wide each, the index of refraction of the guides without bias is 2.205 and the background index is 2.200. The angle between the guides is 1 mrad. Light is assumed to be coupled to the narrow input guide of the structure. As can be seen, the first order mode (double-humped intensity distribution) is excited at the center of the device, which is then routed to the arm with decreased index of refraction.

Using a similar analysis we calculated the switch response as a function of the induced index imbalance between the output arms. Figure 3 shows the power at each of the output guides when the narrow guide is excited. As expected, the output is evenly split between the output guides without any bias. As the bias is increased light is coupled preferentially to the guide with lower index of refraction. Switching with crosstalk smaller than 20dB is obtained when an index imbalance of 0.0002 is induced between the

output guide. This crosstalk drops below 30dB and does not increase above this value as the switching voltage is increased by an order of magnitude above the minimal switching voltage.

The step-like response eliminates the need for precise voltage control, as any voltage in this wide range will be effective. Moreover, this response can be used to generate a polarization independent switching in Ti:LiNbO3. In common z- or x-cut LiNbO3 devices one polarization is affected by an electrooptic interaction which is 3 times weaker than the other polarization. It is obvious that in a switch with the above response both polarizations can be switched by a strong enough bias. Another advantage of this switch is its insensitivity to the precise wavelength. Indeed, the switching voltage may change with wavelength due to changes in optical mode size. However, switching with good crosstalk figure should still be obtained, provided that the waveguides involved are still single mode. It is conceivable then that a single switch will switch two wavelengths, for example 1.3μm and 1.55μm, simultaneously.

In conclusion, we have proposed an electrooptic switch that exhibits a step-like response to the switching voltage. It should be useful in switching arrays and as a polarization and wavelength independent switch.

References

1. R. V. Schmidt and R. C. Alferness, IEEE Trans. Circuit Syst. **CAS-26,** 1099 (1979).
2. M. Papuchon, A. Roy and D. B. Ostrowsky, Appl. Phys. Lett. **31,** 266 (1977).
3. C. S. Tsai, B. Kim and F. R. El-Akkari, IEEE J. Quantum Electron. **QE-14,** 513 (1978).
4. R. A. Forber and E. Marom, IEEE J. Quantum Electron. **QE-22,** 911 (1986).
5. H. Yagima, Appl. Phys. Lett. **12,** 647 (1973).
6. W. K. Burns and A. F. Milton, IEEE J. Quantum Elect. **QE-11,** 32 (1975).

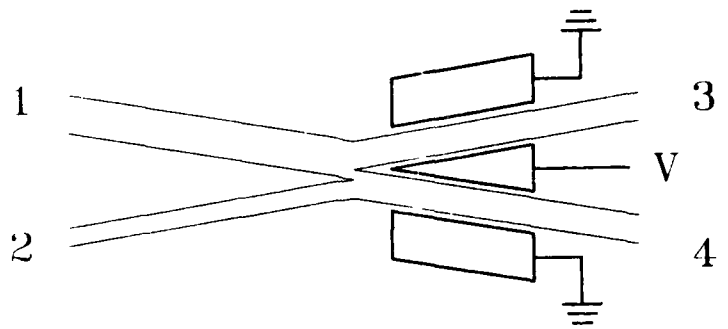

Figure 1. The switch layout.

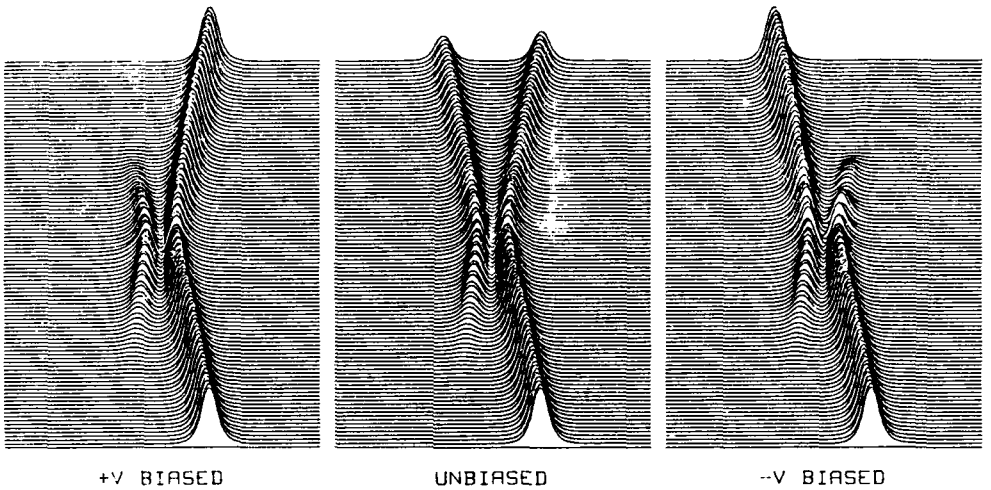

Figure 2. Simulation of light propagation through the structure in three different states: Staight through (left), intermediate (center, no biase) and switched (right). light is launched through the narrow input guide.

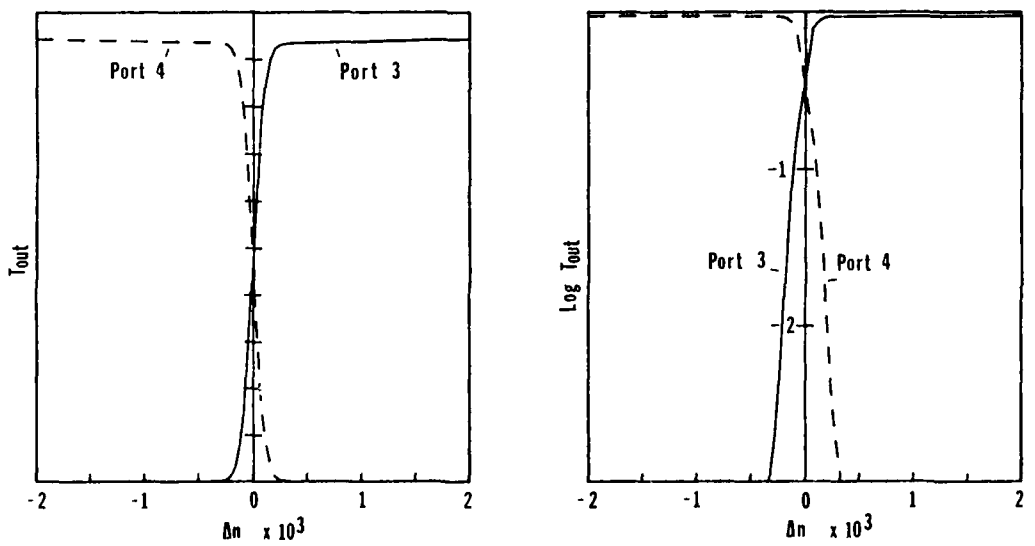

Figure 3. Calculated transmission through ports 3 and 4 as a function of induced index difference. Left: Linear scale. Right: Logarithmic scale.

Fast All Optical Switching in a Silicon on Sapphire Waveguide

H. Chelli, A. Niepceron, N. Paraire, A. Koster,
H. Sauer, M. Carton, S. Laval

Institut d'Electronique Fondamentale - Universite Paris Sud
CNRS UA22, Bat 220, 91405 Orsay Cedex, FRANCE

Using the excitation by a pulsed laser beam of a guided mode in a nonlinear silicon film deposited on sapphire, fast switching and bistability have been observed. A theoretical study, taking into account both electronic and thermal refractive index variations is presented which describes the experimental results accurately.

The device structure consists of a 0.7 μm thick silicon epitaxial layer grown on a sapphire substrate. A diffraction grating is produced at the silicon surface by holographic lithography and ionic etching. The groove spacing and its depth modulation have been chosen to optimize the coupling between a Nd YAG laser beam and one mode of the wave guide. The incident beam generates e-h pairs near the band edge of the semiconductor, inducing electronic refractive index variations.

In the first device studied, the grating was covered with a silver layer to allow 100% coupling efficiency. Observations were performed either on the reflected beam or on the guided one (more precisely on the leading beam associated with the guided wave and coupled out of the guide by the diffraction grating). The use of a shield (see Fig. 1) allows a spatial separation of the reflected and guided beams.

Nonlinear operation has been studied on the TE_0 fundamental beam which presents the sharpest resonance ($\Delta\theta = .16^\circ$), using a Q-switched laser beam with a 0.2 mrad divergence.

If $\delta\theta = \theta - \theta_c$ is the angular shift of the incident beam from resonance, which occurs for θ_c at low power, then
- for $\delta\theta < 0$, no switching appears (which would correspond to an electronic index variation);
- for $\delta\theta > 0$, switching can be seen. The switching time depends on the incident beam power (for power densities of 700 kW/cm^2, switching times of 700 ps have been observed).

These observations can be explained taking into account both thermal ($\delta n_T > 0$) and electronic ($\delta n_e < 0$) index variations. It is shown that $\delta n(t) = \delta n_e + \delta n_T$ depends on 3 main parameters:
- the device geometry (which determines the reflectivity R(O,n) and the heat sink);
- the incident pulse shape and duration (Δt);
- the relative values of Δt and Z which is the recombination time of the electron-hole pairs in silicon on sapphire.

In our experimental conditions (Δt = 20 ns, Z = 100 ps), thermal effects rapidly appear and no pure electronic switching (and consequently no bistability) can be observed. We report in Fig. 2 the experimental and theoretical curves giving the incident (1), reflected (2) and guided (3) intensities for $\delta\theta = +0.04^{\circ}$ and an incident peak intensity of 500 kW/cm^2. However increasing $Z/\Delta t$ allows $\delta n_e(t)/\delta n_T(t)$ to increase at the beginning of the exciting pulse and consequently to observe a pure electronic switching up, followed by an electronic-thermal switching down i.e. bistability.

Indeed, a second device is presently under study, with no silver deposited on silicon, which allows sharper resonances $R(\theta,n)$ and observation of nonlinear phenomena for smaller incident power densities. A chemical treatment has increased the recombination time Z. Under these conditions, observations of the reflected, transmitted or guided beams at incident power densities as low as 50 kW/cm^2 have shown bistability.

Although the use of a waveguide structure prevents a strong reduction of the pixel size, dimensions of 100 x 100 μm^2 are quite realistic and can allow the design of operating systems, owing to the low power densities and fast switching times already observed.

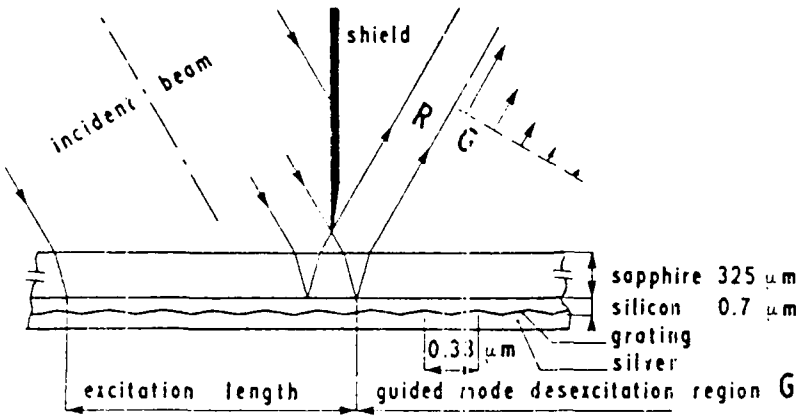

Figure 1 :
Experimental device.

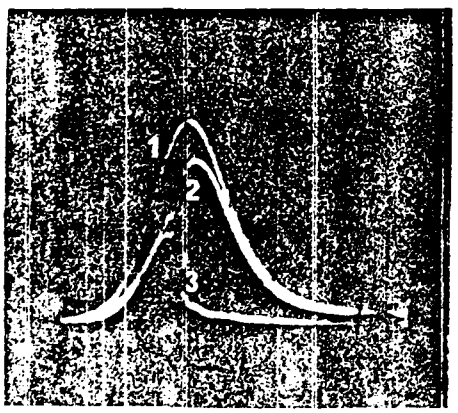

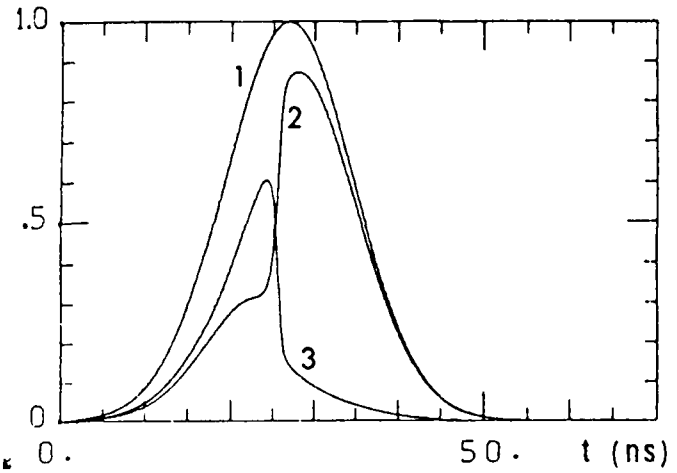

a b figure 2

PDP6-1

Low drive voltage 4X4 Ti:$LiNbO_3$ switch

I. SAWAKI, T. YAMANE, AND H. NAKAJIMA

FUJITSU LABORATORIES LTD.
10-1 MORINOSATO-WAKAMIYA, ATSUGI
KANAGAWA 243-01, JAPAN

An optical matrix switch is one of the most important components in constructing photonic switching systems. Previously, several strictly non-blocking matrix switches fabricated on Ti:$LiNbO_3$ have been reported[1]-[3]. However, drive voltages of less than 10 V have not been obtained in a matrix larger than 4X4 for 1.3 um wavelength. In this paper, we overcame this problem by a new configuration for the waveguide network.

A schematic diagram of the new architecture 4X4 matrix switch is shown in Fig. 1. All crosspoint switches are laid out in a rectangular configuration[4] connected to the next crosspoint through intersecting waveguides[5]. When all switch elements are set to the "cross" state, no output is obtained. An optical path between input #i and output #j is established by switching the element S_{ij} to the "bar" state. The number of crosspoint switches is the same for all possible paths, and the maximum number of switches through paths is reduced from the conventional 2N-1 to N. This architecture makes the number of crosspoint switches the same for all paths, thereby ensuring uniform insertion loss. Moreover, crosspoint switch length can be doubled and the drive voltage can be halved relative to the conventional architecture.

Based on the new architecture, we designed a 4X4 matrix switch on a 65-mm, z-cut $LiNbO_3$ chip using 16 directional coupler switches. Figure 2 shows our waveguide network. Bending radius of connecting and input/output waveguides is 40 mm to prevent radiation loss. The connecting waveguides become 5 mm long with an intersecting angle of 7° which ensures crosstalk of less than -30 dB. The input/output waveguides are also 5 mm long to provide 175 μm pitch fiber arrays. As a result, we obtained 10 mm long directional coupler switches which is about twice the maximum switch length possible using the conventional architecture on the same size chip[1].

Figure 3 shows a photograph of a fabricated 4X4 matrix switch chip. The waveguides were fabricated by diffusing a 7-μm-wide, 700-Å-thick Ti pattern at 1035°C for 8 h in a wet O_2 atmosphere. A 2500-Å-thick CVD SiO_2 buffer layer was deposited, and Δβ-reversal type electrodes (Ti/Au: 3000 Å) were fabricated at each crosspoint. Waveguide gap at the interaction region is 5 um. The switching characteristics were measured for 1.3 μm TM-mode light. The typical voltage needed for "bar" state is 9 V, and that for "cross" state is 18 V. The drive voltage between "bar" state and "cross" state varied from 8 V to 10 V over 16 crosspoints with crosstalk less than -20 dB. These values are about half of those in conventional matrices. Insertion loss was measured using polarization maintaining fibers. The average fiber-to-fiber insertion loss was 4.7 dB and deviations through different paths were only ±0.3 dB. This deviation is due primarily to the different number of intersections for each path. However, the maximum difference in the number of intersections per path is two, independent of matrix size.

In summary, a new architecture matrix switch has been successfully demonstrated. A 4X4 switch was designed and fabricated on a 65-mm-long Ti:$LiNbO_3$ chip. We achieved a reduced drive voltage of 8 V, which is about half that for the conventional matrix and suitable for high-speed control. Average insertion loss was 4.7 dB, and deviations were less than ±0.3 dB for different paths. This architecture can be applied to larger matrices to decrease drive voltage and ensure uniform insertion loss.

Acknowledgments

We wish to express our appreciation to T. Shimoe and K. Murakami for the architecture design. We are also very grateful to T. Iwama and Y. Oikawa for their helpful discussions.

References

[1] G. A. Bogert et al., J. Lightwave Technol., LT-4, p.1542, 1986

[2] P. Granestrad et al., Electron. Lett. 22, p.816, 1986

[3] M. Kondo et al., in Proc. IOOC-ECOC '85 (Venice, Italy), p.861, 1985

[4] T. Shimoe et al., in Proc. OFC-IOOC '87 (Reno), p.144, 1987

[5] T. Shimoe et al., to be presented at ISS '87 (Phoenix), paper C12.2, 1987

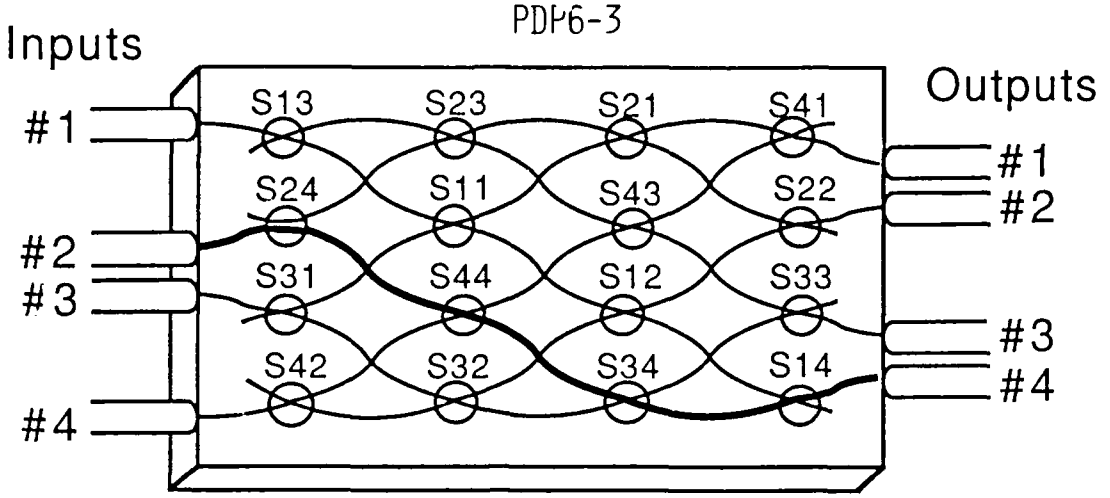

Fig. 1. New architecture 4X4 matrix switch
(An optical path between input #2 and output #4 is established.)

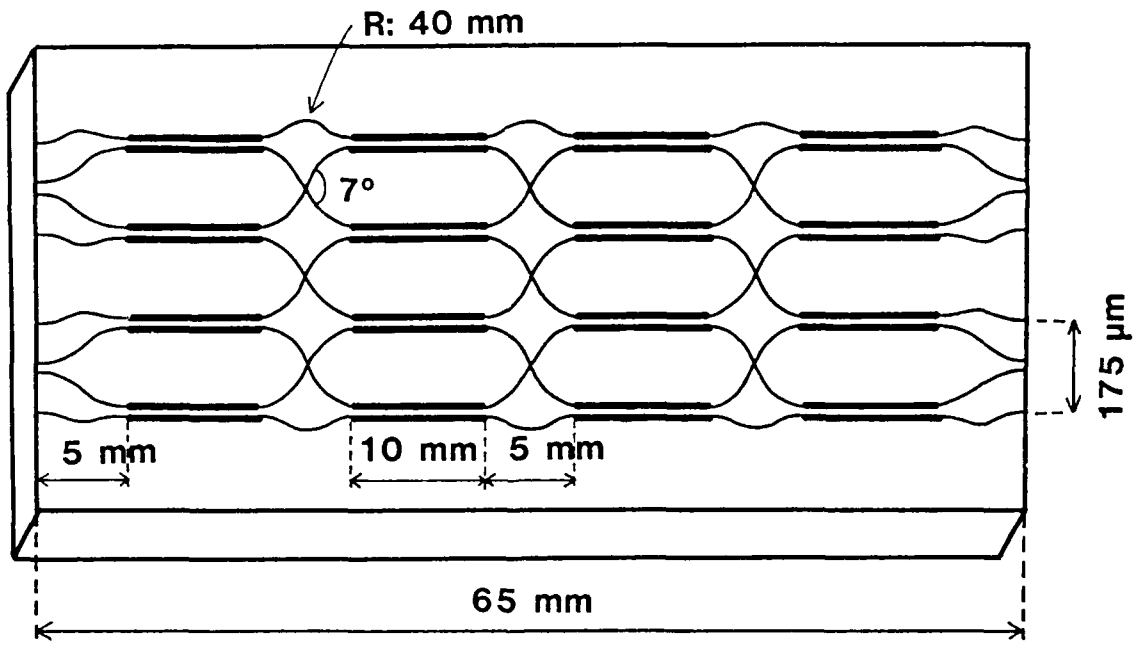

Fig. 2. Design of 4X4 matrix switch

Fig. 3. Photograph of fabricated switch chip

A RIGOROUS ANALYSIS OF INTERSECTING WAVEGUIDES

BY
L. McCaughan and Niraj Agrawal
Dept. of Electrical and Computer Engineering
University of Wisconsin
Madison, WI 53706

Summary

Introduction

Intersecting waveguides are becoming an important guided wave element for integrated optics. The simplicity of the geometry, i.e., an absence of S-bends, makes it possible to achieve higher levels of switch integration with a switch element based on this geometry than is possible with directional couplers. Cross-connections between elements of integrated optical circuits are also possible because inter-waveguide coupling is a strong function of the crossing angle. No unified theory has thus far been constructed to explain all of the observed optical characteristics of various intersecting geometries. We report the derivation of a closed form expression which does quantitatively agree with experimental observations. As the results of our calculations show, intersecting waveguides have unique optical properties which cannot be predicted by seeking analogies with directional couplers.

Theory

Theoretical expressions derived for single-mode intersecting waveguides have been based, at least in part, on previous treatments of directional couplers.(1,2) Central to these derivations are the assumptions of weak coupling and a common propagation direction of the light. The fields are expressed as the sum of a symmetric and antisymmetric mode, which are usually made up from the modes of the individual waveguides. These assumptions not valid for intersecting waveguides. For small angles of intersection, the two waveguides are strongly coupled (to the point of sharing the same volume) over a large distance (c.f. fig. 1). At larger angles, the idea of a common propagation direction is not even qualitatively valid.

In our theoretical approach, two waveguides interact by scattering the optical fields into one another in a self-consistent manner. The solution is formulated in terms of the Green's function of a single-mode planar waveguide. The analysis takes into account the different propagation directions of the optical fields. As a consequence, the fields can be expressed in the form

$$E_{x,2}(y_2,z_2)=i\sin[K(z_2)]\ \Psi_2(y_2,z_2),$$

$$E_{x,1}(y_1,z_1)=\cos[K(z_1)]\ \Psi_1(y_1,z_1).$$

where

$$\kappa_{ij}(z_j') = \frac{\omega}{4}\int_{-\infty}^{\infty} [\varepsilon_j(y_j',z_j') + \iota(y_j',z_j')]\ \Psi_i(y_i',z_i')\Psi_j^*(y_j',z_j')dy_j',$$

$$K_{ij}(z_j) = \int_{-\infty}^{z_j} \kappa_{ij}(z_j')dz_j'$$

Ψ is the fundamental mode of the guide, and ϵ and ι are the dielectric constants in the arms and in the common volume regions, respectively, of the intersecting guides.

Results

A comparison with the results of coupled mode theory for directional couplers suggests that K(z) can be viewed as an effective coupling length. This integrated coupling coefficient, K(z -> ∞), was calculated for two cases: (i) the refractive index in the intersection region is the same as that of the wavguide arms (the so-called single-Δn intersecting waveguides) and (ii) waveguides successively fabricated so that the intersection region contains twice the refractive index of the individual waveguides (2Δn). At small angles (θ < 2°) the fraction of light exchanged between the guides is approximately periodic with intersection angle, and its period increases with increasing angle (figure 2). Experimental results (3) are in agreement with these findings.

As the intersection angle becomes larger than a few degrees, the oscillations broaden and eventually disappear because of the diminished strength of interaction (figure 3). We find an angle of intersection such that the evancescent coupling vanishes, resulting in no crosstalk for the single-Δn case (c.f. figure 3). These findings have recently been verified by experiment(4). Our theory demonstrates that at this zero in the crosstalk coincides with a quasi-phase matching condition for the waveguides. For this condition, the waveguide intersection angle is twice the ray angle and the propagation wave vectors (rays) are parallel for half of their bounce distance.

Finally, for small intersection angles our analysis predicts a stronger coupling with an increased mode confinement. This occurs due to an enhanced overlap of the fields in the intersection region. Previous theory invoking symmetric and antisymmetric modes predict a weaker coupling as a consequence of the reduced difference in progagation constants between the two modes.

References:

(1) A. Neyer, "Electro-optic X-switch using single mode $TiLiNbO_3$ channel waveguides," Electron. Lett., vol. 19, p553 (1983).

(2) A. Neyer, kW. Mevenkamp, L. Thylen, and B. Lagerstrom, J. Lightwave Technol. vol. LT-3, p. 635 (1985).

(3) E. Bergmann, L. McCaughan, and J. Watson, "Coupling of intersecting $Ti:LiNbO_3$ diffused waveguides," Appl. Opt. vol. 23, pp. 3000-3003, (1984).

(4) G. A. Bogert, "$Ti:LiNbO_3$ Intersecting waveguides," Electron. Lett., vol. 23, pp. 72-73 (1987).

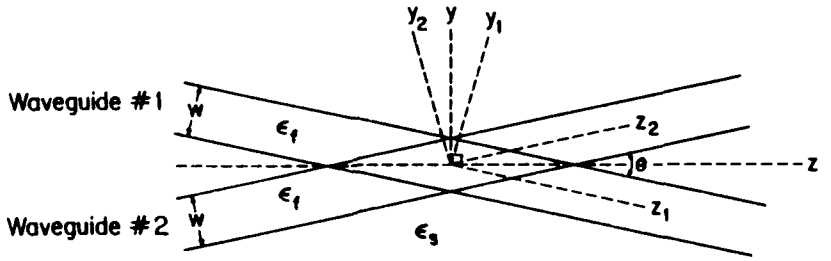

Fig. 1 Schematic diagram of the coordinate system for analysis of intersecting waveguides.

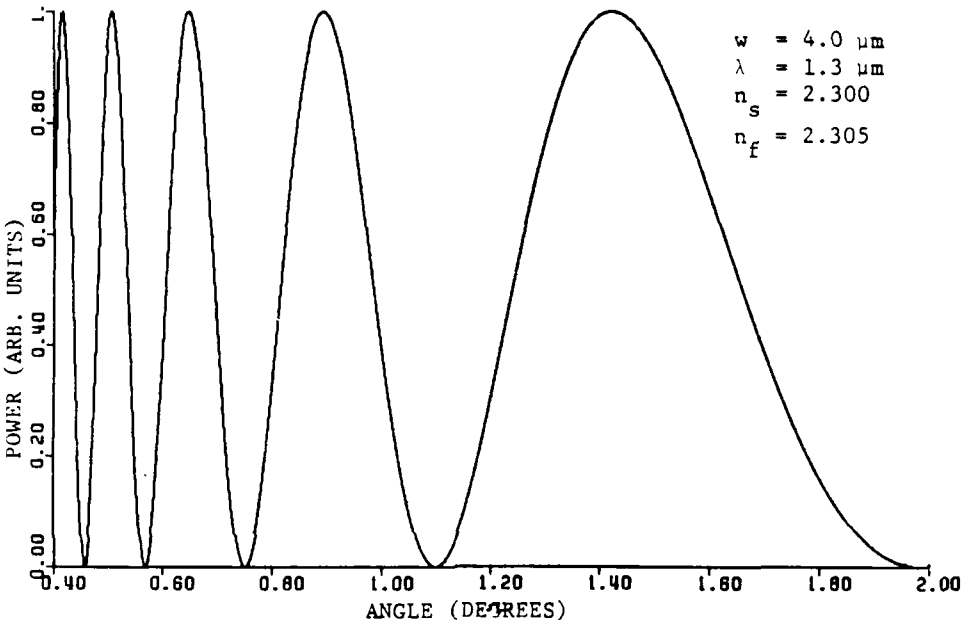

Fig. 2 The optical power exchanged between waveguides as function of intersection angle for the 2-Δn case.

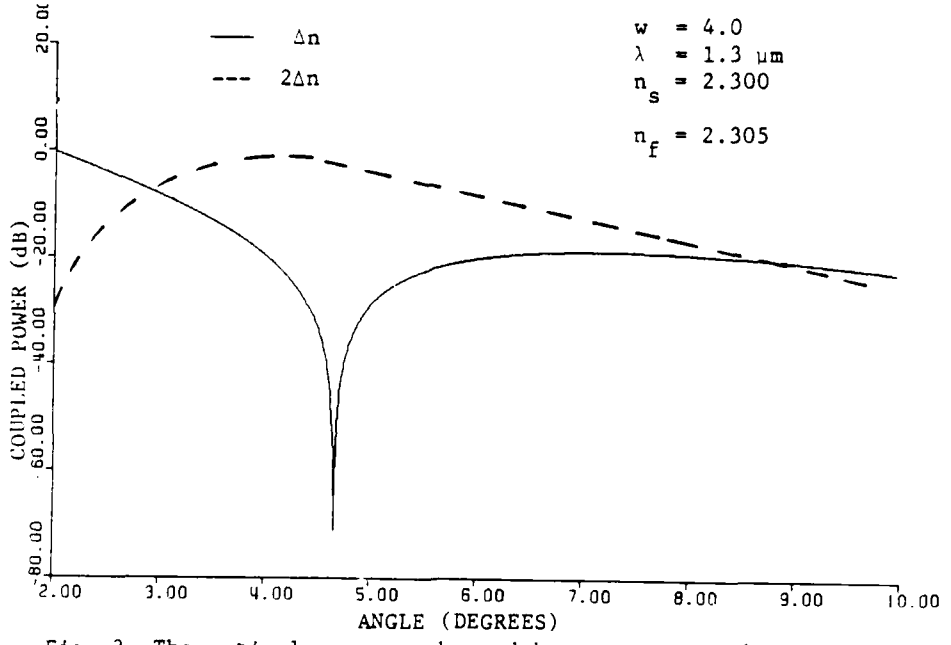

Fig. 3 The optical power exchanged between waveguides as function of intersection angle.

OPTICAL AMPLIFICATION IN SWITCHING NETWORKS

L Thylén, P Granestrand, A Djupsjöbacka
TELEFONAKTIEBOLAGET L M ERICSSON
Ericsson Telecom
Line Transmission and Fibre Optics
S-126 25 STOCKHOLM
SWEDEN

ABSTRACT

We report experimental results involving BER-measurements at 990 Mb/s for a Ti:$LiNbO_3$ integrated optics device cascaded with a semiconductor laser amplifier.

INTRODUCTION

Light amplifiers are expected to play an important role in future optical communications and switching systems. Current efforts are mainly concerned with semiconductor laser amplifiers (SCLA:s) (1) and SCLA:s have been used as preamplifiers (2) and linear repeaters (3). Recent investigations have been concerned with the possibilities of making near travelling wave amplifiers (4) and investigating gain characteristics of long wavelength devices (5). However, the applications mentioned above are generally demanding in the sense that low noise requirements are involved, giving (for direct detection) requirements on a signal to noise ratio limited by signal-spontaneous beat noise and hence requirements on input signal level and/or optical noise bandwidth (6). Such requirements can, however, more easily be accomodated when applying SCLA:s in areas limited in physical size (LAN:s optical switching networks) or generally in situations where the SCLA input signal can be kept high enough to permit cascading of a sizeable number of SCLA:s (5) without impairing signal quality. Here, the SCLA:s can be used to compensate for insertion and power splitting losses occuring in e g integrated optics circuits (IOC:s), thus significantly widening the scope for optical switching, as can be recognized from the comparatively limited complexity of optical systems which can be implemented without the availability of an amplification (or regeneration) function. This paper describes such an application where an SCLA is used to compensate insertion and power splitting losses of a $LiNbO_3$ IOC (7), incorporating two switches in cascade and a travelling wave modulator.

EXPERIMENTAL RESULTS

Fig 1 shows the experimental set-up, where a directly modulated (990 Mb/s) DFB-laser (λ=1.292 µm at room temperature) is coupled via an isolator and a polarization holding (PH) fiber to a pigtailed antireflection coated (AR) IOC (7), which is cascaded (again employing PH-fibers) to an SCLA and subsequently coupled (with an ordinary SM-fiber) to a 50 Ω receiver, incorporating a 10 GHz bandwidth detector diode and an amplifier with 1.7 GHz bandwidth. The receiver sensitivity is approximately -20 dBm.

The insertion loss of the chip is 4 dB and the switches on the chip are used to vary the SCLA input power, simulating power splitting losses. A bit error rate test set is used to generate PN codes and to monitor the transmission quality. The SCLA is an AR-coated FP laser diode with a precoating threshold current of 14 mA, the reflectance of the mirrors is half a percent, as

determined from measurements on the visibility of the gain spectrum. The SCLA is coupled to tapered PH- and SM-fibers and the coupling efficiency is estimated to 20 percent at the input and 30 percent at the output by operating the SCLA above postcoating threshold; these numbers were used for reflectance calculations. Fig 2 shows amplified spontaneous emission power (ASE) from the SCLA as a function of pump current, also shown is the peak ASE-wavelength and the fiber to fiber gains for four pump currents and at low (-20 dBm in the fiber) input power to the amplifier. Calculations of the gain spectrum at the different SCLA pumping levels show that the laser chirping should have little influence on performance, which was also experimentally confirmed.

Fig 3 shows the fiber-to-fiber gain as a function of the power in the fiber coupled to the SCLA with a measured BER $<10^{-10}$ and for a pump current of 40 mA. Too little power is available in this system to saturate the amplifier at this pump current, as can be seen from the figure. Fig 4 shows an oscilloscope photograph of the received bit pattern.

As can be seen, a maximum fiber to fiber gain of 12 dB is obtained and with a 12 dB coupling loss a maximum output power from the FP facet of around 2 dBm is obtained, which is too low to show any appreciable saturation effects. The relatively low fiber to fiber gain is, as is obvious from the above, primarily limited by the comparatively low fiber to SCLA coupling efficiency.

The 50 Ω receiver system employed here has a fairly low sensitivity of approximately -20 dBm. With this sensitivity and the relatively low amplifications employed, the performance of the system should be limited by thermal noise, this is also the case, when the components are properly adjusted to decrease as much as possible the influence of feedback effects. Such feedback effects were shown to have a strong influence on system performance.

In conclusion, we have demonstrated experimentally the feasibility of using a SCLA to compensate insertion and power splitting losses in a system involving an IOC (4 dB insertion and 8 dB power splitting losses in the experiment described here) while retaining transmission quality. The performance of the system can primarily be improved by increasing coupling to the SCLA, using a travelling wave device and by employing a different SCLA-design, as will be discussed. The demonstrated system shows the feasibility to widely enhance the complexity of photonic switching and communications systems.

REFERENCES

1. See e g J C Simon: "Semiconductor laser amplifier for single mode optical fiber communications", J Opt Comm, Vol 4, (1983), pp 51-52.

2. N A Olsson, P Garbinski: "High-sensitivity direct-detection receiver with a 1.5 μm optical preamplifier", Electronics Letters, Vol 22, (1986) pp 1114-1116.

3. I W Marshall, M J O'Mahony, P D Constantine: "Measurements on a 206 km optical transmission experiment at 1.5 μm using two packaged semiconductor laser amplifiers as repeaters", Proc European Conf Opt Commun, ECOC '86, (1986), pp 253-256.

4. T Saitoh, T Mukai, Y Noguchi: "Fabrication and noise characteristics

of a 1.5 μm GaInAsP Travelling wave optical amplifier", Proc First Optoel Conf, OEC '86, (1986), pp 12-13.

5. G Eisenstein, R M Jopson: "Measurements of the gain spectrum of near travelling wave and Fabry-Perot semiconductor optical amplifiers at 1.5 μm", Int J Electron, Vol 60, (1986), pp 113-121.

6. Y Yamamoto: "Noise and error rate performance of semiconductor laser amplifiers in PCM-IM optical transmission systems", IEEE J Quant Electron, Vol QE-16, (1980), pp 1073-1081.

7. L Thylén, A Djupsjöbacka, M Janson, W Döldissen: "Integrated-Optic device for high-speed databuses", Electron Letters, Vol 21, (1985), pp 491-493.

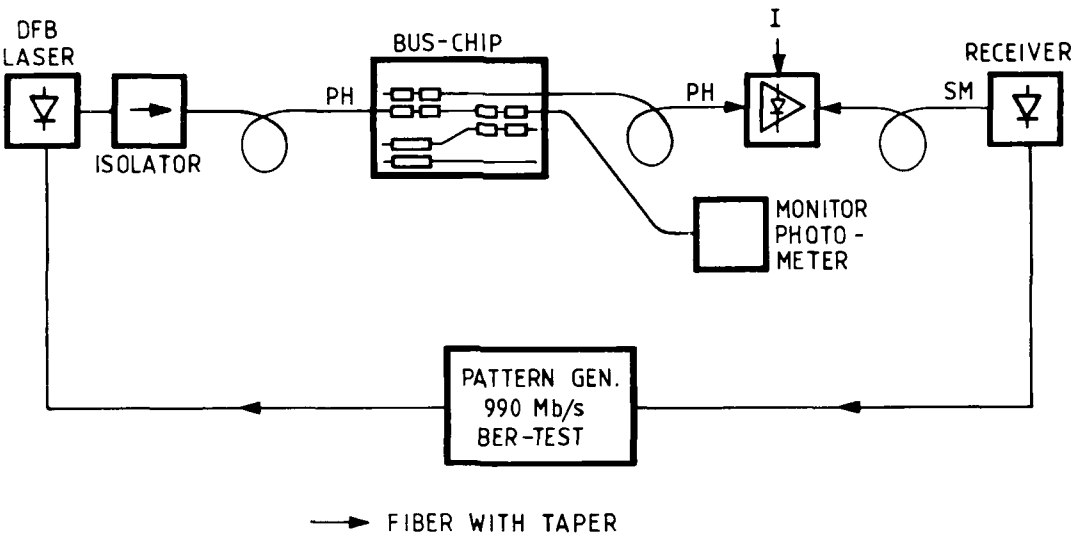

Fig 1: Experimental set-up; all plane fiber ends are index-matched.

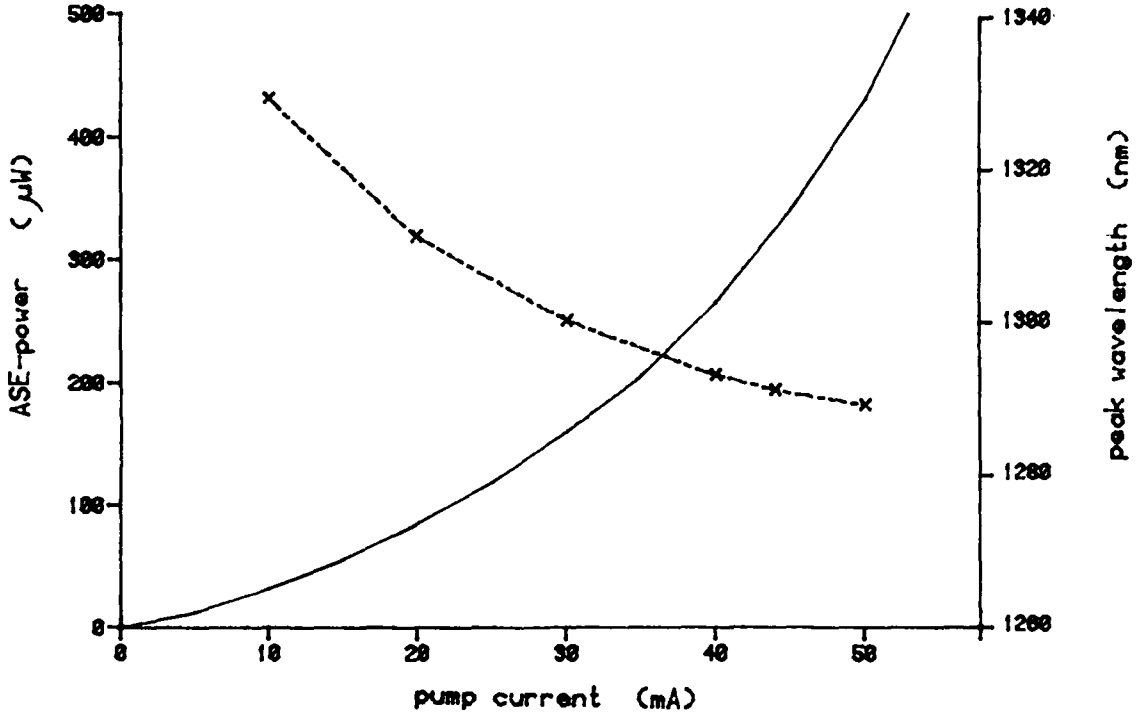

(a)

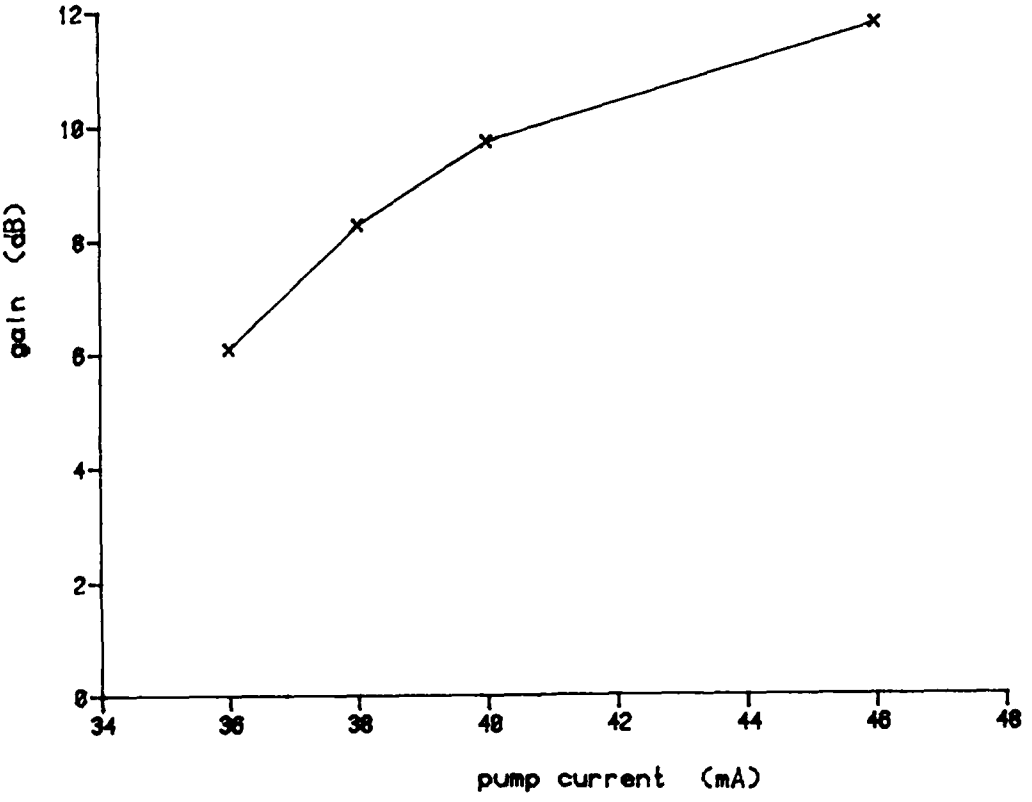

(b)

Fig 2: a) ASE-power (-) and ASE-spectrum peak wavelength (-·-) as a function of pump current is shown. b) Fiber-to-fiber gain at low input power (-20 dBm) is shown for a number of pump currents.

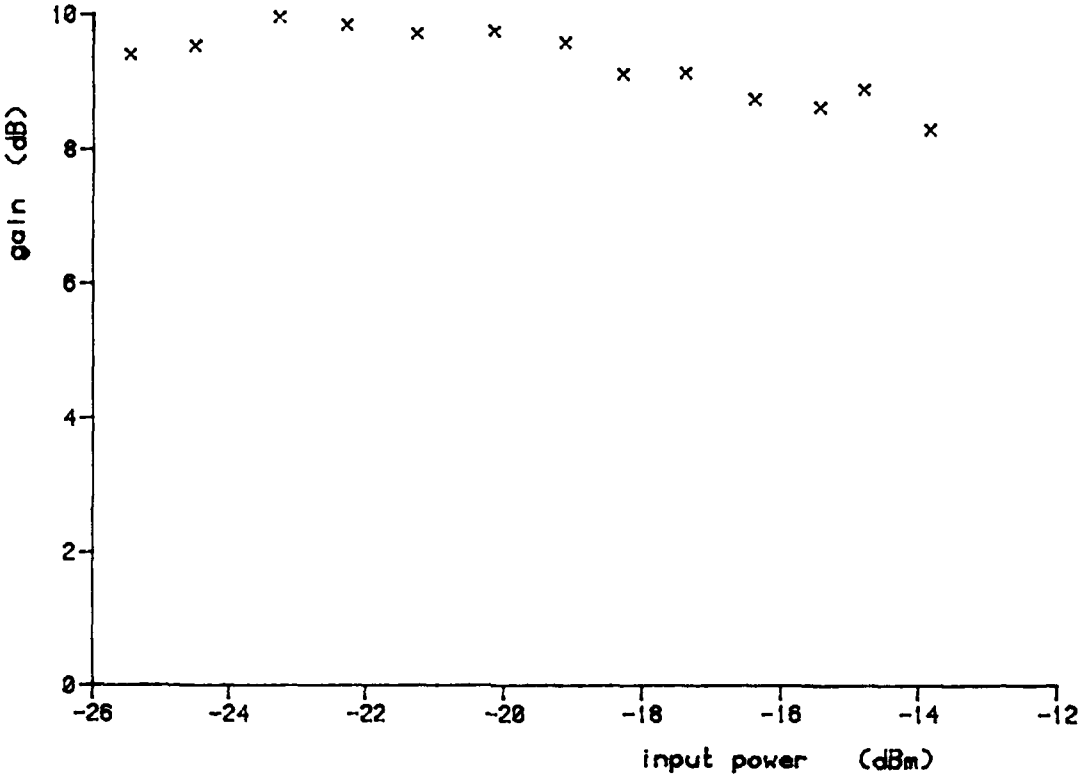

Fig 3: Fiber-to-fiber gain as a function of average input power for a pump current of 40 mA.

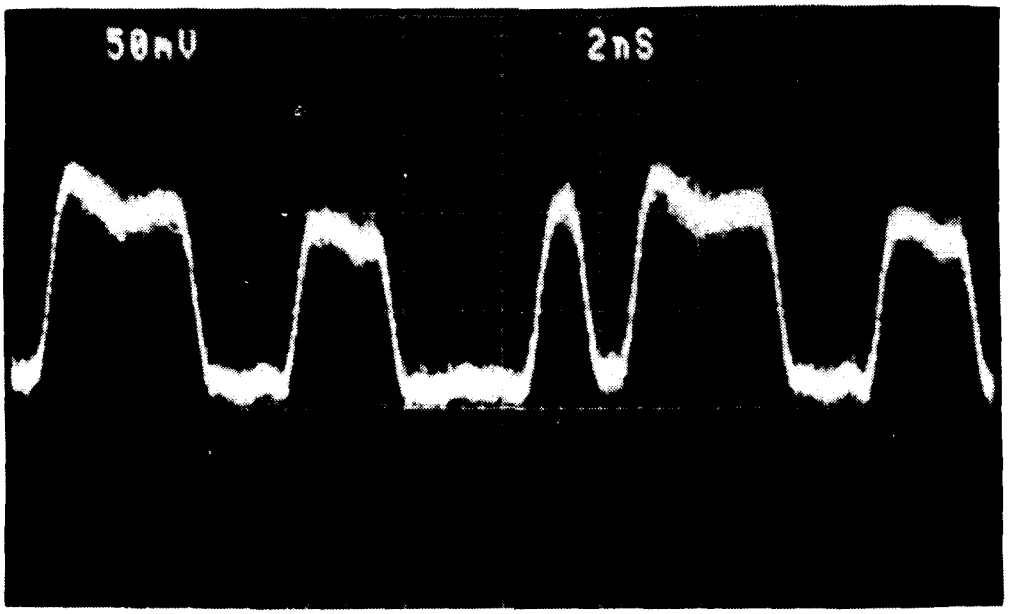

Fig 4: Bit pattern at the receiver output with an input power of approximately -20 dBm and a pump current of 40 mA.

END
DATED
FILM
8-88
DTIC